U.PORTO

PhD IN PHARMACEUTICAL SCIENCES

NANOTECHNOLOGIES SPECIALITY

Optimization of Lyophilization Parameters of Polymeric Nanoparticles for Delivery of Therapeutic Proteins

Pedro Fonte

D

2016

U.PORTO

Pedro Fonte . Optimization of Lyophilization Parameters of Polymeric Nanoparticles for Delivery of Therapeutic Proteins

Optimization of Lyophilization Parameters of Polymeric Nanoparticles for Delivery of Therapeutic Proteins

Pedro Fonte

FACULDADE DE FARMÁCIA

D.FFUP 2016

This page was intentionally left in blank


UCIBIO
@ REQUIMTE


U.PORTO
FACULDADE DE FARMÁCIA
UNIVERSIDADE DO PORTO


CESPU
INSTITUTO UNIVERSITÁRIO
DE CIÊNCIAS DA SAÚDE


INEB
Instituto de Engenharia Biomédica


FACULTY OF HEALTH AND MEDICAL SCIENCES
UNIVERSITY OF COPENHAGEN


FCT
Fundação para a Ciência e a Tecnologia
MINISTÉRIO DA EDUCAÇÃO E CIÊNCIA

Pedro Ricardo Martins Lopes da Fonte

Optimization of Lyophilization Parameters of Polymeric Nanoparticles for Delivery of Therapeutic Proteins

Thesis Submitted in Fulfillment of the Requirements to Obtain the PhD Degree in Pharmaceutical Sciences - Nanotechnologies Speciality

Tese do 3.º Ciclo de Estudos Conducente ao Grau de Doutoramento em Ciências Farmacêuticas na Especialidade de Nanotecnologias

This work was developed and conducted under the supervision of Professor Bruno Sarmento (Instituto Universitário de Ciências da Saúde, Portugal and Instituto de Engenharia Biomédica, Portugal), Professor Salette Reis (Faculty of Pharmacy, University of Porto, Portugal) and Professor Marco van de Weert (Faculty of Health and Medical Sciences, University of Copenhagen, Denmark)

January 2015

ACCORDING TO THE APPLICABLE LAW, THE REPRODUCTION OF THIS THESIS IS NOT ALLOWED.

DE ACORDO COM A LEGISLAÇÃO EM VIGOR, NÃO É PERMITIDA A REPRODUÇÃO DESTA TESE.

“Learn from yesterday, live for today, hope for tomorrow. The important thing is not to stop questioning.”

“If we knew what it was we were doing, it would not be called research, would it?”

Albert Einstein

Preface

This PhD Thesis entitled “Optimization of Lyophilization Parameters of Polymeric Nanoparticles for Delivery of Therapeutic Proteins” has been submitted to meet the requirements for obtaining the PhD degree at the Faculty of Pharmacy, University of Porto. The work contained in this Thesis was performed in the UCIBIO, REQUIMTE, Department of Chemical Sciences - Applied Chemistry Lab, Faculty of Pharmacy, University of Porto, Portugal in collaboration with CESPU, Instituto de Investigação e Formação Avançada em Ciências e Tecnologias da Saúde, Portugal and with the Section for Biologics at the Department of Pharmacy, Faculty of Health and Medical Sciences, University of Copenhagen, Denmark. The project was funded by the Fundação para a Ciência e a Tecnologia, Portugal.

The listed original research articles were prepared under the scope of this Thesis:

I. Pedro Fonte, Sandra Soares, Ana Costa, José Andrade, Vítor Seabra, Salette Reis, Bruno Sarmento, Effect of cryoprotectants on the porosity and stability of insulin-loaded PLGA nanoparticles after freeze-drying, Biomatter, 2 (2012) 329-339.

II. Pedro Fonte, Sandra Soares, Flávia Sousa, Ana Costa, Vítor Seabra, Salette Reis, Bruno Sarmento, Stability study perspective of the effect of freeze-drying using cryoprotectants on the structure of insulin loaded into PLGA nanoparticles, Biomacromolecules, 15 (2014) 3753-3765.

III. Pedro Fonte, Francisca Araújo, Vítor Seabra, Salette Reis, Marco van de Weert, Bruno Sarmento, Co-encapsulation of lyoprotectants improves the stability of protein-loaded PLGA nanoparticles upon lyophilization, Int J Pharm, 496 (2015) 850-862.

IV. Pedro Fonte, Fernanda Andrade, João Pinto, Vítor Seabra, Marco van de Weert, Salette Reis, Bruno Sarmento, Effect of the freezing step in the stability and bioactivity of protein-loaded PLGA nanoparticles upon lyophilization. *Submitted for publication.*

V. Pedro Fonte, Paulo R. Lino, Vítor Seabra, António Almeida, Salette Reis, Bruno Sarmento, Annealing as a tool for the optimization of lyophilization and ensuring of the stability of protein-loaded PLGA nanoparticles. *Submitted for publication.*

Additionally, the following review articles were relevant to the Thesis:

I. Pedro Fonte, Francisca Araújo, Salette Reis, Bruno Sarmento, Oral insulin delivery: how far are we?, J Diabetes Sci Technol, 7 (2013) 520-531.
II. Pedro Fonte, Francisca Araújo, Cátia Silva, Carla Pereira, Salette Reis, Hélder A. Santos, Bruno Sarmento, Polymer-based nanoparticles for oral insulin delivery: Revisited approaches, Biotechnol Adv, 33 (2015) 1342-1354.
III. Pedro Fonte, Salette Reis, Bruno Sarmento, Facts and evidences on the lyophilization of polymeric nanoparticles, J Control Release, *Accepted.*

The work was divulgated through the following communications in scientific meetings:

I. Pedro Fonte, José Carlos Andrade, Vítor Seabra, Domingos Ferreira, Salette Reis, Bruno Sarmento, Optimization of lyophilization parameters of polymeric nanoparticles for therapeutic proteins delivery, 9th International Conference on Protein Stabilization, Lisbon, Portugal, 2012. *Poster presentation.*
II. Pedro Fonte, Sandra Soares, José Carlos Andrade, Vítor Seabra, Domingos Ferreira, Salette Reis, Bruno Sarmento, Effect of cryoprotectants on the stability of protein-loaded PLGA nanoparticles after freeze-drying, 9th Central European Symposium on Pharmaceutical Technology, Dubrovnik, Croatia, 2012. *Poster presentation.*
III. Pedro Fonte, Sandra Soares, Ana Costa, José Carlos Andrade, Vítor Seabra, Domingos Ferreira, Salette Reis, Bruno Sarmento, Freeze-drying of insulin-loaded PLGA nanoparticles: the effect of cryoprotectants on particles stability, 4th International Congress on Nanotechnology, Medicine & Biology, Krems, Austria, 2013. *Poster presentation.*
IV. Pedro Fonte, Sandra Soares, Ana Costa, José Carlos Andrade, Vítor Seabra, Domingos Ferreira, Salette Reis, Bruno Sarmento, Structural stability of proteins encapsulated into PLGA nanoparticles, 6th Meeting of Young Researchers of University of Porto, Porto, Portugal, 2013. *Poster presentation.*
V. Pedro Fonte, Freeze-drying approaches for overcoming instability of therapeutic proteins encapsulated into nanoparticles, IX Cycle of Conferences of the

Advanced Institute of Health Sciences – North, Porto, Portugal, 2013. *Oral presentation.*

VI. Pedro Fonte, Freeze-drying and structure of therapeutic proteins encapsulated into nanoparticles, 3rd AAPS-UP Student Chapter Annual Symposium, Porto, Portugal, 2013. *Oral presentation.*

VII. Pedro Fonte, Sandra Soares, Ana Costa, José Carlos Andrade, Vítor Seabra, Domingos Ferreira, Salette Reis, Bruno Sarmento, Structural stability of proteins encapsulated into PLGA nanoparticles, Vth Training School on Bioencapsulation, National College of Veterinary Medicine, Food Science and Engineering, Nantes, France, 2013. *Poster presentation.*

VIII. Pedro Fonte, Flávia Sousa, Ana Costa, Domingos Ferreira, Vítor Seabra, Salette Reis, Bruno Sarmento, Effect of loaded cryoprotectants on insulin-loaded PLGA nanoparticles, 9th World Meeting on Pharmaceutics, Biopharmaceutics and Pharmaceutical Technology, Lisbon, Portugal, 2014. *Poster presentation.*

IX. Pedro Fonte, Effect of freeze-drying on the structure of therapeutic proteins loaded into nanoparticles, Pharmaceuticals and Biopharmaceuticals: Lyophilization, London, England, 2014. *Oral presentation.*

X. Pedro Fonte, Sandra Soares, Flávia Sousa, Ana Costa, Vítor Seabra, Salette Reis, Bruno Sarmento, Impact of freeze-drying and cryoprotectant loading on the stability of insulin loaded into PLGA nanoparticles, Controlled Release Society Annual Meeting & Exposition, Edinburgh, Scotland, 2015. *Poster presentation.*

The supervisors of the PhD project have been:

- Professor Bruno Sarmento, CESPU, Instituto Universitário de Ciências da Saúde, Portugal and INEB − Instituto de Engenharia Biomédica, University of Porto, Portugal.
- Professor Salette Reis, UCIBIO, REQUIMTE, Department of Chemical Sciences - Applied Chemistry Lab, Faculty of Pharmacy, University of Porto, Portugal.
- Professor Marco van de Weert, Department of Pharmacy, Faculty of Health and Medical Sciences, University of Copenhagen, Denmark.

Biographical Note of the Author

Pedro Fonte was born on April 8, 1986 in Chaves, Portugal. He obtained his graduation in Pharmaceutical Sciences in 2010 from the Instituto Superior de Ciências da Saúde-Norte, Gandra, Portugal. He also obtained a Master of Business Administration (MBA) in Faculty of Economics and Business Management, Lusíada University, Porto, Portugal in 2012.

He has experienced work in Community Pharmacy, Hospital Pharmacy and Clinical Analysis Lab. He was supervisor of the research work of students within the Biochemistry graduation and of students from international exchange programs in the Instituto Superior de Ciências da Saúde-Norte, Gandra, Portugal from 2012 to 2014. He was also invited as a teaching assistant in practical classes of Pharmaceutical Technology of the Pharmaceutical Sciences graduation in Instituto Superior de Ciências da Saúde-Norte, Gandra, Portugal on November 2012-2014.

His research activities has been focused on the development of new drug delivery systems using polymeric and lipid nanoparticles, structural characterization of proteins entrapped into nanoparticles and lyophilization of biopharmaceuticals. He has interest on nanotechnology-based development and up-scale of pharmaceutical and food products, and has obtained awarded entrepreneurship initiatives. In his work he established collaboration with research groups in Portugal and abroad, and has received several awards.

Pedro Fonte is the author of 16 peer-reviewed articles, 5 book chapters and 22 presentations at scientific meetings. He was a founding member of the AAPS-University of Porto Student Chapter in 2010, and has been invited as reviewer by international peer-reviewed scientific Journals.

Acknowledgments

I would like to express my gratitude to all the people and institutions that crossed my path during these years, and supported me during the performance of the Thesis. Therefore, I would like to deeply acknowledge to:

Professor Bruno Sarmento, my supervisor, for his friendship, for giving me the opportunity to join his group and for his professional and enthusiastic guidance. Also, for giving me the opportunity to apply my own ideas in the work. I will always remember that it was him that brought me to the 'research world', so this work would not be definitely possible without him. I cannot find words to properly thank to him;

Professor Salette Reis, my co-supervisor, for her friendship, for receiving me in her group and giving me all the conditions to perform this work. She is also kindly acknowledged for her availability to help me and for the scientific input and advices during these years;

Professor Marco van de Weert, my co-supervisor, for his personal advice and scientific input that improved the quality of the work, and the inspiring and pleasant working atmosphere in his research group.

Professor Vítor Seabra, Instituto Universitário de Ciências da Saúde, Gandra, Portugal, as chair of the Pharmaceutical Sciences graduation, for the scientific formation and skills that I developed during my graduation and it were the starting point of this Thesis. Also for his trust and for receiving me in his laboratory, and for providing me a FTIR equipment that was crucial to the development of the work. He is also acknowledged for the advices on publishing several research articles;

Professor José Costa Lima, as Head of the Applied Chemistry Laboratory of Faculty of Pharmacy, University of Porto, Porto, Portugal for providing the financial support that allowed to present my work in several meetings in Portugal and abroad;

Professor Domingos Ferreira, Pharmaceutical Technology Laboratory of Faculty of Pharmacy, University of Porto, Porto, Portugal for his friendship, and for his availability and for allowing me the use of the lyophilizer in the beginning of the research work;

Professor José Sousa Lobo, as Head of the Pharmaceutical Technology Laboratory of Faculty of Pharmacy, University of Porto, Porto, Portugal for allowing the use of the lab facilities and also the use of the lyophilizer;

Professor João Pinto, Department of Galenic Pharmacy and Pharmaceutical Technology, Faculty of Pharmacy, University of Lisbon, Lisbon, Portugal, for his availability on the established collaboration, and for allowing me to use the freeze-drying microscope that pushed the work forward. He is also acknowledged for his scientific contribution on publishing a research paper;

Professor António Almeida, Department of Galenic Pharmacy and Pharmaceutical Technology, Faculty of Pharmacy, University of Lisbon, Lisbon, Portugal for his friendship and for receiving me so well in his research group, giving me all the available conditions to finish the Thesis with the established collaboration work.

Professor Lene Jørgensen, Department of Pharmacy, Faculty of Health and Medical Sciences, University of Copenhagen, Denmark, for her warm welcome and especially for teaching me about FTIR;

The members of Professor Salette Reis research group, in particular to Ana Rute Neves for her friendship and availability to help me on the use of the facilities and equipments of the lab;

The members of Professor Marco van de Weert research group, in particular to Louise Stenstrup Holm for her friendship, help and support and for making my stay abroad a great time;

Dr. Virgínia Gonçalves, IINFACTS, CESPU, Gandra, Portugal, for her great assistance and help on the lab management and with the HPLC analysis;

Dr. Rui Fernandes, IBMC, Porto, Portugal, for his friendship help and good times spent during the transmission electron analysis;

Dr. Hjalte Trnka and Dorthe Ørbæk, Faculty of Health and Medical Sciences, University of Copenhagen, Copenhagen, Denmark, for their help on the X-ray powder diffraction experiments;

Dr. Mathias Fanø, Faculty of Health and Medical Sciences, University of Copenhagen, Copenhagen, Denmark, for his help on the circular dichroism experiments;

Dr. Artur Pinto, Faculty of Engineering, University of Porto, Porto, Portugal, for his friendship and assistance on the differential scanning calorimetry analysis;

For the staff members of the Instituto Universitário de Ciências da Saúde, Gandra, Portugal, in particular to Paula Vinhas, Isabel Marques, Zélia Ferreira, Paula

Oliveira, Clarinda Carvalho and Fernanda Pereira for their friendship and outstanding environment around the lab, and for their availability on helping me to develop my work in the institution;

For the researchers from the Professor Hassan Bousbaa group, IINFACTS, Cespu, Gandra, Portugal, in particular to Patrícia Silva and Ana Vanessa Nascimento for their friendship and good moments spent together inside and outside the lab;

For the researchers from the Professor Elizabeth Tiritan group, IINFACTS, Cespu, Gandra, Portugal, particularly to Alexandra Maia for her friendship, for the relax times we had outside the lab.

Sandra Soares, Ana Costa, Rute Nunes and Cassilda Reis, IINFACTS, Cespu, Gandra, Portugal for their fellowship, good and funny times spent during the years that became the work much easier to take further, and also for their help and support on several stages of the work;

Fernanda Andrade, Pharmaceutical Technology Laboratory of Faculty of Pharmacy, University of Porto, Porto, Portugal, for her friendship and the great moments spent inside and outside the lab, and also for her help on the *in vivo* experiments;

José das Neves, INEB, Porto, Portugal for his friendship and for his valuable scientific advices and the motivation he gave me to take my work further. He is also kindly acknowledged for the great moments we had outside the lab.

Francisca Araújo, IINFACTS, Cespu, Gandra, Portugal and INEB, Porto, Portugal, for her fellowship and bad mood that entertained me and led us to spent excellent times together. She is deeply acknowledged for being a great friend, and for the personal and scientific contribution on the collaborations we established.

My laboratory friends and colleagues, namely Alexandra Machado, Alexandre Couto, Ana Costa, Ana Vanessa Nascimento, Bárbara Mendes, Carla Pereira, Cassilda Reis, Flávia Sousa, José das Neves, Sara Baptista da Silva, Francisca Araújo, Francisca Rodrigues, João Albuquerque, Luise Lopes, Maria João Gomes, Patrick Kennedy, Pedro Castro, Rute Nunes, Sara Carneiro and Teófilo Vasconcelos, for the good working atmosphere and for the scientific discussions we had in each labmeeting.

My closest friends, André Machado, João Cocharra and Tiago Gonçalves for their friendship, support, companionship, complicity, and for lifting me up in difficult moments.

Tiago Nogueira, for his friendship and for supporting me to follow my dreams. His way of living was always inspiring, and he keeps teaching me every day with his strength and determination. His presence was always in my mind and still, through his example, he gave me energy to keep on moving forward.

Those I love the most, my mother (Fernanda), my father (Cândido) and sister (Alexandra), without whom I would not be who I am today, and for their unconditional love and support. A special acknowledgement goes to my grandmother (Esperança) and aunt (Maria Fernanda), for always believing in me and for their encouragement and support. My parents-in-law (Maria Isabel and Júlio), brothers-in-law (Isabel and Paulo) and nephews-in-law (Gabriela, Ricardo, Inês and Rita), for their friendship and support during all these years. My beloved wife, Cláudia, for her love and for sharing life with me in all the good, and not so good moments. A deep acknowledgement is given to her for being an outstanding wife and friend, and for being the driving force that motivated me to follow my dreams. My dog, Áthila, for being such a good boy and for being there in all the moments, especially during the writing of the Thesis. He is kindly acknowledged for keeping both my feet and my heart warm. This work is dedicated to all of them.

Purac Biomaterials and Abbot Laboratories, Portugal for the free PLGA samples, and Precision Xtra® blood glucose meter and test strips, respectively.

The Bioencapsulation Research Group and its President Dennis Poncelet, for the financial support to attend the BRG's Training School that allowed me to learn more about encapsulation and characterization of nanocarriers.

The SMi Group, for the invitation and for financial support to attend to their annual conference about Lyophilization, and for the opportunity to contribute with an oral presentation;

Fundação para a Ciência e a Tecnologia (FCT), Portugal, (PTDC/SAL-FCT/104492/2008 and SFRH/BD/78127/2011) for financial support. This work was also financed by European Regional Development Fund through the Programa Operacional Factores de Competitividade − COMPETE, by Portuguese funds through FCT in the framework of the project PEst-C/SAU/LA0002/2013, and cofinanced by North Portugal Regional Operational Programme (ON.2 − O Novo Norte) in the framework of Project SAESCTN-PIIC&DT/2011 under the National Strategic Reference Framework.

Abstract

Therapeutic proteins are used to treat specific pathological conditions and severe diseases. The encapsulation into polymeric nanoparticles is a powerful strategy to deliver them in a sustained manner and preserve their stability. However, polymeric nanoparticles may get unstable in aqueous suspension, leading to their aggregation or fusion. The lyophilization comes to the front line as an useful approach to avoid the instability of nanoparticles. Nevertheless, this dehydration process may induce stresses to nanoparticles and encapsulated proteins. The use of excipients such as cryo- and lyoprotectants and the optimization of lyophilization cycle, may be useful strategies to avoid such stresses. Thus, the main aim of this Thesis was to undergo an optimization of lyophilization parameters of polymeric nanoparticles for delivery of therapeutic proteins, to preserve the stability of nanoparticles, and with upmost importance, better preserve the structural stability and bioactivity of proteins. For this purpose, poly(lactic-co-glycolic acid) (PLGA) as polymer and insulin as therapeutic protein were used as models.

The formulation of nanoparticles was optimized and it was demonstrated that the combination of PLGA in a lactic:glycolic ratio of 50:50 and polyvinyl alcohol at 2% (w/v) as surfactant, resulted in nanoparticles with the best features regarding their size, zeta potential and association efficiency, obtaining after insulin encapsulation about 446 nm, -24 mV and 87%, respectively. The lyophilization increased the nanoparticles porosity, being more evident for formulations added with cryoprotectants, namely trehalose, glucose, sucrose, fructose and sorbitol at 10% (w/v). The *in vitro* release of insulin after nanoparticles lyophilization, comparatively to before lyophilization showed an increased release of about 18% in the first 2 hours due to the porosity increase, followed by a sustained release up to 48 hours. The amount of insulin released from lyophilized nanoparticles showed some variability regarding the cryoprotectant used.

The nanoparticles were further used to assess the influence of a standard lyophilization cycle, and different storage conditions over 6 months on their features. The addition of cryoprotectants increased nanoparticles stability upon storage. Fourier transform infrared spectroscopy revealed that cryoprotectants increased insulin structural stability close to 80%, comparatively to formulations without cryoprotectant. Formulations with collapsed cakes had better protein stabilization upon storage, especially that containing sorbitol, preserving 76, 80, and 78% of insulin structure at 4°C, 25°C/60% relative humidity (RH), and 40°C/75% RH, respectively. Principal component analysis also showed that sorbitol added formulation had the most similar insulin structural modifications, among the storage conditions.

A strategy of lyoprotectant co-encapsulation was proposed to better preserve the structure of the loaded protein. Insulin-loaded PLGA nanoparticles with co-encapsulated lyoprotectants achieved a mean particle size of 386-466 nm, and a zeta potential ranging between -34 and -38 mV, dependent on the lyoprotectant used. Formulations had association efficiencies and loading capacities of 85-91% and 10-12%, respectively. X-ray powder diffraction studies revealed that the lyophilizates of nanoparticles with co-encapsulated lyoprotectants were amorphous, whereas formulations with externally added lyoprotectants, except trehalose, showed crystallinity. The co-encapsulation of lyoprotectants better preserved insulin structure upon lyophilization with a spectral area of overlap of 82-87%, comparatively to the lyoprotectants externally added to nanoparticles (66-83%), and to 72% in lyoprotectant absence. Circular dichroism confirmed these results.

The lyophilization cycle was optimized considering the physical-chemical properties of nanoparticles co-encapsulated with cryoprotectants. It was also assessed the influence of different freezing methods, namely freezing at -80ºC, ramped cooling at -40ºC and freezing in liquid nitrogen in the stability and bioactivity of encapsulated insulin. No cake collapse was observed. The cryoprotectants were crucial to mitigate the different freezing stresses and better stabilize insulin structure, as the area of overlap was close to 90%. The structural maintenance was confirmed by circular dichroism and fluorescence spectroscopy. The ramped cooling at -40ºC presented the most structural similarity of insulin among formulations. The use of trehalose and sucrose allowed better protein stabilization than sorbitol in all freezing methods. The *in vivo* studies revealed an enhanced hypoglycemic effect of insulin over 24 h after administration of nanoparticles co-encapsulated with trehalose, comparatively to both nanoparticles without cryoprotectant, and with trehalose added prior lyophilization, mainly due to a superior insulin stabilization and bioactivity.

An annealing step was included in the optimized lyophilization cycle of insulin-loaded nanoparticles co-encapsulated with trehalose to decrease the duration time of lyophilization. The duration time of primary drying was decreased in about 38% and the lyophilization cycle was decreased around 26%. The lyophilizates obtained with and without annealing had similar residual moisture content. The nanoparticles co-encapsulated with trehalose presented higher insulin structural maintenance, and formulations lyophilized with annealing presented similar insulin structural maintenance of those obtained without annealing.

Overall, the optimization of lyophilization of protein-loaded nanoparticles was found to be crucial to preserve the stability of the lyophilizates, the nanoparticles and the loaded protein, in order to formulations completely fulfill their therapeutic proposes.

Resumo

As proteínas terapêuticas são usadas no tratamento de condições patológicas específicas e doenças severas. A encapsulação em nanopartículas poliméricas é uma estratégia poderosa para as administrar obtendo libertação prolongada, e preservar a sua estabilidade. Contudo, as nanopartículas poliméricas podem tornar-se instáveis em suspensão, levando à sua agregação ou fusão. A liofilização está na linha da frente como uma estratégia útil para evitar a instabilidade de nanopartículas. Não obstante, este processo de desidratação pode induzir stresses nas nanopartículas e nas proteínas encapsuladas. O uso de excipientes como crio- e lioprotetores e a otimização do ciclo de liofilização, são estratégias úteis para evitar tais stresses. Assim, o principal objetivo desta Tese é otimizar os parâmetros de liofilização de nanopartículas poliméricas para administração de proteínas terapêuticas, para preservar a estabilidade das nanopartículas, e com maior importância, preservar a estabilidade e bioactividade das proteínas. Para cumprir este objetivo, foram usados como modelos, o ácido poli(láctico-co-glicólico) (PLGA) como polímero e a insulina como proteína terapêutica.

A formulação de nanopartículas foi otimizada e verificou-se que a combinação de PLGA no rácio de ácido láctico:glicólico de 50:50 e álcool polivinílico a 2% (w/v) como surfatante, produziu as nanopartículas com as melhores características considerando o tamanho médio, potencial zeta e eficiência de associação, obtendo após encapsulação de insulina cerca de 446 nm, -24 mV e 87%, respetivamente. A liofilização aumentou a porosidade das nanopartículas, com maior evidência nas formulações adicionadas com os crioprotetores, trealose, glucose, sacarose, frutose e sorbitol a 10% (w/v). A libertação *in vitro* de insulina após liofilização das nanopartículas, comparativamente a antes da liofilização, aumentou cerca de 18% nas primeiras 2 horas devido ao aumento da porosidade, seguida de libertação prolongada até 48 horas. A quantidade de insulina libertada das nanopartículas liofilizadas variou de acordo com o crioprotetor usado.

As nanopartículas foram posteriormente usadas para avaliar a influência de um ciclo de liofilização ‘standard’, e diferentes condições de armazenamento durante 6 meses, nas suas características. A adição de crioprotetores melhorou a estabilidade das nanopartículas durante o armazenamento. Análises de infravermelho com transformada de Fourier revelaram que os crioprotetores preservaram melhor a estrutura da insulina em cerca de 80%, comparativamente às formulações sem crioprotetor. Os liofilizados colapsados tiveram uma melhor estabilização da proteína após armazenamento, especialmente com sorbitol, preservando 76, 80 e 78% da estrutura da proteína a 4°C, 25°C/60% HR, e 40°C/75% HR, respetivamente. A análise de componente principal

também verificou que a formulação com sorbitol apresentou as alterações estruturais mais semelhantes, entre as condições de armazenamento.

Uma estratégia de co-encapsulação de lioprotetor foi proposta para melhor preservar a estrutura da proteína. As nanopartículas co-encapsuladas com lioprotetores obtiveram um tamanho médio de 386-466 nm e um potencial zeta entre -34 e -38 mV, dependendo no lioprotetor usado. As formulações apresentaram eficiências de associação e capacidade de carga de 85-91% e 10-12%, respetivamente. Estudos de difração raio X de pós revelaram que os liofilizados de nanopartículas com lioprotetores co-encapsulados eram amorfos, enquanto quando adicionados externamente, excepto a trealose, revelaram cristalinidade. A co-encapsulação de lioprotetores obteve uma melhor preservação estrutural após liofilização com uma área de sobreposição espetral de 82-87%, comparada com os 66-83% dos lioprotetores adicionados externamente, e com 72% sem lioprotetor. O dicroísmo circular confirmou estes resultados.

O ciclo de liofilização foi otimizado considerando as propriedades físico-químicas das nanopartículas co-encapsuladas com crioprotetor. Foi também avaliada a influência de diferentes métodos de congelação, nomeadamente congelação a -80ºC, arrefecimento em rampa a -40ºC e congelação em azoto líquido, na estabilidade e bioactividade da insulina encapsulada. Os liofilizados não colapsaram. Os crioprotetores foram cruciais para mitigar os stresses da congelação e preservarem melhor a estrutura da insulina, em cerca de 90%. A manutenção estrutural foi confirmada por dicroísmo circular e espetroscopia de fluorescência. O arrefecimento em rampa a -40ºC apresentou a maior semelhança estrutural de insulina entre as formulações. O uso de trealose e sacarose estabilizou melhor a proteína do que o sorbitol, nas três condições de congelação. Estudos *in vivo* durante 24 horas demonstraram um maior efeito hipoglicémico da insulina, após administração de nanopartículas co-encapsuladas com trealose, comparando às nanopartículas sem crioprotetor e adicionadas com trealose antes da liofilização, devido a uma superior estabilização e bioactividade da insulina.

Foi incluída uma etapa de ‘annealing’ no ciclo de liofilização de nanopartículas co-encapsuladas com trehalose de forma a diminuir o tempo de duração da liofilização. A duração da secagem primária foi diminuída em cerca de 38%, e o ciclo de liofilização em cerca de 26%. Os liofilizados obtidos com e sem ‘annealing’ obtiveram um teor de humidade residual semelhante. As nanopartículas co-encapsuladas com trealose apresentaram uma manutenção estrutural de insulina superior, e as formulações liofilizadas com e sem annealing apresentaram uma manutenção estrutural idêntica.

Globalmente, verificou-se que a otimização da liofilização de nanopartículas contendo proteínas é determinante para preservar a estabilidade dos liofilizados, nanopartículas e proteína, para as formulações cumprirem os objetivos terapêuticos.

Table of Contents

List of Figures

Chapter 2. Polymeric Nanoparticles for Oral Administration of Insulin

Chapter 3. Facts and Evidences on the Lyophilization of Polymeric Nanoparticles

Chapter 4. Optimization of Insulin-loaded PLGA Nanoparticles and Effect of Cryoprotectants on their Porosity and Stability upon Lyophilization

Chapter 5. A Stability Study Perspective of the Effect of Lyophilization Using Cryoprotectants on the Structure of Insulin Loaded Into PLGA Nanoparticles

Chapter 6. Co-encapsulation of Lyoprotectants as a Strategy to Improve the Stability of Protein-loaded PLGA Nanoparticles upon Lyophilization

Chapter 7. Optimization of Lyophilization Cycle and Effect of Freezing on the Stability and Bioactivity of Protein-loaded PLGA Nanoparticles upon Lyophilization

Chapter 8. Optimization of Lyophilization Cycle Using Annealing and its Effect on the Stability of Protein-loaded PLGA Nanoparticles

List of Tables

Chapter 7. Optimization of Lyophilization Cycle and Effect of Freezing on the Stability and Bioactivity of Protein-loaded PLGA Nanoparticles upon Lyophilization

Chapter 8. Optimization of Lyophilization Cycle Using Annealing and its Effect on the Stability of Protein-loaded PLGA Nanoparticles

Abbreviations and Acronyms

AAC	Area above the curve
AE	Association efficiency
AFM	Atomic force microscopy
ANOVA	Analysis of variance
AO	Area of overlap
ATP	Adenosine triphosphate
ATR	Attenuated total reflectance
BSA	Bovine serum albumin
CD	Circular dichroism
Cg'	Maximal concentration of the cryoconcentrated solution
CSK	C-Src tyrosine kinase
Cys	Cysteine
DEMC	Diethylmethyl chitosan
DMEC	Dimethylethyl chitosan
DSC	Differential scanning calorimetry
DTPA	Diethylene triamine pentaacetic acid
ELISA	Enzyme linked immuno sorbent assay
ESCA	Electron spectroscopy for chemical analysis
ESEM	Environmental scanning electron microscopy
FITC	Fluorescein isothiocyanate
FTIR	Fourier-transform infrared spectroscopy
HPC	Hydroxypropyl cellulose

HPLC	High performance liquid chromatography
HPMCP	Hydroxypropyl methylcellulose phthalate
HPβCD	Hydroxypropyl-β-cyclodextrin
ICH	International Conference on Harmonization
LCS	Lauryl chitosan
LDH	Lactate dehydrogenase
LC	Loading capacity
MRW	Mean residual weight
NMR	Nuclear magnetic resonance
PA	Pharmacological availability
PAA	Poly(acrylic acid)
PAT	Process analytical technology
PBS	Phosphate buffered saline
PC	Principal component
PCA	Principal component analysis
PCL	Poly(ε-caprolactone)
PdI	Polydispersity index
PEG	Polyethylene glycol
PEO	Polyethylene oxide
PGA	Polyglycolic acid
PIBCA	Poly(isobutylcyanoacrylate)
PIHCA	Poly(isohexylcyanoacrylate)
PLA	Polylactic acid
PLGA	Poly(lactic-co-glycolic acid)

PVA	Polyvinyl alcohol
PVP	Poly(vinyl pyrrolidone)
QbD	Quality by design
RH	Relative humidity
SCC	Spectral correlation coefficient
SD	Standard deviation
SEM	Scanning electron microscopy
Tc	Collapse temperature
TEC	Triethyl chitosan
TEM	Transmission electron microscopy
Teu	Eutectic temperature
Tg	Glass transition temperature
Tg'	Glass transition temperature of the frozen sample
TMC	N-trimethyl chitosan
TPP	Tripolyphosphate
UV	Ultraviolet
UV/Vis	Ultraviolet-visible.
γ-PGA	Poly(γ-glutamic acid)

Chapter 1

Aims and Outline of the Thesis

Benefiting from the developments in the biotechnology field, the use of different therapeutic proteins have been growing in the last years, mainly to treat severe health problems such as autoimmune diseases, cancer and hormone disorders [1]. These drugs may be formulated into polymeric nanoparticles, both from natural and synthetic origin, improving the efficacy of treatment of such diseases [2]. Nanoparticles are used to deliver proteins by different administration routes, mainly due to their ability to preserve the stability of the loaded protein and to deliver in a sustained manner. They are also able to enhance the permeability of proteins through biological barriers such as the intestinal and respiratory epithelium [3, 4]. The nanoparticle polymers may be further functionalized, targeting the delivery to specific tissues and organs, with an increased accumulation of the protein in the action site, both enhancing the therapeutic effect and decreasing the possibility of occurrence of prejudicial side effects [5].

Since nanoparticles are often produced in an aqueous suspension form, they are physically unstable, resulting on nanoparticle aggregation and fusion upon storage. Furthermore, the hydrolytic action of water on the polymers may lead to drug leakage, hampering its sustained release or even leading to the formation of undesirable degradation products [6]. To avoid these issues, the nanoparticle suspension needs to be converted into a solid dosage form. Lyophilization or freeze-drying is an useful process to achieve this purpose by overcoming the instability of nanoparticle suspension, increasing shelf-life and facilitating its handling and storage [7, 8]. In this process, the removal of water occurs by sublimation of ice and desorption of unfrozen water under vacuum. However, freezing and desiccation stresses may occur, leading to detrimental effects to nanoparticle stability. Some excipients such as cryoprotectants and lyoprotectants may be used to minimize the freezing and desiccation stresses, respectively, preserving the stability of nanoparticles. The most common cryo- and lyoprotectants are sugars, mainly because they are easily vitrified during freezing and are chemically innocuous [9]. Additionally, sugars may prevent the inactivation of protein drugs during lyophilization and storage [10].

Most of the research works focusing on the lyophilization of nanoparticles present empiric approaches on the choosing of acceptable protectants and lyophilization cycle, and experiments have been even performed by trial and error. It is imperative to put through a systematic study on the optimization of nanoparticles lyophilization, by evaluating the physical-chemical properties of formulations and understanding the engineering principles of lyophilization. Therefore, it is necessary the optimization of lyophilization parameters of polymeric nanoparticles for delivery of therapeutic proteins, to guarantee the stability of nanoparticles and upmost assure the structural stability of

the loaded protein. There is a lack of knowledge on the effect of lyophilization on the structure of proteins loaded into nanoparticles, with consequences to its bioactivity and the occurrence of possible toxicity problems. To bring some light to this subject, in this PhD Thesis, insulin was used as a model of a therapeutic protein and poly(lactic-co-glycolic acid) (PLGA) polymer was used to produce nanoparticles and encapsulate the protein. In the lyophilization of nanoparticles, several sugars were used as protectants, namely two non-reducing sugars, trehalose and sucrose, two reducing sugars, glucose and fructose and one sugar alcohol, sorbitol.

The title of the present Thesis is “Optimization of Lyophilization Parameters of Polymeric Nanoparticles for Delivery of Therapeutic Proteins”. This optimization focused not only in the lyophilization cycle, but also on the formulation and all the parameters involved in the lyophilization of protein-loaded polymeric nanoparticles. Considering all these motivations, the principal aims pursued in the present Thesis were:

- To optimize and characterize the protein-loaded polymeric nanoparticles;
- To assess the effect of cryoprotectants on the porosity and stability of protein-loaded polymeric nanoparticles, after lyophilization;
- To evaluate the stability of protein-loaded polymeric nanoparticles, upon 6 months at different storage conditions;
- To investigate the structural stability of the protein loaded into polymeric nanoparticles, upon lyophilization using cryoprotectants, and storage;
- To propose the co-encapsulation of lyoprotectants as a strategy to better protect the structural stability of proteins loaded into polymeric nanoparticles;
- To optimize the lyophilization cycle, considering the physical-chemical properties of protein-loaded polymeric nanoparticles;
- To assess the effect of different freezing methods on the stability of both the loaded protein, and on the polymeric nanoparticles upon lyophilization using cryoprotectants;
- To evaluate the *in vivo* performance of protein-loaded polymeric nanoparticles;
- To use annealing as a tool to optimize the lyophilization cycle decreasing the lyophilization time;
- To evaluate the effect of annealing in lyophilization and in the stability of protein-loaded polymeric nanoparticles using cryoprotection.

This Thesis is organized in nine chapters. In *Chapter 1* a brief introduction of the PhD project is performed and the main aims and organization of the Thesis are outlined. The *Chapter 2* and *Chapter 3* contain a state of the art overview on the Thesis subject.

The *Chapter 2* provides a review on the polymeric nanoparticles used in the delivery of insulin with a special focus on the oral route, which is a potential administration route of nanoparticles and the most promising approach to improve the quality of life of diabetic patients. This chapter provides many examples of polymers used to encapsulate proteins, which may be subjected to lyophilization and used in other administration routes. In *Chapter 3* it is performed a review on the lyophilization process and on its application in polymeric nanoparticles, with a special regard to protein-loaded polymeric nanoparticles. The optimization and characterization of protein-loaded nanoparticles is described in *Chapter 4*. The effect of cryoprotectants on nanoparticles porosity and stability upon lyophilization is also discussed in this chapter. The *Chapter 5* provides a stability study perspective about the effect of lyophilization using cryoprotectants, on the structure of insulin loaded into polymeric nanoparticles. In *Chapter 6* it is proposed the co-encapsulation of lyoprotectants as a strategy to better protect the protein loaded into nanoparticles. The optimization of the lyophilization cycle and the evaluation of the effect of the freezing step, on the stability of protein-loaded polymeric nanoparticles are described in *Chapter 7*. The *in vivo* performance of nanoparticle formulations is also assessed in this chapter. Further, the *Chapter 8* describes the utility of annealing in the optimization of the lyophilization cycle and the evaluation of its effect on the stability of protein-loaded nanoparticles. Finally, the *Chapter 9* provides the general conclusions of the Thesis and future perspectives of the work.

Chapter 2

Polymeric Nanoparticles for Oral Administration of Insulin

Partially published in:

Pedro Fonte, Francisca Araújo, Salette Reis, Bruno Sarmento, Oral insulin delivery: how far are we?, J Diabetes Sci Technol, 7 (2013) 520-531.

Pedro Fonte, Francisca Araújo, Cátia Silva, Carla Pereira, Salette Reis, Hélder A. Santos, Bruno Sarmento, Polymer-based nanoparticles for oral insulin delivery: Revisited approaches, Biotechnol Adv, 33 (2015) 1342-1354.

1. Introduction

The International Diabetic Federation reported that 366 million people were affected by diabetes in 2011 and estimates that by 2030 this number will raise up to 552 million [11]. Due to its high prevalence and secondary effects, diabetes *mellitus* is one of the most lethal diseases and responsible for almost three million deaths per year worldwide, as reported by the World Health Organization [12]. On average, life expectancy is reduced by more than 20 years in people with type 1 diabetes and by up to 10 years in people with type 2 diabetes [13]. Type 1 and type 2 diabetes are characterized by a progressive decrease of *β*-cell function. The maintenance of blood glucose levels at near-normal levels reduces the risk of long term complications of diabetes. These complications may range from adult blindness, cardiovascular diseases such as heart attacks and strokes, non-traumatic amputation in adults and the possible necessity of renal dialysis due to the diabetic nephropathy [14].

In 1922, the discovery of insulin from dog pancreas was a milestone in the history of diabetes therapy with a Nobel Prize winning, which had a great importance in biomedical research [15]. Indeed, insulin is the most used and effective drug to control diabetes. Intensive insulin in type 1 diabetes patients is able to reduce the risks of nephropathy by 35% to 56%, neuropathy by 60% and retinopathy by 50% to 70% [16-18]. From the time of this discovery, peptides and proteins have been used as biopharmaceuticals due to their advantages such as high activity, specificity and effectiveness comparatively to conventional drugs [19]. However, suitable oral formulations of proteins are still under development, facing countless challenges despite all the efforts, time and money spent on the research [19]. Hence, parenteral delivery remains the most common route for insulin administration [20].

The use of biocompatible and biodegradable nanoparticles has been described as a promising strategy towards oral administration of proteins and peptides [13]. In order to enhance the oral bioavailability of insulin, as well as to provide a stable and biocompatible environment to the encapsulated drug, polymeric nanoparticles have been claimed to be the perfect candidates for the oral delivery of insulin [21].

In this chapter, the benefits and drawbacks on the oral insulin delivery as well as the different pathways of insulin-loaded nanoparticles uptake through intestinal epithelium will be discussed. The different polymeric nanoparticles developed for delivery of insulin orally developed so far will be presented. In addition, it will be reviewed the efforts of the pharmaceutical industry to develop an insulin oral delivery system and the toxicity concerns about the use of polymer-based nanoparticles

2. Benefits and drawbacks on oral insulin delivery

Despite all the successes achieved after insulin discovery, diabetes therapy tends to fail in long-lasting treatments, followed by a number of side-effects. Thus, more than a few improvements are urgently needed, especially regarding the administration of insulin. On one hand, parenteral delivery of insulin is hindered by the lack of patient compliance to treatment due to the uncomfortable use of injections with needles. On the other hand, oral administration is the most accepted delivery route due to its convenience, painless and easy for self-medication. Based on efficacy and toxicity, it is possible to tune the dosing schedule of insulin to the responses of individual patients [22]. Moreover, the oral route mimics the endogenous pathway of insulin after secretion, as it suffers the first pass to the liver instead of going to the systemic bloodstream [19, 20]. Owing to its role in blood glucose level control, the liver is the first and foremost important target of pancreas-secreted insulin [23]. Indeed, only a small amount (approximately 20%) of subcutaneously administered insulin reaches the liver [24]. The reproduction as faithful as possible of the physiological mechanisms of glucose metabolism, allows the control and/or decrease of the side effects that are commonly described by patients under insulin therapy. Encountered first in the liver, insulin levels are reduced in systemic circulation, which minimizes the risk of hypoglycemia episodes, immune responses as well as insulin resistance in type 2 diabetic patients [23]. Other problems such as allergic reactions, lipodystrophy around the injection site and risk of infectious diseases transmission, can also be avoided with oral administration of insulin [13]. Finally, the oral route is more cost-effective since there is no need of specialized people for the administration, decreasing the number of visits to the hospital and avoiding costs in injection materials [25].

However, the path is not straightforward and achieving an effective oral formulation for delivery of insulin is still a goal to pursue. Along the gastrointestinal tract there are several barriers that must be overcome to increase the bioavailability of insulin. For instance, the harsh pH conditions in the stomach, the enzymatic activity, the presence of mucus and the poor permeability across the intestinal epithelium are the main concerns for the activity and effectiveness of the protein [13, 20, 26]. Besides the physiological features of the gastrointestinal tract, also a better knowledge of the differences between animal models and humans would guarantee a more reliable extrapolation of the results obtained from preclinical to clinical studies, as well as a better understanding of how diet, fasting states, patient-to-patient variability and disease states affect the protein absorption [25, 27, 28].

3. Mechanisms of the intestinal uptake of polymeric nanoparticles

Regardless of the protection of insulin by nanoparticles from the hostile conditions of the gastrointestinal tract, the transport across the intestinal epithelium still remains a barrier to overcome. As a gatekeeper, the epithelium acts by thwarting proteins from being absorbed, making it the major restrictive barrier to the nanoparticles passage from the lumen to the *lamina propria* [25]. The epithelial cells maintain this protection because of the tight junctions between adjacent cells [29]. Thus, the transport and the absorption mechanism may be either paracellular (between the cells) or transcellular (through the cells), and are mainly regulated by the characteristics of the mucosa and by the physicochemical properties of the nanoparticles such as size, charge and lipophilicity [30, 31]. The Figure 2.1 shows the pathways for insulin nanoparticle translocation through the intestinal epithelium.

It is commonly accepted that due to the features of the paracellular route, which has a small surface area (less than 1% of the total intestine) and a limited space owing to the tightness of the junctions between cells (3 and 10 Å of diameter), this is not the most common mechanism of nanoparticles uptake [22, 23, 30]. However, it has been described that some natural polymers used in nanoparticles composition such as chitosan, may reversibly affect the tight junctions opening by mechanisms that are still not very well understood. For instance, some materials may act on the tight junctions inducing a structural reorganization of their proteins and others may modulate tight junctions by chelating calcium and inducing their disruption [22, 32-37]. The transcellular transport is thus the most probable mechanism of nanoparticles absorption [38]. This transport pathway may be divided into different endocytic mechanisms: phagocytosis, macropinocytosis, clathrin-mediated endocytosis and caveole-mediated endocytosis, which are adenosine triphosphate (ATP) dependents, and clathrin- and caveolae-independent endocytosis, which are not ATP dependents. These uptake mechanisms occur at the apical cell membrane, where nanoparticles are taken-up, and then the transport occurs through cells within vesicles, releasing their contents at the basolateral pole [26].

In the epithelial cells, phagocytosis is restricted to M cells, which is a receptor-mediated process where the cellular membrane projects itself to engulf nanoparticles [26, 30]. M cells have several properties that favor the transport of nanoparticles such as lack of mucus secretion, a scant glycocalyx and reduced proteases, making the transport through M cells higher than the transport through enterocytes [30, 39]. However, since M cells are part of the immune Peyer's patches, it may stimulate the immune responses

compromising further the nanoparticles administration [25]. Similar to phagocytosis, also macropinocytosis is an actin-dependent process capable of engulf large volumes of fluid containing nanoparticles; however, this is not restricted to a cellular type and it is non-specific receptor mediated. The vesicles may have a large size (between 0.15–5 µm) and after formed, they fuse with the early endosomes [40]. Clathrin-mediated endocytosis, in turn, is a receptor-mediated uptake where the cellular membrane forms pits originating small vesicles coated by proteins (mainly clathrin protein), which also fuse with early endosomes. One strategy to enhance the nanoparticles uptake by the intestinal cells is to conjugate ligands to nanoparticles surface that would facilitate cell–nanoparticle interactions and enhance the nanoparticles internalization [41]. Bacterial adhesins, lectins, monoclonal antibodies and specific amino acid sequences are some examples of ligands that can be found in more detail elsewhere [30, 42]. Finally, caveole-mediated endocytosis is a non-specific uptake process where small caveolae-coated vesicles (50-80 nm) can escape from the endolysosomes and lead to direct exocytosis. However, the small size of the vesicles makes this a non-probable route of nanoparticles uptake [22, 40].

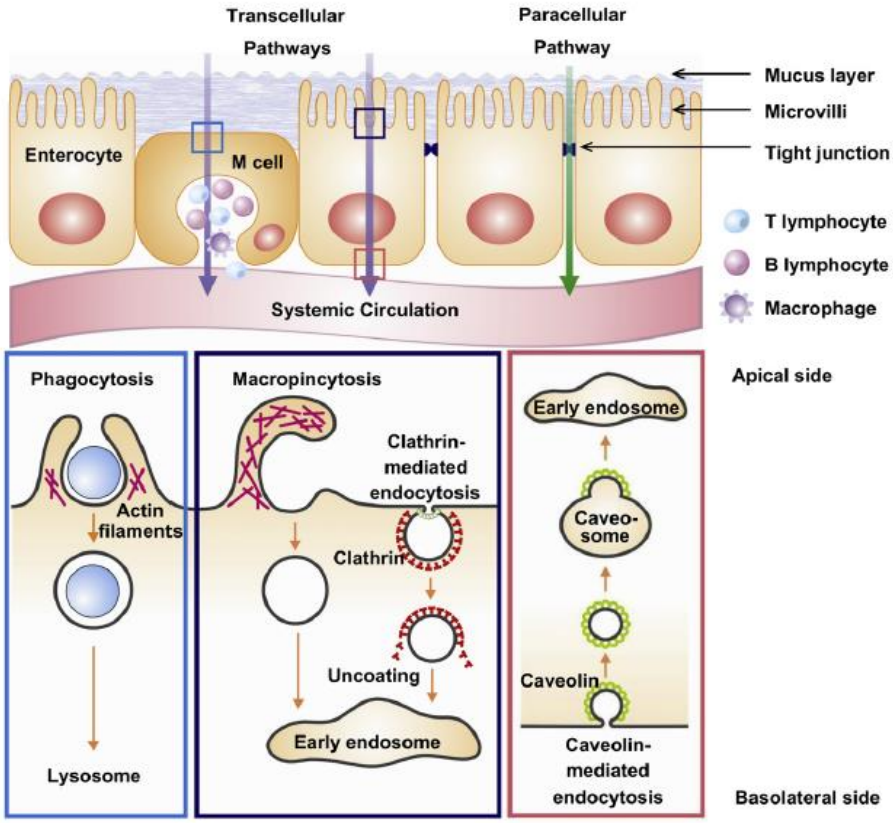

Figure 2.1. Pathways for insulin nanoparticle translocation through the intestinal epithelium. Schematic focus on phagocytosis, macro-pinocytosis, and caveolin-mediated endocytosis. *Reprinted with permission from* [26].

4. Polymer-based delivery systems for oral administration of insulin

In the nanotechnology field, nanoparticles may be subcategorized into nanospheres and nanocapsules. In nanospheres, insulin is dispersed in the nanoparticles matrix, whereas in nanocapsules, insulin is retained in a compartment surrounded by a polymer membrane [43]. Different methods and technologies may be used to prepare these nanoparticle types, so the best production protocol needs to be inferred regarding the polymer nature and also insulin stability. Indeed, the majority of the production protocols use heat, sonication, strong agitation and organic solvents, which may damage the insulin structure.

Polymer science has increased in the last decades with better understanding of polymers backbones and possible modifications of their structure. In addition, also the drug delivery field has evolved in developing new and improved polymer-based drug delivery systems. Due to the amount of different existing polymeric materials, the physicochemical properties of nanoparticles such as charge and association efficiency (AE), can be modulated and nanoparticles can be tailored to retain insulin stability, increase its bioavailability, control the release profiles, stabilize the systems and modulate the biological behavior [13, 44]. Overall, polymers may be from natural or synthetic sources, and can be used individually or together [21].

In this section, the focus goes to the most commonly natural and synthetic polymers used to produce nanoparticles for oral delivery of insulin. Thus, chitosan, dextran, alginate, poly(γ-glutamic acid) (γ-PGA) and hyaluronic acid as natural polymers, and polylactic acid (PLA), PLGA, poly(ε-caprolactone) (PCL), acrylic polymers and polyallylamine as synthetic polymers are used to encapsulate insulin for oral delivery, and will be briefly discussed in this section. Additionally to the properties of the different polymer-based nanoparticles, they may be modified to increase the interactions with the intestinal mucosa, for example, by modifying its surface by adsorption or grafting of hydrophilic molecules conferring mucoadhesion (e.g., chitosan) or hydrophilicity (e.g. polyethylene glycol (PEG)). The nanoparticles surface may be also modified for targeting purposes by grafting ligands such as peptides, glycoproteins or antibodies [27], carbohydrates (e.g., decanoic acid) [45], and vitamins (e.g., vitamin B12) [46, 47].

Formulations of nanoparticles may also contain excipients such as enzyme inhibitors and absorption enhancers, which may help on preserving insulin stability and promote its absorption through the intestinal epithelium, respectively [3]. Duck and chicken ovomucoid, leupeptin and sodium cholate are used as enzyme inhibitors due to their ability to avoid insulin degradation [48, 49]. Regarding the absorption enhancers,

bile salts [50], ethylenediaminetetraacetic acid [51], surfactants and *zonula occludens* toxin [52], as well as cell-penetrating peptides such as l-penetratin [53] and octarginine R8 [54], have been used to promote insulin absorption through the intestinal epithelium.

4.1. Chitosan nanoparticles

Among the natural polymers, polysaccharides have particular interest in the oral delivery of insulin, because they are biocompatible, biodegradable, non-toxic and hydrophilic. From these polymers, chitosan is by far the most widely used for the delivery of insulin. Chitosan is a mucoadhesive polycationic polymer composed by N-acetyl-D-glucosamine and D-glucosamine and it is produced by the alkaline deacetylation of chitin [55-57]. Together with tripolyphosphate (TPP) or even just polyelectrolyte complexation with insulin are the most common methods to produce chitosan nanoparticles. The interaction of chitosan and polyanions leads to a spontaneous formation of nanoparticles with high AE in an aqueous media in mild conditions, with no need for using organic solvents or heat, avoiding cytotoxicity concerns and threats to insulin stability, thus being the main advantages of these carriers [37, 58].

Pan *et al*. showed that chitosan when structured in nanoparticles is able to enhance the intestinal absorption of insulin comparing to chitosan in solution, with an AE up to 80% [59]. The release profile of insulin presented a great initial burst with pH-sensitivity and when administered *in vivo*, insulin-loaded chitosan nanoparticles had a hypoglycemia effect for 15 h with higher bioavailability of insulin, up to 14.9%, in comparison with the subcutaneous administration of insulin [59]. Another study conducted by Mukhopadhyay *et al.* showed an average AE of insulin with self-assembled chitosan nanoparticles of approximately 85%. The nanoparticles retained insulin efficiently in simulated gastric conditions with significant amount of insulin released in simulated intestinal conditions. When administered *in vivo*, insulin-loaded nanoparticles were effective in dropping the blood glucose level [60].

Despite promising results, other studies were performed showing that chitosan nanoparticles are greatly influenced by the pH of the formulations, either in the AE of insulin or in its release profile [61-63]. Chitosan dissolves easily in acidic conditions due to its basic nature (pKa ≈ 6.5), compromising the protection of insulin from the harsh gastric conditions [64]. In order to overcome this issue, a combination of chitosan with other polymers, peptides and other chitosan derivatives emerged as possible solutions to achieve high insulin bioavailability at the intestinal level. Makhlof *et al.* formulated chitosan nanoparticles with hydroxypropyl methylcellulose phthalate (HPMCP), a pH-sensitive polymer, by ionic cross-linking [58]. HPMCP pKa is approximately 5.2, which

makes the polymer only soluble at high pH-values, thus protecting insulin from the harsh conditions of the stomach. As expected, chitosan/HPMCP nanoparticles revealed a superior acid stability with a significant control over insulin release. After oral administration, the hypoglycemic effect conferred by the insulin-loaded chitosan/HPMCP nanoparticles increased by more than 9.8 and 2.8 folds as compared to an oral insulin solution and insulin-loaded chitosan/TPP nanoparticles, respectively [58]. Due to the backbone features of chitosan with free amino and hydroxyl groups, it is also possible the substitution or modification with different chemicals to achieve desired properties for oral drug delivery [44].

In this context, *N*-trimethyl chitosan (TMC) chloride is the most used chitosan derivative. It is a partially quaternized derivative of chitosan, which is soluble under neutral and basic conditions [64]. Similar to chitosan, TMC has mucoadhesive properties and acts as an absorption enhancer (it has been showed a pronounced reduction in the transepithelial electrical resistance in Caco-2 cell monolayers) but, in contrast with chitosan, TMC plays an important role, especially in neutral environments where chitosan is ineffective as an absorption enhancer [64]. The synthesis of TMC without O-methylation is important to obtain good enhancing permeation properties [65]. Sandri *et al.* performed a study in which it was evaluated the penetration enhancement properties of insulin-loaded chitosan and TMC nanoparticles. The *in vitro* studies using a Caco-2 cell monolayer, evaluated the effect of nanoparticles in the enhancement of insulin uptake and it was verified the same enhancement effect for both chitosan and TMC nanoparticles, but this enhancement occurred respectively through different mechanisms, opening of the tight junctions and endocytosis [66]. Furthermore, the *ex vivo* studies showed the important role of the mucus layer, where the chitosan and TMC nanoparticles were more efficient towards jejunum tissue (pH 6–6.5) due to their high mucoadhesive potential. As referred above, the modification of nanoparticles with specific ligands increases their cellular uptake. Jin *et al.* used TMC nanoparticles modified with the targeting peptide C-Src tyrosine kinase (CSK) and proved that the uptake of nanoparticles and the permeation of drugs across the epithelium were higher when they were conjugated with the peptide, which induced a significantly higher internalization of drugs via clathrin- and caveolae-mediated endocytosis on goblet cell-like HT29-MTX cells [67]. Also, in co-culture models of Caco-2/HT29-MTX the CSK peptide modification showed higher transport for peptide conjugated nanoparticles. Regarding the pharmacological and pharmacokinetic studies *in vivo* using diabetic rats, the CSK-nanoparticles improved the hypoglycemic effect with a 1.5-fold higher relative bioavailability compared with unmodified nanoparticles [67].

Besides TMC, other quaternized chitosan derivatives such as diethylmethyl chitosan (DEMC), triethyl chitosan (TEC) and dimethylethyl chitosan (DMEC), were developed aiming to the successful delivery of proteins and peptides at neutral or weakly alkaline pH in the small intestine [68-71]. When evaluating these three systems for the oral delivery of insulin, it was possible to observe that the AE of insulin was 70% for TMC and DEMC, and 90% for TEC and DMEC. TEC and DMEC nanoparticles presented a 5 h sustained release with minimum burst release effect at the initial hours in phosphate buffered saline (PBS) without significant differences for pH 6.8 and 7.4, which was a higher insulin release than chitosan nanoparticles, and more sustained when compared to the *ex vivo* studies. Similar to what happened in the *in vitro* and *ex vivo* experiments; in the *in vivo* experiments the modified chitosan nanoparticles presented enhanced colonic absorption of insulin in comparison with an insulin solution or insulin-loaded chitosan nanoparticles [68-70].

TMC-cysteine conjugate (TMC-Cys) was synthesized in an attempt to combine the mucoadhesion and the permeation enhancing effects of TMC and thiolated polymers. TMC-Cys with several molecular weights and quaternization degrees were allowed to form polyelectrolyte nanoparticles with insulin through self-assembly. These nanoparticles presented high AE of insulin and presented a 2.1- to 4.7-fold increase in mucoadhesion compared to TMC nanoparticles. Moreover, compared to a insulin solution and TMC nanoparticles, TMC-Cys nanoparticles promoted Caco-2 cell internalization by 7.5–12.7 and 1.7–3.0 folds, inducing an insulin uptake increase in the rat intestine by 3.3–11.7 and 1.7–2.6 folds, and augmented uptake in Peyer's patches by 14.7–20.9 and 1.7–5.0 folds, respectively. Insulin-loaded TMC-Cys nanoparticles showed also significant decrease in the blood glucose levels after oral and ileal administration (Figure 2.2). In addition, the biocompatibility assessment revealed lack of toxicity of TMC-Cys nanoparticles [72].

A chitosan derivative with lauryl group substituted succinic anhydride via an amide link formation between the carboxyl group and the amine group in the chitosan, lauryl chitosan (LCS), was developed by Recka *et al.* [73]. This study showed an inhibitory effect by the succinyl carboxyl groups on the release kinetics of insulin at pH 1.2 and also showed that the hydrophobic moieties of LCS were able to control the release of insulin at the intestinal pH. Moreover, the LCS nanoparticles were capable of reducing blood glucose levels in diabetic rats for 6 h. This system proved to be better not only in the release profiles, but also at the permeability of insulin compared to unmodified chitosan nanoparticles [73]. Another study carried out by Elsayed *et al.* showed that LCS nanoparticles were stable in simulated gastric fluids protecting insulin from the gastrointestinal tract barriers [74]. Additionally, the *in vivo* results clearly indicated that

insulin-loaded nanoparticles could effectively reduce the blood glucose levels in a diabetic rat model. Nevertheless, additional modifications in the insulin formulation are still required to improve the oral bioavailability of insulin.

Other studies combining chitosan with arabic gum [75, 76], *N,O*-carboxymethyl chitosan [77], cationic β-cyclodextrin polymers [78, 79] have also been conducted, and were reviewed in more detail by Mukhopadhyay *et al*. [80] and Chen *et al.* [81].

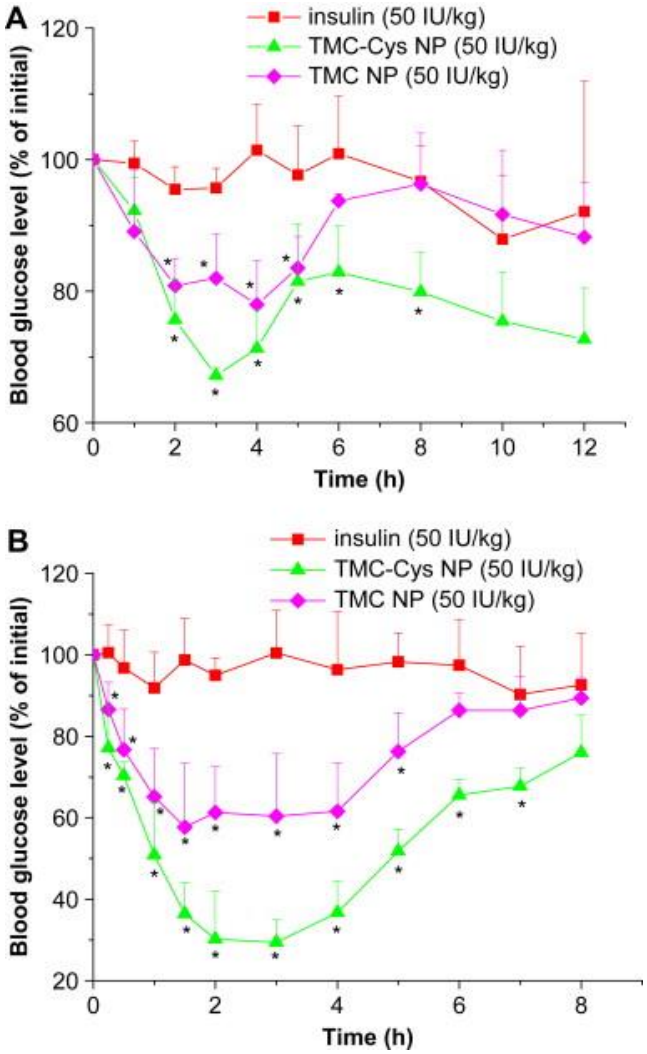

Figure 2.2. Blood glucose levels in rats after oral (A) and ileal (B) administration of TMC and TMC-Cys nanoparticles (50 IU/kg). Mean ± standard deviation (SD) (n = 4). Significant difference from insulin solution: $p < 0.05$. NP stands for nanoparticles. *Reprinted with permission from* [72].

4.2. Dextran nanoparticles

Dextran is a polysaccharide composed by α-D-glucose units that bind to each other through glycosidic bonds. Similar to chitosan, dextran is also used in biomedicine as a constituent of nanoparticles for insulin delivery. Chalasani *et al.* prepared

nanoparticles by an emulsion method using different dextran molecular weights. The nanoparticles surface was then modified and conjugated with vitamin B12, a specific target ligand. The AE was between 45 and 70% and from that, 65 to 83% of insulin was protected against gut proteases. Moreover, the *in vitro* release experiments showed a burst, followed by a controlled release step, up to 95% within 48 h. Regarding the *in vivo* tests, after 5 h of oral administration (20 IU/kg), the plasma glucose levels decreased 70 to 75% reaching basal levels in 8-10 h and this effect was prolonged for 54 h. According to their results, the pharmacological availability (PA) of vitamin B12-conjugated nanoparticles was significantly higher than for the nanoparticles without conjugation, which was 29.4% higher compared to the subcutaneous injection of insulin [46, 47]. This insulin carrier based on vitamin B12-conjugated nanoparticles is further addressed in Section 5 of this chapter.

In another study, dextran sulfate was complexed with chitosan in aqueous media to obtain insulin-loaded nanoparticles. This system was able to retain insulin in simulated gastric medium, and sustained the release of insulin up to 24 h in simulated intestinal medium [82]. Moreover, these nanoparticles were able to reduce the basal serum glucose levels in approximately 35% in diabetic rats for more than 24 h. For doses of 50 and 100 IU/kg, the PA of insulin was 5.6 and 3.4%, respectively, which was a significant increase compared to the administration of oral insulin solution (1.6%) [83].

4.3. Alginate nanoparticles

Alginate is an anionic polysaccharide of (1–4)-linked β-D-mannuronic acid (M) and a-L-guluronic acid (G); these G residues, with divalent ions, have gelling properties that allow the formation of nanoparticles [84]. Moreover, in contrast to chitosan, alginate is soluble in high pH and insoluble in low pH [44]. Sarmento *et al.* showed that alginate/chitosan polyelectrolyte complexes after optimization formed nanoparticles with high AE (92%) and loading degrees (14.3%), which were able to preserve the secondary structure of insulin, essential to its bioactivity [85, 86]. Moreover, the nanoparticles retained approximately 50% of the protein in gastric pH conditions for 24 h while in intestinal pH environment the release was more extensive, around 75% [84]. When orally administered, insulin-loaded nanoparticles decreased the glucose levels of serum by more than 40%, sustaining the hypoglycemia for more than 18 h. For doses of 50 and 100 IU/kg, the pharmacological bioavailability of insulin was 6.8 and 3.4%, respectively. These values represent a significant increase of more than 1.6% when compared to solutions of oral insulin alone, and are over other related studies at the same dose levels [86].

Woitiski *et al*. produced nanoparticles formed by alginate and dextran sulfate that nucleated around calcium and bond to poloxamer, stabilized by chitosan, and subsequently coated with albumin [87, 88]. Albumin was applied to nanoparticles as the outermost coat, in order to protect insulin through shielding from proteolytic degradation. The effect of this albumin layering on insulin permeation was compared with albumin-free nanoparticles that mimic the action of albumin being enzymatically removed during gastric and intestinal transport. The results showed that albumin layering was important toward improving insulin uptake across the intestinal membrane, possibly by stabilizing insulin in the intestinal conditions. Moreover, insulin permeation through different intestinal *in vitro* and *ex vivo* models was also studied. For the gold-standard Caco-2 cell monolayer, the permeation of insulin loaded into the nanoparticles was enhanced 2.1-fold comparatively to insulin in solution, 3.7-fold for the mucus-secreting Caco-2:HT29 co-culture and 3.9-fold for excised intestinal mucosa of Wistar rats [88]. Regarding the *in vivo* studies, insulin-loaded nanoparticles proved to reduce plasma glucose levels to 40% of the basal values, with a sustained hypoglycemic effect over 24 h. Moreover, in an administered dose of 50 IU/kg, nanoencapsulated insulin had a bioavailability of 13% which was a 3.0-fold increase in comparison to an insulin solution. Confocal microscopy studies were also performed, showing internalization of nanoencapsulated insulin in the small intestinal mucosa [87]. The same group also studied the histopathological effects of nanoparticles administration, by analysing organs and tissues of diabetic rats dosed daily for 15 days with insulin nanoparticles. The results showed that no morphological or pathological alterations were observed in rat liver, spleen, pancreas, kidney or intestinal sections [89].

4.4. Poly(γ-glutamic acid) nanoparticles

Lin *et al*. developed γ-PGA and chitosan nanoparticles prepared by an ionic-gelation method. γ-PGA is a biodegradable, water-soluble anionic peptide, originated from the members of genus Bacillus [90]. After nanoparticles loading, the release profiles of insulin were significantly affected by the pH environment, being the highest amount of insulin released at pH 7.4. However, despite of the nanoparticles remained intact between pH 2.0–7.2, at lower pH they disintegrated, compromising insulin protection in the gastric acidic pH environment. Moreover, at pH 7.4, chitosan was deprotonated making the nanoparticles unstable, which lead to their disintegration. This also affected the ability of the formulation to open tight junctions, and thus, to increase insulin uptake. Nevertheless, the *in vivo* results clearly indicated that the administration of insulin-loaded nanoparticles in a dose of 15 IU/kg of insulin could effectively reduce the blood glucose

levels in a diabetic rat model, being this effect more pronounced when it was administered higher doses of insulin (30 IU/kg). The hypoglycemic effect lasted for 10 h. Due to the short effective time and to the pH sensitivity of the system, the same group improved it by lyophilizing the nanoparticles and delivering them within an enteric-coated capsule [91]. This process did not affect the activity of loaded insulin, which kept its secondary structure and its release remained pH-dependent. The enteric-coated capsule did not dissolve in the acidic environment of the stomach, crumbling in the high intestinal pH where it freed the insulin-loaded nanoparticles. As all the encapsulated nanoparticles reached the intestine, the intestinal absorption of insulin was enhanced and the reduction of blood glucose levels was prolonged, with 20% of insulin bioavailability observed [91]. Another study conducted by the same research group, presented a pH-responsive multi-ion-crosslinked nanoparticles, prepared from γ-PGA and chitosan with TPP and $MgSO_4$ [92]. These nanoparticles showed stability in the ionically cross-linked network structure for 10 weeks suspended in deionized water and over a wide pH range of 1.2-7.4. When orally administered to diabetic rats, the nanoparticles demonstrated a hypoglycemic action for at least 10 h, with a bioavailability of 15.1 ± 0.9%. The toxicity studies showed that even at a dose 18 times higher than the one tested, the nanoparticles were well tolerated and not presented any toxicity [93].

Diethylene triamine pentaacetic acid (DTPA) is known for disrupting the intestinal tight junctions and inhibiting the intestinal proteases by chelating divalent metal ions. Su and Lin conjugated DTPA with chitosan/γPGA nanoparticles (chitosan/γPGA-DTPA), a pH-sensitive system that disintegrated at pH above 7.0, producing a transient and reversible enhancement of paracellular permeability which increased the insulin uptake, producing a prolonged reduction of blood glucose levels [94]. When administered orally in an enteric-coated capsule, the system presented a maximum insulin concentration at 4 h after treatment with a relative oral bioavailability of insulin of about 20%.

4.5. Hyaluronic acid nanoparticles

Hyaluronic acid is an anionic non-sulfated glycosaminoglycan natural polymer, used as carrier for the administration of insulin. Han and Zhao prepared insulin-loaded hyaluronic acid nanoparticles by the reverse-emulsion freeze-drying method [95]. The nanoparticles showed high insulin AE of about 95%. Due to the pH sensitivity of hyaluronic acid nanoparticles, the system was able to protect insulin from the low pH of the stomach. The results of the uptake experiments showed more than 2.0-fold increase in the apparent permeability coefficient comparatively to insulin in solution, and the main uptake mechanism of insulin was through active transport. The *ex vivo* experiments

showed that the hyaluronic acid nanoparticles significantly enhanced insulin uptake through the duodenum and ileum. When orally administered, hyaluronic acid nanoparticles also showed stronger hypoglycemic effects than insulin in solution (Figure 2.3).

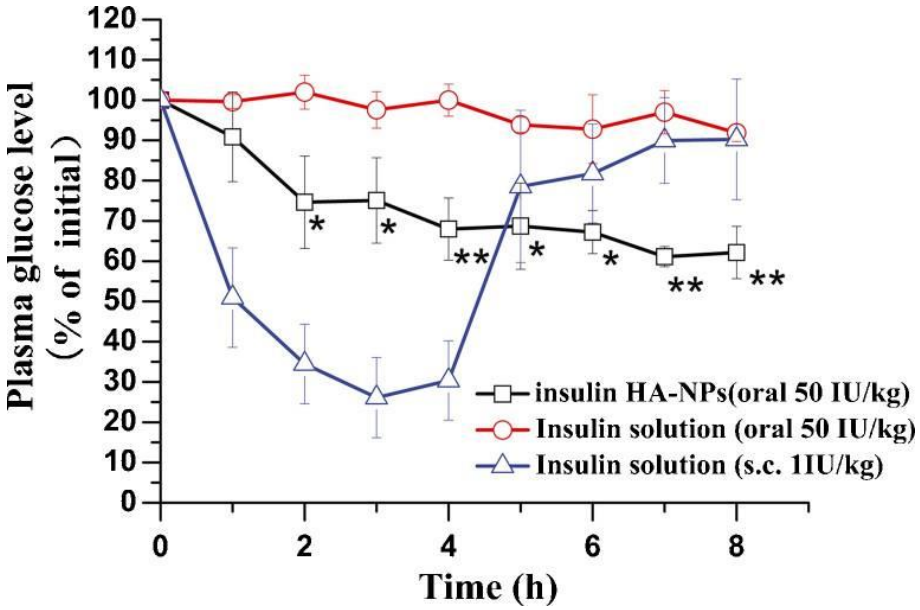

Figure 2.3. Blood glucose levels after oral administration of insulin-loaded hyaluronic acid nanoparticles (50 IU/kg, squares) and insulin solution (50 IU/kg, circles); and subcutaneous administration of insulin solution (1 IU/kg, triangles) to diabetic rats. Statistically significant difference were observed for insulin-loaded hyaluronic acid nanoparticles comparatively to insulin solution (*p < 0.05; **p < 0.01). Mean ± SD (n = 6). HA and NPs stands for hyaluronic acid and nanoparticles, respectively. *Reprinted with permission from* [95].

4.6. Polylactic acid nanoparticles

PLA is an aliphatic polyester polymer considered biodegradable and biocompatible due to its hydrolysis into monomeric units in the body. Xiong *et al.* developed PLA-*b*-pluronic-*b*-PLA (PLA-F127-PLA) vesicles intended to deliver insulin orally [96]. The *in vitro* release study showed a biphasic release profile of insulin from the PLA-F127-PLA vesicles. The pluronic block copolymer showed a high permeability profile of insulin across the cell membrane, due to its amphiphilic properties and strong affinity to the small intestine caused by its polyethylene oxide (PEO) blocks. Insulin-loaded PLA vesicles were orally administered to diabetic mice (50 IU/kg), and the blood glucose concentration decreased from 18.5 to 5.3 mmol/L in the first 4.5 h, reaching the lowest blood glucose concentration of 4.5 mmol/L after about 5 h. The same level of blood glucose concentration was maintained for more about 18.5 h. These results

showed the potential of insulin-loaded PLA-F127-PLA vesicles to be administered orally, due to its prolonged hypoglycemic effect. In a more recent study from the same group, PLA-*b*-pluronic-*b*-PLA (PLA-P85-PLA) vesicles were produced for the same purpose, obtaining a mean diameter of 178 nm [97]. The biocompatibility of the obtained vesicles was proved in cytotoxicity studies using human ovarian cancer cells OVCAR-3. *In vitro* and *in vivo* release studies revealed that insulin was sustainably released, and almost completely after 7.5 h of its administration. The oral administration of insulin-loaded PLA-P85-PLA vesicles (200 IU/kg) in diabetic mice showed that the blood glucose levels were reduced, reaching its minimum (15% of the initial blood glucose level) 2.5 h after the administration. Upon 10.5 h, the blood glucose levels increased gradually up to 31.8% of the initial blood glucose concentration, keeping the same level for more 14 h.

4.7. Poly(lactic-co-glycolic acid) nanoparticles

PLGA an aliphatic polyester co-polymer is one of the most used synthetic polymers to produce nanoparticles for the oral delivery of insulin, mainly due to its biodegradability and biocompatibility properties as well as sustained release profiles. In fact, PLGA allows the production of versatile nanoparticles since it may be combined to other polymers or coated with different ligands, attributing to nanoparticles important features that may enhance the uptake of loaded drugs [98]. The ability of insulin-loaded PLGA nanoparticles to permeate across Caco-2 cell monolayer models, was demonstrated with nanoparticles produced by a double emulsion solvent evaporation technique, achieving an AE above 80%, and it was observed a profile of insulin absorption based on clathrin-mediated endocytosis in a time-dependant manner [99]. After intraduodenal administration to diabetic rats, the nanoparticles remained stable in the intestine for a period necessary to allow its uptake, and delivery of insulin into the bloodstream. The *in vivo* hypoglycemic effect was very similar to long-acting insulin. In another study, insulin was encapsulated into PLGA nanoparticles also using the double emulsion solvent evaporation technique [100], and it was found that insulin was released in a lower rate in pH 1.0 reaching about 90% of release in 11 days. On contrary, at pH 7.8 the release was faster, since about 90% of the total amount of insulin was released in 3 days. The developed carriers were further administered orally to diabetic rats, and it was observed that blood glucose levels decreased while insulin levels in the blood increased. These results showed clearly the sustained release properties of PLGA nanoparticles, and its ability to protect insulin and consequently decrease the blood glucose levels upon oral administration. Indeed, the release profile of insulin from PLGA nanoparticles was characterized by a first burst release, followed by a sustained release

profile overtime [101]. The initial burst release may be mitigated by the combination of PLGA and β-cyclodextrin in nanoparticles production, which allows prolonging the effect of insulin for a longer period of time [102].

The encapsulation of hydrophilic insulin into the hydrophobic PLGA matrix may be challenging, thus different strategies may be used to improve the liposolubility of insulin as well as its loading efficiency. For instance, the complexation of insulin with lipophilic substances is one of these strategies. An insulin-phospholipid complex made by soybean phosphatidylcholine was produced to improve insulin liposolubility and increase its loading efficiency when encapsulated into PLGA nanoparticles [103]. The optimized formulation achieved an AE of about 90%, and the *in vitro* release study of insulin demonstrated an initial burst release at pH 1.2 with further slower release at pH 6.8. Insulin complex-loaded PLGA nanoparticles (20 IU/kg) were further administered orally to diabetic rats and it was observed a decrease of fasting plasma glucose levels to about 57% in the first 8 h, which was prolonged for another more 12 h. It was also observed that insulin loaded into nanoparticles had 7.7% of oral bioavailability comparatively to the subcutaneous administration. In another study, a complex of insulin and sodium oleate, was loaded into PLGA nanoparticles by an emulsion solvent diffusion method [104]. After optimization of the formulation, it was obtained an AE of insulin of about 91%. Insulin:sodium oleate-loaded PLGA nanoparticles (20 IU/kg) were further administered orally to diabetic rats, and 12 h after the administration it was observed a decrease on the plasma glucose levels to about 23.9% of the initial insulin, which was also prolonged for 24 h.

As stated above, one of the main issues in the oral delivery of insulin is the acid environment in the stomach and the action of proteolytic enzymes in the gastrointestinal tract. Thus, different strategies have been developed to mitigate their influence. Previously, it was proposed two types of nanocarriers made of a blend of PLGA and two polyoxyethylene derivatives, poloxamer (Pluronic F68) and poloxamine (Tetronic T904) for insulin oral delivery [105]. The stability of unloaded nanoparticles was assessed in gastric and intestinal fluids, and it was observed a strong interaction of unblended PLGA nanoparticles and digestive enzymes, whereas such interaction was mitigated by the blended formulations. *In vitro* results showed that insulin-loaded PLGA:Pluronic F68 nanoparticles were able to avoid the gastrointestinal barrier. However, despite these positive results, *in vivo* studies are still needed to confirm these findings. Another creative strategy was to encapsulate both insulin and an antacid into PLGA nanoparticles [106]. Magnesium hydroxide or zinc carbonate at 2% were used as antacids, and the AE of insulin ranged between 81% and 85%, respectively. Using Fourier transform infrared spectroscopy (FTIR), circular dichroism (CD) and fluorescence

spectroscopy it was observed that the structural stability of insulin was maintained after formulation. Upon oral administration of insulin:antacid-loaded PLGA nanoparticles in healthy rats, the oral bioavailability of insulin increased 6-fold comparatively to an insulin solution. After administration to diabetic rats (120 IU/kg), the blood glucose levels decreased similarly to a 20 IU/kg subcutaneous administration of insulin. Despite these good results, the oral dose of insulin was significantly higher than the subcutaneous insulin in order to reach the same hypoglycemic effects, which from a cost-benefit point of view is less attractive.

Another important strategy to overcome the harsh environment of the stomach is to use enteric coating materials. Thus, the prevention of insulin burst release in the stomach has been achieved by using HPMCP to produce PLGA/HPMCP nanoparticles to deliver insulin orally [107]. This pH-sensitive polymer was used as an enteric coating able to deliver insulin specifically to the small intestine. Insulin AE into the produced nanoparticles was about 65%, whereas insulin loaded into PLGA nanoparticles had an AE of about 50%. The *in vitro* release of insulin in simulated gastric fluid revealed that PLGA/HPMCP nanoparticles mitigated the initial burst release profile, characteristic of PLGA nanoparticles with about 20% release of insulin in the first hour, whereas PLGA nanoparticles released 50% of insulin in the same period. The relative bioavailability of insulin-loaded PLGA/HPMCP nanoparticles and insulin-loaded PLGA nanoparticles, comparatively to subcutaneous insulin (1 IU/kg) in diabetic rats was about 6.3% and 3.7%, respectively. These results showed the potential of PLGA/HPMCP nanoparticles to deliver insulin orally. Wu *et al.* produced also insulin-loaded PLGA/HPMCP nanoparticles by a modified multiple emulsion solvent evaporation method, achieving an insulin AE of 94% [108]. It was also observed the release of insulin in a pH dependent manner at simulated gastrointestinal conditions. After oral administration to diabetic rats (50 IU/kg), the blood glucose levels decreased with a maximal effect between 1 and 8 h. Comparatively to the subcutaneous injections (5 IU/kg), the relative bioavailability was about 11.3%, which could be explained by the burst release of insulin in the upper intestine. The same research group, developed a two-stage delivery system based on a enteric capsule coated by the pH-sensitive HPMCP, able to selectively release insulin loaded into PLGA nanoparticles in the intestine [109]. Eudragit® RS was also used on PLGA nanoparticles production to increase the uptake of insulin across the intestinal mucosa, due to its enhanced mucoadhesive properties. The optimized nanoparticles were produced by a multiple emulsion solvent evaporation method achieving a zeta potential of +42 mV and an AE of about 74%, and the *in vitro* studies showed that the burst release of insulin was greatly reduced at pH 1.2. The capsule containing insulin-loaded PLGA/Eudragit® RS nanoparticles was further administered to diabetic rats

inducing a prolonged reduction on blood glucose levels, and the PA of insulin was about 9.2%.

The modification of PLGA nanoparticles surface is also a good strategy to improve its properties, and its ability to enhance the uptake of insulin across the intestinal membrane. Indeed, the negative charge of PLGA nanoparticles may decrease the oral bioavailability of insulin, thus insulin-loaded PLGA nanoparticles can be coated with cationic chitosan to overcome this issue. In this context, Zhang *et al*. prepared chitosan-coated PLGA nanoparticles and demonstrated their higher bioadhesive properties when delivered orally, comparatively to uncoated PLGA nanoparticles, and also a higher relative pharmacological bioavailability of insulin comparatively to an insulin solution [110]. These results clearly showed the importance of the mucoadhesive properties of chitosan. In another work, nanoparticles made of PLGA and poly(fumaric-co-sebacic anhydride) were produced and administered orally to rats, achieving a pharmacological bioavailability of insulin of 11% [111]. The polyanhydride compound was considered essential due to its bioadhesive properties. Despite of this fact, the nanoparticles prepared with poly(fumaric-co-sebacic anhydride) were much less efficient than nanoparticles prepared by the combination of poly(fumaric-co-sebacic anhydride) and PLGA, thus further improvements in the proposed carrier are still needed. The PEGylation of PLGA nanoparticles may be also used to improve the bioavailability of loaded insulin. Thus, a folate coupled PEGylated PLGA (FA-PEG-PLGA) nanoparticles were developed to improve the oral uptake of insulin [112]. The nanoparticles were produced by a double-emulsion solvent evaporation method, obtaining a loading of insulin of about 6.5% (w/w) and an AE of 87%. Insulin-loaded FA-PEG-PLGA nanoparticles (50 IU/kg) were further administered to diabetic rats, and it was observed a 2-fold increase in the oral bioavailability of insulin, comparatively to subcutaneous administration of insulin. It was also observed the maintenance of the blood glucose levels for 24 h. In another approach, insulin-loaded PEGylated PLGA nanoparticles were functionalized with two different cell-penetrating peptides (poly[arginine]8 enantiomers, l-R8 and d-R8) [113]. The *in vitro* studies in Caco-2 cell monolayers showed that functionalized nanoparticles significantly enhanced the permeation of insulin across the monolayers. Upon intestinal administration in rats, it was observed that functionalized nanoparticles improved the relative bioavailability of insulin in about 3.2 and 4.4-folds, and increased the hypoglycemic action in 2.5 and 3.7-folds, respectively for l-R8 and d-R8 functionalized nanoparticles. This approach showed that d-R8 was better on promoting insulin uptake that l-R8.

4.8. Poly(ε-caprolactone) nanoparticles

PCL is a biodegradable and biocompatible polyester, recognized for its good sustained release properties. The slower degradation profile of PCL comparatively to PLGA, for instance, makes it excellent for prolonged drug delivery. Damgé *et al*. developed a nanocarrier for oral insulin administration made of a mix of PCL and Eudragit® RS, achieving an insulin AE of about 96% [114]. Insulin-loaded nanoparticles (25, 50 and 100 IU/kg) were orally administered to diabetic rats, decreasing fasted glycemia levels with a dose dependant profile, reaching the maximal decrease at 100 IU/kg. In addition, nanoparticles containing fluorescein isothiocyanate (FITC) labelled insulin adhered strongly to the intestinal mucosa, mainly due to the mucoadhesive properties of Eudragit® RS, allowing the uptake of insulin mainly by the Peyer's patches.

In another work from the same group, the same type of nanoparticles were used to encapsulate two different commercial insulins, Actrapid® and Novorapid®, achieving an AE of about 96% and 35%, respectively [115]. The *in vitro* release studies showed a burst release profile of insulin, and the *in vivo* studies in diabetic rats revealed that the Novorapid-loaded nanoparticles delivered orally decreased the glycemia, comparatively to empty nanoparticles. In another study, the authors used the same nanocarrier to encapsulate insulin aspart (short-acting insulin analogue) and obtained an AE of about 98% [116]. The *in vitro* release study revealed that nanoparticles were able to release about 70% of insulin after 24 h. After oral administration of insulin-loaded nanoparticles (50 IU/kg) to diabetic rats, fasted glycemia decreased for an extended time and enhanced the glycemic response in a time-dependent manner, reaching a maximal effect at 12-24 h. Overall, it was observed that the produced nanoparticles allowed the suppression of postprandial peak more than 24 h comparatively to regular insulin, that had effect for 6-8 h only. This could be explained by the ability of insulin aspart to be better taken-up by the intestinal membrane than the 'pure' insulin.

4.9. Acrylic polymers nanoparticles

Acrylic polymers have been used in the oral delivery of insulin due to its ability to inhibit proteases activity, enhance mucoadhesion and alter the cell tight junctions improving the intestinal uptake. In fact, acrylic acid and its derivatives are used to produce nanoparticles with different properties that may improve the oral bioavailability of insulin. The mucoadhesive poly(acrylic acid) (PAA) was used to produce PAA-Cys nanoparticles to deliver insulin orally to non-diabetic rats [117]. This combination allows good enzymatic protection properties, and permeation enhancement due to the

increased mucoadhesion ability. Upon administration, it was observed a reduction of blood glucose levels and a significant increase of insulin concentration in serum. The insulin area under the curve of thiolated PAA nanoparticles was 2.3-fold higher than unmodified PAA nanoparticles, mainly due to the enhancement of the mucoadhesive properties of thiolated polymers. A similar carrier was developed in another study with the intention to protect loaded insulin from proteases in the intestine [118]. The *in vitro* studies showed that comparatively to insulin in solution, nanoparticles showed protection of respectively about 44%, 21% and 45% of the initial amount of insulin from degradation by trypsin, α-chymotrypsin and elastase degradation.

Methacrylates are also useful to encapsulate insulin into nanoparticles. Nanospheres of crosslinked networks of methacrylic acid grafted with PEG and nanospheres of acrylic acid grafted with PEG, were previously developed [119]. The size of the copolymer gel nanospheres was dependent on the pH of the medium, as well as the release profile of insulin showed to be higher at pH 7.0. The *in vivo* studies in diabetic rats demonstrated that insulin-loaded copolymer nanospheres, caused a significant reduction of glucose level in serum, which lasted for 6 h. Methacrylates demonstrated to be useful for the tight junctions opening, enhancing the intestinal permeation, whereas PEG conferred the protein stability and promoted mucoadhesion.

Nanoparticles prepared by the blend of methacrylic copolymers with chitosan have been used to encapsulate insulin [120]. These systems enhanced the bioavailability of insulin due to its pH-sensitive property, which allowed insulin protection in stomach and promoted its interaction with the intestinal mucosa. In a different study, a complex of insulin and hydroxypropyl β-cyclodextrin (HPβCD) was encapsulated into polymethacrylic acid-chitosan-polyether PEG-polypropylene glycol copolymer) nanoparticles [121]. An evaluation by an enzyme linked immuno sorbent assay (ELISA) showed that insulin retained its biological activity after complexation and encapsulation. *Ex vivo* results using excised intestinal mucosa of rat showed good mucoadhesive properties of the nanoparticles. Insulin-loaded poly(isobutylcyanoacrylate) (PIBCA) nanoparticles produced by anionic *in situ* polymerization were also previously developed [122]. The nanoparticles were administered orally to diabetic rats, and it was observed positive results on oral absorption of loaded insulin.

Eudragit® is a copolymer of ethyl acrylate, methyl methacrylate and methacrylic acid ester with quaternary ammonium groups, widely used as an excipient in pharmaceutical products. The enteric coating and controlled release properties of this copolymer make it helpful in the formulation of insulin-loaded nanoparticles intended to be administered orally. For instance, insulin-loaded thiolated Eudragit® L100 (with Cys) nanoparticles have been prepared by a precipitation method [123]. Thiolated and non-

thiolated Eudragit® L100 nanoparticles containing insulin, achieved a loading efficiency of about 92% and 96%, respectively. The *in vitro* release profiles showed an insulin release in a pH-dependent manner, and CD measurements showed that the released insulin maintained its secondary structure. The *in vitro* mucoadhesion studies in the rat jejunum and ileum showed that thiolated nanoparticles had a 3.0 and 2.8-fold increase, respectively, comparatively to non-thiolated nanoparticles. This was attributed to the immobilization of the thiol groups on Eudragit® L100. The nanoparticles were further administered orally to rats, and the thiolated nanoparticles showed a higher and prolonged hypoglycemic action, with an insulin relative bioavailability of 7.33%, which represented a 2.8-fold increase comparatively to non-thiolated nanoparticles. In a different approach, nanoparticles produced by a complex coacervation method using Eudragit® L100-55 and chitosan polymers, were used to deliver insulin orally, achieving a loading efficiency of about 31%, mean particle size of about 200 nm and with a non-spherical shape [124]. CD studies revealed that the insulin structure was not significantly changed after encapsulation, and its release was pH-dependent. Gelatin and Eudragit® L100 have been combined to produce pH-sensitive nanoparticles [125]. These nanoparticles were able to retain insulin, showing only about 20% of protein release during 90 min at pH 2.5. In contrast, at pH 7.4 the release was about 40% in the first 30 minutes. This pH-sensitive release pattern conferred protection to insulin from the harsh gastric conditions along the gastrointestinal tract. Eudragit® RS, a polycationic acrylic polymer, was also combined with PCL achieving a relative bioavailability of insulin over 13% [116]. The success of such carrier on insulin oral delivery is mostly attributed to the bioadhesive character of Eudragit® RS.

4.10. Insulin-polyallylamine nanocomplexes

The complexation of insulin with polymers may be a good strategy to obtain a different type of nanoparticles, which may be valuable in the oral delivery of insulin. Thompson *et al*. developed a nanocomplex made of polymeric self-assemblies of comb-shaped amphiphilic polyallylamine that may be used to deliver insulin orally [126]. Polyallylamine was synthesized by randomly grafting palmitoyl pendant groups and further quaternized with methyl iodide. The obtained transmission electron microscopy (TEM) images showed that non-quaternized polymer complexes presented vesicular structures at low polymer:insulin concentrations, whereas at high concentrations they formed solid nanoparticles. The obtained complexation efficiency of insulin ranged between 78 and 93%. *In vitro* studies showed that the formed complex was able to protect insulin from degradation by pepsin and trypsin. It was also verified that

quaternized polymers had better protective effect against trypsin, mainly due to the electrostatic interaction with insulin, whereas non-quaternized polymers increased significantly the degradation of insulin by α-chymotrypsin. These results suggested that quaternized polymers could be a good option for oral delivery of insulin.

In a different study, it was assessed the impact of the polymer architecture of nanocomplexes on insulin protection from degradation by trypsin, α-chymotrypsin and pepsin [127]. The polymer-insulin nanocomplexes were produced using quaternized derivatives of polyallylamine. It was verified that the polymer architecture could have influence on the complexes morphology, but had just a few impact on complexation efficiency. The polymers showed ability to reduce insulin degradation by trypsin, whereas it was verified that the polymer architecture played a crucial role against α-chymotrypsin and pepsin degradation. Thus, quaternized cetyl polymers were effective against pepsin degradation of insulin, whereas cholesteryl polymers significantly limited the degradation by α-chymotrypsin. These results indicated that to increase insulin protection against all the tested enzymes upon oral insulin administration, it is needed a combination of the used polymers.

Further work of the same group, evaluated the effect of polymer architecture on the uptake of the nanocomplexes across a Caco-2 cell model [128]. It was observed that the nanocomplexes were able to reversibly open the tight junctions of cells increasing insulin uptake. Despite promising, the potential of these nanocomplexes to deliver insulin orally needs to be further addressed in *in vivo* models.

Overall, the most relevant carriers for oral insulin delivery discussed all over the Section 4 of this chapter, and their features and pharmacological activity/bioavailability are summarized in Table 2.1.

Table 2.1. The most relevant polymer-based nanocarriers and their pharmacological activity/bioavailability studies developed so far.

Polymer	Mean diameter	Dose	Glucose level reduction	Pharmacological bioavailability	Ref.
Chitosan	250-400 nm	21 IU/kg	58%	14.9%	[59]
	200-550 nm	50 IU/kg	29%	NA	[60]
		100 IU/kg	33%	NA	
	269 nm	50 IU/kg	44.9%	4.4%	[62]
		100 IU/kg	51.4%	3.2%	
	339 nm	100 IU/kg	40%	3.5%	
TEC	175 nm	25 IU/kg	30%	NA	[70]
DMEC	172 nm		34%	NA	
TMC-CSK	180-350 nm	50 IU/kg	28%	5.7%	[67]
TMC-Cys	100-200 nm	50 IU/kg	35%, 70%	NA	[72]
Chitosan-γ-PGA	110-150 nm	15 IU/kg	25%	NA	[90]
		30 IU/kg	50%		
	230-390 nm	30 IU/kg	45%	20.1%	[91]
	218 nm	30 IU/kg	60%	15.1%	[93]
Chitosan-γ-PGA-DTPA	245-432 nm	30 IU/kg	50%	19.7%	[94]
LCS	270 nm	60 IU/kg	34%	NA	[73]
Chitosan-dextran sulfate	500 nm	50 IU/kg	35%	5.6%	[83]
		100 IU/kg		3.4%	
Chitosan-alginate	750 nm	50 IU/kg	40%	6.8%	[86]
		100 IU/kg		3.4%	

Alginate–dextran + poloxamer + chitosan + albumin	396 nm	50 IU/kg	40%	13.2%	[87, 88]
Chitosan-HPMCP	255 nm	12.5 IU/kg	35%	8.5%	[58]
Dextran + Vitamin B12	192 nm	20 IU/kg	70%	29.4%	[46, 47]
Hyaluronic acid	182 nm	50 IU/kg	40%	NA	[95]
PLA-F127-PLA	56 nm	50 IU/kg	75%	NA	[96]
PLA-P85-PLA	178 nm	200 IU/kg	85%	NA	[97]
PLGA	247 nm	30 mg/kg	50%	NA	[100]
	200 nm	20 IU/kg	43%	1.7%	[103]
	160 nm	20 IU/kg	76%	NA	[104]
PLGA-HPMCP	169 nm	20 IU/kg	65%	6.3%	[107]
	182 nm	50 IU/kg	88%	11.3%	[108]
PLGA-Eudragit® RS	285 nm	50 IU/kg	40%	9.2%	[109]
PLGA-cell penetrating peptide	190-200 nm	10 IU/kg	30%, 50%	7.5%, 11.2%	[113]
	358 nm	100 IU/kg	80%	13.2%	[114]
PCL-Eudragit® RS	700 nm	50 IU/kg	60%	NA	[116]
PIBCA	85-182 nm	100 U/kg	75%	NA	[122]
Eudragit® L100-Cys	324 nm	50 IU/kg	28%	7.33%	[123]

NA: Not available

5. Walkthrough on pipeline products

Pharmaceutical companies are trying their best efforts on achieving a good formulation for oral delivery of insulin. Although the majority of the products are still in the development phase, some products are now in clinical trials. The main strategies focus on avoiding insulin degradation in the gastrointestinal tract and promoting its intestinal uptake. Strategies under development are concentrating efforts more on the use of excipients, such as protease inhibitors and absorption enhancers, together with insulin in conventional dosage forms like tablets or capsules, rather than the use of polymeric nanoparticles. Fonte *el al.* published a work discussing these different products to deliver insulin orally by pharmaceutical products recently developed [3]. This section is directed to describe the known delivery products based on polymer-based nanoparticles.

Access Pharmaceuticals, Inc. (Dallas, TX, USA) developed CobOral™ technology, which consists in a polymer-based delivery system that takes advantage of vitamin B12 uptake mechanisms in the intestine to improve oral delivery of insulin. After oral administration, vitamin B12 attached to nanoparticles surface binds to haptocorrin in the stomach, and such complex migrates to the duodenum and dissociates. The intrinsic factor released in the stomach binds to vitamin B12 forming a complex, which binds to intrinsic factor receptor in the ileum. Then, the conjugated nanoparticles with vitamin B12 reach the bloodstream by an endocytotic process. Chalasani and Russell-Jones, used a developed carrier to deliver insulin orally [46]. The nanoparticles produced using dextrans with different molecular weights and coated with vitamin B12, were loaded with 2, 3 and 4% w/w of insulin and showed an AE of 45-70%. *In vitro* trials demonstrated that the conjugated nanoparticles were able to protect the loaded insulin from proteases activity in about 65-83%. The *in vitro* release studies revealed a first burst release followed by a controlled release profile, releasing 75-95% of insulin in 48 h. Insulin-loaded nanoparticles were further administered orally to diabetic rats (20 IU/kg), leading to a plasma glucose reduction of 70-75% after 5 h, reaching basal levels at 8-10 h and obtaining a prolonged second phase until 54 h. The conjugated nanoparticles of Mw 70,000 dextran loading insulin at 2, 3 and 4% w/w obtained a PA of 1.1, 1.9 and 2.6-fold, respectively, which was higher than the nanoparticles with no conjugated vitamin B12. It was also found that nanoparticles of Mw 70,000 dextran had a PA 1.4-fold higher than Mw 10,000 dextran nanoparticles. Despite of some promising results, this approach of insulin-loaded dextran nanoparticles coated with vitamin B12 needs further

investigations. Phase I clinical trials of Access Pharmaceuticals oral insulin product were announced, but no significant results were revealed so far [129].

NanoMega Medical Corporation (Lake Forest, CA, USA) developed a patented novel nanoparticle deliver system, made of a core of neutral γ-PGA coated with positively charged chitosan. This carrier is intended to facilitate the transient opening of tight junctions of cells promoting insulin uptake. Chitosan that is located on the outer surface of nanoparticles also allows the mucoadhesion of nanoparticles, and γ-PGA located inside the chitosan shell allows nanoparticle stabilization. The produced nanoparticles (30 U/kg) and an insulin solution (30 U/kg) were orally administered to diabetic rats, and the subcutaneously administered insulin was used as control [130]. The results shown in Figure 2.4 demonstrated that insulin-loaded nanoparticles were able to decrease blood glucose levels in a sustained manner over 8 h. The oral insulin solution was ineffective in decreasing the blood glucose levels and as expected, the subcutaneous administration of insulin decreased the blood glucose levels faster, but this effect was mitigated after 3 h. These results proved the ability of nanoparticles on increasing the intestinal uptake of insulin. No information about the current development stage of the developed product has been reported yet.

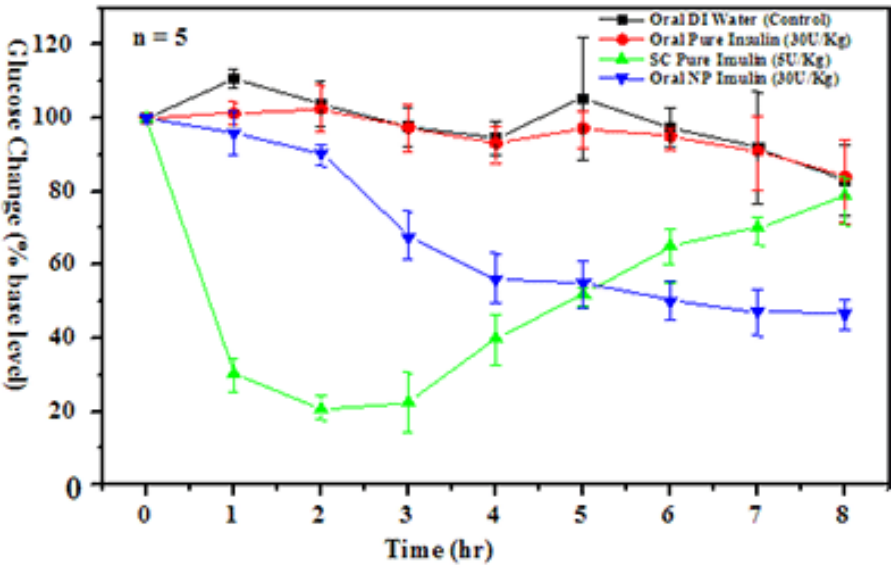

Figure 2.4. Levels of glucose change after oral administration of insulin-loaded γ-PGA/chitosan nanoparticles. Water and insulin administered orally, and subcutaneously administered insulin were used as controls. *Source*: [130].

It is important to highlight that only a few results were revealed by the pharmaceutical companies regarding the oral delivery of insulin and the results described above are the most relevant presented so far. Despite the positive results, it

seems that a lot of work is still needed in the upcoming years in order to take the research on oral delivery of insulin to the next level. Even though, there are other companies trying their efforts to achieve a good polymer-based nanoparticle system for the oral delivery of insulin such as Aphios Corp. (Woburn, MA, USA) and NOD Pharmaceuticals, Inc. (San Diego, CA, USA), however the information about the used polymers and the products under development is too scarce. Aphios Corp. developed APH-0907 that is in pre-clinical development and consists in patented biodegradable polymer nanospheres loading insulin. NOD Pharmaceuticals, Inc., developed a formulation based on insulin-loaded bioadhesive nanoparticles, which are further formulated in unidirectional dosage forms for basal insulin supplementation. Their product Nodlin, which has been developed by their subsidiary Biolaxy (Shangai, China), uses NOD technology patented in US, EU, China and Mexico, and is currently in clinical phase trials I [131]. These latter companies present a lot of claims on the research of oral delivery of insulin, but no relevant results were reported so far.

6. Toxicity concerns regarding insulin-loaded polymeric nanoparticles

The toxicity assessment regarding oral administration of insulin-loaded polymer-based nanoparticles needs to be focused both on insulin and on the carrier. Comparatively to the subcutaneous route, higher amounts of insulin are needed to be administered orally to have the same effect. However, the administration of such amounts in the intestine may raise toxicological problems that the majority of investigations usually neglect or underestimate. For instance, insulin released in a large amount may cause gastroparesis [132], being the effect of the prolonged administration of insulin on intestinal epithelium not well known so far. Regarding the carrier, the majority of the used polymers are recognized for being biocompatible and biodegradable, but the biodegraded polymeric products may accumulate inside the cells, which may affect unexpectedly the cellular responses [133]. Besides cytotoxicity, the immunological response may also be hindered.

The excipients or adjuvants used in the formulation of nanoparticles, such as surfactants and absorption enhancers, may also damage the intestinal epithelium. The latter when continuously administered may compromise the epithelium integrity allowing the permeation of toxins and pathogens, which may lead to unexpectable side effects [134]. Other putative problems are, protease inhibitors that may interfere with proteins digestion leading to dietary problems and also mucoadhesive materials that may change the mucus turnover affecting the physiology of the intestine [135]. The developments in the oral insulin delivery field has focused more on improving the bioavailability of oral

insulin, rather than assessing the toxicity of the developed carriers, since it is assumed they are biocompatible. However, the toxicity in a long term of the carriers has been neglected. Nevertheless, some studies have been reported addressing some toxicity concerns.

I*n vivo* studies were performed upon oral administration in rats of a daily dose of self-assembled γ-PGA/chitosan nanoparticles during 14 days [93]. Neither significant difference in clinical signs nor in body weight was observed between experimental and control groups. No relevant pathological changes were observed in kidney, liver and intestine and no inflammatory reactions were also observed. The nanoparticles were well tolerated even at a higher dose of 18-fold than used in the pharmacokinetic/pharmacodynamic study. The toxicity assessments in rats, after administration of insulin-loaded decanoic acid grafted oligochitosan nanoparticles on the intestine were also performed [45]. Animals were sacrificed after a few hours and the histopathology studies revealed that the nanoparticles had no adverse effects on the intestine. Another biocompatibility assessment of TMC-Cys conjugate nanoparticles in Caco-2 cells after 8 h of incubation, and in rats after 2 h of administration showed no significant toxicity [72]. In another study, the cytotoxicity of PLGA nanoparticles and chitosan-coated PLGA nanoparticles was determined by 3-(4,5-dimethylthiazol-2-yl)-2,5-diphenyltetrazolium bromide in Caco-2 cells and showed to be harmless to cell survival, since the cell viability was above 85% of the controls [110].

Insulin-loaded alginate–dextran complexed with chitosan–PEG–albumin nanoparticles were orally administered to diabetic rats for 15 days, and its toxicity effects were also evaluated [136]. There was no significant liver damage or biliary obstruction, since it was showed lower levels of alkaline phosphatase, alanine transaminase and aspartate aminotransaminase. In another study from the same group, the same type of insulin-loaded nanoparticles was administered to diabetic rats. No changes were observed in the liver and kidney, since some modifications on hepatic parameters and kidney functions were similar to normal rats and this was attributed to the chemical inducement of diabetes [137]. More recently, similar nanocarriers were administered to diabetic rats at a daily dose for 15 days, and a histopathological study was performed [89]. Neither pathological nor morphological modifications were observed in the intestine, kidney, spleen, pancreas or liver.

7. Conclusion

A major problem in insulin oral administration is the enzymatic degradation, as well as the low intestinal permeability and consequently low oral bioavailability. Thus,

different strategies using insulin encapsulation in polymer-based nanoparticles have been used to overcome these problems. The polymers used in nanoparticles production may be obtained from natural or synthetic sources, taking advantage of their properties such as the ability to preserve insulin stability, mucoadhesion, control the release and targeting of drugs. The combination of different polymers may accommodate all these properties together in the same nanocarrier.

The research progress on finding an alternative system to deliver insulin orally has been concentrated more in academic research, rather than developments in the pharmaceutical industry. Thus, the focus has been on testing and proposing different carriers that have the ability to promote insulin intestinal uptake in a much larger extension than an oral administrated insulin solution. Positive results have been found, although obtained results are far from the hypoglycemic effect achievable by using subcutaneous insulin. In fact, the insulin amount used to formulate the oral delivery systems is much higher than that used for subcutaneous formulations. This is a critical point since the AE of the developed nanocarriers is crucial from a cost-effective point a view. The delivery of large amounts of insulin in the intestine also may lead to adverse effects. Thus, the future research developments needs to be more focused on becoming the developed oral insulin nanocarriers more effective and with similar biopotency of the subcutaneous route. Toxicity assessments of the developed nanocarriers, in a long term use need to be performed and their safety has to be clearly demonstrated.

The pharmaceutical industries are trying their best efforts to develop an insulin oral delivery system; however, the focus on polymeric nanoparticles has been rather scarce, where only few industries have tried this strategy and the known results are very preliminary. A lot of work needs to be done still to become possible to bring to the market a nanoparticle-based delivery system to deliver insulin orally. Even though, the path is well-marked and the strategy of using polymeric nanoparticles may become in the future a possible answer to the search for an insulin oral delivery system.

Overall, with the focus on the most promising administration route of insulin, the oral route, this chapter gave an overview about the potential polymeric nanoparticles used for delivery of therapeutic proteins. For therapeutic proposes, such carriers may be subjected to lyophilization and administered by several administration routes.

Chapter 3

Facts and Evidences on the Lyophilization of Polymeric Nanoparticles

To be published as:

Pedro Fonte, Salette Reis, Bruno Sarmento, Facts and evidences on the lyophilization of polymeric nanoparticles, J Control Release, *Accepted.*

1. Introduction

Nanoparticles are often produced in form of an aqueous suspension. However, in an aqueous suspension they are physically unstable, so particle aggregation and fusion are frequent phenomena during long storage periods. The hydrolytic action of water on the polymer matrix can lead to drug leakage, hamper or eliminate the sustained release properties or even lead to the formation of undesirable degradation products [6]. A nanoparticle suspension is also prone to the development and growth of microorganisms [138]. To overcome all these problems, the transformation of the nanoparticle suspension into a solid dosage form is the obvious solution.

Lyophilization or freeze-drying is a dehydration process used to overcome the instability of nanoparticle suspension, increasing shelf-life and simultaneously facilitating its handling and storage [7, 8]. This process has three main steps, the freezing, the primary drying and the secondary drying. Thus, water is removed from the formulation by sublimation of ice and further desorption of unfrozen water under vacuum. The processing conditions at which formulation are subjected may generate freezing and desiccation stresses, with detrimental consequences to nanoparticle structure and stability. Different excipients such as cryoprotectants and lyoprotectants may be used to minimize the lyophilization stresses and preserve the physical-chemical properties of nanoparticles. Sugars are the preferable cryo- and lyoprotectants, mainly because they are chemically innocuous and may be easily vitrified during the freezing step [9]. Therapeutic proteins are often encapsulated into nanoparticles, and sugars are also important in the protection of protein drugs from inactivation, during lyophilization and storage [10]. Another important property of sugars is that they also affect the glass transition temperature (Tg and Tg') of formulations, which have major importance on the optimization of the lyophilization cycle [8]. A higher cryoprotectant concentration and faster freezing rate lead to better nanoparticle redispersibility [139, 140]. However, there is some controversy, so the selection of an adequate cryo- or lyoprotectant and freezing rate is not straightforward, and it may depend both on the formulation properties and on the lyophilization cycle [7]. In most of the works focusing on lyophilization of nanoparticles, the choice of a good cryo- or lyoprotectant and lyophilization cycle has been relied in empirical approaches, and experiments have been even performed by trial and error. Therefore, it is crucial to perform a systematic study on the optimization of nanoparticles lyophilization, by assessing the physical-chemical properties of formulations and understanding the engineering principles inherent to lyophilization.

Several analytical techniques may be used to achieve this purpose, and also characterize the properties of both the nanoparticles and the cake upon lyophilization.

The use of therapeutic proteins have been grown in the last years, due to their therapeutic benefits in severe health problems such as cancer and autoimmune diseases [1]. These drugs have been also loaded into polymeric nanoparticles with potential benefits to patients. However there is a lack of knowledge on the effect of lyophilization on the structure of proteins loaded into nanoparticles, and whether the interaction of polymers and proteins inside nanoparticles core may affect the conformation of proteins, in such a way that could hinders their bioactivity or even lead to undesirable side effects. To address such lack of knowledge, in this Thesis it was used as models, insulin as therapeutic protein, PLGA as nanoparticles polymer and several lyophilization protectants, namely trehalose, sucrose, glucose, fructose, and sorbitol. These compounds are briefly described below:

Insulin

Insulin is a protein hormone involved in the metabolism of carbohydrates, which lowers blood sugar and is used to treat both type 1 and type 2 diabetes *mellitus.* Insulin has a molecular weight of about 5.8 kDa, and is composed of two polypeptide chains, the A- and B- chain, with 21 and 30 amino acids, respectively, linked together by two disulphide bonds [141]. In Figure 3.1 is shown the organization of the primary structure of human insulin. This structure may slightly variate between animal species.

Insulin is produced and stored in the body as a hexamer, but the active form is the monomer [142]. The hexamer is an inactive form with long-term stability, and is more stable than the monomer. In solution, insulin may exist as an equilibrium mixture of monomers, dimers, tetramers and hexamers depending on concentration, solvent composition, pH, metal ions and ionic strength. Upon exposure to harsh conditions, such as high temperatures, organic solvents, low pH and agitation, insulin can aggregate and even form fibrils [143].

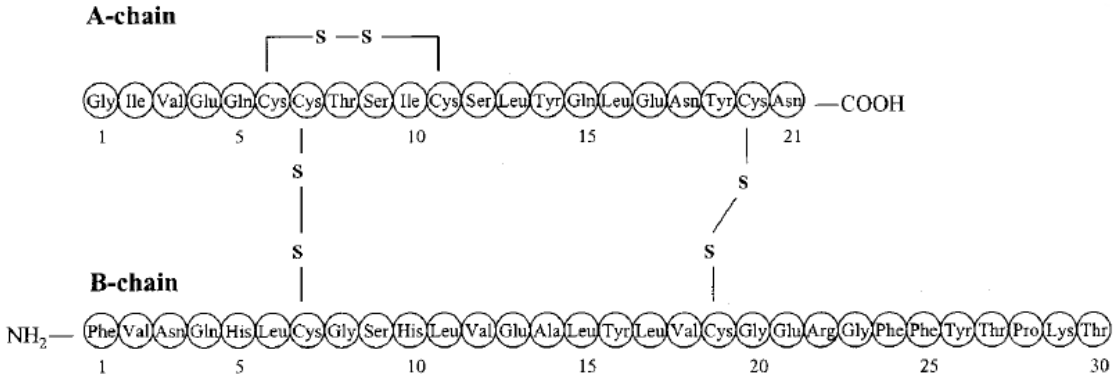

Figure 3.1. The structure of human insulin composed of A-chain with 21 amino acids, and B-chain with 30 amino acids. Adapted from [144].

PLGA

PLGA is a polyester and a copolymer of PLA and polyglycolic acid (PGA). PLA has an asymmetric α-carbon, usually stereochemically described as L or D form. Figure 3.2 shows the chemical structure of PLGA. Different forms of PLGA may be obtained depending on the ratio of lactide and glycolide used for polymerization, and are identified regarding the molar ratio of the monomers used [145]. The chemical properties of PLGA depend on that ratio, and the polymer may variate from crystalline to amorphous form depending on both the molar ratio and block structure. The Tg is usually in the range of 40-60ºC.

PLGA is used to encapsulate molecules of a large size range, and it is soluble in chlorinated solvents, acetone, ethyl acetate and tetrahydrofuran [146]. Water may lead to the biodegradation of PLGA by hydrolysis of its ester linkages. The Tg, molecular weight and residual moisture content may variate accordingly to the hydrolysis of PLGA, and the modification of PLGA properties during its biodegradation influences the rate of release and degradation of loaded drugs [145]. PLGA is useful in drug delivery due to its biodegradation by hydrolysis in the body originating its monomers, lactic acid and glycolic acid [147]. Such monomers are by-products of different metabolic pathways, so its toxicity is considered negligible.

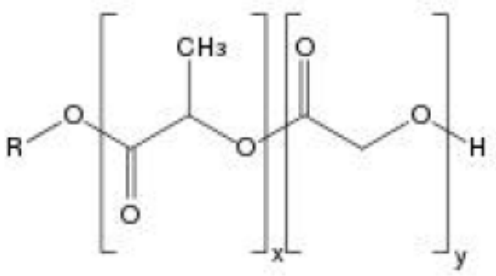

Figure 3.2. Chemical structure of PLGA. The x represents the number of units of lactic acid, and y represents the number of units of glycolic acid.

Trehalose

Trehalose is a non-reducing disaccharide formed by a linkage of two d-glucose molecules (Figure 3.3). The typical commercial product is trehalose in the dehydrate form with a molecular formula and weight of $C_{12}H_{26}O_{13}$ and 378.33 g/mol, respectively [148].

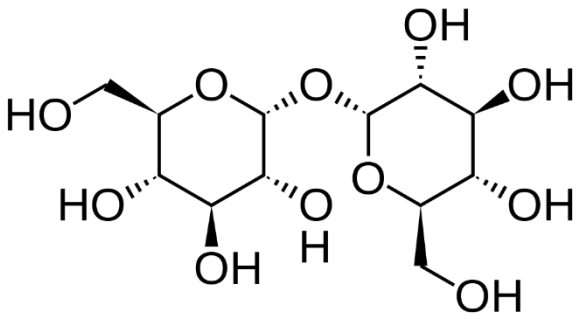

Figure 3.3. Chemical structure of trehalose.

Sucrose

Sucrose is a non-reducing disaccharide formed by a linkage of glucose and fructose (Figure 3.4), with a molecular formula and weight of $C_{12}H_{22}O_{11}$ and 342.30 g/mol, respectively [148].

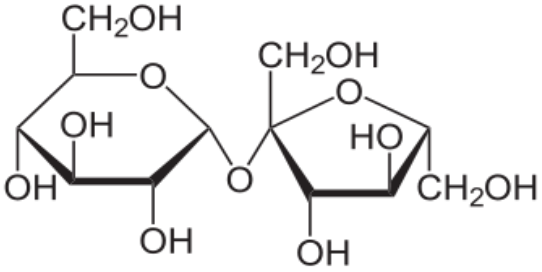

Figure 3.4. Chemical structure of sucrose.

Glucose

Glucose is a reducing monosaccharide (Figure 3.5), with a molecular formula and weight of $C_6H_{12}O_6$ and 180.16 g/mol, respectively [148].

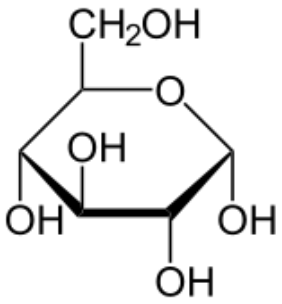

Figure 3.5. Chemical structure of glucose.

Fructose

Fructose is a reducing monosaccharide (Figure 3.6), with a molecular formula and weight of $C_6H_{12}O_6$ and 180.16 g/mol, respectively [148].

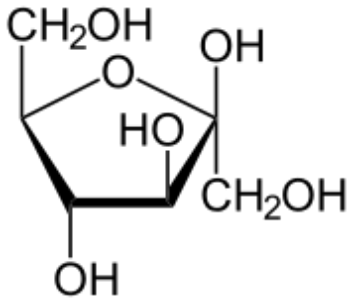

Figure 3.6. Chemical structure of fructose.

Sorbitol

Sorbitol is a sugar alcohol (Figure 3.7), with a molecular formula and weight of $C_6H_{14}O_6$ and 182.17 g/mol, respectively [148]. Sorbitol is an isomer of mannitol, differing only in the orientation of the hydroxyl group on carbon 2.

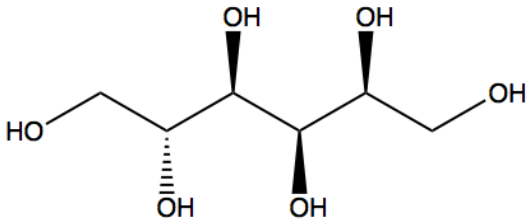

Figure 3.7. Chemical structure of sorbitol.

The main aim of this chapter was to perform an up-to-date insight on the fundaments involved in the lyophilization of polymeric nanoparticles, mainly regarding the binomial formulation-lyophilization cycle and their storage stability. A special focus is given to the need of optimization of the mentioned binomial to obtain a good lyophilized product, discussing also the analytical methods for its characterization. Finally, the effect of lyophilization on the stability and structure of proteins loaded into polymeric nanoparticles is also scrutinized.

2. Lyophilization of nanoparticles

Lyophilization is commonly used to improve the long-term stability of nanoparticles [149]. A good lyophilizate should have some important characteristics, i.e., maintain the physical and chemical properties of the original product, obtain a cake with good aspect, possess short reconstitution time, low residual moisture content and good long-term stability [150]. Furthermore, after lyophilization, the nanoparticles need to be easily resuspendable, presenting no modification of particle size distribution, and the activity of the loaded drug must be preserved. To achieve all these purposes, it is crucial to optimize and focus on three main aspects involved in the stability of nanoparticles, which are the formulation, the lyophilization process and the storage conditions.

2.1. Formulation matters

The thermo-physical properties of the nanoparticle suspension need to be properly known, and further considered to obtain a good lyophilizate. These properties are essentially the glass transition temperature of the frozen sample (Tg') and the collapse temperature (Tc) of the formulation. The different constituents of the formulations such as the nanoparticles polymer, the type of surfactants, the chemical

groups attached on nanoparticle surface, and the nature and concentration of cryo- or lyoprotectant used, may influence those properties, and have important effects on the different stresses caused by lyophilization [7]. All these components should be regarded before inferring the lyophilization process, and distinguished between the components of the formulation with origin in the production of nanoparticles, and others added to the formulation prior to lyophilization, such as cryo- and lyoprotectants. Since the latter are specifically added to avoid the lyophilization stresses, they will be fully discussed in section 2.1.1 of this chapter.

Surfactants are frequently used to stabilize the nanoparticles suspension and avoid their aggregation [151, 152]. Polyvinyl alcohol (PVA) is one of the most common surfactants used to produce nanoparticles, enabling the production of stabilized nanoparticles with small size and narrow distribution [151, 152]. Simultaneously, surfactants may also have a stabilizing effect on nanoparticles during lyophilization. It was reported that PCL nanoparticles formulated with 2.5% (w/v) and 5% (w/v) of PVA, used as surfactant, were stable with no significant aggregation upon lyophilization with no cryo- or lyoprotectant added [153]. Another surfactant, pluronic F68 2% (w/v), was also able to stabilize poly(isohexylcyanoacrylate) (PIHCA) and PIBCA nanoparticles, after lyophilization [154]. The PVA may remain on nanoparticles surface even after washing, improving the freezing resistance of nanoparticles [151, 152, 155]. Different studies reported that for nanoparticles without cryoprotectant the residual PVA was able to preserve nanoparticle structure upon lyophilization [156-159]. However, not even all surfactants may have a stabilization effect on nanoparticles during lyophilization. For instance, PLA nanoparticles stabilized with pluronic F68 were not stable upon lyophilization, due to the increase of this surfactant solubility in the bulk solution during freezing, leading to nanoparticles aggregation [160].

The drug present in formulation may also influence the lyophilization process, whether the drug is entrapped into the nanoparticles or free in the formulation. The presence of free drug may reduce the zeta potential of nanoparticles, leading to their aggregation [7]. The lyophilization process itself may lead to the leakage of the drug, or in the case of protein drugs, lead to the degradation of its structure. Previously, it was observed that the lyophilization of PCL nanoparticles resulted in desorption of itraconazole located at nanoparticles surface, due to the crystallization of pluronic F68 used as stabilizer [161]. However, the modification of pluronic F68 by sodium deoxycholate in presence of sucrose 10% (w/v) fully stabilized the nanoparticles upon lyophilization. The sodium deoxycholate did not crystallize and maintained the drug-nanoparticle association. In another work, the cyclosporine association with PCL

nanoparticles was enhanced upon lyophilization, in presence of pluronic due to the adsorption of free drug on nanoparticles surface [162].

2.1.1. Cryo- and lyoprotectants

During freezing, occurs a separation of phases into ice and a cryoconcentrated suspension. The cryoconcentrated phase is constituted by the nanoparticles and other excipients like cryo- and lyoprotectants, buffers, surfactants and even unloaded drugs [140]. The high concentration of nanoparticles in the cryoconcentrated phase may motivate aggregation or even fusion of nanoparticles. Furthermore, the ice crystallization may induce a mechanical stress onto nanoparticles leading to their destabilization. To avoid these issues, some excipients may be added to the nanoparticles suspension prior lyophilization. Such excipients may be mainly cryoprotectants to protect from freezing stresses, and lyoprotectants to protect from drying stresses. The Table 3.1 summarizes the most used cryo- and lyoprotectants in the lyophilization of polymeric nanoparticles. Generally, the cryoprotectants may also act as lyoprotectants and vice-versa.

Overall, the cryoprotectants may form a protective glassy matrix in which the nanoparticles are immobilized, avoiding its aggregation and protecting them from the mechanical stresses of ice crystals. They are known to vitrify at a specific glass Tg', so to guarantee the complete solidification of the formulation, the freezing step needs to be performed below Tg' of a frozen amorphous formulation or below the Teu (eutectic temperature) for crystalline formulations [163]. Another theory of nanoparticles stabilization by cryoprotectants is the particle isolation hypothesis, stating that cryoprotectants separate the nanoparticles in the unfrozen phase, avoiding their aggregation upon freezing above Tg' [164].

The most commonly used cryoprotectants are sugars, such as trehalose, glucose, sucrose and mannitol [7]. Other cryoprotectants such as polymers are also often used. Most of the works present a trial and error approach, on choosing the best cryoprotectant for the nanoparticle formulation. For instance, it was evaluated the performance of the cryoprotectants, glucose, sucrose, PVA and γ-PGA in the lyophilization of PCL nanoparticles [165]. It was found that glucose 1% (w/w) had the best stabilizing effect achieving spherical, uniform and biocompatible PCL nanoparticles upon lyophilization. Among the most used cryoprotectants, trehalose present some advantages over the other sugars mainly because of its absence of internal hydrogen bonds, allowing more flexible formation of hydrogen bonds with nanoparticles during lyophilization, less hygroscopicity, higher Tg' and low chemical reactivity [166]. The stabilization effect of sugars is also directly related to their concentration. It was

described that PLGA and PCL nanoparticles, respectively, added with sucrose and glucose at a concentration of 20% (w/w), presented no macroscopic aggregation after reconstitution [167]. The mass ratio of nanoparticles:cryoprotectant seems to be also important on nanoparticles stabilization. A complete redispersion of poly(lactide acid-co-ethylene oxide) (PLA-PEO) nanoparticles was observed after lyophilization, when trehalose was added at a mass ratio of 1:1 [157]. However, the exaggerated increase of the cryoprotectant concentration may overcome the stabilization limit, and even destabilize the nanoparticles. For instance, the aggregation of silica nanoparticles increased with higher concentration of glucose [168].

To infer the right type of cryoprotectant and its concentration, a freeze-thawing study may be performed to optimize the formulation and guarantee the stabilization of nanoparticles. It was performed a freeze-thawing at -20ºC, -80ºC and -196ºC on PCL-PEG-PCL micelles testing as cryoprotectants, maltose, glucose, HPβCD and PEG of distinct molecular weights [169]. When not properly used, cryoprotectants may have a detrimental effect on nanoparticles stability. For example, the crystallization of cryoprotectants such as mannitol may originate a phase separation in the cryoconcentrated phase, without a stabilization effect on nanoparticles [7]. This is because in the nanoparticles enriched phase, they may interact and form aggregates. In addition, the ice crystals and mannitol can lead to mechanical stresses leading to nanoparticles fusion. Thus, to have a stabilization effect it is necessary to have mannitol in the amorphous phase of nanoparticles [140].

The removal of ice and unfrozen water may also destabilize the nanoparticles, so lyoprotectants may be used to avoid the drying stresses. The water replacement hypothesis, may explain the mechanism of nanoparticles stabilization by lyoprotectants [170, 171]. This theory states that lyoprotectants may form hydrogen bonds, with the polar groups at the nanoparticles surface, at the end of the drying steps. Nanoparticles are stabilized because lyoprotectants act as water substitutes. The amorphous state of nanoparticles and lyoprotectant facilitates a maximal H-bonding between them. Thus, the crystallization of a lyoprotectant hampers the formation of such hydrogen bonds [140]. The concentration of nanoparticles may also impact the outcome of lyophilization. This was observed in the lyophilization of PLA-PEO copolymer nanoparticles, in which the concentration of nanoparticles played an important role in the lyoprotective mechanism, independently of the amount of trehalose added [172]. It was observed that the highest lyoprotective efficiency was obtained for the highest nanoparticles concentration.

Table 3.1. Cryo- and lyoprotectants commonly used in the lyophilization of polymeric nanoparticles.

Cryo- and lyoprotectant	Polymer	Drug	Ref.
Dextran	PLGA	Ciprofloxacin HCl	[173]
		Cyclosporine	[174]
Fructose	PLGA	Insulin	[101, 175]
Glucose	BSA	Abacavir	[176]
	PCL	Cyclosporine	[167]
		Itraconazole	[161]
		-	[140, 153]
	PCL-PEG-PCL	Rifampicin	[169]
	PIBCA	Itraconazole	[177]
	PLA	-	[160]
	PLGA	Ciprofloxacin HCl	[173]
		Cyclosporine	[174]
		Insulin	[101, 175]
		-	[167]
HPβCD	PCL	-	[140, 153]
	PCL-PEG-PCL	Rifampicin	[169]
Lactose	PIBCA	Itraconazole	[177]
	PLGA	Testosterone	[178]
Maltose	PCL-PEG-PCL	Rifampicin	[169]
Mannitol	Chitosan	Docetaxel	[179]
	PLGA	Ciprofloxacin HCl	[173]
		Cyclosporine	[174]
		Testosterone	[178]
PEG	PCL-PEG-PCL	Rifampicin	[169]
PVP	PCL	-	[140, 153]
PVA	PCL	-	[153]
	PLA	-	[160]
	PLGA	-	[158]
Sorbitol	PCL	Cyclosporine	[167]
	PLGA	Insulin	[101, 175]
		-	[167]
Sucrose	PCL	Cyclosporine	[167]
		Itraconazole	[161]
		-	[140, 153]

	PIBCA	Itraconazole	[177]
	PLA	-	[160]
	PLGA	Insulin	[101, 175]
		Testosterone	[178]
		-	[167]
Trehalose	PIBCA	Itraconazole	[177]
	PLA	-	[160]
	PLGA	Ciprofloxacin HCl	[173]
		Cyclosporine	[174]
		Insulin	[101, 175]
		Testosterone	[178]

2.2. Lyophilization process matters

After optimizing the formulation and knowing its thermo-physical properties, it is necessary to adequate the lyophilization parameters in order to obtain a lyophilizate with good quality. The lyophilization occurs in three main steps: freezing, primary drying and secondary drying. Thus, this dehydration process occurs in the following stages: i) cooling of the formulation, and conversion of water into ice. In this stage occurs the crystallization of crystallizable solutes and/or formation of an amorphous matrix containing unfrozen moisture with noncrystallizing solutes; ii) sublimation of ice using vacuum; iii) removal of water by evaporation from the amorphous matrix and desorption of residual moisture.

The required conditions to the lyophilization process may induce some stresses and damage the products. That damage occurred in early stages such as during freezing may be drastically augmented in further stages. Although lyophilization is a robust technique, even trivial changes in the process such as changes in the vials type or trays, may be enough to transform an acceptable process into unacceptable. In Figure 3.8 it is shown examples of lyophilization cycles for sucrose and mannitol solutions representing amorphous and crystalline formulations, respectively. It is possible to observe differences in processing conditions, mainly regarding the shelf temperature and the chamber pressure. The product temperature is influenced both by the shelf temperature and the formulation itself, loaded into recipients with different sizes and distinct product volumes. Different temperatures and duration of steps are necessary to lyophilize the solutions. The primary drying of the amorphous formulation often requires a low temperature, leading to a lower sublimation rate and consequently to a required longer time. On its turn, in the lyophilization of the crystalline formulation it may be applied more

aggressive processing conditions. Thus, the sublimation rate may be quite higher, leading to a required shorter time for primary drying.

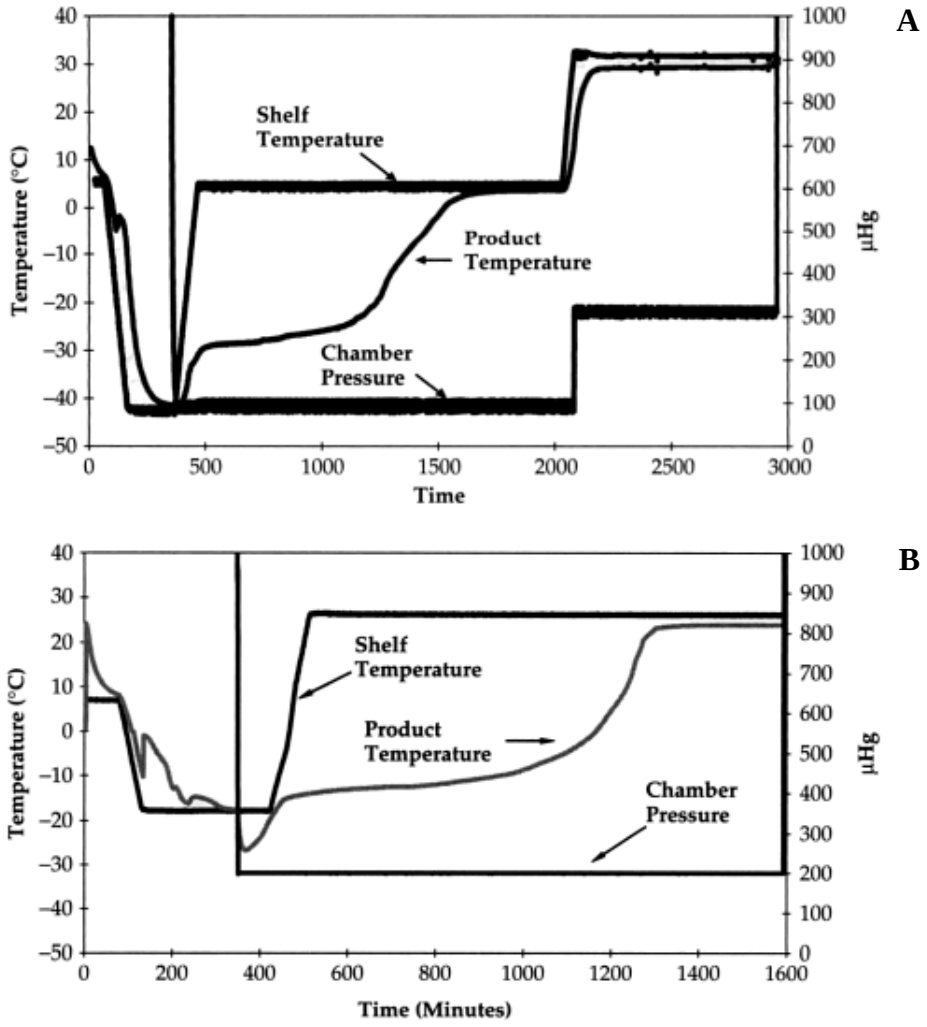

Figure 3.8. Lyophilization process of (A) 6 mL fill in 20 mL vial of a sucrose solution 5% w/v, and (B) 18 mL fill in 50 mL vial of a mannitol solution 5% w/v. *Reprinted with permission from* [180].

Upon freezing, the formulation constitutes a solid amorphous phase that contains about 15-30% of unfrozen water. After this step is complete, the temperature of the shelves is increased, and the ice-vapor is evacuated by the vacuum pump to promote the sublimation of water. After being removed, the ice crystals form a network of pores, that allows the exit of water vapor from the product [181]. The sublimation process occurs from the top to the bottom of the vial, being the primary drying the most time consuming step in lyophilization. After the primary drying, the shelf temperature is increased to remove the remainder unfrozen water and the secondary drying begins, normally at 20-50ºC for a few hours. Although the lyophilization purpose is to improve stability, some formulations may get unstable during the following events: occurrence of

a cold shock during the cooling of the formulation; formation of a cryoconcentrated phase, during the formation of ice; collapse of the formulation during drying; in the case of protein formulations, high shelf temperatures during secondary drying may lead to protein denaturation; presence of reactive gases such as oxygen, during drying and storage; Maillard reactions occurred during storage; and damage of formulation upon reconstitution when it is difficult to resuspend it.

Overall, the lyophilization of nanoparticles is a complex process and demands a good comprehension of the process specificity. Most of the research works use the lyophilization of nanoparticles in a trial and error way, using different processing conditions and formulation excipients, and choosing the best after lyophilization and product characterization. Standard lyophilization cycles are frequently used, and all the three steps of lyophilization, mainly the secondary drying, are even unspecified in many papers. Therefore, the best approach is to assess the thermo-physical properties of the formulation, and the engineering principles of lyophilization to obtain a good lyophilizate, without having a trial and error approach [8]. Still, there are some research works in which the thermo-physical properties of formulations were assessed prior lyophilization [140, 182]. The evaluation of the critical properties of the nanoparticle formulation is crucial to infer an optimum lyophilization cycle. Those properties are mainly the Tg' and the Tc of the formulation; as well as the stability of the loaded drug, the nanoparticles and excipients used. Usually, the Tg' is about 2ºC lower than the Tc. In the following sections, all the lyophilization steps will be fully described.

2.2.1. Freezing

The freezing step is the first one in the lyophilization process, in which the formulation is cooled and ice crystals are formed. During freezing, while water freezes, an increase in the concentration of the remaining suspension occurs, increasing its viscosity and hampering further crystallization. Then, this cryoconcentrated phase solidifies, originating a lyophilizate with a crystalline, amorphous or a combination of both form [183]. The water that does not solidify during freezing is denominated bound water. The freezing step may be understood, by the analysis of the phase diagram of a water/solute system (Figure 3.9). The diagram shows that a solution increases its concentration during freezing until the Tg', in which reaches the maximal concentration of the cryoconcentrated solution (Cg'). At this value, further cooling of the solution will not change its concentration. Therefore, the freezing temperature needs to be performed below Tg' to obtain complete freezing. During freezing, the crystallization of a crystallizable solute occurs below the Teu.

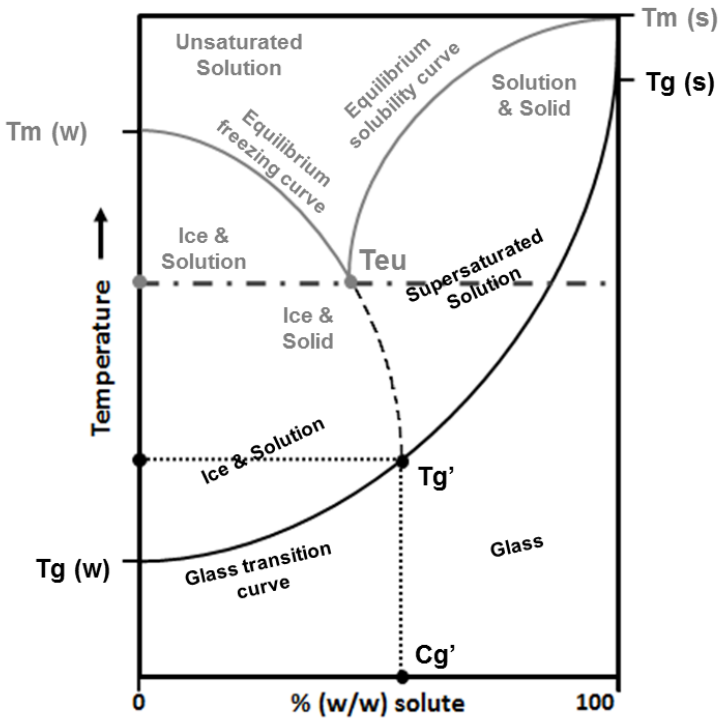

Figure 3.9. Phase diagram for a system of water (w) / solute (s). Tm, Teu, Tg, Tg' and Cg' stand for melting temperature, eutectic temperature, glass transition temperature, glass transition temperature of the frozen sample and concentration of the cryoconcentrated solution, respectively. The crystallization of the solute occurs below Teu (gray line). There is no crystallization of the solute at Teu in the case of vitrification (black line), and the cryoconcentration follows into a glass state at Tg. *Adapted from* [184].

The terms cooling and freezing are usually not properly distinguished. Cooling is related to the decrease of the temperature of the lyophilizer shelves, the lyophilizer chamber and the formulation. On its turn, freezing is related with the modification of the physical state of the formulation from liquid to solid. During freezing the water starts to nucleate, and ice crystals are formed and the remainder solute phase is a mixture of solute concentrate and ice. When a formulation is cooled below its freezing point it occurs a supercooling. Thus, in an optimized lyophilization process, it is necessary to induce supercooling in the formulation to promote the uniform cooling and freezing [183]. The cooling rates may be distinctly inferred, namely in terms of, the rate that the shelf temperature is cooled per period of time, the rate that solution cools per period of time and the depth of formulation in the vial that cools per period of time. There is a difference between the temperature of the formulation and the shelf temperature, so the shelf-cooling rate may not precisely define the formulation thermic behaviour. Furthermore, the cooling or freezing rates of the formulation may variate from vial to vial depending on

their position on the shelves, or even present intravial variation if the formulation is heterogeneous. For instance, the random freezing pattern may lead to differences in the ice structure from vial to vial, leading to different drying profiles, since the ice and crystal structure of the solute impacts the drying behaviour. At the end of sample cooling it is necessary a hold time, in which the temperature is maintained to assure that all vials are properly frozen.

Regarding the lyophilization of nanoparticles, the freezing step is the one in which most of the water is removed. This is because it is in this step, that there is a formation of many phases and interfaces between ice and nanoparticles. However, such formation of phases may induce stresses to nanoparticles leading to their aggregation or fusion in the cryoconcentrated phase. To assure that the formulation freezes, nanoparticles need to be cooled below the Tg' of the formulation if it is amorphous, or below the Teu if it is in the crystalline state. Thus, the shelf temperature needs to be below this critical temperature, and hold it for enough time to assure complete solidification of the suspension. Just a few papers have been reported the thermo-physical properties of nanoparticles before lyophilization [140, 161, 167]. To freeze the nanoparticle suspension it have been used different freezing methods [184]. Such methods may occur by placing vials onto precooled shelves, a ramped cooling on the shelves, freezing in an external freezer, freezing in liquid nitrogen or others. These freezing methods originate distinct supercooling effects, which lead to a distinct ice crystallization. Commonly, the freezing in liquid nitrogen result in the highest supercooling, whereas the freezing onto precooled shelves originates the lowest one. Thus, a larger surface area of ice resulting from smaller ice crystals is originated by a higher supercooling [185]. These smaller ice crystals may decrease the mechanical stress on nanoparticles, hampering their aggregation.

There is some controversy about if a slow or fast freezing rate is better for nanoparticles redispersibility and prevention of irreversible aggregation. It was previously observed that a faster freezing originated less aggregation of mannan-coated cationic nanoparticles upon thawing, comparatively to slow freezing [186]. However, when the formulation was added with a cryoprotectant, the freezing rate did not affect the particle size upon thawing. Similar results were found for PCL nanocapsules containing no cryoprotectant [153] In another research work, even in presence of mannitol, the freezing method influenced the particle size of monensin nanoparticles, and the fast freezing demonstrated to have a lower change of nanoparticles size, comparatively to slow freezing [187]. However, when trehalose was added, the freezing method showed no significant effect on particle size. This result may be explained by the capacity of mannitol to crystallize during slow freezing, and upon a fast freezing it may be produced

more amorphous mannitol able to protect nanoparticles. Previously, it was also reported that the addition of 5% (w/v) of glucose, sucrose and trehalose preserved the features of PCL and PLGA nanoparticles upon freeze-thawing, regardless the freezing at -70ºC or in liquid nitrogen [167]. Sorbitol was an effective cryoprotectant for PLGA nanoparticles frozen at -70ºC, and it was able to avoid the formation of macroscopic aggregates upon freezing of PLGA in liquid nitrogen and of PCL nanoparticles at -70ºC.

Other studies found that a slow freezing was beneficial for the lyophilization of nanoparticles, mainly because it originates a more cryoconcentrated phase, in which the present cryoprotectant better protects the nanoparticles. For instance, it was previously assessed the effect of the cryoprotectant in function of the freezing rate, on the redispersibility of hydroxypropyl cellulose (HPC) based nanoparticles [9]. Generally, it was found that a fast freezing rate and high concentration of cryoprotectants produced better redispersibility. However, the excessive addition of cryoprotectants was prejudicial in many cases. In other occasions, slower freezing rates originated a better redispersibility, due to the formation of a more cryoconcentrated phase. In another study, it was determined the effect of the molecular weight of cryoprotectants and the freezing rate, on nanoparticles aggregation [149]. An irreversible aggregation occurred mainly during drying than during freezing, but an adequate freezing rate was found to be essential. More homogeneous formulations originated better redispersible powders, and the maintenance of the local concentration of nanoparticles and cryoprotectant was crucial. The nanoparticles redispersibility increased, with an increase in cryoprotectants molecular weight. For the formulation containing PEG, the redispersibility was better in the case of a slow freezing. Such result was explained by the tendency of solutes to be excluded from growing ice crystals. Thus, the differences in the excluding behaviour of nanoparticles and cryoprotectants, may explain the dependence of the redispersibility both on the molecular weight and the freezing rate. Overall, besides the controversy about the best freezing rate may still exist, it is clear that the thermo-physical properties of the formulation have a crucial impact in the nanoparticles aggregation and redispersibility.

2.2.2. Annealing importance in the lyophilization process

The freezing step influences the morphological characteristics of the lyophilized cake [188]. Being the first step in lyophilization and influencing the size of ice crystals, it impacts the primary and secondary drying. Generally, the optimization of lyophilization focus on decreasing the time of the primary drying that is the longest step. Annealing is defined to keep formulations at a subfreezing temperature, above the Tg' for a period of

time, immediately before the primary drying. This process has a crucial influence on the size of ice crystals, which consequently influences the time required for the sublimation process, and improves the homogeneity and appearance of the cake [189]. The Figure 3.10 shows an example of a typical lyophilization cycle containing an annealing step. It has been reported that annealing motivates an increase in the size of ice crystals, and leads to an accelerated primary drying due to the increased diameter of pores in the plug structure that were occupied by ice crystals [190]. Furthermore, annealing decreased also the heterogeneity of the drying rate between samples, achieving a more homogeneous cake aspect. The annealing process may also avoid the formation of the skin layer on the top of the cake, increasing the sublimation rate [7]. This layer may be formed by the deposition of nanoparticles or cryoprotectants during the ice crystallization, hampering the sublimation of water.

Annealing was used in the lyophilization of PCL using as cryoprotectants poly(vinyl pyrrolidone) (PVP) (Tg' of −22 °C) and sucrose (Tg' of −31 °C), and was applied at different temperatures for 1 hour (20 °C, −15 °C and −10 °C) [191]. It was noticed that the sublimation rate was accelerated 17% and 30% for PVP and sucrose, respectively, without influencing the size of nanocapsules. The proposed explanation was due to the increase of the size of ice crystals upon annealing and the decrease of mass transfer resistance by the dried layer. The impact of annealing on secondary drying was dependent on the used cryoprotectant, since it was observed no effect for PVP and a slowdown of the kinetics of secondary drying for sucrose. The use of annealing may also influence the long-term stability of nanoparticles. It was found that annealing and cryoprotectants may change the glass transition temperature (Tg) of starch nanoparticles in about 52-57ºC [192]. However, the residual moisture content was significantly higher for annealed formulations, comparatively to those lyophilized without annealing. This may be explained by the higher size of ice crystals in the annealed samples, leading to more difficult sublimation of water. Besides its benefits, further studies on the application of the annealing process on the lyophilization of nanoparticles are needed.

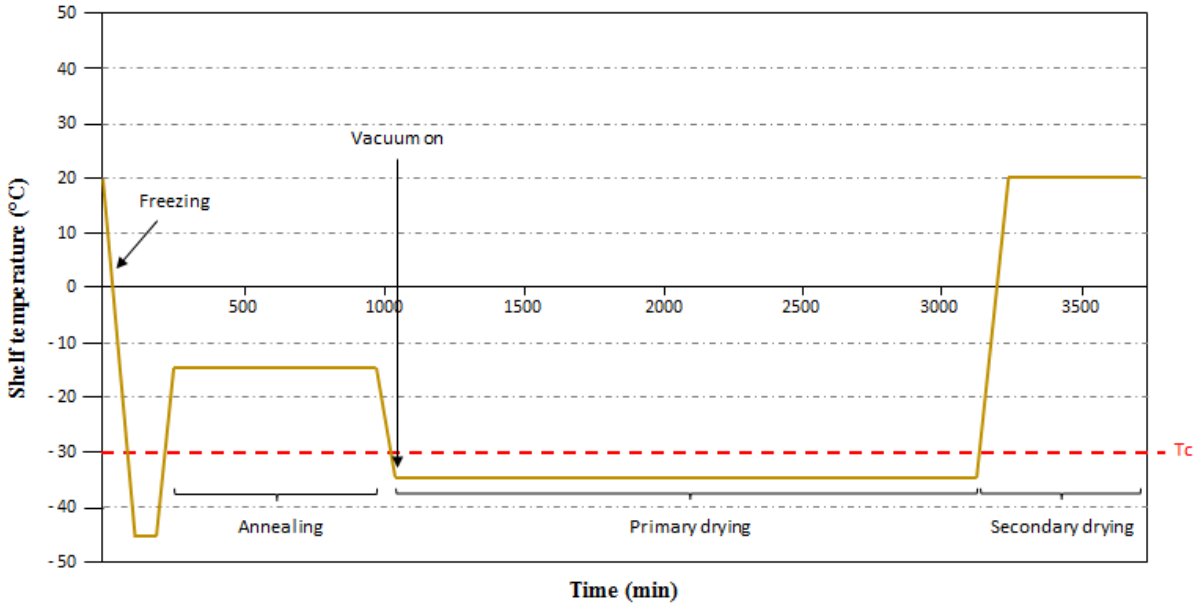

Figure 3.10. Example of a lyophilization cycle showing the steps: freezing, annealing, primary drying and secondary drying. The brown line represents the shelf temperature, and Tc stands for collapse temperature.

2.2.3. Primary drying

During the primary drying step, the water is removed by sublimation from the frozen formulation. To achieve this, the temperature of samples is raised under vacuum. Then, a porous plug is formed, which correspond to the spaces occupied by ice crystals [150]. Generally, the primary drying time depends on the formulation and its depth in the vial. The heat comes from the bottom to the top, and the sublimation front occurs from the top to the bottom of the vial. To avoid product collapse, the primary drying needs to be below the Tc of the product [193]. If product is dried above this critical temperature, it loses its macroscopic structure. The Figure 3.11 shows the difference between a collapsed and a non-collapsed cake. A collapsed cake shrinks upon lyophilization, whereas a non-collapsed cake is characterized by occupying the same volume of the initial suspension.

The natural consequences of product collapse are long reconstitution times and high residual moisture content, which may negatively impact the long-term storage of nanoparticles. In different types of nanoparticles, it was demonstrated that the reconstitution of a collapsed cake was difficult, due to the absence of a porous structure [168, 173, 194]. Most of the research works do not assess the Tc of formulations to infer the lyophilization cycle, and the processing conditions of chamber pressure and shelf temperature are selected empirically. The cake collapse and difficulty of reconstitution may even influence the nanoparticles aggregation upon lyophilization. However,

cryoprotectants may still avoid nanoparticles aggregation in collapsed caked. It was observed no significant changes in the diameter of PCL nanoparticles using glucose, but the product collapse obtained an unacceptable aspect of the cake [153].

Figure 3.11. Lyophilized insulin-loaded PLGA nanoparticles. Non-collapsed cake of nanoparticles dried below its Tc (left vial); and collapsed cake of nanoparticles dried above its Tc (right vial).

2.2.4. Secondary drying

The secondary drying implicates the elimination of the adsorbed water from the product, that did not sublimate upon primary drying because did not previously separate as ice during freezing [193]. The secondary drying removes about 5-10% of the total moisture, and water desorption is facilitated by increasing the shelf temperature, using high-vacuum. However, the temperature of the product during the secondary drying needs to be below its Tg, otherwise it may occur product collapse.

The unfrozen water may be located in the solute phase, both dissolved in an amorphous solid or as hydrate water in a crystalline hydrate, or also adsorbed on the surface of the crystalline product [195]. It is present in an enough amount to cause the rapid degradation of the product. The residual moisture content required for a product influences the time needed for the secondary drying, and it is desirable that for pharmaceutical products, the residual moisture content should be around 1% [150]. Many papers are quite strange, since do not distinguish the secondary drying from the primary drying, and do not show any evaluation of the residual moisture content of the product. It has been demonstrated that a high residual moisture content may destabilize nanoparticles upon storage, due to the crystallization of the containing cryoprotectant [140]. Indeed, the crystallization of amorphous sugars may occur by placing the

formulation at a temperature above its Tg, being also a time-dependent process. Since the residual moisture content may shift the Tg of the formulation to below the temperature of storage, it may cause the crystallization of the formulation upon storage.

In a recent study, the drying time and shelf temperature were optimized, considering the residual moisture content of pharmaceutical products, by a new simulation program of the secondary drying [196]. Using such program, it was possible to predict the secondary drying conditions to obtain the desired residual moisture content, without a trial and error approach.

2.3. Storage of nanoparticles

The enhancement of the long-term stability of a product is the main purpose of lyophilization. Thus, it is important to assure its physical and chemical stability, and prevent degradation reactions such as hydrolysis. Formulations should be stored below its Tg, to guarantee the formulation stability [7]. Every year, different polymeric nanoparticle systems both in suspension and in the lyophilizate form are developed, however their long-term storage stability is often neglected. The long-term stability during storage at 25ºC and 60% of relative humidity (RH) during 12 months, or even at accelerated conditions at 40 ºC and 75% RH during 6 months, as recommended by the International Conference on Harmonization (ICH) guidelines are conditions to assess in stability studies [197]. Additionally to these recommendations, other stability storage conditions have also been used. During the stability studies, at specified time points, at least the drug loading, particle size and zeta potential must be evaluated to assess the stability of nanoparticles. Indomethacin-loaded PIBCA nanoparticles were lyophilized and their stability was assessed during 12 months upon storage at, -30ºC, 4ºC and room temperature [198]. Nanoparticles physical stability was assessed by the drug retained in the nanoparticles upon storage; however the particle size was not evaluated. It was found that upon storage at 4ºC the loss of drug content was 9.3% after 12 months. However, during storage at room temperature the drug loss was 8.5%, 26% and 50.5% upon 2, 4, 6 months, respectively.

Regarding the lyophilizates, other properties such as the cake volume, reconstitution time and residual moisture content, should be also monitored during the stability study. Previously, doxorubicin-loaded $(PEG)_3$–PLA nanopolymersome formulations were lyophilized using different lyoprotectants and stored at 2–8 ºC, 25 ºC/65% RH and 40 ºC/75% RH [199]. The carriers showed no significant change in particle size, polydispersity index (PdI) and zeta potential when stored at 2-8ºC over 12 months. No modifications were observed in terms of cake volume, reconstitution time

and residual moisture content, as well as in the drug content at this storage condition. However, when stored at 40 ºC/75% RH it was observed a significant increase in particle size, PdI and zeta potential. There is a clear influence of the formulation composition in the long-term stability of nanoparticles, since the presence of distinct cryoprotectants in a similar formulation may lead to different outcomes in terms of storage stability. Previously, it was assessed the storage stability of PLGA nanoparticles lyophilized with sucrose, trehalose, and mannitol at 3% (w/v) and stored at 4 ºC, 25 ºC/60% RH, and 40 ºC/75% RH over 3 months [182]. No significant changes on nanoparticles properties were verified, after 3 months of storage at 4ºC in all the formulations. PLGA nanoparticles containing trehalose and sucrose at 3% (w/v) were also stable at 25 ºC/60% RH upon 3 months. In the other storage conditions it was verified considerable changes after 3 months of storage in terms of residual moisture content and particle size and size distribution, which were dependent on the formulation composition.

After lyophilization, the lyophilizate may be exposed to air and reabsorb it into the product. Thus, an adequate stoppering of the product is crucial, since both water and air may cause damages to the lyophilizate, leading to poor product stability. It is advisable that the stoppering of the products should be performed inside the lyophilizer chamber. Stoppering the product under vacuum may be also a good choice to assure product stability. Indeed, a high residual moisture content originated by a poor secondary drying or by a bad stoppering of the product, may originate the cryoprotectant crystallization, leading to nanoparticles destabilization [140]. Other technological methods may be used to estimate the shelf-life of a product. Shelf life computations revealed a shelf-life time of at least 18 months at -20ºC of lyophilized HI-6-loaded albumin nanoparticles containing trehalose 3% (w/v), with no significant degradation of the containing drug [200].

3. The lyophilization equipment

The three parameters to be controlled during lyophilization are shelf temperature, chamber pressure and time. Thus, the lyophilizer needs to be properly designed to manage these processing conditions, and obtain a good lyophilizate. The lyophilization equipment must hold a differential pressure from vacuum to atmosphere, to operate in a low-pressure atmosphere, facilitating the water sublimation. This ability is important to obtain vacuum, however the driving force of water removal is influenced by the condenser. The condenser may be located inside the drying chamber, or be positioned in a separated place between the sample chamber and the vacuum pump. The diagram of a typical lyophilizer is shown in Figure 3.12.

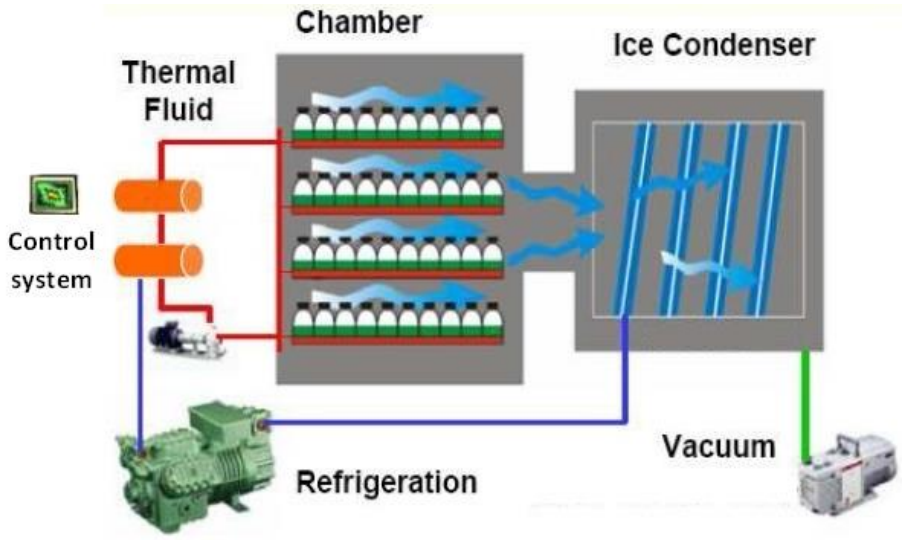

Figure 3.12. Diagram of a tray style lyophilizer. *Adapted from* [201].

A lyophilizer is constituted by a vacuum chamber, in which vials of products are placed on shelves that supply cooling and heating, through a thermal fluid [163]. To the vacuum chamber is also associated a refrigeration unit and a vacuum pump. After product freezing, the chamber is evacuated by the vacuum pump, and the product heating and drying begins. The chamber of the lyophilizer is made of stainless steel, to allow an easy cleaning and thermal conductivity [180]. The door of the chamber may be also made of stainless steel or a clear acrylic material, with an elastomer seal to facilitate vacuum inside the chamber. The shelves may supply or remove thermal energy to the product in function of the lyophilization step. They may be also organized to serve as stoppering platforms, to facilitate the stoppering of vials inside the chamber avoiding the exposition of the product to the atmospheric air [180]. As mentioned above, it is the condenser, which is usually refrigerated by direct expansion of a refrigerant, that produces the driving force to remove water from products [180]. During the primary drying, the temperature of the condenser needs to be usually at least 20ºC lower than the temperature of the product. Therefore, it is the vacuum pump and the condenser that provide the conditions to the removal of water during the product drying.

The control system manages all processing conditions and may be fully automatic. More recent lyophilizers may be connected to a computer, in which all the processing conditions are managed and recorded in real-time. This ability also allows defining different lyophilization cycles, suitable to lyophilize different products. The temperature of the products may be also monitored real-time, by 100-ohm platinum resistance temperature detectors or T-type copper-constantan thermocouples.

4. Characterization of the lyophilized product

To validate an acceptable lyophilization process, it is crucial to characterize both the lyophilizate and the containing nanoparticles upon lyophilization and reconstitution. In this section, several essential characterization methods will be described.

4.1. Macroscopic aspect and reconstitution time of the lyophilizate

The macroscopic appearance of the cake and the occupied volume are important features to assess, and infer a good lyophilization cycle. After lyophilization, the cake should occupy the same volume as the original frozen mass. Otherwise, cake shrinkage or collapse may be observed with prejudicial consequences to product appearance and reconstitution time. The shape, texture and colour modifications of the cake may also indicate detrimental changes in the physical-chemical properties of nanoparticles.

The lyophilizate should be reconstituted in the same volume as the nanoparticle suspension prior to lyophilization, and the time needed to achieve complete reconstitution may be recorded. A good lyophilizate should rehydrates immediately, however in some cases such as cake collapse, the reconstitution time can be long. The complete reconstitution of nanoparticles may be performed immediately by water addition, or by swirling, shaking, vortexing or even sonication. The presence of excipients in formulation may be also important in the nanoparticles resuspension. It was previously demonstrated that cryo- and lyoprotectants facilitated the reconstitution of lyophilized PLA nanoparticles [139]. In another study, it was assessed the influence of different cryoprotectants on the reconstitution of surfactant-free PLGA nanoparticles [178]. No significant change of particle size and a complete reconstitution were verified when trehalose, sucrose and lactose at 2% (w/v) were used, however no satisfactory reconstitution was observed when mannitol 1% (w/v) was used.

4.2. Microscopic observation of the lyophilizate

The microscopic visualization may assess both the microstructure of the lyophilizate, and the maintenance of nanoparticles morphology and stability upon lyophilization. The nanoparticles may be visualized by TEM, scanning electron microscopy (SEM), cryogenic TEM, cryogenic SEM, environmental SEM (ESEM) and atomic force microscopy (AFM). The Figure 3.13 shows the SEM microphotographs of a lyophilizate, and insulin-loaded PLGA nanoparticles after reconstitution. Through such

microscopic techniques, it is possible the visualization of both the morphology and pore network of the lyophilizate, and the shape and size of nanoparticles.

The amorphous matrix of the cryoprotectant PVP, could be visualized by TEM in the outer surface of PCL nanoparticles after reconstitution [191]. Silica nanoparticles lyophilized using trehalose at 5% as cryoprotectant were observed by AFM, and it was found that trehalose formed a matrix embedding the nanoparticles [168]. In another study, lyophilized PCL nanoparticles stabilized by HPβCD were also visualized after reconstitution by SEM and ESEM [140]. An amorphous continuous matrix embedding the nanoparticles was also observed. ESEM demonstrated that PCL nanoparticles maintained their spherical monodisperse shape upon lyophilization. These results showed that the observation of nanoparticles by AFM and SEM is difficult, when the concentration of cryo- or lyoprotectant is higher than 5%. On its turn, TEM facilitates the observation of lyophilized nanoparticles after samples dilution.

The ESEM technique allows managing the sample dehydration, by reduction of temperature and pressure in the sample chamber. Nanoparticles may be observed in a hydrated form without a complete drying, preventing the observation of individual nanoparticles. Furthermore, it is not required a sample preparation prior microscopic visualization. Overall, the ESEM is the best technique to observe lyophilized nanoparticles in a hydrated form, and present an advantage over SEM, since do not requires any conductive coating of hydrated samples.

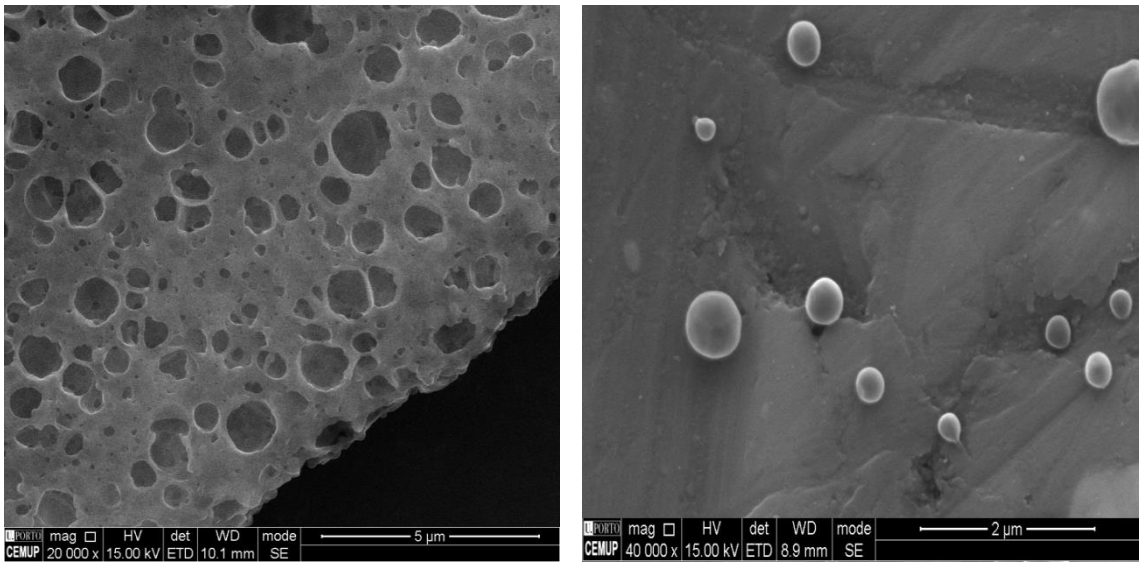

Figure 3.13. SEM microphotograph of the lyophilizate of insulin-loaded PLGA nanoparticles, containing sucrose 10% (w/v) (left microphotograph); and SEM microphotograph of insulin-loaded PLGA nanoparticles after reconstitution (right microphotograph).

4.3. Analysis of powder surface

The elemental composition of the lyophilizate of nanoparticles may be assessed by electron spectroscopy for chemical analysis (ESCA). Such technique is based on the emission of electrons from materials, at a characteristic energy of atoms. It has been used to assess the surface of ice crystals during lyophilization [202], and the modification of nanoparticles surface [203]. The adsorption of proteins into an ice/liquid interface during freezing may lead to the loss of its native structure, resulting in its surface induced denaturation [204]. The surface tension of protein solutions in such interface may be decreased by surfactants, and this ability may be evaluated by ESCA. This kind of analysis may be also applied to nanoparticle formulations. ESCA assessments revealed the presence of PCL nanoparticles, at the powder surface of lyophilized formulation, containing a matrix of PVP and sucrose as cryoprotectants [140]. Thus, ESCA may be used to locate the presence of nanoparticles, ligands or even drugs in a lyophilizate.

4.4. Thermal analysis and lyophilization microscopy

The thermal analysis may be performed by differential scanning calorimetry (DSC). The critical temperatures of a formulation, such as Tg' and Tg may be assessed by this technique, and then used to infer an adequate lyophilization cycle. As mentioned above, to guarantee a good quality of the lyophilizate and long-term storage stability, a nanoparticle formulation should be frozen below its Tg', and both the secondary drying and storage should occur below its Tg. Furthermore, DSC allows evaluating the interaction between the nanoparticles and cryoprotectants.

Besides being an analysis performed prior to nanoparticles lyophilization, the lyophilization microscopy is an important technique to guarantee the achievement of a product with good quality. Such technique allows the assessment of the Tc or Teu, for amorphous or crystalline formulations, respectively, which are crucial to define the temperature at which the primary drying should occur. The lyophilization microscopy allows the study of the lyophilization process in real-time, and the observation of the sublimation front. Thus, it is possible to determine the exact temperature at which the formulation starts to lose its structure and collapses.

4.5. Determination of residual moisture content

The residual moisture content of a lyophilizate is mainly caused by an inefficient secondary drying, with a poor desorption of water from the product. This may drastically influence the structure and the thermal properties of lyophilized nanoparticles. High residual moisture content may lead to an unexpected dissolution of the lyophilizate immediately after lyophilization, and to a poor long-term storage stability of nanoparticles. Several analytical methods such as a gravimetric technique, thermal gravimetric analysis or Karl Fischer titration, may be used to quantify the residual moisture content of the lyophilizate. For pharmaceutical products, the residual moisture content should be around 1% [150].

4.6. Particle size and zeta potential of nanoparticles, and drug content upon lyophilization

The particle size after reconstitution may be assessed by photon correlation spectroscopy or other technique. The maintenance of the diameter of nanoparticles after lyophilization is a good indicator of a good lyophilization process. The ratio of nanoparticles size between that after and before lyophilization should be evaluated. A ratio around 1 indicates the maintenance of nanoparticles physical stability, whereas a ratio different from 1 may indicate aggregation or degradation of nanoparticles. Simultaneously, the PdI may be also evaluated upon lyophilization and compared with that obtained before lyophilization.

The evaluation of the zeta potential may be performed by phase analysis light scattering, and is useful to assess if any modification of nanoparticles surface occurred during lyophilization. It may be also used to assess the interaction between nanoparticles and the excipients present in formulation. It was reported that after addition of sucrose 10% (w/v), the zeta potential of PCL nanoparticles modified from −40.9 mV to −20.4 mV [161]. This could be explained by the hydrogen bonding between sucrose and nanoparticle surface that masks the nanoparticles surface. After lyophilization, the decrease in the negative charge was accentuated, due to a rearrangement of the surfactant at nanoparticles surface.

The drug content of nanoparticles may be determined by a high performance liquid chromatography (HPLC), ultraviolet-visible (UV/Vis) spectroscopy or other quantification method. It is important to evaluate if occurs any leakage of the drug upon lyophilization. An adequate lyophilization process, that do no damages the nanoparticles

integrity, allows the retention of the drug entrapped into nanoparticles, which is crucial to the desired therapeutic effect.

5. Lyophilization of protein-loaded nanoparticles

Through the developments of the biotechnology field in the last decades, peptide and protein drugs have been developed with the aim of improving the patients quality of life [205]. They have been used to treat severe health problems, such as genetic and enzymatic disorders, autoimmune diseases and infections or even cancer [206]. Therapeutic proteins are mainly delivered in an invasive way, such as through subcutaneous injection, with a repeated administration to obtain therapeutic levels, mainly due to its rapid degradation and elimination [207]. Furthermore, the low permeation through biological barriers, such as the intestinal epithelium, turns their administration to be limited to the parenteral route. The encapsulation of therapeutic proteins into polymeric nanoparticles is a good strategy to avoid all these issues, since the polymeric matrices may protect proteins from *in vivo* hydrolytic and enzymatic degradation, preserving their structural stability and bioactivity, and consequently improve their *in vivo* half-life and bioavailability [2]. The ability of nanoparticles to enhance the permeability of proteins through epithelial barriers is important to improve their bioavailability [3]. Additionally, nanoparticles may be useful to deliver proteins in a sustained manner, reducing the required number of administration, and to target protein delivery to specific organs or tissues [208].

The lyophilization of therapeutic proteins is commonly used to improve their long-term stability. Similar stresses suffered by nanoparticles during lyophilization, are also suffered by proteins, which may lead to their instability and loss of bioactivity [7]. The influence of lyophilization on the stability of proteins have been investigated, and it has been described that protein denaturation and aggregation may occur both during the freezing or drying steps [209, 210]. Distinct findings have been reported, showing that the stresses suffered have a great dependence both on the protein type and on the lyophilization process. For instance, it was previously described that the ice formation was the critical process that influenced the stability of lactate dehydrogenase (LDH) [211]. It was also reported that proteins can be lyophilized above Tg' without vitrification, mainly because the protein unfolding occurs slowly during lyophilization, since this process is directly related with the system viscosity [212]. However, in another study, it was compared the effect of the primary drying and secondary drying stresses, and it was observed that the latter was the one that critically influenced the LDH stability [213]. A complementary study revealed that the stability of LDH was significantly influenced by

the duration and temperature of the secondary drying [214]. The vitrification and direct interaction of excipient was found to be essential on protein stabilization. Several excipients such as sugars and surfactants may be used to improve the stability of proteins [215]. It may be inferred that proteins loaded into nanoparticles are subjected to similar stresses suffered by protein formulations upon lyophilization. In addition, it is expected that both the nanoparticles and used excipients may be useful in the preservation of the structural stability of the loaded protein. Studies on lyophilization of protein-loaded nanoparticles have been focused more on the carrier stability, rather than in the stability of the loaded protein [216-218]. The therapeutic activity of proteins is directly related with their conformational structure and integrity, so this characterization is important to assess the influence of lyophilization in the stability of proteins loaded into polymeric nanoparticles. An important problem in the analysis of protein loaded into nanoparticles upon lyophilization is that many analytical techniques require the extraction of protein from nanoparticles [219]. However, there are other techniques that allow a non-invasive analysis of proteins in solid state, such as FTIR, ESCA, dielectric spectroscopy and solid-state nuclear magnetic resonance (NMR). The extraction method may originate artifacts, prejudicial to the protein characterization [220-222]. For example, the protein quantification may be difficult since it may occur a preferential extraction of protein molecules that are easier to diffuse out of nanoparticles. Furthermore, the aggregation extension may be over- or underestimated when the extraction method lead to aggregates formation or aggregates dissolution, respectively. The extraction media itself may induce irreversible conformational modifications, which is a problem when it is required the study of the conformation and bioactivity of the loaded protein.

Most of the works on the lyophilization of protein-loaded nanoparticles focus more on the analysis of the bioactivity of proteins, rather than the characterization of their conformation. Previously, it was demonstrated that the combination of lyophilization and a cross linking treatment was important to stabilize, and increase the bioefficiency of insulin-loaded chitosan nanoparticles [223]. In another work, it was evaluated the ability of amino functionalized mesoporous silica nanoparticles to stabilize ovalbumin, a model antigen, at room temperature [224]. The protein was adsorbed to nanoparticles and lyophilized using trehalose 5% (w/v) and PEG8000 1% (w/v). Ovalbumin has a shelf-storage stability at room temperature of just 16 hours, and using the proposed approach it was observed maintenance of the immunological activity of ovalbumin and the structure of nanoparticles after 2 months of storage. After reconstitution, nanoparticles were administered to mice and they induced humoral and cell-mediated immune responses, demonstrating the bioactivity of ovalbumin.

Besides there are just a few works that evaluate the structural stability of proteins loaded into nanoparticles upon lyophilization, this characterization is crucial to better predict and understand both the activity of proteins and potential detrimental side effects after administration. CD assessments demonstrated that the secondary structure of bovine serum albumin (BSA) was preserved upon *in vitro* release from lyophilized poly(lactic-co-glycolic-co-hydroxymethylglycolic acid) nanoparticles [225]. Using the same technique, it was demonstrated that the structure of insulin present in a polyelectrolyte complex nanoparticles of amino poly(glycerol methacrylate)s, was preserved after lyophilization [226]. Insulin has been used as a model of therapeutic protein, in the study of structural stability of proteins loaded into polymeric nanoparticles upon lyophilization [175, 227]. It was evaluated the influence of lyophilization using cryoprotectants, on the structure of insulin loaded into PLGA nanoparticles upon 6 months of storage [175]. FTIR assessments demonstrated that insulin structure was preserved in about 88% after encapsulation, decreasing to 71% upon lyophilization. The cryoprotectants used were trehalose, glucose, sucrose, fructose and sorbitol at 10% (w/v), and they presented different performances on the stabilization of the loaded protein. Interestingly, the formulations collapsed upon lyophilization, revealed better protein stabilization during storage. Lyophilized nanoparticle formulation containing sorbitol, demonstrated the most similar structural changes of insulin within the storage conditions, achieving an insulin structural preservation of about 76, 80, and 78% after stability at 4 °C, 25 °C/60% RH, and 40 °C/75% RH, respectively. In another study from the same authors, an interesting approach was developed by co-encapsulating lyoprotectants into PLGA nanoparticles together with insulin [227]. FTIR and CD evaluations revealed that the co-encapsulating lyoprotectants better preserved the structure of insulin after lyophilization in about 82-87%, comparatively to just 72% in absence of lyoprotectant.

6. Conclusion

The lyophilization process is fundamental in the improvement of the long-term stability of nanoparticles. The lyophilization of nanoparticles has been mostly based on empiric principles and trial and error approaches, without considering the main principles involved. Therefore, prior lyophilization, the nanoparticle formulation should be physical-chemically characterized and the processing parameters of lyophilization need to be optimized regarding the formulation characteristics. The use of excipients, such as cryo- and lyoprotectants with the purpose of nanoparticles stabilization should also be carefully thought, since there is no straightforward relationship between their use and the

stabilization of nanoparticles. The storage conditions are also important, on the long-term stability of the lyophilized nanoparticles. The needed processing conditions of the lyophilization process, should also be inferred considering the architecture of the lyophilizer. The proper characterization of both the lyophilizates and nanoparticles upon lyophilization is fundamental to achieve a good lyophilized product, and also to guarantee the preservation of nanoparticles stability. Regarding the lyophilization of protein-loaded polymeric nanoparticles, together with the analysis of the stability of the carrier, it is also crucial to assess the conformation and the maintenance of protein structure upon lyophilization.

This chapter may contribute to highlight all the parameters involved in the lyophilization of polymeric nanoparticles, in order to obtain a good lyophilizate and nanoparticles with long-term stability. Thus, hereafter empirical approaches on lyophilization of nanoparticles should be abandoned, and the focus should go on optimizing the lyophilization process to meet the specificity of the physical-chemical properties of nanoparticles. Furthermore, it is important to bring the recent developments on the lyophilization technology into the nanoparticles lyophilization. Such developments allow a more precise control and management of lyophilization processing conditions in real-time. In addition, the application of quality by design (QbD) and process analytical technology (PAT) approaches need to be more deeply applied in the nanoparticles lyophilization. Finally, another important concern that is one of the major challenges to focus in the future is the scaling up of the lyophilization of nanoparticles, assuring their stability, allowing polymer-based nanoparticle products to reach the market.

Chapter 4

Optimization of Insulin-loaded PLGA Nanoparticles and Effect of Cryoprotectants on their Porosity and Stability upon Lyophilization

Partially published in:

Pedro Fonte, Sandra Soares, Ana Costa, José Andrade, Vítor Seabra, Salette Reis, Bruno Sarmento, Effect of cryoprotectants on the porosity and stability of insulin-loaded PLGA nanoparticles after freeze-drying, Biomatter, 2 (2012) 329-339.

1. Introduction

The delivery of therapeutic proteins may occur under stress conditions, leading to their aggregation or denaturation with unpredictable side effects, such as toxicity or immunogenicity [228]. To mitigate these problems, proteins are often encapsulated into nanoparticles. These carriers are submicron sized colloidal systems prepared from natural or synthetic polymers, suitable to deliver both small and macro- molecules on a targeted or localized manner. They are able to further protect proteins from a harsh environment, as observed for instance in the gastrointestinal tract due to pH and proteolytic action of enzymes, and deliver it on a sustained manner avoiding repeated dose administration. PLGA is one of the most used synthetic polymers on nanoparticles production, mainly because of its good sustained release properties, biodegradability, biocompatibility, variable mechanical properties and nontoxic properties [147]. A minimal systemic toxicity is observed on the use of this polymer for drug delivery and biomaterial applications [229].

As delivery systems the most important characteristics of nanoparticles are the size, AE and release profile. Their shape and surface charge are also important features to control. Since nanoparticles are produced to be administered to the human body and interact with cells, it is imperative to produce them with a proper size, shape and surface charge, otherwise severe toxicity problems may occur. From an industrial and economic perspective, the AE is crucial especially in the case of proteins which are expensive products. Different techniques of production may be employed to control all these features, and for hydrophilic molecules such as proteins, the double emulsion solvent evaporation technique is one of the most used methods. This technique may be responsible for the formation of pores on the nanoparticles surface due to the evaporation of the solvent. These pores may play a role on protein release rate and on its stability, they may form open pathways for protein denaturation by external factors. The use of nanoparticles formulation has some limitations mainly due to problems related with the integrity of the liquid suspension [167]. To avoid some stability problems, surfactants are usually included in formulation to stabilize the suspension by its direct adsorption to nanoparticles surface. However, some aggregation may still be observed during storage [157, 162]. In addition, the chemical stability of the polymeric matrix of nanoparticles [6], and the protein must be taken into account in order to avoid the formation of undesired degradation products and premature release of protein.

Lyophilization is regarded as one of the most useful methods to stabilize and handle colloidal systems. Otherwise, nanoparticles formulation may suffer detrimental

changes during storage. Proteins instability in aqueous systems is also overcome by removing water by lyophilization [204]. Various stability problems affecting nanoparticles have been reported [168]. Regarding PLGA-based nanoparticles, the principal concern is the hydrolytic instability of the polymer in aqueous suspension. Hence, lyophilization is an important method to stabilize PLGA nanoparticles, by avoiding hydrolytic degradation in aqueous suspensions [182].

As discussed above, the control of nanoparticles characteristics is crucial, so it is necessary to improve its stability during storage to assure that the characteristics are maintained during shelf-life. The lyophilization process may also result in changes of nanoparticles physical properties, affecting particle size and release characteristics, with consequent effect on the encapsulated protein release and stability. Therefore, different excipients like trehalose, sucrose, fructose, glucose and sorbitol may be used as cryoprotectant agents to increase nanoparticles physical stability during lyophilization, preventing their aggregation and protecting them against the mechanical stress of ice crystals. These sugars used as cryoprotectants are important, because they affect the glass transition temperature (Tg' and Tg), which is important to obtain a lyophilized cake with a stable amorphous form, a high redispersion speed, an appropriate residual moisture content, and a good protein protection and stabilization upon storage [8, 230]. How the different cryoprotectants may influence the porosity of nanoparticles, and therefore the protein release and stability is barely known.

The main objective of this chapter was to develop and optimize a formulation of insulin-loaded PLGA nanoparticles with good physical-chemical properties and assess how lyophilization using a standard cycle and different cryoprotectants may influence the stability and porosity of nanoparticles, which is an important feature on PLGA nanoparticles release properties, constituting also a pathway for protein instability.

2. Materials and Methods

2.1. Materials

For the production of nanoparticles, it were used PLGA 50:50 (Evonik Industries AG, Resomer® RG 503 H), PLGA 75:25 (Purac Biomaterials, Purasorb® PDLG 7502), PVA (Sigma-Aldrich, P1763), Pluronic® F-127 (Sigma-Aldrich, P2443), Tween® 80 (Merck, 822187), dichloromethane (Sigma-Aldrich, 32222) and recombinant human insulin (Sigma-Aldrich, 91077C). The cryoprotectants used were trehalose (Sigma-Aldrich, 90210), sucrose (Sigma-Aldrich, 84100), fructose (Sigma-Aldrich, 47740), glucose (Sigma-Aldrich, 49152) and sorbitol (Sigma-Aldrich, 97336). Acetonitrile HPLC

Gradient Grade (Fischer Scientific, A/0627/17) and trifluoroacetic acid (Acros Organics, 139721000) were used in the HPLC measurements and PBS (Sigma-Aldrich, P4417) was used in the *in vitro* release study. Milli-Q water was produced in-house.

2.2. Preparation of PLGA nanoparticles

Different formulations of nanoparticles were prepared with PLGA 50:50 and PLGA 75:25. Using each polymer to produce the nanoparticles, it was used different surfactants at two different concentrations, namely PVA, Pluronic and Tween at 1% and 2% (w/v). The method for the nanoparticles preparation was a modified solvent emulsification-evaporation method, based on a w/o/w double emulsion technique [231, 232]. Briefly, 200 mg of polymer was dissolved in 2 ml of dichloromethane. Then, 0.2 mL of a 20 mg/mL insulin solution in HCl 0.1 M was added to the polymeric solution, and homogenized using a Bioblock vibracell 75186 sonicator (Fischer Bioblock Scientific, Illkirch, France), during 30 seconds with 70% of amplitude. This primary emulsion was poured into 25 mL of each PVA, Pluronic or Tween solution at the two different concentrations and then homogenized for 30 seconds using the same equipment. The organic solvent was then removed by evaporation, during 3 hours under magnetic stirring. The nanoparticles were purified three times by centrifugation using a Heraeus Megafuge 1.0 R centrifuge (Thermo Scientific, Asheville, NC, USA) at 4300 rpm for 50 minutes, and redispersed in water before storage at 4ºC for further analysis.

After optimization of the formulation, the optimal formulation was produced by the same methodology using PLGA 50:50 and PVA 2% as a surfactant and 0.2 mL of a 150 mg/mL insulin solution in HCl 0.1 M. The produced nanoparticles were then purified three times by centrifugation at 4300 rpm for 50 minutes at 4ºC, and redispersed in water prior to lyophilization and storage.

2.3. Lyophilization of nanoparticles

The cryoprotectants used were trehalose, sucrose, fructose, glucose and sorbitol at a concentration of 10% (w/v). A control group of nanoparticles lyophilized with no cryoprotectant was also included in the study, and all this different cryoprotectant conditions were performed in triplicate. Samples were poured into semi-stoppered glass vials with slotted rubber closures and frozen at -80°C for 2h and then dried in a Modulyo 4K lyophilizer (Edwards, Crawley, West Sussex, UK) at 0.09 mbar for 72h, being maintained at the condenser surface temperature of -60ºC.

2.4. Lyophilized samples reconstitution

The lyophilizates were reconstituted by slowly adding distilled water in the inside wall of the vial, and then maintained during 10 minutes to ensure the proper cake wetting. After such period of time, samples were gently shaken in a Vortex Mixer ZX Classic (Velp Scientifica, Usmate, Italy) for 3 minutes to complete homogenization. After reconstitution, samples were physical-chemically characterized.

2.5. Particle size and zeta potential analyses

Samples were diluted with Milli-Q water to a suitable concentration for both particle size and zeta potential analyses. Particle size was analysed by dynamic light scattering using a 90Plus Particle Size Analyzer (Brookhaven Instruments Corporation, NY, USA). The zeta potential was determined by phase analysis light scattering using a ZetaPALS Zeta Potential Analyzer (Brookhaven Instruments Corporation, NY, USA). All measurements were performed in triplicate.

2.6. Insulin association efficiency

The AE was determined indirectly. The amount of insulin entrapped into the PLGA nanoparticles was calculated by the difference between the total amount used to prepare the nanoparticles, and the amount of insulin that remained in the supernatant after nanoparticles isolation by centrifugation in a Beckman Optima TL ultracentrifuge (Beckman Coulter, Brea, CA, USA) at 20,000 rpm for 15 min at 4ºC. The equation below summarizes this concept:

$$AE = \frac{\text{Total amount of insulin} - \text{Free insulin in supernatant}}{\text{Total amount of insulin}} \text{ x } 100 \qquad \textbf{(Eq. 4.1)}$$

The insulin concentration was determined by a HPLC-UV method previously developed and validated by our group [233]. Thus, the measurements were performed on a Merck-Hitachi LaChrom HPLC instrument (Merck, Whitehouse Station, NJ, USA) equipped with a XTerra RP 18 column, 5 µm particle size, 4.6 mm internal diameter × 250 mm length (Waters, Milford, MA, USA) and a LiChrospher 100 RP-18, 5 µm particle size guard column (Merck, Darmstadt, Germany). All measurements were performed in triplicate.

2.7. Transmission electron microscopy analysis

Nanoparticles were observed by TEM, in order to characterize its morphology. Samples were placed on a grid, treated with uranil acetate and then observed in a JEOL JEM-1400 Electron Microscope (JEOL Ltd.,Tokyo, Japan).

2.8. Scanning electron microscopy analysis

The surface morphology of nanoparticles was observed by SEM on a FEI Quanta 400 FEG SEM (FEI, Hillsboro, OR, USA). Nanoparticles were resuspended and purified three times with distilled water by centrifugation in a Beckman Optima TL ultracentrifuge (Beckman Coulter, Brea, CA, USA) at 20,000 rpm for 15 min at 4ºC, to remove the dissolved cryoprotectant. Then, samples were mounted onto metal stubs and vacuum-coated with a layer of gold/palladium before observation.

2.9. Insulin *in vitro* release study

Insulin-loaded PLGA nanoparticles were dispersed in 20.0 mL of pH 7.4 PBS solution and incubated at 37°C under magnetic stirring at 100 rpm. Aliquots were taken at predetermined time intervals of 0.5, 1, 2, 4, 8, 24 and 48 hours and replaced with fresh medium kept at the same temperature. The collected samples were centrifuged, and the content of insulin in the supernatant was determined by HPLC. All samples were run in triplicate.

2.10. Statistical analysis

The statistical analysis was done using the GraphPad Prism Software vs. 5.0 (GraphPad Software Inc., La Jolla, CA, USA), and differences between the formulations were compared within a Tukey *post hoc* test, and considered to be significant at a level of $p < 0.05$.

3. Results and discussion

3.1. Optimization of PLGA nanoparticles formulation

Two different ratios of PLGA, 50:50 and 75:25, were used to produce the insulin-loaded PLGA nanoparticles. Dichloromethane was used to dissolve PLGA in each formulation, and as it is removable after nanoparticles preparation, its possible toxicity is avoided. It was also used three different surfactants, namely PVA, Pluronic and Tween at two different concentrations, 1% and 2%, to increase nanoparticles stability. Thus, these preliminary studies aimed to produce nanoparticles both with the lower obtainable mean particle size and higher AE. Furthermore, the surface charge of nanoparticles must be negatively charged due to its polymeric matrix. These results are shown in Table 4.1. The optimization was performed to obtain the formulation with the best physical-chemical properties to be used on further experiments.

Table 4.1. Physical-chemical properties of insulin-loaded PLGA nanoparticles (n = 3, mean ± SD).

Polymer	Surfactant	Particle Size (nm)	PdI	Zeta Potential (mV)	Insulin AE (%)
PLGA 50:50	PVA 1%	437 ± 4^{b}	0.37 ± 0.03	10.1 ± 2.4^{b,c}	61.1 ± 11.4^{a}
	PVA 2%	256 ± 17^{c}	0.20 ± 0.07	-13.2 ± 1.8^{d}	78.9 ± 4.1^{c}
	Pluronic 1%	1289 ± 232^{a}	0.57 ± 0.06	10.8 ± 2.9^{b,e}	21.7 ± 15.9^{b}
	Pluronic 2%	426 ± 13^{b}	0.22 ± 0.04	-9.6 ± 3.4^{f}	31.4 ± 7.8^{d}
	Tween 1%	455 ± 23^{b}	0.21 ± 0.05	-8.3 ± 0.5^{a}	0
	Tween 2%	565 ± 34^{d}	0.35 ± 0.01	-8.3 ± 1.8	0
PLGA 75:25	Pluronic 1%	419 ± 28^{b}	0.31± 0.05	-12.3 ± 1.5^{a,e}	12.9 ± 7.1
	Pluronic 2%	357 ± 22^{b}	0.21± 0.03	13.4 ± 2.3^{c,f}	8.7 ± 5.4
	Tween 1%	374 ± 61^{b}	0.25 ± 0.15	14.7 ± 1.6^{b}	6.6 ± 2.3
	Tween 2%	121 ± 12^{a}	0.49 ± 0.04	-9.4 ± 2.3^{b,d}	7.2 ± 1.1

If the formulations were significantly different between them ($a \neq b$; $c \neq d$; $e \neq f$, $p < 0,05$).

Insulin-loaded PLGA nanoparticles were produced to take advantage of the better sustained release properties and protection of the encapsulated protein. A clear advantage of the used encapsulation technique, is the avoidance of thermal or pressure stresses that can damage the protein structure. This technique also allows to produce other kind of nanoparticles such as lipid-based nanoparticles [234]. The preliminary study (Table 4.1) showed that both PLGA ratios were able to produce nanoparticles, with the exception of PLGA 75:25 when combined with PVA. Thus, it may be concluded that with the used methodology, such combination was not able to produce stable nanoparticles.

The results of mean particle size showed that generally, the higher concentrations of surfactant resulted in a reduction of the particle size, however with just

a significant difference ($p < 0.05$) for PLGA 50:50/Pluronic formulations. This occurs mainly because the surfactant is able to reduce the surface tension, and promote the particle division during homogenization. The decrease in particle size highly increases the surface area, stabilizing the nanoparticles, however, when higher concentrations of surfactants are used, the risk of toxic side effects increases [235]. This problem was mitigated by removing the surfactant after nanoparticles production. Overall, it was also verified that when the surfactant concentration increased the PdI decreased, except for formulations in which Tween was used. This may be also explained by the higher stabilization of higher concentrations of surfactants, during nanoparticles production.

The surface charge is an important feature, since nanoparticles are intended to interact with cells, the charge may play an important role on such interaction. The PLGA nanoparticles have negative surface charge due to its polymeric matrix [208]. This negative surface charge was observed in the majority of the formulations, thus being an indicator of a good nanoparticles production. In other formulations, the surface charge was positive which may be explained by an ineffective nanoparticles formation. It is also shown in Table 4.1, that for the PLGA 50:50/PVA, PLGA 50:50/Pluronic, and PLGA 75:25/Tween formulations, at a surfactant concentration of 1% the surface charges of nanoparticles were positive and at 2% the surface charges were negative. This is because for those formulations, the higher concentration of surfactant better stabilized the nanoparticles, thus achieving the expected negative values characteristic of the polymeric matrix. Therefore, at a higher concentration of surfactants, the emulsification may have occurred more effectively and faster, forming a good emulsion and nanoparticles. When a lower concentration of surfactant was used, the emulsification process was not so effective and the surfactant remained attached to the polymer, becoming the surface charge of nanoparticles positively charged.

From an industrial point of view, the AE is a crucial feature, since most of the therapeutic proteins encapsulated into nanoparticles are quite expensive. It was observed that nanoparticles produced with PLGA 75:25 obtained nanoparticles in a range of 100-450 nm but with low values of AE. Thus, the higher proportion of lactic acid of the polymer may hinder the ability of nanoparticles to encapsulate proteins. Essentially considering this result, the formulations containing PLGA 75:25, were not considered for further experiments. On one hand, formulations using PLGA 50:50/PVA, obtained significantly higher ($p < 0.05$) AE values for both surfactant concentrations, being even higher for the higher surfactant concentration. On the other hand, formulations using PLGA 50:50/Tween obtained 0% of AE for both surfactant concentrations, probably because the surfactant did not promote the emulsification properly, and therefore insulin was not encapsulated. This may be due to a possible interaction between the surfactant

and the polymer itself leading to an extrusion of insulin from the inner core of the forming particle. This may be also the explanation why it was achieved such a low AE when Tween 1% and 2% were used to produce PLGA 75:25 nanoparticles.

Regarding all the results, it was selected just one formulation of PLGA 50:50 nanoparticles for further experiments because the AE obtained for PLGA 75:25 nanoparticles, even using different surfactants, was not satisfactory. Thus, the formulation produced using PLGA 50:50/PVA 2% was selected for further experiments regarding its lower mean particle size, higher AE and the negatively charged surface. The mean particle size of these nanoparticles was around 250 nm and the AE was about 80%, which was a good achievement. In fact, the AE of hydrophilic molecules is improved by the double-emulsion technique, allowing the encapsulation of therapeutic proteins [235]. PVA is able to produce stable nanoparticles with a small size and a narrow PdI [151, 152]. It was also reported, that a fraction of PVA remains associated with the surface of nanoparticles even after nanoparticles washing. Thus, the presence of the PVA layer on nanoparticles surface may improve also their freezing resistance, which stabilizes nanoparticles during lyophilization [236].

3.2. Physical-chemical characterization of PLGA 50:50/PVA 2% nanoparticles

The optimized formulation, PLGA 50:50/PVA 2%, was formulated encapsulating a higher amount of insulin (0.2 mL of 150 mg/mL insulin solution) to be used in further experiments. It was produced loaded and unloaded PLGA nanoparticles and their properties are shown in Table 4.2.

Table 4.2. Physical-chemical properties of PLGA 50:50/PVA 2% nanoparticles after production (*n* = 3, mean ± SD).

Formulation	Particle Size (nm)	PdI	Zeta Potential (mV)	Insulin AE (%)
Insulin-loaded nanoparticles	446 ± 30	0.26 ± 0.03	-24.2 ± 3.4	87.4 ± 0.2
Unloaded nanoparticles	247 ± 21	0.20 ± 0.06	-7.5 ± 2.3	-

After insulin loading into PLGA nanoparticles, its particle size increased about 1.8 fold comparatively to the unloaded nanoparticles. This may be explained by a higher encapsulation and adsorption of insulin on the particle surface increasing the particle size, which may also explain the increase of the negative charge on the loaded nanoparticles surface up to -24.2 ± 3.4 mV, since at pH 7.4 the charge of insulin is

negative [237]. This increase allows the increment of nanoparticles stability in the formulation. An AE of 87.4 ± 0.2 % was observed, which is a very good achievement. Therefore, even encapsulating a higher amount of insulin, the AE was even higher. This may be also explained by a higher amount of insulin encapsulated and of insulin that is associated with the nanoparticles surface and more electrostically linked, thus increasing insulin AE. Furthermore, comparatively to the results shown on Table 4.1 for the PLGA:PVA 2% formulation, after encapsulating a higher amount of insulin it was obtained an increase on particle size up to 446 ± 30 nm, and the surface charge became more negative which is once more explained by a higher adsorption of insulin on the particle surface.

3.3. Physical-chemical characterization of PLGA 50:50/PVA 2% nanoparticles after lyophilization

As discussed above, the major problem limiting the use of nanoparticles in a colloidal suspension is its physical instability by aggregation and particle fusion or/and the chemical instability due to hydrolysis of the polymer and the chemical reactivity during extended periods of storage [174]. Hence, lyophilization comes to the front line as an optimal method to stabilize nanoparticles. However, during lyophilization in the freezing step, the concentration of the nanoparticles system increases during time, which may induce aggregation and sometimes irreversible fusion of nanoparticles. In addition, the ice crystallization induces mechanical stresses, which leads to nanoparticles destabilization. Thus, cryoprotectants must be added to nanoparticles formulation prior freezing to protect and further stabilize nanoparticles. The presence of cryoprotectants in formulation is also important to avoid aggregation after redispersion of the lyophilizate [178]. Trehalose for instance showed to facilitate the resuspension of PLA-PEO nanoparticles after lyophilization [157]. The insulin-loaded PLGA nanoparticles were lyophilized with and without cryoprotectants added, and their physical-chemical properties were assessed after lyophilization and resuspension (Table 4.3).

Table 4.3. Physical-chemical properties of insulin-loaded PLGA nanoparticles after lyophilization with and without cryoprotectants (*n* = 3, mean ± SD).

Formulation	Particle Size (nm)	PdI	Zeta Potential (mV)
PLGA nanoparticles	422 ± 60	0.37 ± 0.02	-28.2 ± 5.8
PLGA nanoparticles + 10% (w/w) Trehalose	396 ± 16	0.32 ± 0.05	-42.9 ± 1.7
PLGA nanoparticles + 10% (w/w) Sucrose	559 ± 16	0.35 ± 0.03	-39.5 ± 2.9
PLGA nanoparticles + 10% (w/w) Glucose	365 ± 28	0.39 ± 0.01	-36.7 ± 6.0
PLGA nanoparticles + 10% (w/w) Fructose	712 ± 55	0.39 ± 0.01	-38.2 ± 1.7
PLGA nanoparticles + 10% (w/w) Sorbitol	469 ± 23	0.37 ± 0.03	-36.3 ± 1.9

It was observed that after lyophilization with no cryoprotectant added, the particle size and the zeta potential values remained in the same order of values. The negative surface charge even slightly increased, which showed the better colloidal stability of nanoparticles after lyophilization. It was also verified that further adding cryoprotectants prior lyophilization, the negative surface charge increased more than 1.5 fold for all the cryoprotectants. The trehalose-added sample showed the highest negative value of -42.9±1.7 mV, which may be due to the adsorption of cryoprotectants on nanoparticles surface. These results prove that the different cryoprotectants have a more stabilizing effect on nanoparticles upon lyophilization. Regarding the particle size values, it was verified that on one hand, adding trehalose and glucose decreased the particle size after lyophilization respectively to 396 ± 16 nm and 365 ± 28 nm, and on the other hand sucrose, fructose and sorbitol increased the particle size to 559 ± 16, 712 ± 55 and 469 ± 23, respectively. These changes on particle size may be related with the behaviour of each cryoprotectant during lyophilization, and its adsorption on nanoparticles surface.

3.4. Transmission and scanning electron microscopy analyses

The morphology of nanoparticles may be evaluated through the visualization of its microscopic appearance by TEM and SEM. TEM may characterize the shape of PLGA nanoparticles, whereas SEM may characterize the nanoparticles surface. However, the evaluation of nanoparticles surface by SEM with a good definition is very difficult, and focusing the electron beam on such a small area may also damage the nanoparticles. To avoid these drawbacks, during the visualization by SEM it were observed particles with the highest particle size that could be visualized. Therefore, it was possible to visualize the larger particles, and correlate its morphology and surface characteristics with the nanoparticles. TEM allows the observation of the lyophilized

nanoparticles after their suspension, however the visualization of nanoparticles by SEM is very difficult when the cryoprotectant concentration is more than 5 %, since a continuous matrix covering the nanoparticles may be observed [7]. Therefore, the purification of the lyophilized nanoparticles to remove the cryoprotectant was crucial, to allow the properly visualization of particles by SEM.

As discussed above, the processing conditions employed in the nanoparticles production, influences their characteristics. The nanoparticles porosity for instance, plays an important role on insulin release since a large amount of pores may increase the release rate of the protein [238]. The porosity of nanoparticles is originated by their hardening during the evaporation of dichloromethane in the preparation process and by the rate of its evaporation, or even by the temperature of nanoparticles preparation [239]. Furthermore, porosity may also influence insulin structure, since pores may open a pathway to external factors that can lead to protein denaturation. This loss of protein structure may occur in different extents depending on the different nanoparticles used, since they may have different porosity. In addition, the influence of cryoprotectants on nanoparticles porosity after lyophilization, which may influence the protein release rate and stability, is not well established.

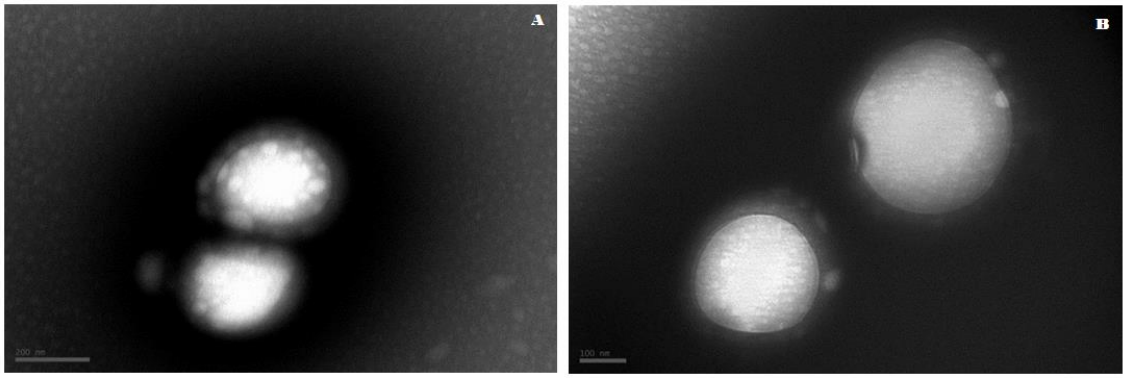

Figure 4.1. TEM microphotographs of insulin-loaded PLGA nanoparticles after production (A) and after lyophilization with no cryoprotectant added (B) (Figure A, bar shows 200 nm; Figure B, bar shows 100 nm).

The Figure 4.1 shows the microscopic appearance by TEM of insulin-loaded PLGA nanoparticles after production and lyophilization. The nanoparticles exhibited a spherical shape and a smooth surface, characteristic of the polymeric matrix. These characteristics were maintained after lyophilization with no added cryoprotectant (Figure 4.1-B) and with added cryoprotectants (Figure 4.2). The maintenance of nanoparticles morphology after lyophilization showed that the lyophilization process was effective on

nanoparticles stabilization. The size of nanoparticles showed in Figure 4.1 and 4.2 was in agreement with the previous particle size evaluations.

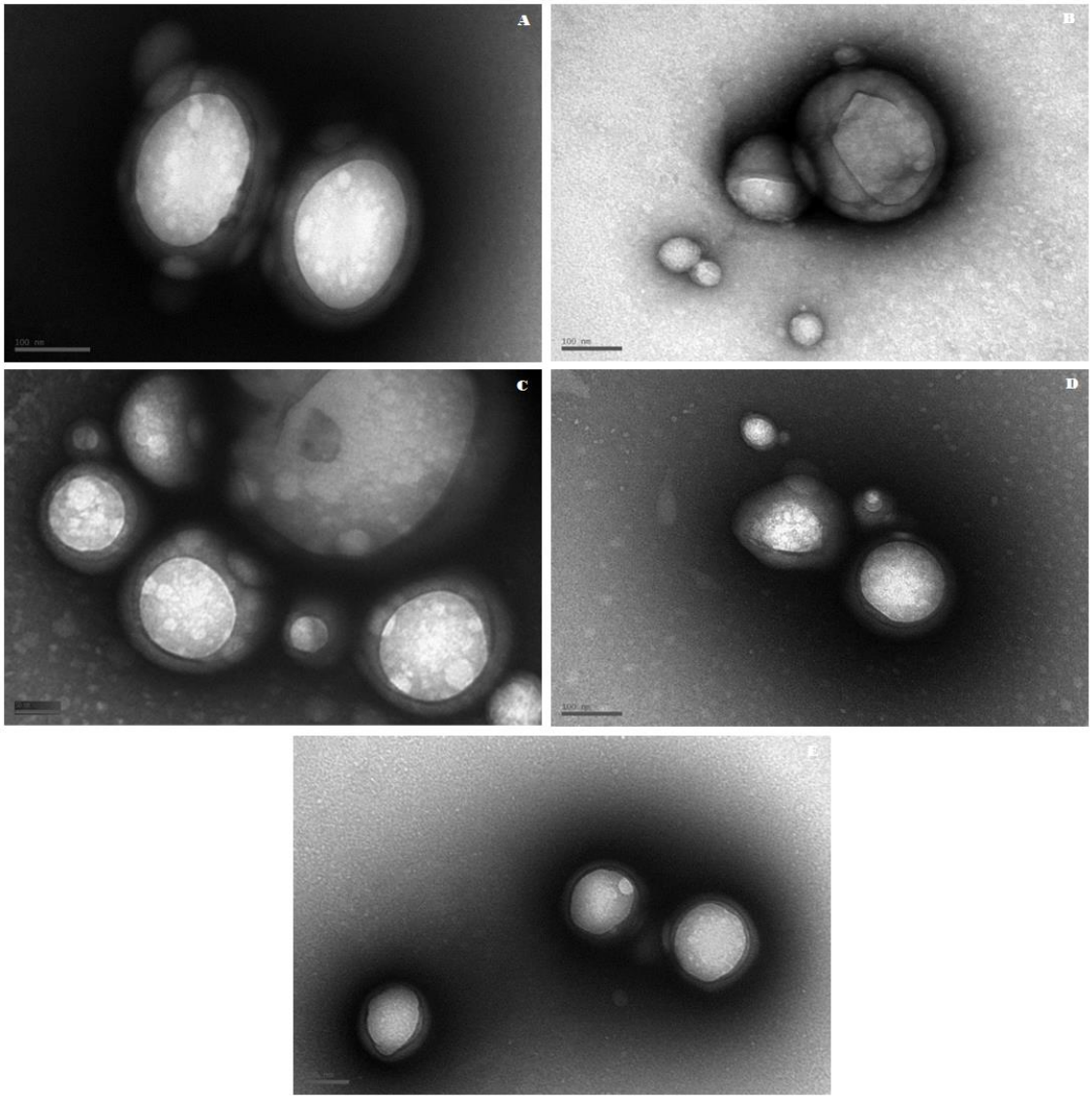

Figure 4.2. TEM microphotographs of insulin-loaded PLGA nanoparticles after lyophilization with: 10% (w/v) trehalose (A); 10% (w/v) sucrose (B); 10% (w/v) glucose (C); 10% (w/v) fructose (D) and 10% (w/v) sorbitol (E) (Figure A-B, bar shows 100 nm; Figure C, bar shows 50 nm; Figure D-E, bar shows 100 nm).

SEM was used to assess the nanoparticles surface. The Figure 4.3-A shows the presence of some depressions and pores on insulin-PLGA nanoparticles surface after production, that were caused by the evaporation of the organic solvent. Such morphology was similar for nanoparticles upon lyophilization (Figure 4.3-B).

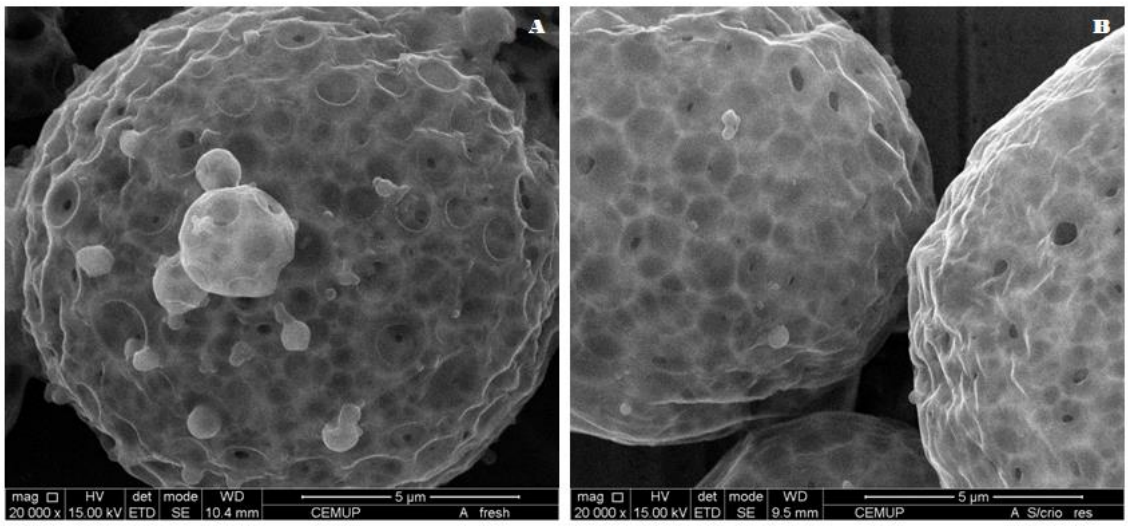

Figure 4.3. SEM microphotographs of insulin-loaded PLGA particles after production (A) and after lyophilization with no cryoprotectant added (B) (Figure A-B, bar shows 5 µm).

It was also observed that lyophilization of nanoparticles added with cryoprotectants, significantly increased the number of pores on nanoparticles surface (Figure 4.4). This occurred because after solidification of all solutes and water, the ice-vapor is evacuated and the shelf temperature increases supplying energy for sublimation, and thus beginning the primary drying. The elimination of ice crystals by sublimation creates an open network of pores, which are pathways for water removal from nanoparticles [7]. This increase on nanoparticles porosity after lyophilization with cryoprotectants added may open a pathway for a faster insulin release from nanoparticles and for its degradation. The freezing step may also influence the porosity of nanoparticles, since this step may affect the morphological characteristics of the cake [184]. Therefore, the freezing step influences the size of ice crystals and subsequently the drying steps and thus, the surface of nanoparticles and porosity of the final cake strongly depends on it. The presence of such pores are necessary on a lyophilizate, since the absence of a porous structure such as in a collapsed cake, becomes the reconstitution of the lyophilizate very hard to accomplish [173, 194].

Both the higher release rate and insulin degradation could be mitigated by the adsorption of the cryoprotectant on nanoparticles surface obstructing some of the formed pores. This was particularly evident in Figure 4.4-A, 4.4-B and 4.4-C.

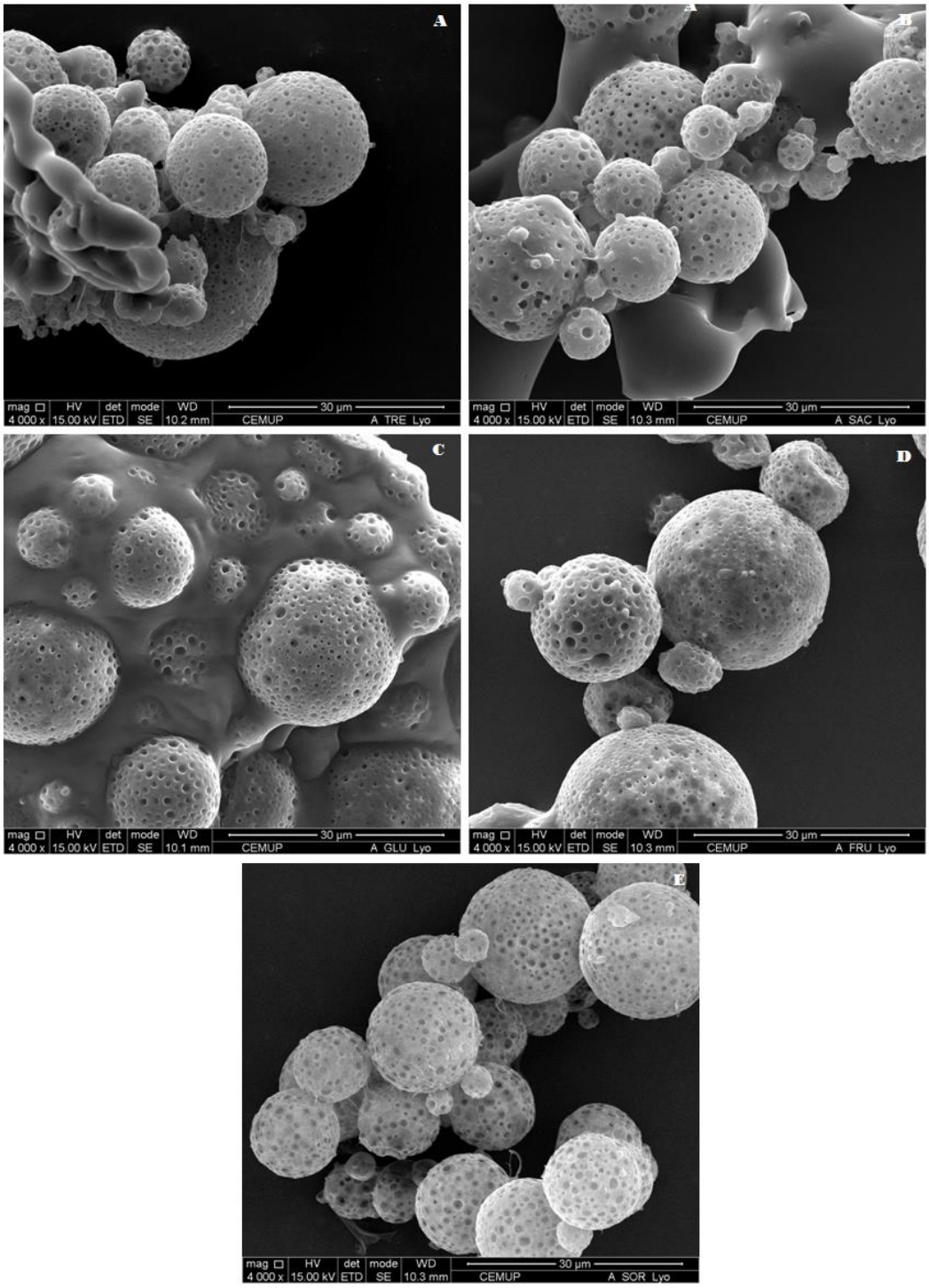

Figure 4.4. SEM microphotographs of insulin-loaded PLGA particles after lyophilization with: 10% (w/v) trehalose (A); 10% (w/v) sucrose (B); 10% (w/v) glucose (C); 10% (w/v) fructose (D) and 10% (w/v) sorbitol (E) (Figure A-E, bar shows 30 µm).

3.5. Evaluation of insulin *in vitro* release from nanoparticles

Several studies have been assessing the release pattern of drugs by PLGA nanoparticles [105, 239, 240]. However, just a few is known about the release pattern of

drugs from PLGA nanoparticles after lyophilization with cryoprotectants added. In addition, the relationship between the porosity and the surface characteristics of nanoparticles lyophilized with cryoprotectants, and the release pattern of insulin is not well established yet.

In Figure 4.5, it is shown the cumulative release profile of insulin from nanoparticles in 48 hours, after formulation and after lyophilization with no cryoprotectant added. The release pattern for both samples was very similar, with an initial burst release within the first 2 hours and a sustained release pattern until the 48 hours, which is characteristic of the PLGA-based nanoparticles [239]. The initial burst release may be explained by the release of insulin which is still adsorbed on nanoparticles surface, and then the encapsulated insulin is released during time achieving a sustained release pattern.

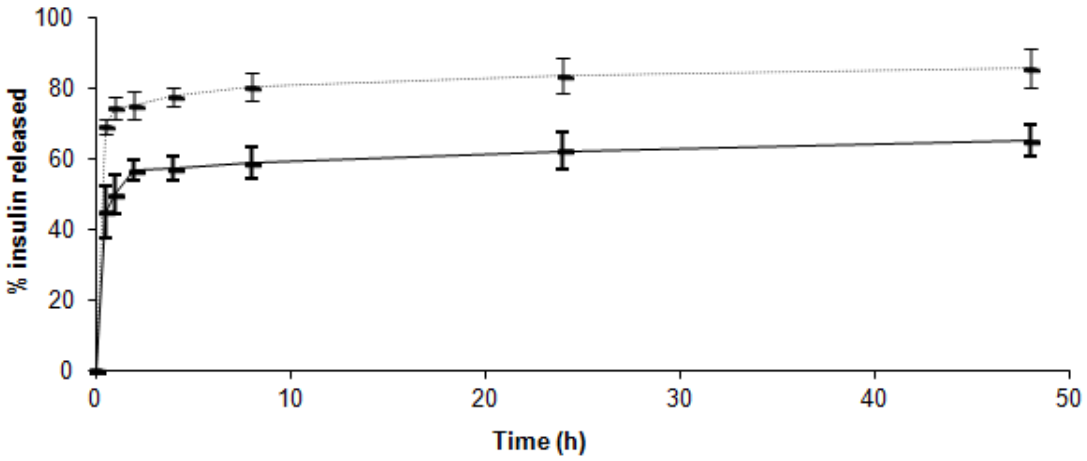

Figure 4.5. Cumulative release profile of insulin from PLGA nanoparticles after formulation (solid line) and after lyophilization with no cryoprotectant added (dotted line) (*n* = 3, bars represent SD).

The PLGA nanoparticles after formulation released about 57% of the insulin in the first 2 hours, and maintained a sustained release achieving 65% of insulin released after 48 hours. On other hand, PLGA nanoparticles after lyophilization with no cryoprotectant added released about 75% of insulin in the first 2 hours, which was an increment of 18% of insulin released, comparatively to nanoparticles after formulation. Such increment of insulin release may be related to the possible increase of pores size of nanoparticles as could be visualized in Figure 4.3-B. Thereby, a method to precisely assess the diameter of nanoparticles pores is required to support this possibility. The lyophilized nanoparticles further released about 86% of insulin after 48 hours.

Regarding the release patterns obtained for cryoprotectant added samples shown in Figure 4.6, it was possible to observe that the release pattern of insulin remained

similar to that with no cryoprotectant due to the polymeric matrix, with an initial burst release in the first 2 hours and a sustained release pattern until 48 hours. Comparatively to the lyophilized sample with no cryoprotectant added, the sample with trehalose added achieved a higher released amount of insulin while samples with the other used cryoprotectants added, led to a lower amount of insulin released. In fact, trehalose added nanoparticles released almost 91% of the insulin amount in the first 2 hours, releasing up to 96% of insulin after 48 hours. This could be due to the increase of the porosity of nanoparticles, as stated in Figure 4.4-A and to trehalose properties as cryoprotectant. In fact, it was reported that trehalose seems to be the best cryoprotectant for biomolecules, due to its many advantages comparatively with the other sugars. Such advantages are a higher Tg', less hygroscopicity and the absence of internal hydrogen bonds which during lyophilization, allows a more flexible formation of hydrogen bonds with nanoparticles [166]. Due to these more flexible bonds, trehalose is removed more easily from nanoparticles surface and insulin is released in a higher amount.

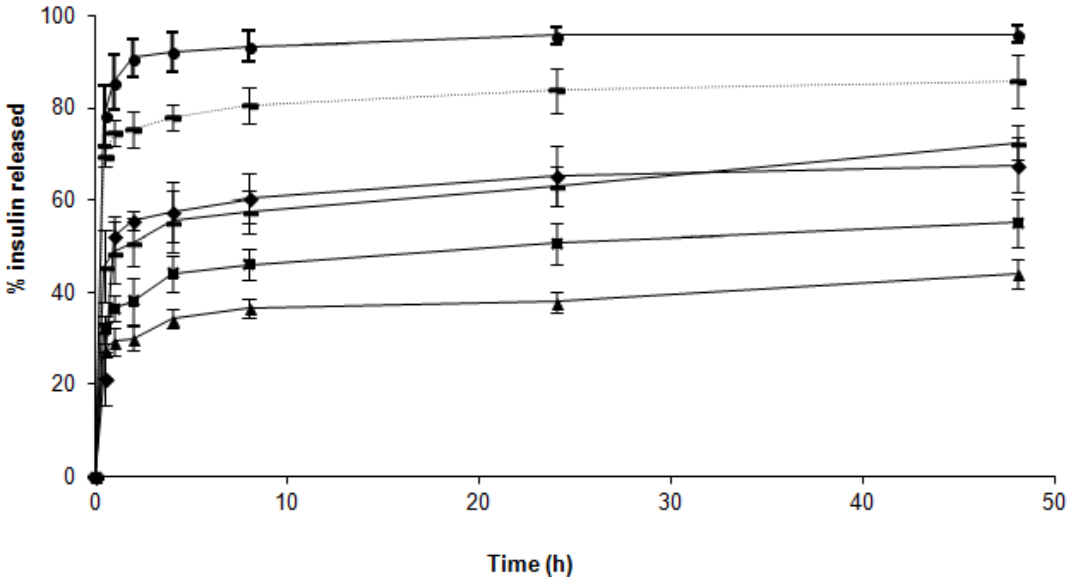

Figure 4.6. Cumulative release profile of insulin from PLGA nanoparticles after lyophilization with: no cryoprotectant (dotted line), 10% (w/v) trehalose (●); 10% (w/v) sucrose (■); 10% (w/v) glucose (▲); 10% (w/v) fructose (◆) and 10% (w/v) sorbitol (–) added (*n* = 3, bars represent SD).

Even increasing the porosity after lyophilization, the others cryoprotectant added samples showed a lower insulin released amount, mainly due to the presence of the sugars on the nanoparticles surface, which may obstruct the pores leading to a lower release. Indeed, cryoprotectants may stabilize nanoparticles during the drying steps due to the formation of hydrogen bonds between the cryoprotectant and the polar groups, at the nanoparticles surface at the end of the drying step [171]. Therefore, is harder to

remove these cryoprotectants from nanoparticles surface and the insulin release rate is lower. The glucose-added nanoparticles sample released the lowest amount of insulin with just almost 30% released in the first 2 hours, which was less 45% comparatively to the non-added cryoprotectant sample, and releasing just 44% of the total amount of insulin after 48 hours.

These results showed that the porosity of nanoparticles and the presence of cryoprotectants on nanoparticles surface may affect the release of insulin from nanoparticles. This was particularly important because the increase of the porosity of nanoparticles after lyophilization may open a pathway for insulin release, and simultaneously for insulin degradation. Additionally, the cryoprotectants bonding to nanoparticles surface may obstruct nanoparticles pores leading to a lower insulin release rate.

4. Conclusion

The aim of this chapter was to optimize the formulation of insulin-loaded PLGA nanoparticles and analyze the influence of cryoprotectants on nanoparticle stability and porosity after lyophilization, which may influence protein release and stability. The formulation containing PLGA 50:50 as polymer and PVA 2% as surfactant was the one that presented a better combination of size, zeta potential and AE, and was chosen for further experiments. It was verified that the lyophilization significantly increased the number of pores on PLGA nanoparticles surface, being more evident when cryoprotectants were added. The presence of pores is important in a lyophilizate to facilitate its reconstitution in water, although this may have consequences to protein release and stability. The release profile of insulin encapsulated into PLGA nanoparticles showed an initial burst in the first 2 h and a sustained release up to 48 h. After nanoparticles lyophilization the insulin release increased due to the formation of pores, maintaining a sustained release during time. After lyophilization with cryoprotectants, the amount of insulin released was higher for trehalose and lower for sucrose, glucose, fructose and sorbitol comparatively to lyophilized PLGA nanoparticles with no cryoprotectant added. Besides the porosity, the ability of cryoprotectants to be adsorbed on the nanoparticles surface may also play an important role on insulin release and stability.

Chapter 5

A Stability Study Perspective of the Effect of Lyophilization Using Cryoprotectants on the Structure of Insulin Loaded Into PLGA Nanoparticles

Partially published in:

Pedro Fonte, Sandra Soares, Flávia Sousa, Ana Costa, Vítor Seabra, Salette Reis, Bruno Sarmento, Stability study perspective of the effect of freeze-drying using cryoprotectants on the structure of insulin loaded into PLGA nanoparticles, Biomacromolecules, 15 (2014) 3753-3765.

1. Introduction

During encapsulation, proteins may suffer structural modifications due to the exposure to organic solvents, hydrophobic interfaces, dehydrations, shearing stresses and prejudicial reactions upon storage [10]. In addition, the introduction of hydrophilic proteins into hydrophobic polymeric carriers is a challenge, thus complex protein-protein and protein-polymer interactions are expected to occur. FTIR is considered the reference technique to assess the secondary structure of proteins loaded into nanoparticles in a non-invasive way.

The removal of water from protein-loaded nanoparticles by lyophilization may be fundamental to avoid the hydrolytic degradation of the nanoparticle matrix in aqueous suspension and to prevent loaded protein instability [182, 204]. However, this process also produces changes on nanoparticle properties, which may affect its robustness and size, with ultimately consequences to protein stability. Some sugars such as trehalose, glucose, sucrose, fructose and sorbitol may be used as cryoprotectants to minimize nanoparticles instability upon lyophilization, preventing their aggregation and protecting them from mechanical stress of ice crystals. Cryoprotectants may affect the Tg' of the formulation, which is crucial to obtain a cake with a stable amorphous form, appropriate residual moisture content, good redispersibility, and, of upmost importance, good protein stabilization upon storage [8, 230]. Cryoprotectants are known to preserve the native structure of proteins after lyophilization [241, 242].

Comparatively to other colloidal systems, there are just a few works focusing on the lyophilization process of polymeric nanoparticles. Most of the investigations on nanoparticle lyophilization are performed by trial and error, without considering the scientific principles of the lyophilization process. These chemical, physical and engineering principles need to be regarded in order to obtain a product with good quality and acceptable shelf-life. Generally, researchers just use this process as a way to remove water without considering the physical-chemical stability of the formulation. In this work it is demonstrated the influence of a standard lyophilization cycle, on the stability of insulin-loaded PLGA nanoparticles, after lyophilization and storage.

Thus, the aim of this chapter was to evaluate the stability of PLGA nanoparticles upon lyophilization and storage, and using insulin as a model of therapeutic protein, evaluate the maintenance of insulin secondary structure after encapsulation into PLGA nanoparticles. It was also evaluated the influence of lyophilization, using different cryoprotectants, on insulin structure. In addition, it were evaluated the modifications on

insulin secondary structure encapsulated into PLGA nanoparticles and on its features, over 6 months at different storage conditions following the ICH guidelines

2. Materials and methods

2.1. Materials

PLGA 50:50 Resomer® RG 503 H (Mw 24,000-38,000 g/mol; viscosity 0.32-0.44 dL/g; Tg 44-48 ºC; end group: free carboxylic acid) was from Evonik Industries AG (Essen, Germany). PVA, dichloromethane and recombinant human insulin, trehalose (Mw 378.33 g/mol), glucose (Mw 180.16 g/mol), sucrose (Mw 342.30 g/mol), fructose (Mw 180.16 g/mol) and sorbitol (Mw 182.17 g/mol) were from Sigma-Aldrich (Steinheim, Germany). Acetonitrile HPLC gradient grade was from Fischer Scientific (Loughborough, UK) and trifluoroacetic acid from Acros Organics (Morris Plains, NJ, USA). Milli-Q water was produced in-house and all other reagents were of analytical grade.

2.2. Preparation of PLGA nanoparticles

PLGA nanoparticles were produced using a modified solvent emulsification-evaporation method, based on a w/o/w double emulsion technique [101]. Briefly, 200 mg of PLGA 50:50 were dissolved in 2 mL of dichloromethane. Then, 0.2 mL of a 150 mg/mL insulin solution in HCl 0.1 M was added to the polymeric solution and mixed using a Bioblock vibracell 75186 sonicator from Fischer Bioblock Scientific (Rungis Complexe, France), during 30 seconds with 70% of amplitude. After this homogenization, the primary emulsion was poured onto 25 mL of PVA 2% (w/v) at pH 7.4 and mixed using the same sonication conditions. Finally, the organic solvent was completely evaporated under magnetic stirring.

The nanoparticles were washed with Milli-Q water three times by centrifugation using a Heraeus Megafuge 1.0 R centrifuge (Thermo Scientific, Asheville, NC, USA) at 15,000 rpm for 30 min, and redispersed in water prior lyophilization and storage. The same procedure was followed to produce unloaded PLGA nanoparticles.

2.3. Insulin association efficiency

The insulin AE was indirectly determined. The amount of insulin entrapped into the PLGA nanoparticles was calculated using the concept of the equation 4.1 (*see* Chapter 4). The insulin free in supernatant correspond to the amount of insulin that

remained in the aqueous phase after nanoparticles isolation by centrifugation using a Beckman Optima TL ultracentrifuge from Beckman Coulter (Brea, CA, USA) at 20,000 rpm for 15 min at 4°C, and it was quantified by a HPLC-UV method previously validated [233]. Measurements were performed using a Merck-Hitachi LaChrom HPLC instrument from Merck (Whitehouse Station, NJ, USA) equipped with a XTerra RP 18 column, 5 µm particle size, 4.6 mm internal diameter × 250 mm length from Waters (Milford, MA, USA) and a LiChrospher 100 RP-18, 5 µm particle size guard column also from Merck (Whitehouse Station, NJ, USA). Samples were run in triplicate.

2.4. Lyophilization of nanoparticles

The PLGA nanoparticles were poured into semi-stoppered glass vials with slotted rubber closures at a maximal formulation height of 10 mm, and added in a set of 3 replicates with different cryoprotectants: trehalose, glucose, sucrose, fructose and sorbitol at a concentration of 10% (w/v) of the final volume in each vial. All samples including those with no cryoprotectant added were then frozen at -80ºC for 6 hours and transferred to a Modulyo 4K lyophilizer from Edwards (Crawley, West Sussex, UK) at 0.09 mbar for 72 h, being maintained at the condenser surface temperature of -60 ± 5 ºC.

2.5. Reconstitution of lyophilized samples

After lyophilization, samples were reconstituted by slowly adding distilled water in the inside wall of the vial and maintained during 10 minutes to ensure the proper cake wetting. Then, samples were shaken in a Vortex Mixer ZX Classic from Velp Scientifica (Usmate, Italy) during 3 minutes to obtain complete homogenization.

2.6. Long-term storage study

A 6 month study was performed to evaluate the long-term stability of insulin loaded into PLGA nanoparticles under different storage conditions, following the ICH guidelines [197]. Samples were stored at three different storage conditions: 4 ± 2ºC , 25 ± 2ºC / 60 ± 5% RH and 40 ± 2ºC / 75 ± 5% RH in a Climacell chamber from MMM Medcenter Einrichtungen GmbH (Planegg, Germany) and at all storage conditions samples were protected from light. Samples were analyzed in triplicate at four different time points, for each storage condition: after lyophilization (t0), and after 1, 3 and 6 months of storage (t1, t3 and t6, respectively).

2.7. Particle size and zeta potential analyses

Both formulations in suspension and after reconstitution were diluted with Milli-Q water to a proper concentration for both particle size and zeta potential assessments. The particle size and zeta potential were analyzed respectively, by dynamic light scattering using a 90Plus Particle Size Analyzer and by phase analysis light scattering using a ZetaPALS Zeta Potential Analyzer, both from Brookhaven Instruments Corporation (Holstville, NY, USA). All measurements were performed in triplicate.

2.8. Transmission electron microscopy analysis

PLGA nanoparticles morphology was characterized by TEM, by placing formulations in suspension and reconstituted samples on a grid, treated with uranyl acetate and then observed in a JEOL JEM-1400 Electron Microscope from JEOL Ltd (Tokyo, Japan).

2.9. Scanning electron microscopy analysis

The surface morphology of PLGA nanoparticles was observed by SEM on a FEI Quanta 400 FEG SEM from FEI (Hillsboro, OR, USA). The lyophilized nanoparticles containing cryoprotectants were resuspended in distilled water and washed three times by centrifugation at 20,000 rpm for 15 min at 4°C, to remove the dissolved cryoprotectant. The lyophilizates were also observed. Samples were mounted onto a metal stub and vacuum-coated with a layer of gold/palladium prior observation.

2.10. Attenuated total reflectance-Fourier transform infrared spectroscopy analysis

The secondary structure of insulin loaded into the PLGA nanoparticles upon 6 months of storage, was assessed by FTIR. The analyses were performed in an ABB MB3000 FTIR spectrometer from ABB (Zurich, Switzerland) equipped with a MIRacle single reflection attenuated total reflectance (ATR) accessory from PIKE Technologies (Madison, WI, USA).

All spectra were collected with 256 scans and a 4 cm^{-1} resolution in the region of 4000-600 cm^{-1}, and a triplicate of each formulation was analyzed. Insulin spectra were obtained following a double subtraction procedure [243], followed by a 15 points Savitsky-Golay second derivative, and a baseline correction using 3-4 point adjustment

at the amide I region (1710-1590 cm^{-1}). Finally, all spectra were area-normalized for further comparison. The spectral treatment was performed using the HorizonMB FTIR software from ABB (Zurich, Switzerland).

2.10.1. Spectral similarity analysis

The quantitative comparison of the similarity of FTIR spectra between the insulin loaded into the PLGA nanoparticles and native insulin was determined using the area of overlap (AO) [244] and spectral correlation coefficient (SCC) [245] algorithms. The area normalized second-derivative amide I spectra were used for both methods considering as reference a 30 mg/mL insulin solution in HCl 0.1 M, and the results are presented as percentage, so the higher the percentage most similar are the spectra. This protein solution was used as reference, because it is generally recognized that the stability of a solid protein formulation increases with the increase of similarity to the FTIR spectra in solution [246].

2.10.2. Multivariate data analysis

The principal component analysis (PCA) is a helpful method for protein structure characterization [247]. Therefore, it was performed a correlation of the loaded protein secondary structure with the influence of the lyophilization process, used cryoprotectant and storage condition upon 6 months of storage. A data set consisting of N objects (average spectra of the second-derivative spectra of insulin loaded into PLGA nanoparticles formulations and native insulin structure) and X variables (amide I region wavenumbers) was the PCA input matrix, that resulted in the scores and loadings matrix for each estimated principal component (PC). The PCA was performed using the Matlab 7.9 software from MathWorks (Natick, MA, USA) with a PLS Toolbox 5.5 software from Eigenvector Research Inc. (Wenatchee, WA, USA).

2.11. Statistical analysis

The statistical analyses were performed using a one-way analysis of variance (ANOVA) Tukey *post hoc* test, with a significance level of $p < 0.05$ in the OriginPro 8 software from OriginLab Corporation (Northampton, MA, USA).

3. Results and discussion

3.1. Nanoparticles characterization

3.1.1. Particle size, zeta potential and association efficiency

3.1.1.1. Before lyophilization

Insulin-loaded PLGA nanoparticles were characterized after production and lyophilization using different cryoprotectants, and also upon 6 months at different storage conditions. The nanoparticles were successfully produced by a formulation protocol previously optimized [101]. These carriers were used mainly by its recognized biocompatibility, ability to protect the loaded drug and sustained release properties. The production method is also widely used to encapsulate protein drugs, since it is very easy to reproduce and obtain nanoparticles with good properties. The Figure 5.1 shows the particle size, PdI and zeta potential characterization of all the formulations upon 6 months of storage. These results are also represented in numeric values in Table 5.1. Insulin-loaded PLGA nanoparticles in suspension (insulin-PLGA nanoparticles) were obtained with a mean particle size of 446 ± 30 nm, PdI of 0.26 ± 0.03 and zeta potential of -24.2 ± 3.4 mV, which was a good indicator of nanoparticles stability. Insulin AE was 87.4 ± 0.2 %, being a very good achievement regarding the hydrophilic nature of insulin, loaded into the hydrophobic polymeric matrix.

3.1.1.2. After lyophilization

Nanoparticles were lyophilized without cryoprotectant added (freeze-dried insulin-PLGA nanoparticles) or added with trehalose (freeze-dried insulin-PLGA nanoparticles + trehalose), glucose (freeze-dried insulin-PLGA nanoparticles + glucose), sucrose (freeze-dried insulin-PLGA nanoparticles + sucrose), fructose (freeze-dried insulin-PLGA nanoparticles + fructose) and sorbitol (freeze-dried insulin-PLGA nanoparticles + sorbitol) at a cryoprotectant concentration of 10% (w/v). The criteria to choose these excipients as cryoprotectants was to use two non–reducing sugars (trehalose and sucrose) two reducing sugars (glucose and fructose) and one sugar alcohol (sorbitol). Comparatively to mannitol, the latter is not commonly used as cryoprotectant, so its potential as a cryoprotectant was evaluated. The mentioned cryoprotectant concentration was used to obtain the highest acceptable cryoprotectant effect level. Thus, it was intention of this work to demonstrate how these different cryoprotectants may impact the stability of the carrier and the loaded protein. These cryoprotectants were expected to avoid aggregation and facilitate redispersion of the lyophilizate [178].

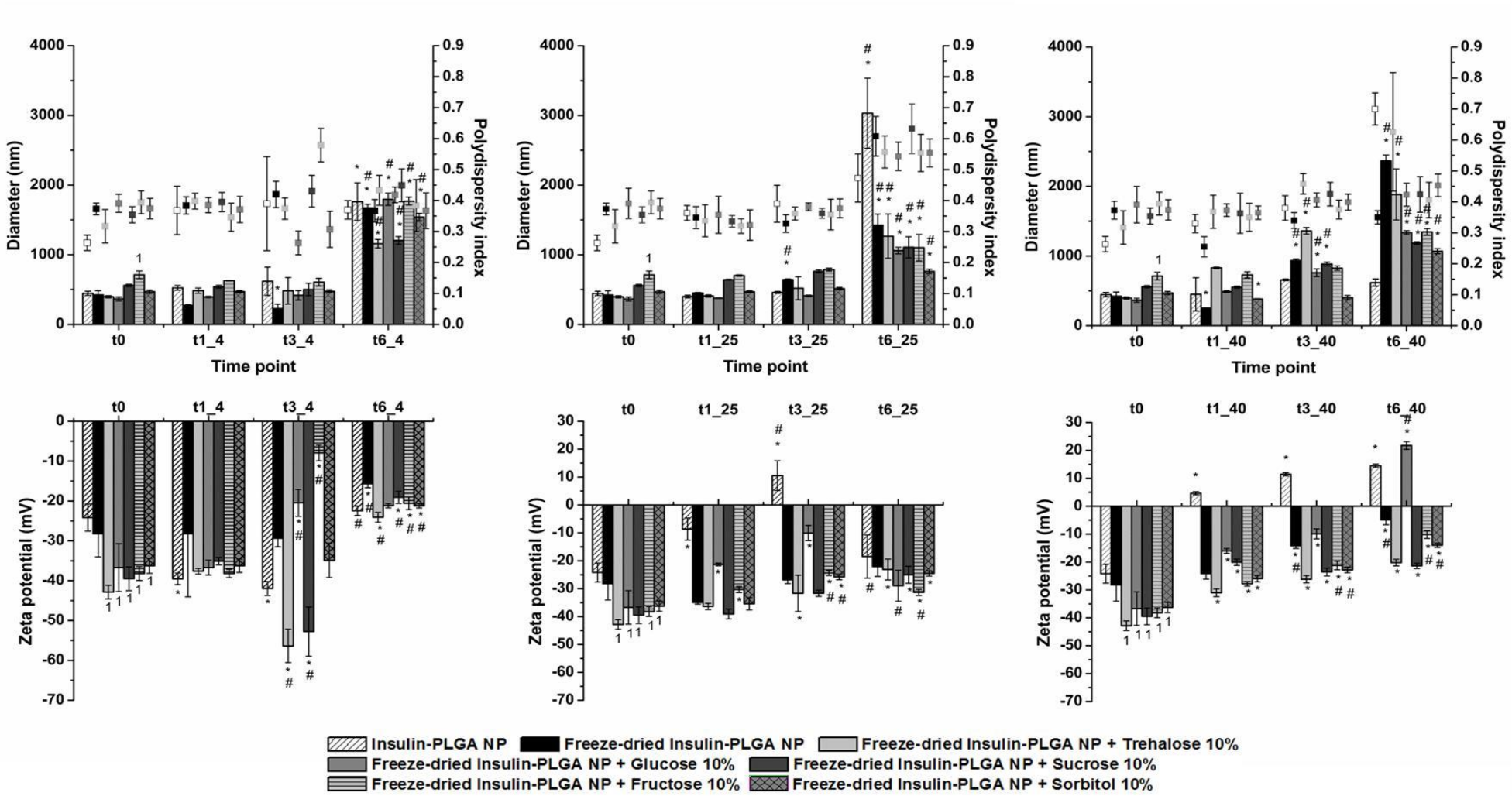

Figure 5.1. Mean particle size (top bars), PdI (square symbols) and zeta potential (bottom bars) characterization of insulin-loaded PLGA nanoparticles formulations. Results are significantly different ($p < 0.05$) from insulin-PLGA nanoparticles after formulation, when marked with 1. When marked with * and #, results are significantly different ($p < 0.05$) from the corresponding formulation at t0, and from the corresponding formulation at the previous time point, respectively. NP stands for nanoparticles. Left, middle and right graphs are referred to 4ºC, 25ºC / 60% RH and 40ºC / 75% RH, respectively.

After lyophilization, it was noticed that all formulations, except freeze-dried insulin-PLGA nanoparticles and freeze-dried insulin-PLGA nanoparticles + trehalose 10%, were collapsed. The obtained collapsed cakes were more difficult to resuspend comparatively to non-collapsed cakes. Even though, all tested formulations did not significantly change its particle size after lyophilization, with the exception of freeze-dried insulin-PLGA nanoparticles + fructose 10%. The natural consequences of product collapse are indeed the long reconstitution time and the high residual moisture content. Concerning to zeta potential analyses, the overall obtained results showed that nanoparticles presented negative surface charge, which is characteristic of the acidic PLGA [147]. However, some exceptions were found indicating that nanoparticles surface suffered modifications. The removal of free drug from formulations supernatant prior lyophilization was important, since its presence in formulation may increase the zeta potential near to neutrality, increasing the probability of particle aggregation [7]. The zeta potential values decreased after lyophilization, and mainly when cryoprotectants were added, showing that nanoparticles became more stable. This may be explained by the presence of sugars that expand the location of the slipping plan during electrophoretic movement due to the formation of a viscous hydration layer on nanoparticles surface [248].

Table 5.1. Mean particle size, PdI and zeta potential characterization of insulin-loaded PLGA nanoparticle formulations upon 6 months of storage at the tested storage conditions (*n* = 3, mean ± SD).

Time point	Formulation	Diameter (nm)	PdI	Zeta potential (mV)
t0	Insulin-PLGA nanoparticles	446 ± 30	0.26 ± 0.03	-24.2 ± 3.4
	Freeze-dried Insulin-PLGA nanoparticles	422 ± 60	0.37 ± 0.02	-28.2 ± 5.8
	Freeze-dried Insulin-PLGA nanoparticles + Trehalose 10%	396 ± 16	0.32 ± 0.05	-42.9 ± 1.7
	Freeze-dried Insulin-PLGA nanoparticles + Glucose 10%	365 ± 28	0.39 ± 0.01	-36.7 ± 6.0
	Freeze-dried Insulin-PLGA nanoparticles + Sucrose 10%	559 ± 16	0.35 ± 0.03	-39.5 ± 3.0
	Freeze-dried Insulin-PLGA nanoparticles + Fructose 10%	712 ± 55	0.39 ± 0.01	-38.2 ± 1.7
	Freeze-dried Insulin-PLGA nanoparticles + Sorbitol 10%	469 ± 23	0.37 ± 0.03	-36.3 ± 1.9
	4°C			

t1	Insulin-PLGA nanoparticles	524 ± 34	0.37 ± 0.08	-39.6 ± 1.4
	Freeze-dried Insulin-PLGA nanoparticles	272 ± 10	0.38 ± 0.01	-28.2 ± 15.8
	Freeze-dried Insulin-PLGA nanoparticles + Trehalose 10%	484 ± 37	0.40 ± 0.02	-37.6 ± 0.7
	Freeze-dried Insulin-PLGA nanoparticles + Glucose 10%	393 ± 10	0.39 ± 0.01	-36.7 ± 1.9
	Freeze-dried Insulin-PLGA nanoparticles + Sucrose 10%	540 ± 21	0.40 ± 0.01	-35.1 ± 0.9
	Freeze-dried Insulin-PLGA nanoparticles + Fructose 10%	628 ± 4	0.35 ± 0.01	-38.2 ± 1.0
	Freeze-dried Insulin-PLGA nanoparticles + Sorbitol 10%	469 ± 16	0.37 ± 0.01	-36.3 ± 1.7
t3	Insulin-PLGA nanoparticles	618 ± 203	0.39 ± 0.15	-42.0 ± 1.8
	Freeze-dried Insulin-PLGA nanoparticles	227 ± 63	0.42 ± 0.04	-29.4 ± 2.1
	Freeze-dried Insulin-PLGA nanoparticles + Trehalose 10%	482 ± 191	0.37 ± 0.03	-56.4 ± 4.2
	Freeze-dried Insulin-PLGA nanoparticles + Glucose 10%	417 ± 68	0.26 ± 0.04	-20.5 ± 3.4
	Freeze-dried Insulin-PLGA nanoparticles + Sucrose 10%	502 ± 90	0.43 ± 0.05	-52.8 ± 6.2
	Freeze-dried Insulin-PLGA nanoparticles + Fructose 10%	606 ± 55	0.58 ± 0.05	-8.0 ± 2.0
	Freeze-dried Insulin-PLGA nanoparticles + Sorbitol 10%	475 ± 21	0.31 ± 0.01	-34.9 ± 4.3
t6	Insulin-PLGA nanoparticles	1761 ± 271	0.37 ± 0.01	-22.4 ± 1.2
	Freeze-dried Insulin-PLGA nanoparticles	1671 ± 53	0.37 ± 0.01	-15.7 ± 1.0
	Freeze-dried Insulin-PLGA nanoparticles + Trehalose 10%	1158 ± 61	0.43 ± 0.01	-24.1 ± 1.3
	Freeze-dried Insulin-PLGA nanoparticles + Glucose 10%	1795 ± 88	0.42 ± 0.02	-21.2 ± 0.6
	Freeze-dried Insulin-PLGA nanoparticles + Sucrose 10%	1205 ± 57	0.45 ± 0.05	-19.1 ± 1.5
	Freeze-dried Insulin-PLGA nanoparticles + Fructose 10%	1770 ± 56	0.38 ± 0.01	-20.6 ± 1.6
	Freeze-dried Insulin-PLGA nanoparticles + Sorbitol 10%	1540 ± 54	0.37 ± 0.01	-21.2 ± 0.5

25°C / 60% RH

t1	Insulin-PLGA nanoparticles	400 ± 19	0.36 ± 0.01	-8.7 ± 4.0
	Freeze-dried Insulin-PLGA nanoparticles	451 ± 8	0.35 ± 0.01	-35.0 ± 0.6
	Freeze-dried Insulin-PLGA nanoparticles + Trehalose 10%	408 ± 16	0.34 ± 0.01	-36.4 ± 1.1
	Freeze-dried Insulin-PLGA nanoparticles + Glucose 10%	378 ± 6	0.35 ± 0.01	-21.3 ± 0.5
	Freeze-dried Insulin-PLGA nanoparticles + Sucrose 10%	643 ± 7	0.33 ± 0.02	-39.1 ± 1.8
	Freeze-dried Insulin-PLGA nanoparticles + Fructose 10%	702 ± 10	0.32 ± 0.01	-30.3 ± 1.1
	Freeze-dried Insulin-PLGA nanoparticles + Sorbitol 10%	470 ± 12	0.32 ± 0.01	-35.4 ± 2.2
t3	Insulin-PLGA nanoparticles	460 ± 14	0.39 ± 0.01	10.5 ± 5.3
	Freeze-dried Insulin-PLGA nanoparticles	644 ± 10	0.33 ± 0.03	-26.9 ± 1.3
	Freeze-dried Insulin-PLGA nanoparticles + Trehalose 10%	519 ± 165	0.36 ± 0.02	-31.7 ± 6.5
	Freeze-dried Insulin-PLGA nanoparticles + Glucose 10%	411 ± 11	0.38 ± 0.01	-10.1 ± 2.7
	Freeze-dried Insulin-PLGA nanoparticles + Sucrose 10%	763 ± 21	0.36 ± 0.02	-31.7 ± 1.1
	Freeze-dried Insulin-PLGA nanoparticles + Fructose 10%	787 ± 21	0.36 ± 0.01	-24.4 ± 0.9
	Freeze-dried Insulin-PLGA nanoparticles + Sorbitol 10%	514 ± 17	0.38 ± 0.01	-25.8 ± 1.0
t6	Insulin-PLGA nanoparticles	3032 ± 504	0.47 ± 0.08	-18.5 ± 7.7
	Freeze-dried Insulin-PLGA nanoparticles	1425 ± 159	0.61 ± 0.06	-22.1 ± 3.5
	Freeze-dried Insulin-PLGA nanoparticles + Trehalose 10%	1267 ± 318	0.56 ± 0.05	-23.1 ± 3.8
	Freeze-dried Insulin-PLGA nanoparticles + Glucose 10%	1060 ± 47	0.55 ± 0.05	-29.0 ± 5.5
	Freeze-dried Insulin-PLGA nanoparticles + Sucrose 10%	1107 ± 152	0.63 ± 0.08	-25.0 ± 3.0
	Freeze-dried Insulin-PLGA nanoparticles + Fructose 10%	1102 ± 190	0.55 ± 0.06	-31.4 ± 1.1
	Freeze-dried Insulin-PLGA nanoparticles + Sorbitol 10%	763 ± 31	0.55 ± 0.05	-24.6 ± 0.9

40°C / 75% RH

t1	Insulin-PLGA nanoparticles	450 ± 239	0.33 ± 0.03	4.6 ± 0.6
	Freeze-dried Insulin-PLGA nanoparticles	252 ± 4	0.26 ± 0.01	-24.2 ± 2.0
	Freeze-dried Insulin-PLGA nanoparticles + Trehalose 10%	830 ± 11	0.37 ± 0.01	-31.1 ± 1.4
	Freeze-dried Insulin-PLGA nanoparticles + Glucose 10%	489 ± 13	0.37 ± 0.01	-16.0 ± 0.8
	Freeze-dried Insulin-PLGA nanoparticles + Sucrose 10%	552 ± 15	0.36 ± 0.01	-20.1 ± 1.1
	Freeze-dried Insulin-PLGA nanoparticles + Fructose 10%	729 ± 44	0.35 ± 0.02	-27.8 ± 0.8
	Freeze-dried Insulin-PLGA nanoparticles + Sorbitol 10%	382 ± 5	0.37 ± 0.01	-26.0 ± 1.1
t3	Insulin-PLGA nanoparticles	657 ± 12	0.38 ± 0.01	11.4 ± 0.6
	Freeze-dried Insulin-PLGA nanoparticles	936 ± 21	0.34 ± 0.03	-14.2 ± 0.9
	Freeze-dried Insulin-PLGA nanoparticles + Trehalose 10%	1360 ± 48	0.46 ± 0.03	-26.2 ± 1.3
	Freeze-dried Insulin-PLGA nanoparticles + Glucose 10%	760 ± 55	0.41 ± 0.02	-9.9 ± 1.8
	Freeze-dried Insulin-PLGA nanoparticles + Sucrose 10%	885 ± 29	0.43 ± 0.02	-23.6 ± 1.4
	Freeze-dried Insulin-PLGA nanoparticles + Fructose 10%	826 ± 32	0.38 ± 0.03	-21.2 ± 1.5
	Freeze-dried Insulin-PLGA nanoparticles + Sorbitol 10%	403 ± 30	0.40 ± 0.03	-22.9 ± 1.0
t6	Insulin-PLGA nanoparticles	619 ± 52	0.70 ± 0.01	14.5 ± 0.6
	Freeze-dried Insulin-PLGA nanoparticles	2366 ± 82	0.35 ± 0.02	-4.9 ± 1.7
	Freeze-dried Insulin-PLGA nanoparticles + Trehalose 10%	1884 ± 367	0.63 ± 0.19	-20.2 ± 1.2
	Freeze-dried Insulin-PLGA nanoparticles + Glucose 10%	1337 ± 27	0.42 ± 0.04	21.8 ± 1.4
	Freeze-dried Insulin-PLGA nanoparticles + Sucrose 10%	1186 ± 19	0.42 ± 0.03	-21.4 ± 0.9
	Freeze-dried Insulin-PLGA nanoparticles + Fructose 10%	1346 ± 47	0.41 ± 0.02	-10.2 ± 1.4
	Freeze-dried Insulin-PLGA nanoparticles + Sorbitol 10%	1070 ± 37	0.45 ± 0.04	-14.0 ± 0.8

3.1.1.3. Upon storage

The formulations were stored at different storage conditions during 6 months and particles were characterized at time points of 1, 3 and 6 months. Regarding the storage of formulations at 4ºC, during the first 3 months, particle size of nanoparticles did not significantly changed, except for freeze-dried insulin-PLGA nanoparticles that obtained a particle size of 227 ± 63 nm. This decrease was probably due to the absence of cryoprotectant that has the ability to form hydrogen bonds with the polymer and cover nanoparticles surface protecting them from hydrolytic degradation motivated by the residual moisture content [101]. After 6 months of storage at 4ºC (t6_4) the particle size significantly changed in all formulations comparatively to the corresponding formulation at t0, and the lyophilized formulations also significantly changed from t3 to t6. Overall, particle size increased more than 3-fold from t0. This fact may be explained by the particles aggregation upon 6 months of storage at 4ºC, which was also evident by the gradual difficulty to resuspend particles over time. Regarding zeta potential results, formulations maintained similar results upon 1 month of storage, but after 6 months the zeta potential of lyophilized formulations significantly increased, providing another indicator of nanoparticles modification.

At 25ºC / 60% RH, after 3 months all nanoparticle formulations maintained its particle size except freeze-dried insulin-PLGA nanoparticles that showed a significantly increased particle size of 644 ± 10 nm. At t6, particle size highly increased up to 3032 ± 504 nm which shows up also the great aggregation suffered. This particle size increase for all the formulations was also particularly evident by the increase of its PdI. This indicator shows clearly the variable size range of nanoparticles originated by the formation of aggregates, resulting in low homogeneity and low particle suspension stability. In addition, comparatively to other storage conditions the PdI values demonstrated that the reconstitution of the lyophilizates was more difficult at 25ºC / 60% RH. Even though, after 6 months of storage, all the formulations remained colloidally stable since nanoparticles presented negative zeta potential values not higher than -20 mV.

Concerning the stability of the formulations at more extreme storage conditions, 40ºC / 75% RH, instability was observed earlier. Although at t1 most of the formulations maintained its particle size, freeze-dried insulin-PLGA nanoparticles and freeze-dried insulin-PLGA nanoparticles + sorbitol particle size significantly changed. Freeze-dried insulin-PLGA nanoparticles after one month decreased its particle size down to 253 ± 4 nm, probably due to partial surface degradation of the polymer. This degradation may be

particularly augmented by the increase of the number of pores on nanoparticles surface after lyophilization, which increases the surface area for hydrolytic processes motivated by residual moisture content, combined with the absence of cryoprotectants on nanoparticles surface [101]. Besides this decrease suffered by particle degradation, at t3 particle size significantly increased due to particle aggregation. Indeed, the degradation suffered by particles led them to destabilize and have more tendency to aggregate overtime, increasing particle size values. At this storage condition, insulin-PLGA nanoparticles in suspension did not significantly changed the particle size, but it was clearly noticed a completely change of the formulation aspect over time, changing from a milky to a more aqueous aspect due to the constant degradation of particles because the storage temperature was close to the PLGA Tg (44-48ºC). It is recommended that the Tg value of a stable formulation, needs to be at least 20ºC above the storage temperature [249]. At t6, all the lyophilized formulations significantly increased the particle size comparatively to t0 and t3, which was particularly evident for freeze-dried insulin-PLGA nanoparticles and freeze-dried insulin-PLGA nanoparticles + trehalose. Regarding zeta potential, insulin-PLGA nanoparticles presented positive zeta potential values at t1, t3 and t6 showing that the stability of nanoparticles in suspension were really compromised at 40ºC / 75% RH. The increased degradation suffered by PLGA nanoparticles at this storage condition could turned the formulation into an acidic pH, and at this condition the zeta potential of PLGA nanoparticles may become positive [151]. Indeed, the surface charge reverse may be due to a transfer of protons from the bulk solution into nanoparticles surface, so hydroxyl groups may be protonated at the surface. After 6 months of storage, the zeta potential significantly increased for all the formulations and freeze-dried insulin-PLGA nanoparticles + glucose increased its zeta potential into positive values.

In an overall view, it may be stated that for the storage conditions except for 40ºC / 75% RH, the formulations maintained similar levels of particle size upon 3 months comparatively to t0. The highest particle size increase was noticed from t3 to t6 at all the storage conditions, however it must be noticed that particles remained suitable for intravenous administration even after 6 months of storage. It is generally accepted that the particle size of intravenously administered formulations should not exceed 5 µm. In addition, it was particularly evident that cryoprotectant added formulations led to a less particle increase upon 6 months, showing that additionally to its better performance during lyophilization, they were able to increase particles stability upon 6 months of storage. The zeta potential increased over time, however besides the mentioned exceptions, particles demonstrated good stability upon 6 months of storage. Regarding

zeta potential results, cryoprotectant added formulations showed once more to have a higher level of particles stabilization presenting lower negative zeta potential values.

Most of the modifications occurred on nanoparticles stability over the 6 months of storage were explained by the collapse of formulations after lyophilization, which leads to a high residual moisture content. The inappropriate residual moisture content of formulations is a natural consequence of product collapse. During storage nanoparticles may adsorb enough moisture leading to a reduction of its Tg below the storage temperature, accelerating formulations instability and product collapse [250]. It is known that at the early stage of storage time, moisture inside the vials may increase due to water transfer from stoppers, and over time moisture content may increase due to its permeation through vials stoppers [251]. These gradual modifications over time were noticed by the increasing nanoparticles aggregation and resuspension difficulty over time. Indeed, the use of a standard lyophilization process led to this instability upon storage. First of all, prior lyophilization, the different formulations need to be physical and chemical characterized, so the critical properties of the formulations such as the Tg' and the collapse temperature Tc need to be known. To prevent the collapse during lyophilization and storage, the product temperature must be set below the glass transition temperature (Tg' and Tg, respectively) and the lyophilized product collapses and changes its macroscopic shape during lyophilization, when it is dried above the Tc [163]. Indeed, in most of the cases, lyophilization process is usually developed by trial and error or even in a 'blind way' in which samples are just dropped inside the lyophilizer, and attention on formulation critical properties, and the three steps of lyophilization are completely neglected. The intention of this chapter was to demonstrate what may happen to formulations stability when these procedures occur. For instance, when the primary drying does not begin immediately after freezing, the frozen water may start to liquefy which combined with an ineffective secondary drying step leads to a high level of residual moisture content that destabilizes formulations.

3.1.2. Nanoparticles morphology

The morphology of PLGA nanoparticles may be visualized by TEM and SEM, since these techniques provide essential information about the shape and the surface of nanoparticles, respectively. As previously reported [101], the visualization of nanoparticles surface by SEM with good definition is not easy and all the visualized nanoparticles surfaces may look similar, so differences between them are not possible to distinguish. Thus, taking advantage of formulations polydispersity, by visualizing the largest particles it is possible to correlate its surface and morphology with the obtained

nanoparticles, and then better understand the influence of storage conditions on nanoparticles over time. The information about nanoparticles surface is crucial to infer its stability, and the stability of the loaded protein. On its turn, TEM visualizations helped to confirm particles size and shape.

3.1.2.1. Lyophilizate morphology

In Figure 5.2 it is shown the microphotographs of the lyophilizates. It was noticed a clear difference between the lyophilizate of freeze-dried insulin-PLGA nanoparticles and the cryoprotectant-added formulations, since the latter presented a compact aspect. These structures may be advantageous since the nanoparticles inside may get more protected from degradation, thus the structure of the loaded protein may be also more protected with the addition of cryoprotectants. Considering the freeze-dried insulin-PLGA nanoparticles + sucrose formulation, the lyophilizate did not show clearly the particles, but in all the other formulations it was possible to visualize the containing particles that maintained its characteristic spherical shape after lyophilization. The lyophilizate of formulations at the different storage conditions showed that particles could be perfectly observed in all formulations after 1 month of storage (Figure 5.3), but structural modifications of the lyophilizate of some formulations started to be observed after 3 months (Figure 5.4). For freeze-dried insulin-PLGA nanoparticles it was noticed that at 4ºC and 25ºC / 60% RH particles maintained their shape, however at 40ºC / 75% RH after 3 months particles lost their stability. In the cryoprotectant-added formulations the compact structure of the lyophilizate obtained after lyophilization could still be observed. Upon 6 months, at 4ºC and 25ºC / 60% RH it was possible to notice that particles maintained their shape. However it was predictably at 40ºC / 75% RH that particles shape mostly changed and when fructose was used the shape of the cake was really compromised, since no particles were visualized (Figure 5.5). These results indicate that the other cryoprotectants offered superior stability to the lyophilizate upon 6 months of storage, which was mostly noticed at 40ºC / 75% RH.

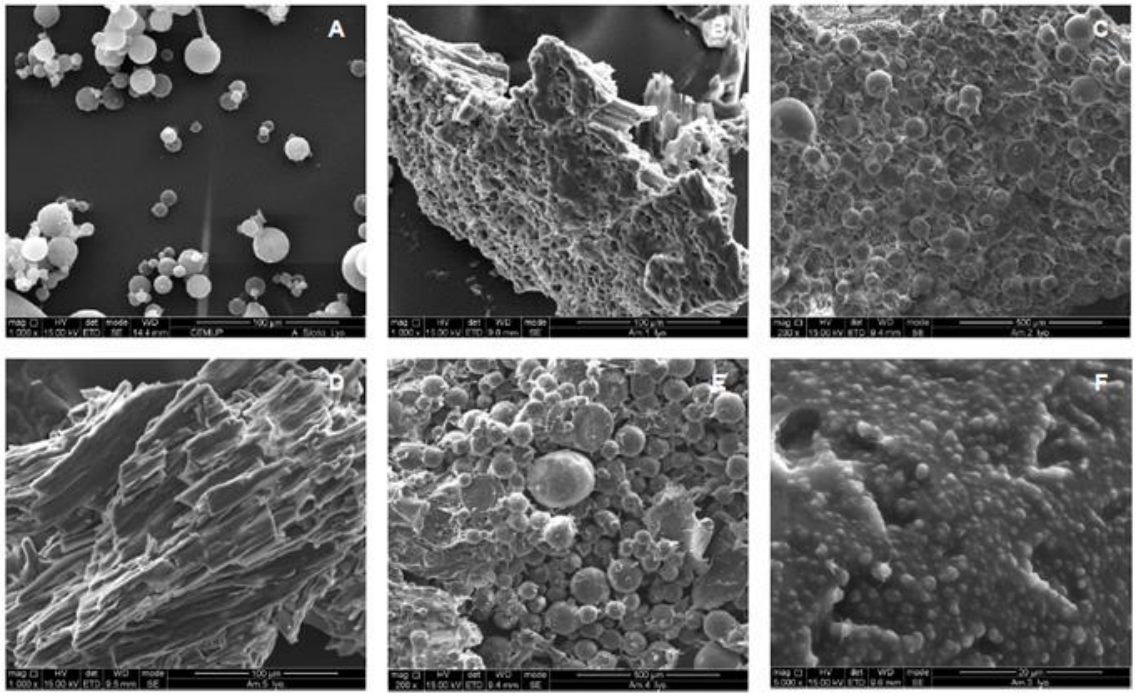

Figure 5.2. SEM microphotographs of the lyophilizates at t0. Freeze-dried insulin-PLGA nanoparticles (A), freeze-dried insulin-PLGA nanoparticles + trehalose (B), freeze-dried insulin-PLGA nanoparticles + glucose (C), freeze-dried insulin-PLGA nanoparticles + sucrose (D), freeze-dried insulin-PLGA nanoparticles + fructose (E) and freeze-dried insulin-PLGA nanoparticles + sorbitol (F). Scale bar: 20 µm (F), 100 µm (A, B, D) and 500 µm (C, E).

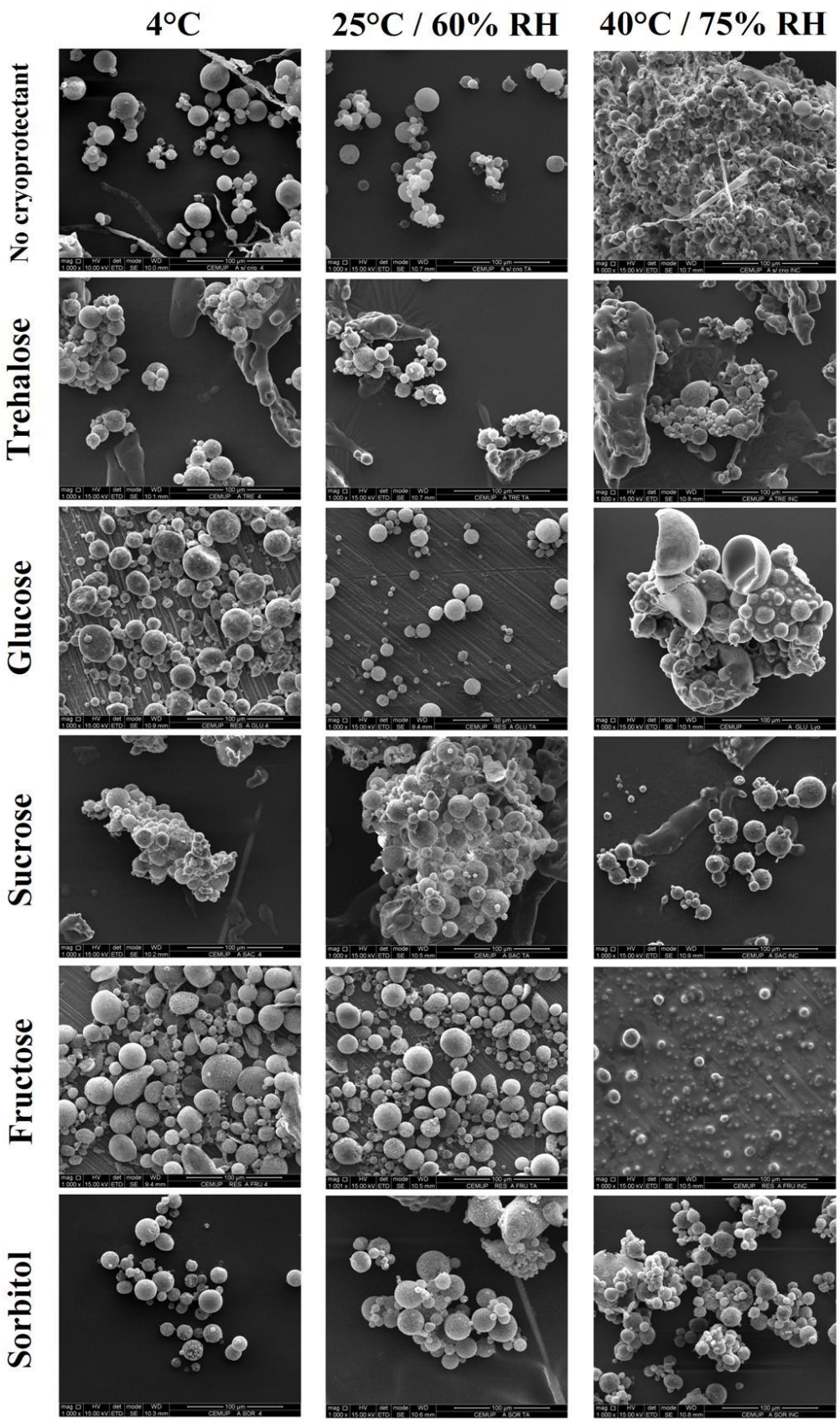

Figure 5.3. SEM microphotographs of the lyophilizates after 1 month of storage (t1) at the tested storage conditions. Scale bar: 100 µm**.**

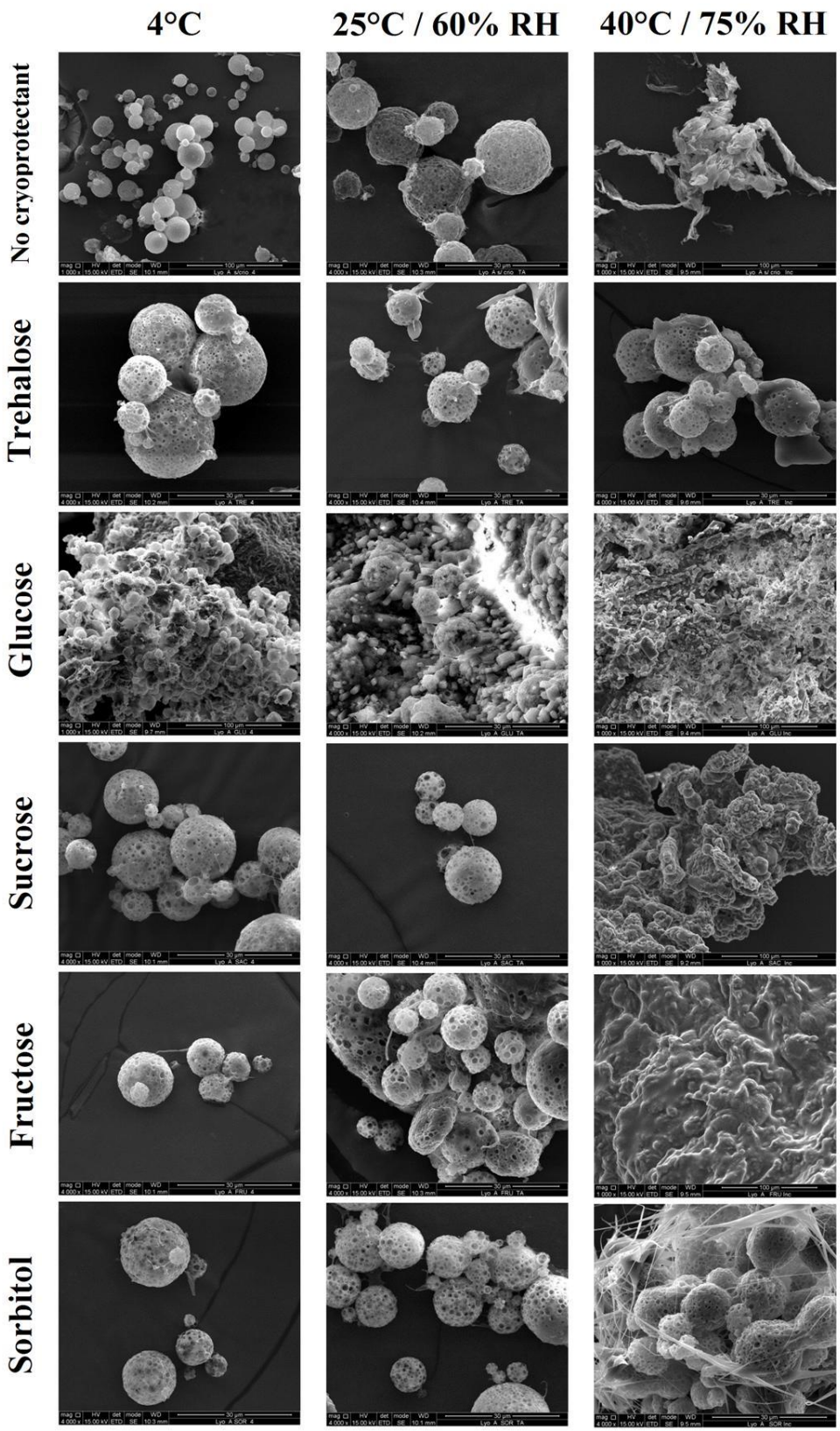

Figure 5.4. SEM microphotographs of the lyophilizates after 3 months of storage (t3) at the tested storage conditions. Scale bar: 30 µm (all microphotographs except, no cryoprotectant 4ºC and 40ºC / 75% RH, glucose 4ºC and 40ºC / 75% RH, sucrose 40ºC / 75% RH and fructose 40ºC / 75% RH at 100 µm).

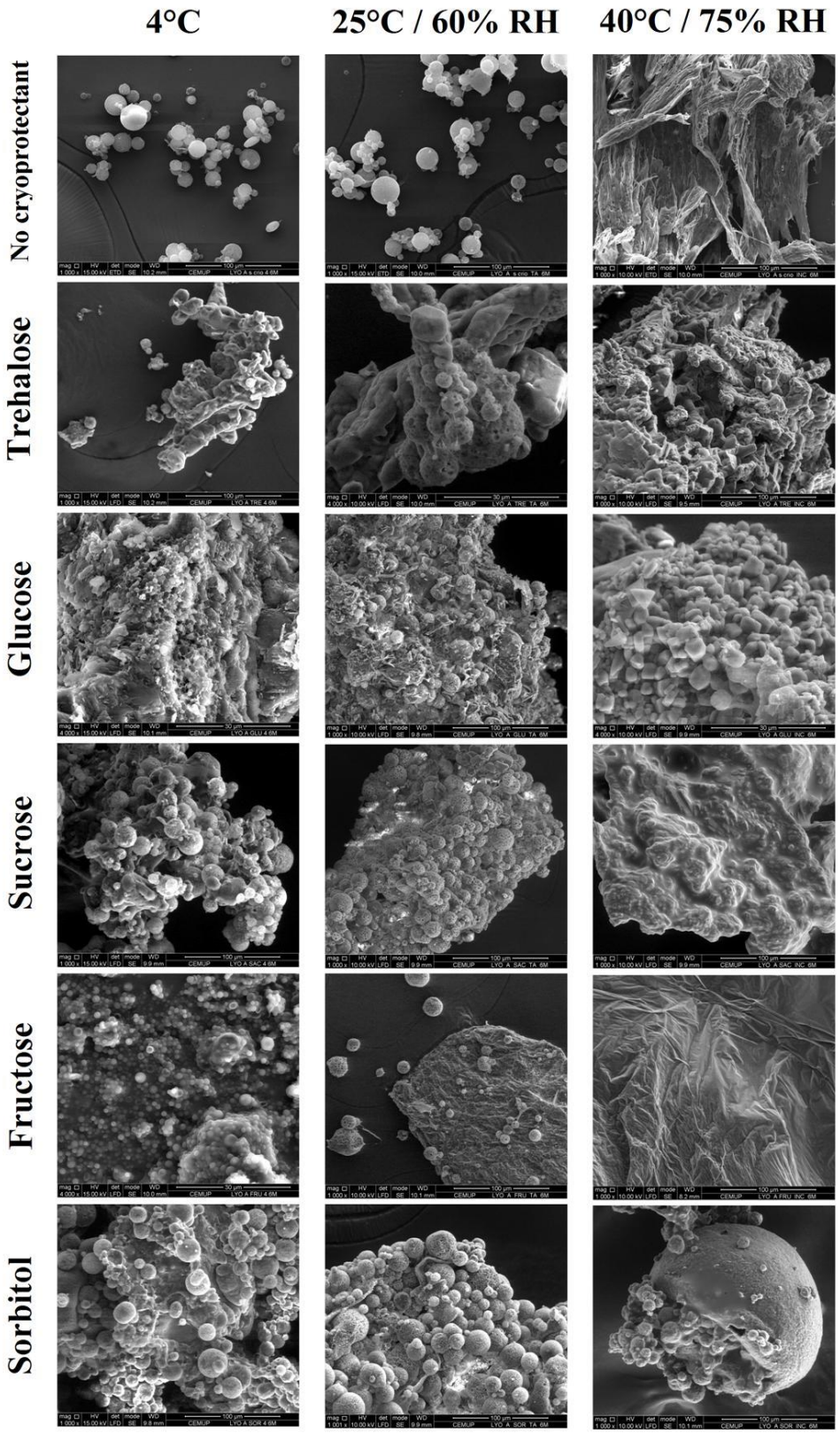

Figure 5.5. SEM microphotographs of the lyophilizates after 6 months of storage (t6) at the tested storage conditions. Scale bar: all microphotographs at 100 µm, except trehalose - 25ºC / 60% RH, glucose - 4ºC and 40ºC/75% RH; and fructose - 4ºC at 30 µm.

3.1.2.2. Particles morphology after lyophilizate resuspension

Figure 5.6 shows the TEM microphotographs of formulations at t0, and it was confirmed that nanoparticles maintained its characteristic spherical shape after lyophilization with and without added cryoprotectants, which was also proved by SEM visualizations in Figure 5.7. In Figure 5.8 and 5.9 it is shown the SEM microphotographs of all formulations after 6 months of storage.

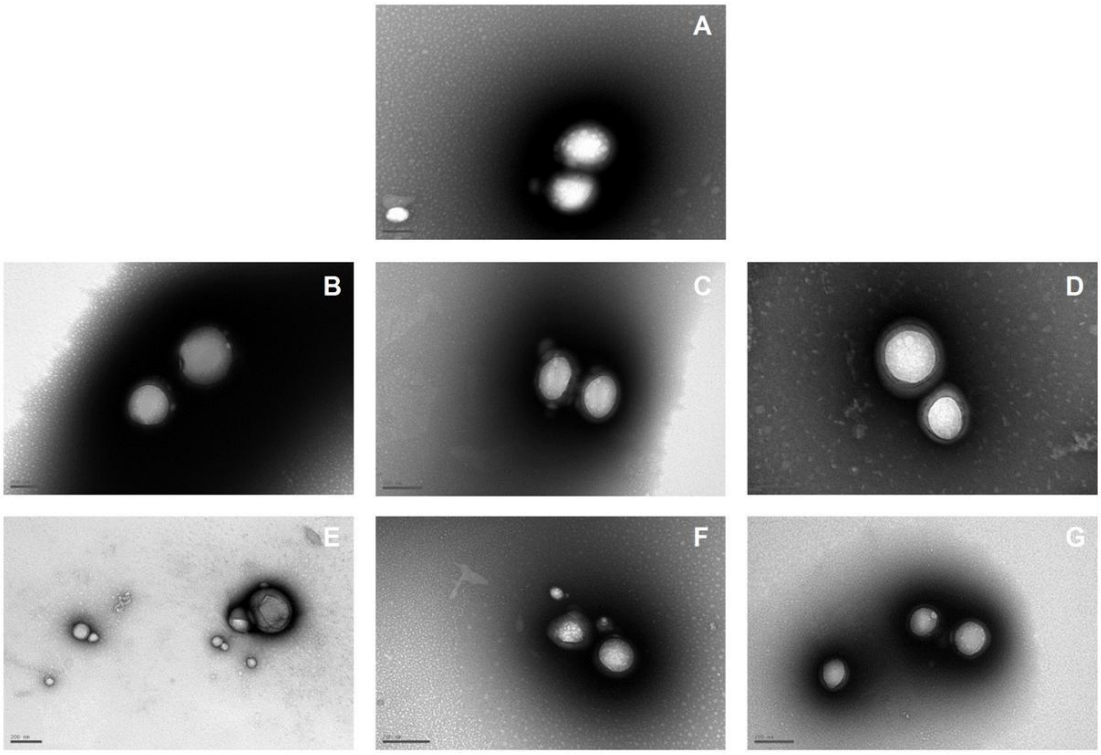

Figure 5.6. TEM microphotographs of insulin-PLGA nanoparticles after production (A) and after lyophilization. Freeze-dried insulin-PLGA nanoparticles (B), freeze-dried insulin-PLGA nanoparticles + trehalose (C), freeze-dried insulin-PLGA nanoparticles + glucose (D), freeze-dried insulin-PLGA nanoparticles + sucrose (E), freeze-dried insulin-PLGA nanoparticles + fructose (F) and freeze-dried insulin-PLGA nanoparticles + sorbitol (G). Scale bar: 200 nm.

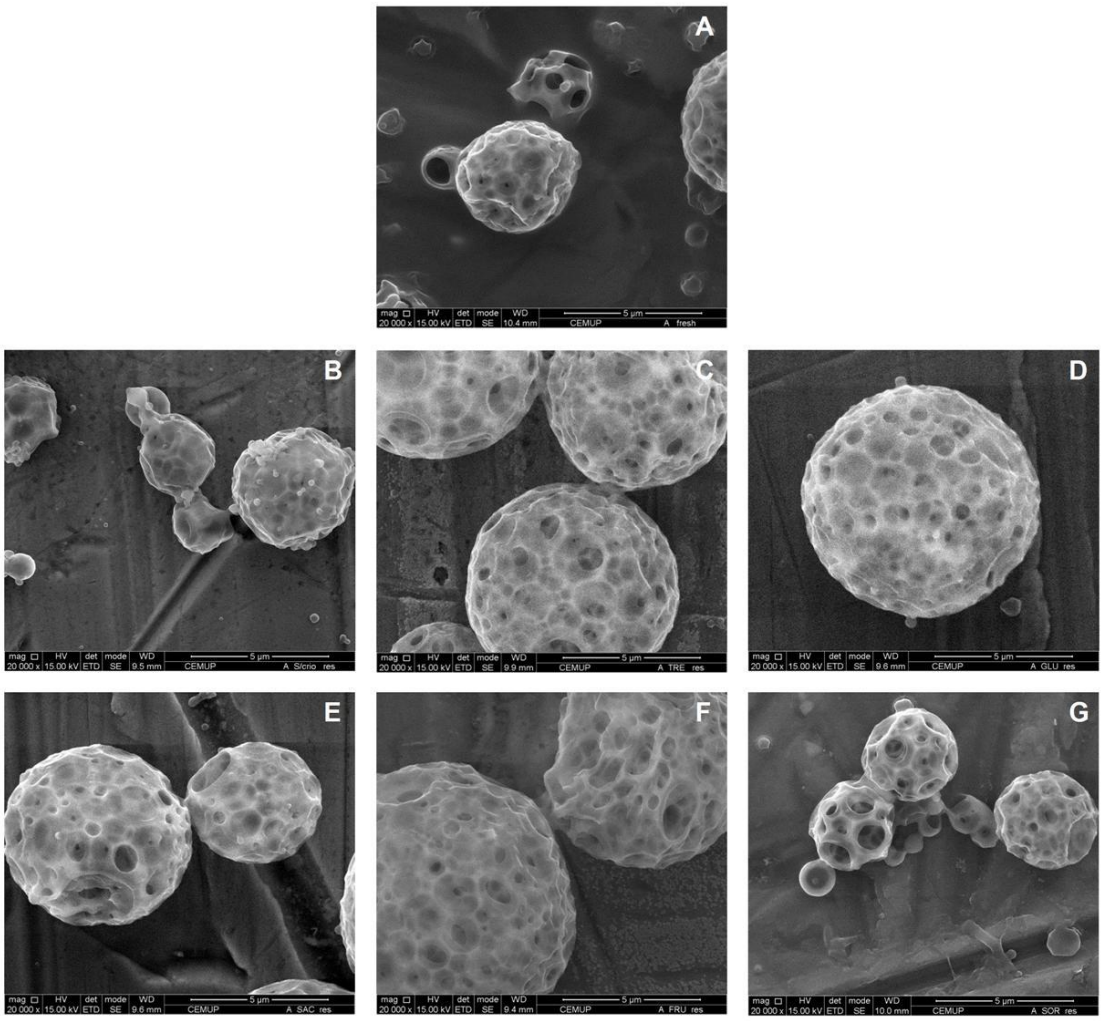

Figure 5.7. SEM microphotographs of insulin-PLGA nanoparticles after production (A) and after lyophilization. Freeze-dried insulin-PLGA nanoparticles (B), freeze-dried insulin-PLGA nanoparticles + trehalose (C), freeze-dried insulin-PLGA nanoparticles + glucose (D), freeze-dried insulin-PLGA nanoparticles + sucrose (E), freeze-dried insulin-PLGA nanoparticles + fructose (F) and freeze-dried insulin-PLGA nanoparticles + sorbitol (G). Scale bar: 5 µm.

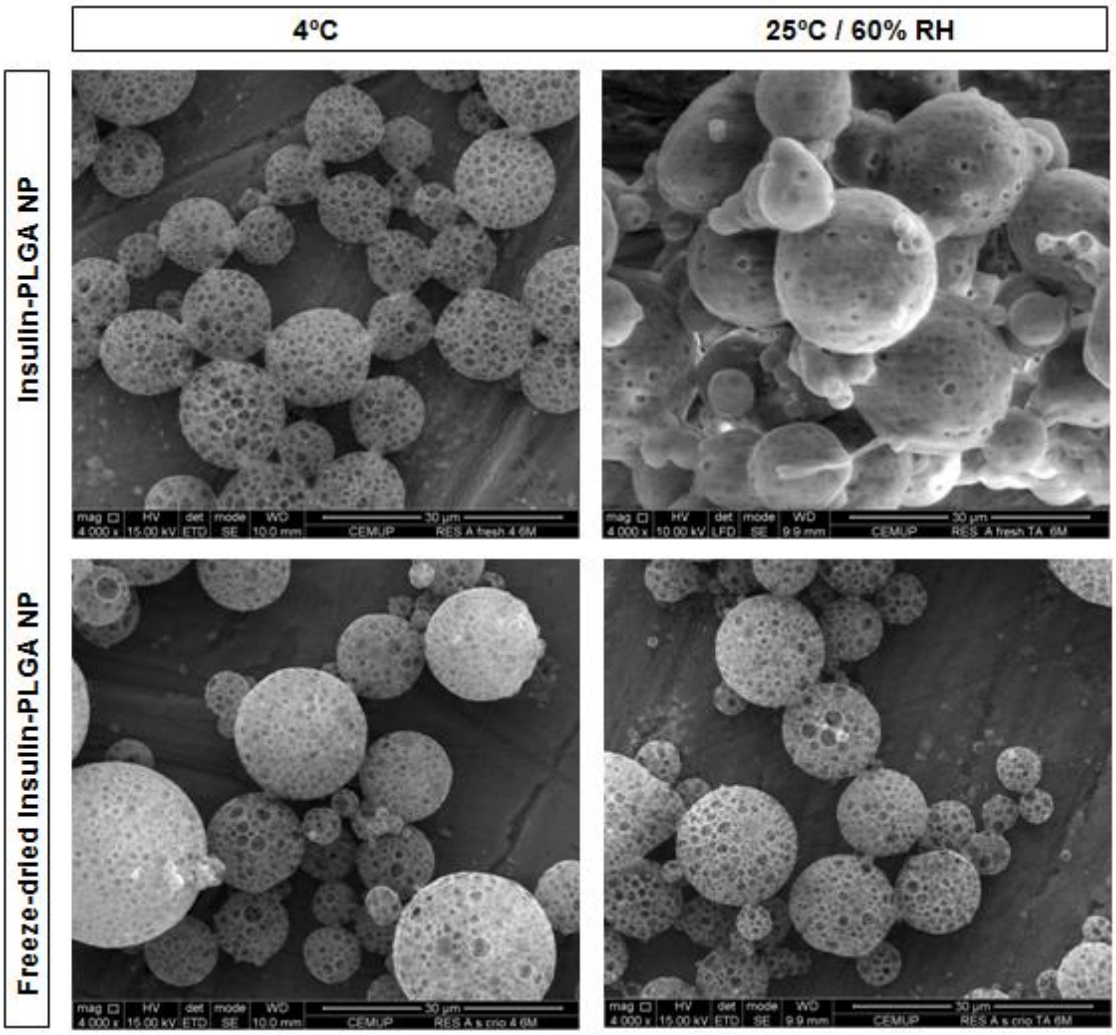

Figure 5.8. SEM microphotographs of insulin-PLGA nanoparticles and freeze-dried insulin-PLGA nanoparticles upon 6 months of storage at 4ºC and 25ºC/60% RH. Scale bar: 30 µm. NP stands for nanoparticles.

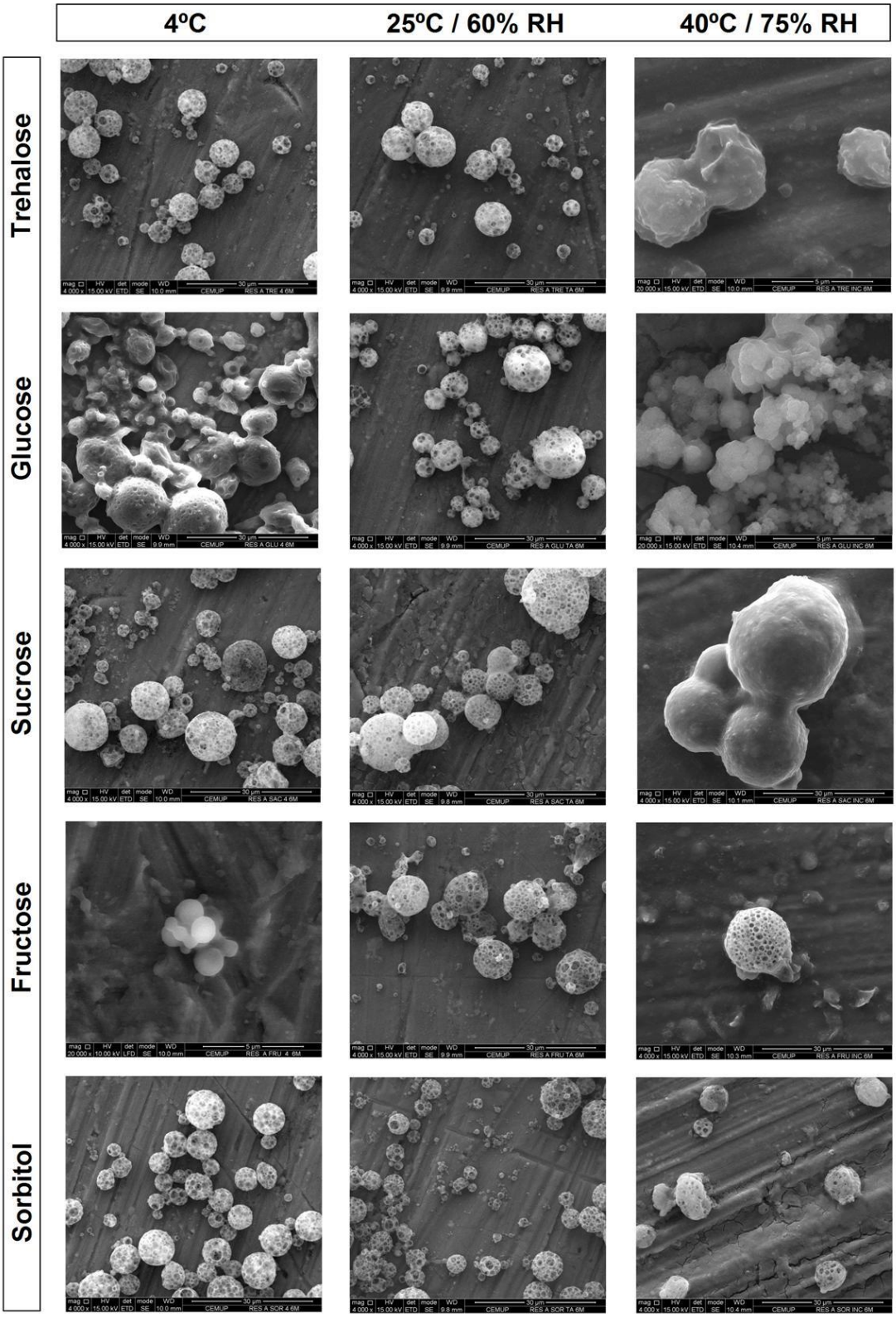

Figure 5.9. SEM microphotographs of lyophilized insulin-PLGA nanoparticles added with cryoprotectants upon 6 months of storage at 4ºC, 25ºC/60% RH and 40ºC/75% RH. Scale bar: all microphotographs at 30 µm, except trehalose 40ºC / 75% RH, glucose 40ºC / 75% RH and fructose 4ºC at 5 µm.

3.1.2.2.1. Insulin-PLGA nanoparticles

The TEM and SEM microphotographs of insulin-PLGA nanoparticles at the storage conditions at t0, t1, t3 and t6 are shown respectively, in figures 5.10 and 5.11. Insulin-PLGA nanoparticles maintained its spherical shape at 4ºC and 25ºC / 60% RH upon 6 months, however as referred above, at 40ºC / 75% RH the formulation completely changed and from a milky aspect at the beginning over time became to a more aqueous aspect with an increasing deposit of aggregated polymer. Comparatively to other formulations and as expected, these results showed that lyophilization improved the stability of nanoparticles upon storage. At 40ºC / 75% RH insulin-PLGA nanoparticles macroscopic shape presented agglomerated polymer pieces in suspension, and in SEM visualizations no particles were found because most of them got degraded (Figure 5.8). Even though, the remainder particles did not significantly changed its particle size, upon 6 months at this storage condition (Figure 5.1). Besides of maintained their spherical shape at 4ºC and 25ºC / 60% RH after 6 months, insulin-PLGA nanoparticles surface was considerable distinct, which revealed the degradation suffered under these storage conditions. In addition, the ability of particles to be more permissive relatively to external degradation factors, for instance through nanoparticles pores, may be different under these two conditions that might play a different role on the ability of the carrier to protect the loaded protein.

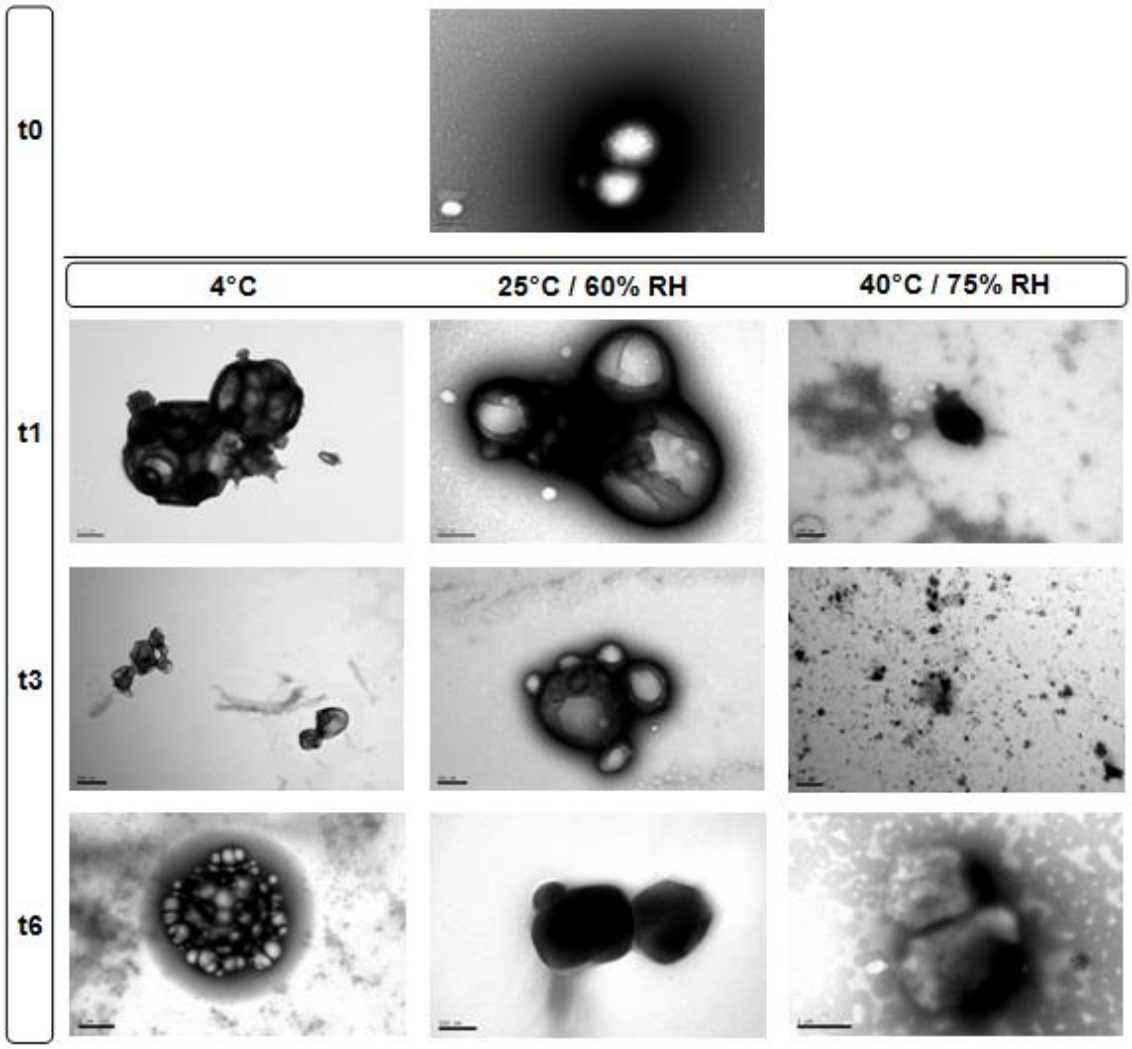

Figure 5.10. TEM microphotographs of insulin-PLGA nanoparticles formulations at t0, t1, t3 and t6, under the storage conditions. Scale bar: 100 nm (t1 25ºC / 60%RH, t6 25ºC / 60%RH); 200 nm (t0, t1 40ºC / 75%RH, t3 4ºC, t3 25ºC / 60% RH); 0.5 µm (t1 4ºC, t3 40ºC / 75% RH) and 1 µm (t6 4ºC, t6 40ºC / 75% RH).

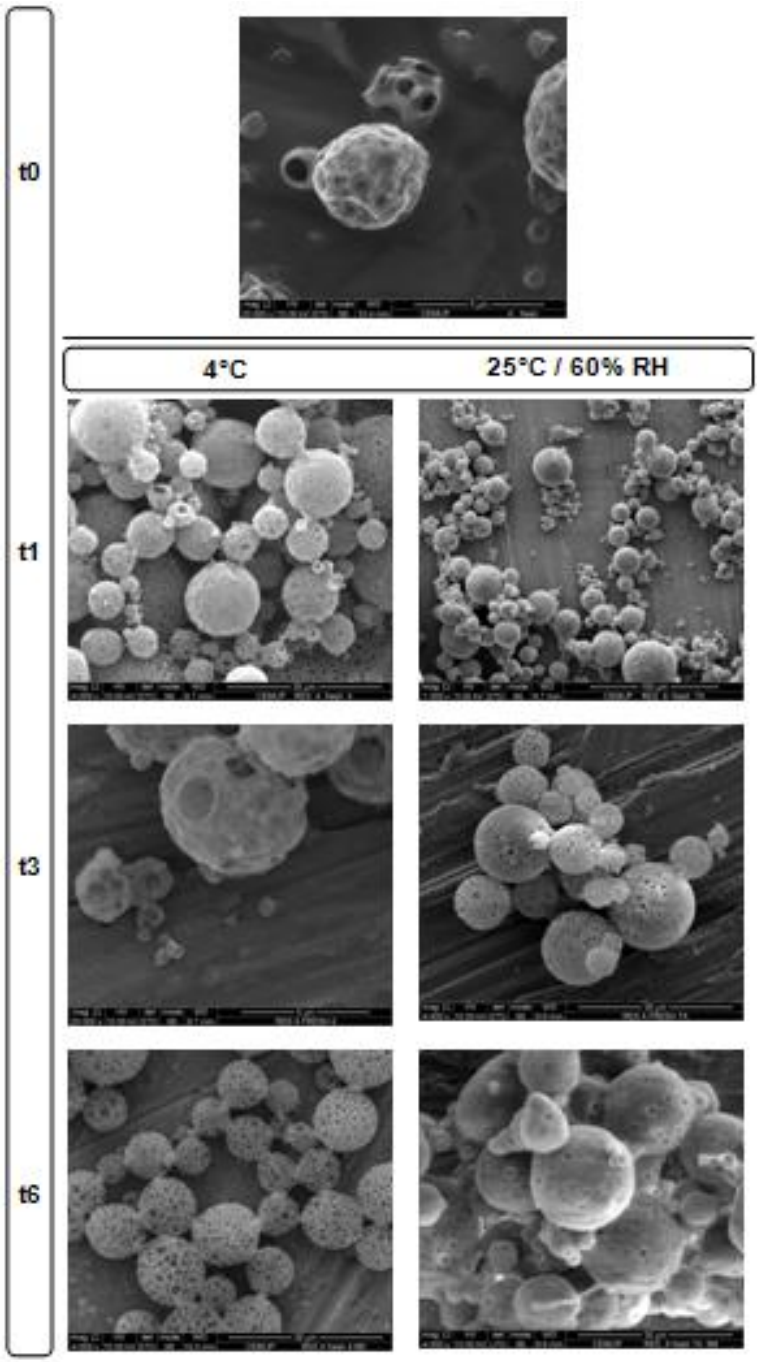

Figure 5.11. SEM microphotographs of insulin-PLGA nanoparticle formulations at t0, t1, t3 and t6, under the tested storage conditions. No particles found at 40ºC / 75% RH due to degradation suffered. Scale bar: 5 µm (t3 4ºC); 30 µm (t1 4ºC, t3 25ºC / 60% RH, t6 4ºC, t6 25ºC / 60% RH); 100 µm (t1 25ºC / 60% RH) and 500 µm (t0).

3.1.2.2.2. Lyophilized nanoparticles

Freeze-dried insulin-PLGA nanoparticles maintained its spherical shape in all time points and tested storage conditions except for 40ºC / 75% RH at t6. Particles surface was maintained after storage at 4ºC and 25ºC / 60% RH and at the latter condition after 6 months the surface seemed to maintain better than insulin-PLGA nanoparticles. At 40ºC / 75% RH particles maintained its shape upon 3 months; however it was not possible to visualize stable nanoparticles after 6 months storage due to surface degradation (Figure 5.8). The TEM and SEM microphotographs of lyophilized PLGA nanoparticles at the tested storage conditions at t0, t1, t3 and t6 are shown respectively, in figures 5.12 and 5.13. The microscopy findings for these formulations showed that the addition of cryoprotectants was necessary to improve nanoparticles stability, especially at 40ºC / 75% RH.

SEM microphotographs of cryoprotectant added formulations, upon 6 months of storage are shown in Figure 5.9. Freeze-dried insulin-PLGA nanoparticles + trehalose maintained its spherical shape at all the tested storage conditions and time points. At 40ºC / 75% RH after 6 months particles maintained its shape, showing that the presence of the cryoprotectant during lyophilization better stabilized the nanoparticles comparatively to lyophilized insulin-PLGA nanoparticles. Particles maintained its surface characteristics at all the storage conditions upon 6 months of storage except for 40ºC / 75% RH at t6, in which particles surface completely changed due to suffered degradation.

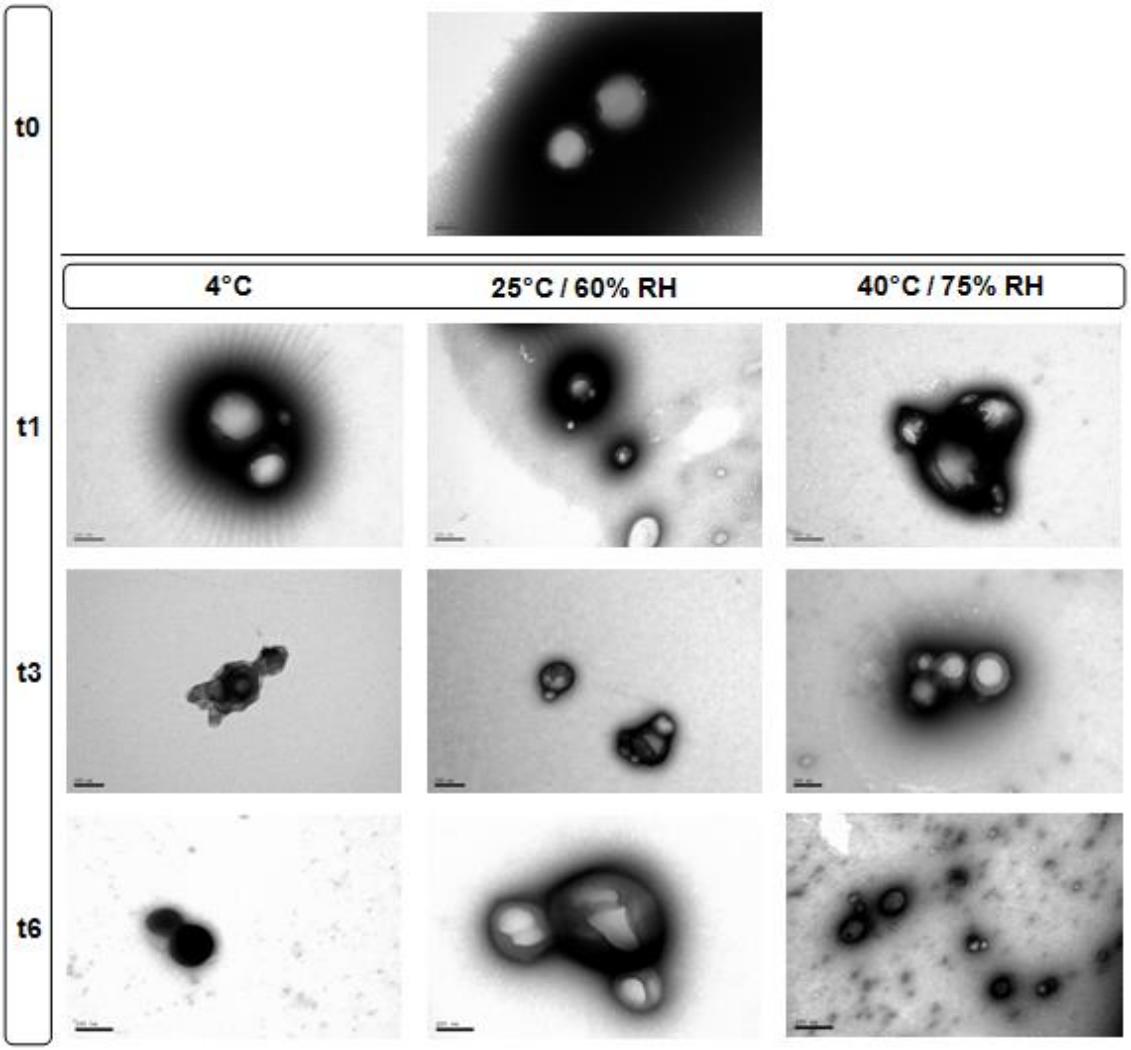

Figure 5.12. TEM microphotographs of freeze-dried insulin-PLGA nanoparticle formulations at t0, t1, t3 and t6, under the tested storage conditions. Scale bar: 200 nm, all microphotographs except t3 40ºC / 75%RH, t6 25ºC / 60% RH at 100 nm.

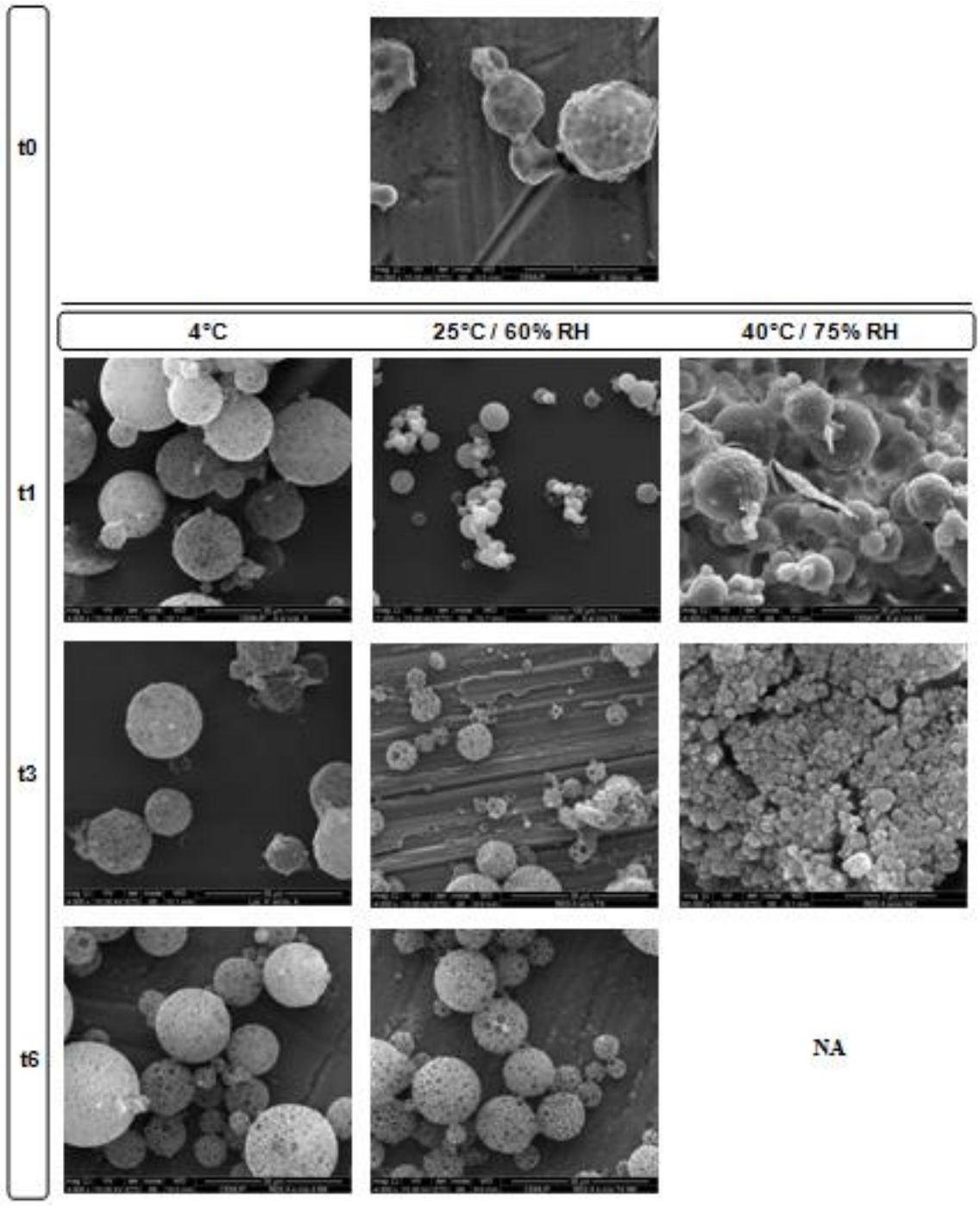

Figure 5.13. SEM microphotographs of freeze-dried insulin-PLGA nanoparticle formulations at t0, t1, t3 and t6, under the tested storage conditions. NA: Not available due to particle degradation. Scale bar: 30 µm, all microphotographs except t3 40ºC / 75% RH at 1 µm; t0 at 5 µm; and t1 25ºC / 60% RH, t6 40ºC / 75% RH at 100 µm.

Lyophilized insulin-PLGA nanoparticles + glucose were stable and maintained their shape upon 6 months of storage at 4ºC and 25ºC / 60% RH, but at 40ºC / 75% RH after 3 months were degraded and changed into a cubical shape, which was also observed at t6. This showed that glucose was not effective to protect the lyophilized nanoparticles in such a way that could preserve its stability upon storage at 40ºC / 75% RH. After 6 months of storage at 4ºC, the particles surface seem to change more significantly than those stored at 25ºC / 60% RH, showing that freeze-dried insulin-PLGA nanoparticles + glucose at the latter storage condition remained more stable during that period of time. SEM microphotographs also showed that the shape of the particles stored at 40ºC / 75% RH was completely different from the particles stored at other conditions.

Freeze-dried insulin-PLGA nanoparticles + sucrose maintained its spherical shape at all the tested storage conditions and time points except at 40ºC / 75% RH in which seems to be degraded. SEM microphotographs showed precisely this fact in which, comparatively to other storage conditions, particles surface stored at 40ºC / 75% RH after 6 months were completely changed indicating the suffering of degradation upon storage (Figure 5.9). It was observed that sucrose was able to preserve particles surface after 3 months stored at 40ºC / 75% RH and after 6 months at the other storage conditions.

Regarding freeze-dried insulin-PLGA nanoparticles + fructose, they maintained its shape at all the storage conditions and time points except for 4ºC at t6, and its surface was also maintained after 6 months at the storage conditions, however for 4ºC at t6 the visualized particles did not gave information about the surface.

Freeze-dried insulin-PLGA nanoparticles + sorbitol maintained its spherical shape after 6 months at the storage conditions. Furthermore, the particles surface also maintained its characteristics upon storage which indicated that sorbitol was effective on protecting particles from degradation upon storage. Indeed, it was also the lyophilized formulation that less increased its particle size after 6 months at 25ºC / 60% RH and 40ºC / 75% RH. The TEM and SEM microphotographs of all the cryoprotectant added formulations at the tested storage conditions at t0, t1, t3 and t6 are shown in figures 5.14-5.23. The visualization of lyophilized nanoparticles by TEM after its resuspension is feasible, but difficult to occur by SEM whenever cryoprotectant concentration exceeds 5%, due to a continuous amorphous matrix embedding the nanoparticles [7, 101, 168]. This is mainly due to the ability of cryoprotectants to form hydrogen bonds with the polar groups at nanoparticles surface, replacing water as it freezes [7]. This property is favorable for nanoparticles protection, but interferes with SEM measurements. It was also reported that PVA remained associated with the surface of nanoparticles even after

washing, acting as a cryoprotectant by improving nanoparticles freezing resistance and stability [236].

Considering the overall results it was noticed that insulin-PLGA nanoparticles were not stable after storage at 40ºC / 75% RH, and this was mitigated by lyophilization of the formulation. Even improving the stability at this condition, it was noticed that the addition of cryoprotectants was necessary to improve the stability of particles upon 6 months of storage. In all the lyophilized formulations it was visualized that particles surface changed over time until the 6 months of storage, which is due to the degradation suffered upon storage and the hydrolytic action of the residual moisture content in the lyophilizate, which may be noticed by the 'melted' shape of particles surface. Indeed, cryoprotectants are amorphous but tend to crystallize with the increase of the residual water content or during heating and storage at high temperatures, becoming a source of instability. It was reported that high residual water content may destabilize nanoparticles during storage due to cryoprotectant crystallization [140]. The crystallization of amorphous sugars occurs when the formulation is hold above its Tg. The containing water may induce a shift in the Tg of the formulation to below the storage temperature, so a high residual water content may promote the crystallization of the formulation upon storage. The rate of crystallization increases with the increase of temperature and RH [252]. These changes on nanoparticles surface and stability may affect the stability of the loaded protein, since the surface modifications may lead to the open of pathways for loaded protein instability. Regarding, all the tested formulation it was the freeze-dried insulin-PLGA nanoparticles + sorbitol that seemed to be more stable at all the storage conditions upon 6 months of storage.

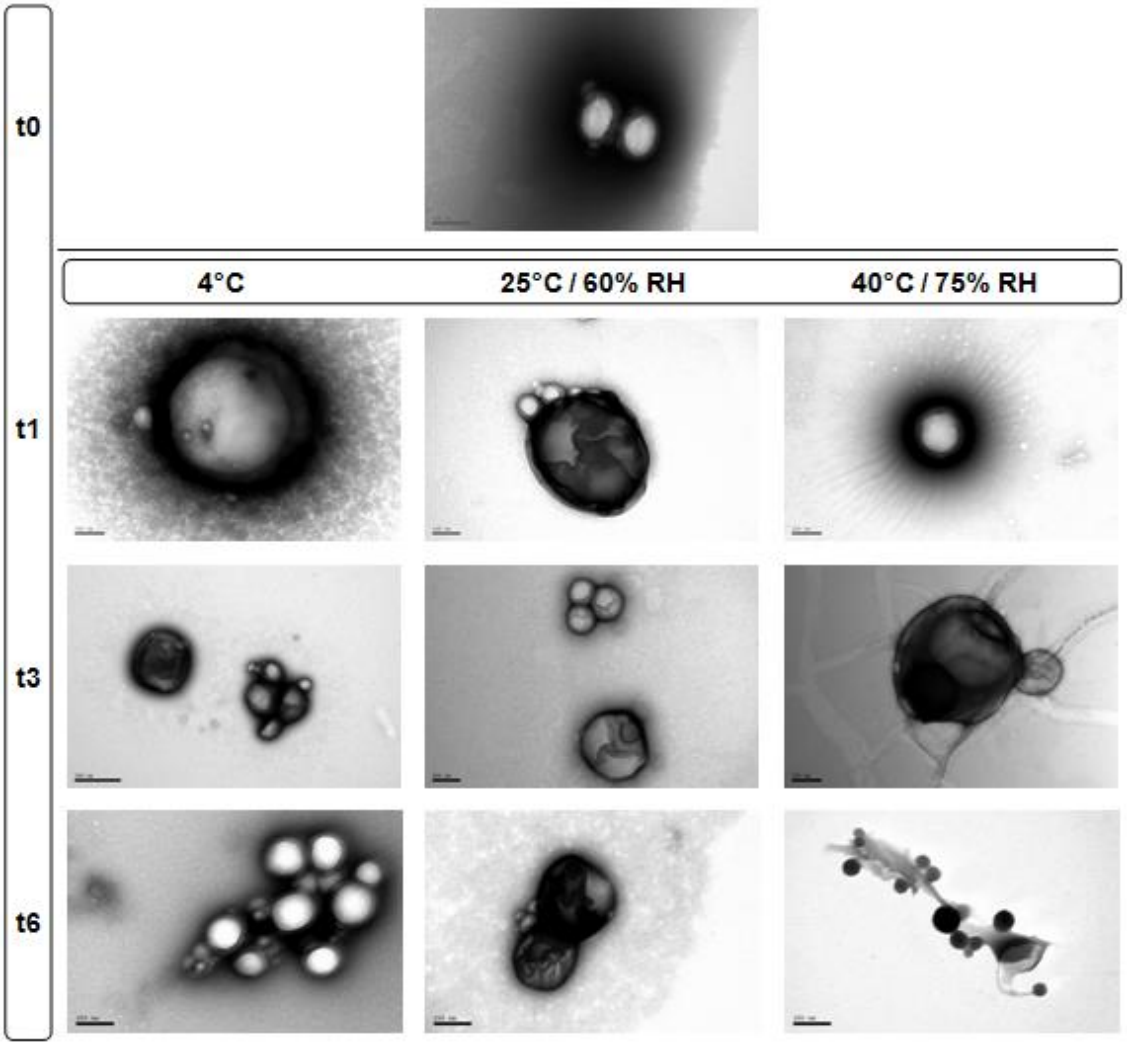

Figure 5.14. TEM microphotographs of freeze-dried insulin-PLGA nanoparticles + trehalose formulations at t0, t1, t3 and t6, under the tested storage conditions. Scale bar: 200 nm, all microphotographs except t1 25ºC / 60% RH, t3 25ºC / 60% RH at 100 nm; and t3 - 4ºC at 500 nm.

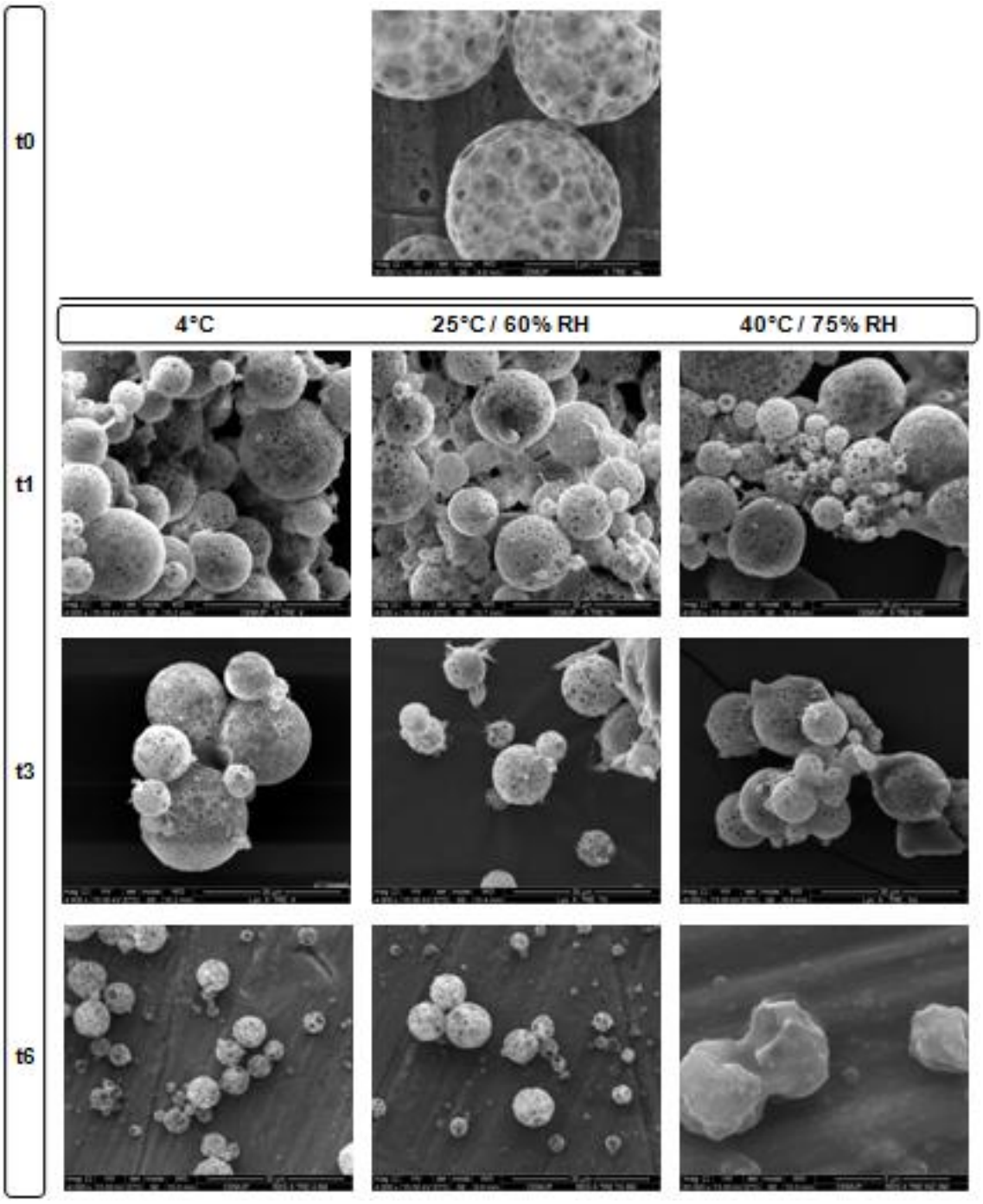

Figure 5.15. SEM microphotographs of freeze-dried insulin-PLGA nanoparticles + trehalose formulations at t0, t1, t3 and t6, under the tested storage conditions. Scale bar: 30 µm, all microphotographs, except t0, t6 40ºC / 75% RH at 5 µm.

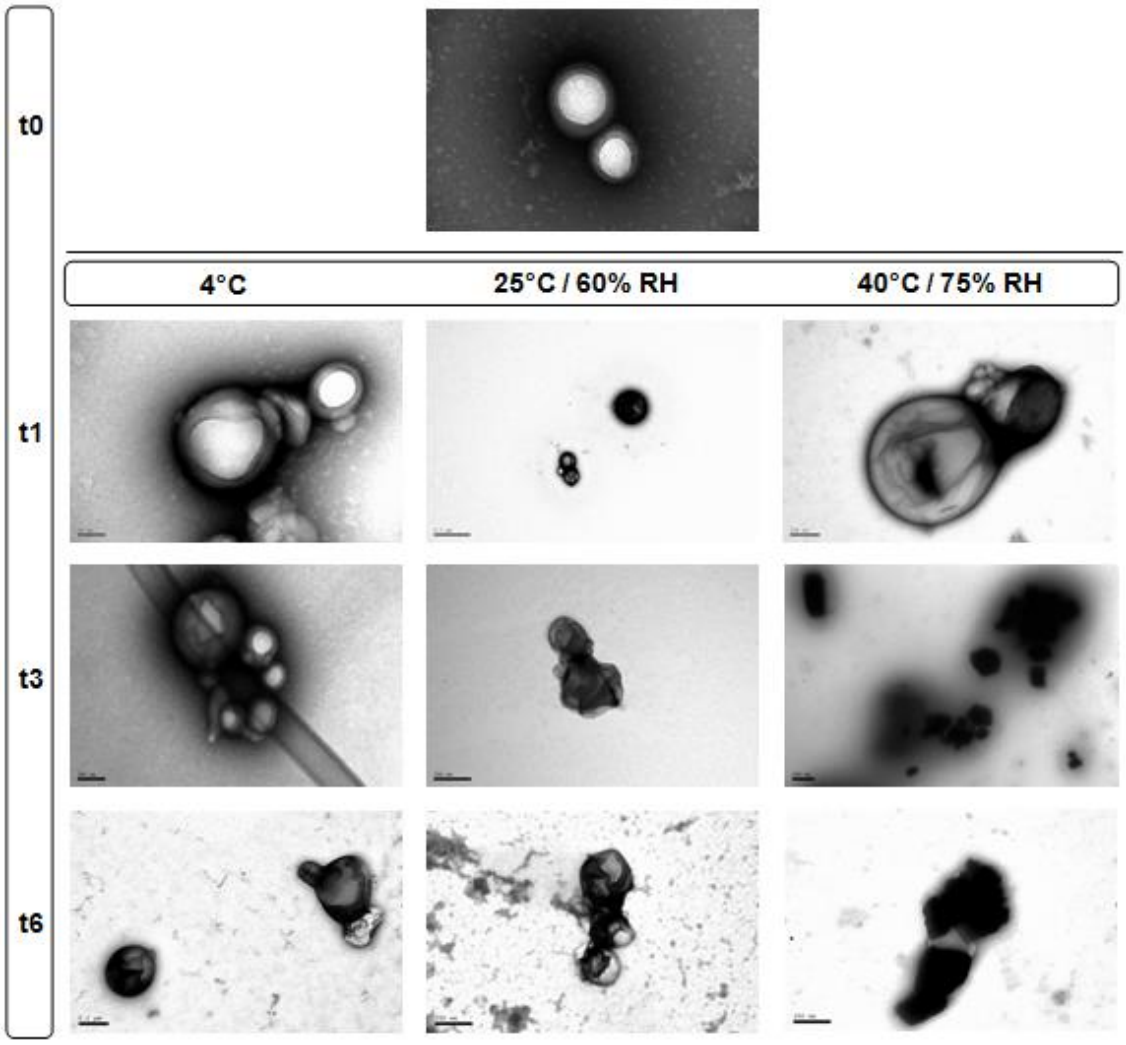

Figure 5.16. TEM microphotographs of freeze-dried insulin-PLGA nanoparticles + glucose formulations at t0, t1, t3 and t6, under the tested storage conditions. Scale bar: 200 nm, all microphotographs except t1 4ºC at 50 nm; t3 4ºC at 100 nm; and t1 25ºC / 60% RH at 0.5 µm.

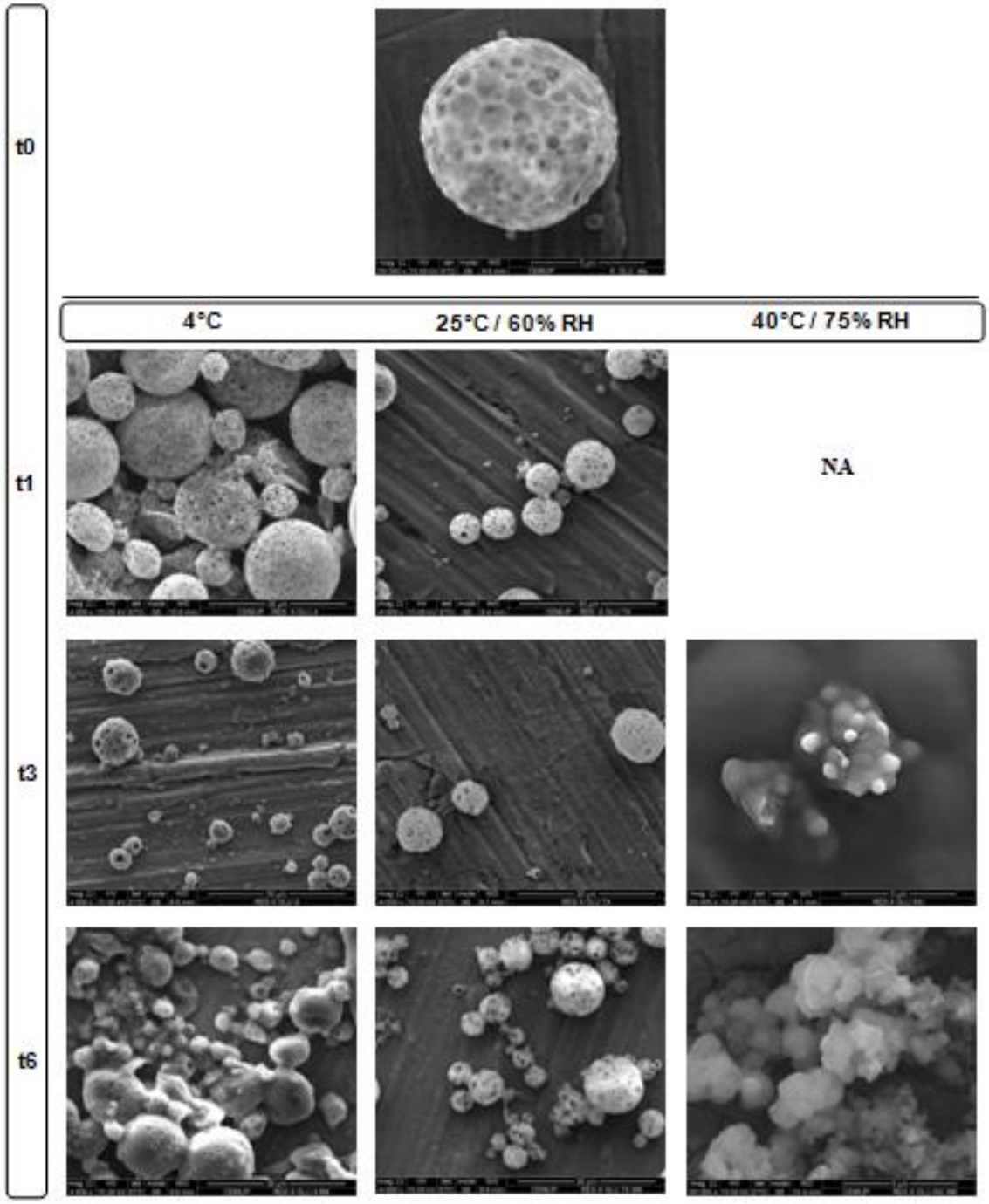

Figure 5.17. SEM microphotographs of freeze-dried insulin-PLGA nanoparticles + glucose formulations at t0, t1, t3 and t6 under, the tested storage conditions. NA: Not available due to particle degradation. Scale bar: 30 µm, all microphotographs except t0, t3 40ºC / 75% RH, t6 40ºC / 75% RH at 5 µm; and t1 40ºC / 75% RH at 100 µm.

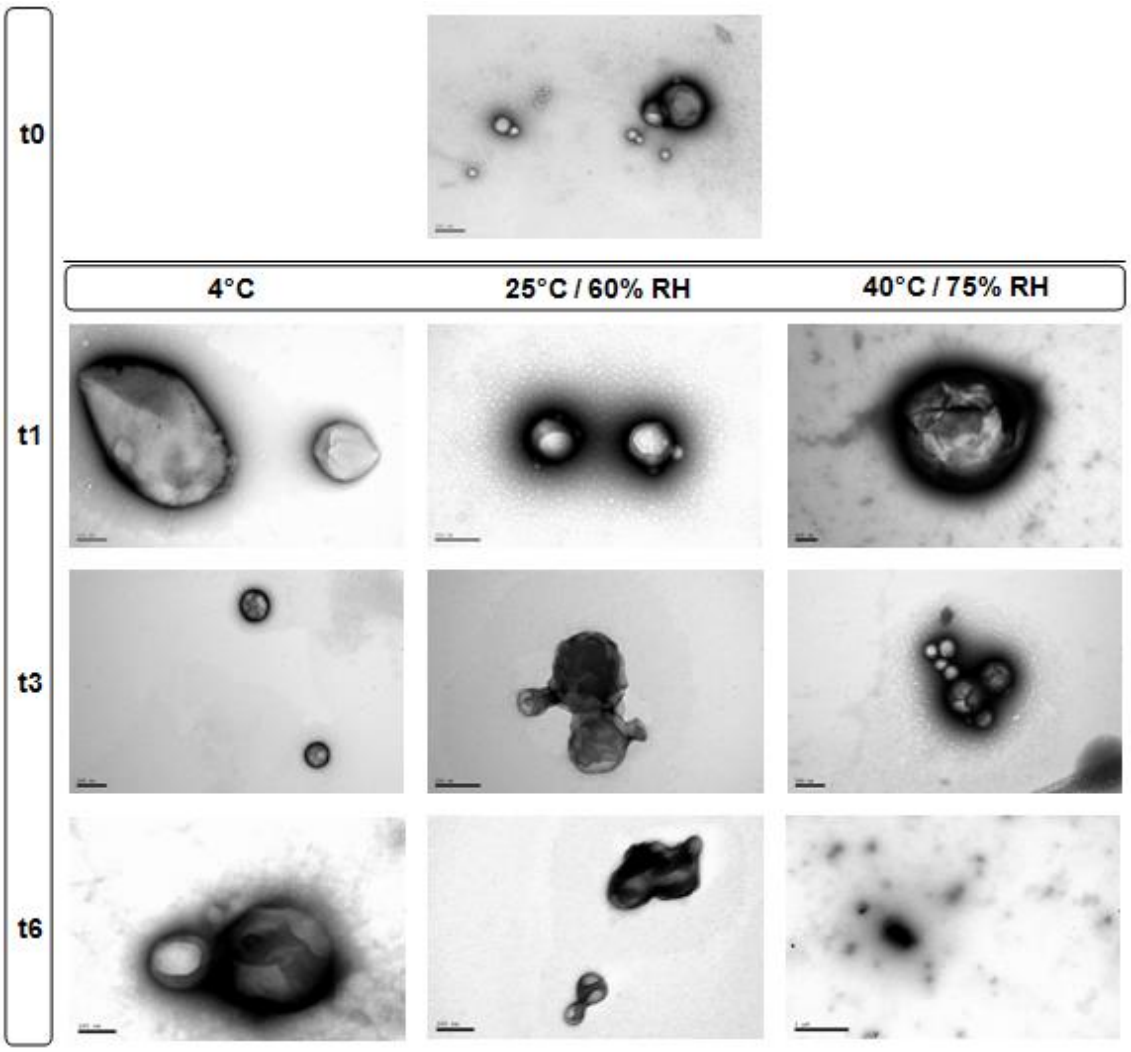

Figure 5.18. TEM microphotographs of freeze-dried insulin-PLGA nanoparticles + sucrose formulations at t0, t1, t3 and t6, under the tested storage conditions. Scale bar: 200 nm, all microphotographs except t6 4ºC at 100 nm; and t6 40ºC / 75% RH at 1 µm.

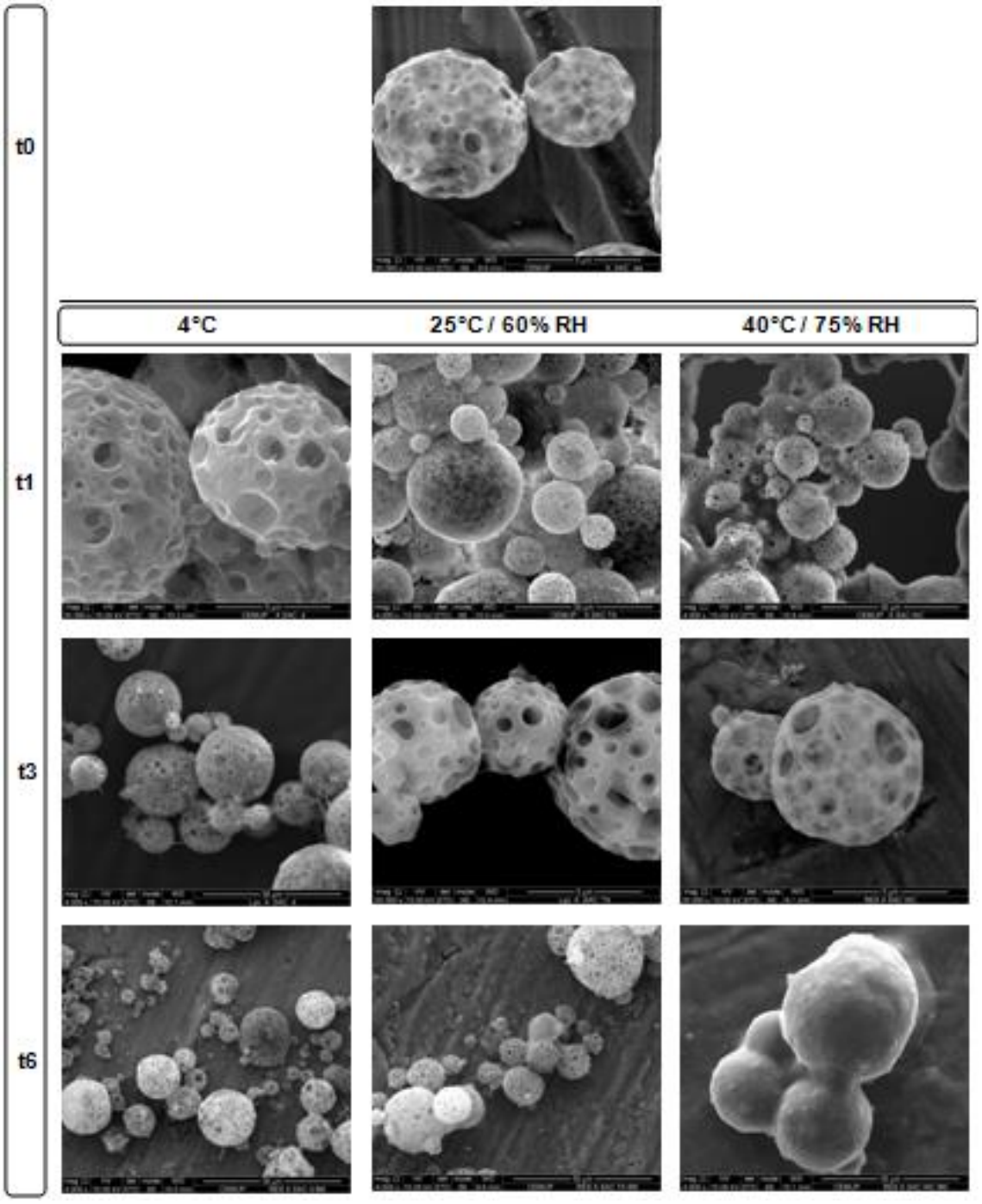

Figure 5.19. SEM microphotographs of freeze-dried insulin-PLGA nanoparticles + sucrose formulations at t0, t1, t3 and t6, under the tested storage conditions. Scale bar: 30 µm, all microphotographs except t0, t1 4ºC, t3 25ºC / 60% RH, t3 40ºC / 75% RH at 5 µm.

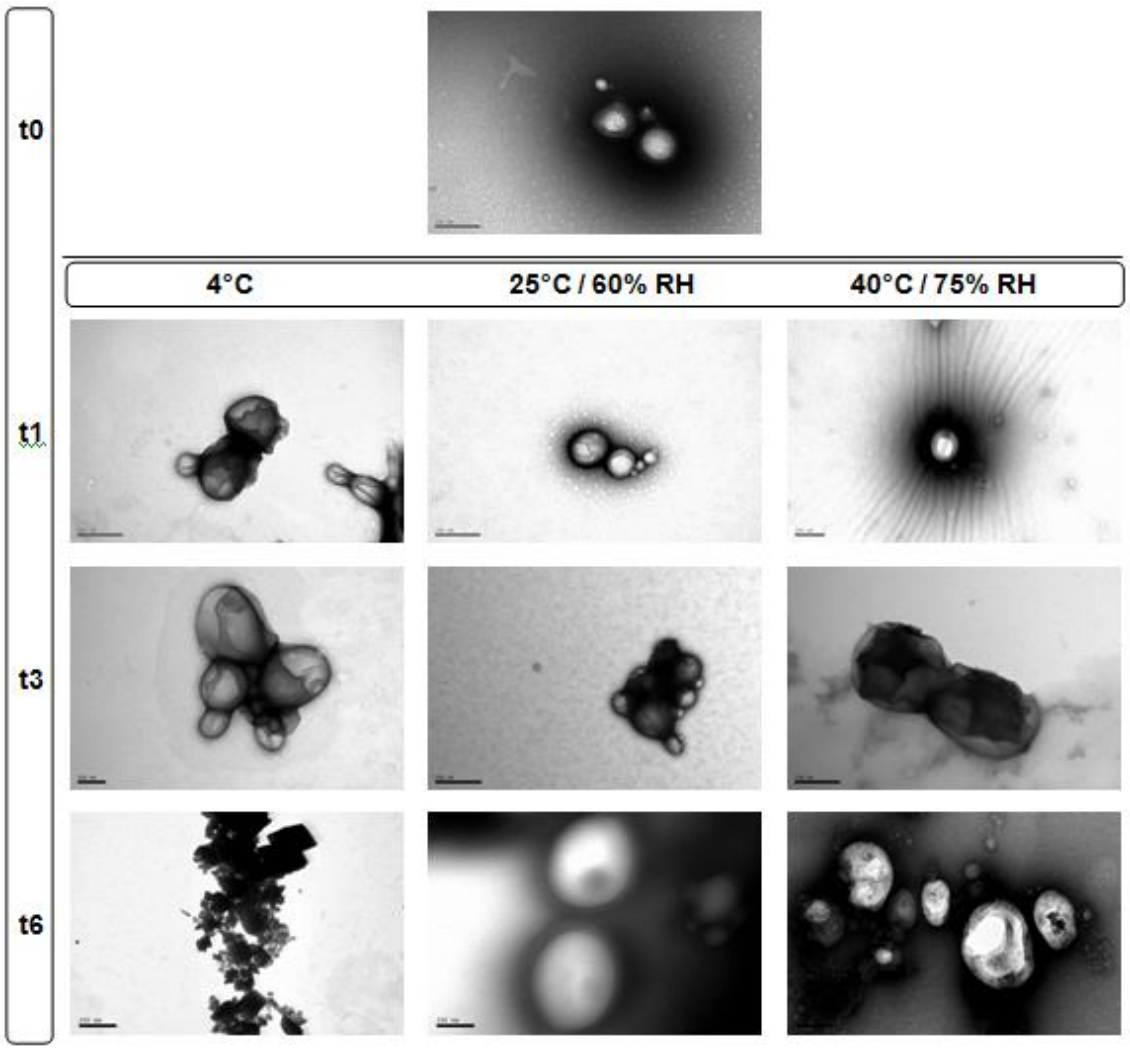

Figure 5.20. TEM microphotographs of freeze-dried insulin-PLGA nanoparticles + fructose formulations at t0, t1, t3 and t6, under the tested storage conditions. Scale bar: 200 nm, all microphotographs except t3 4ºC at 100 nm; and t3 25ºC / 60% RH at 500 nm.

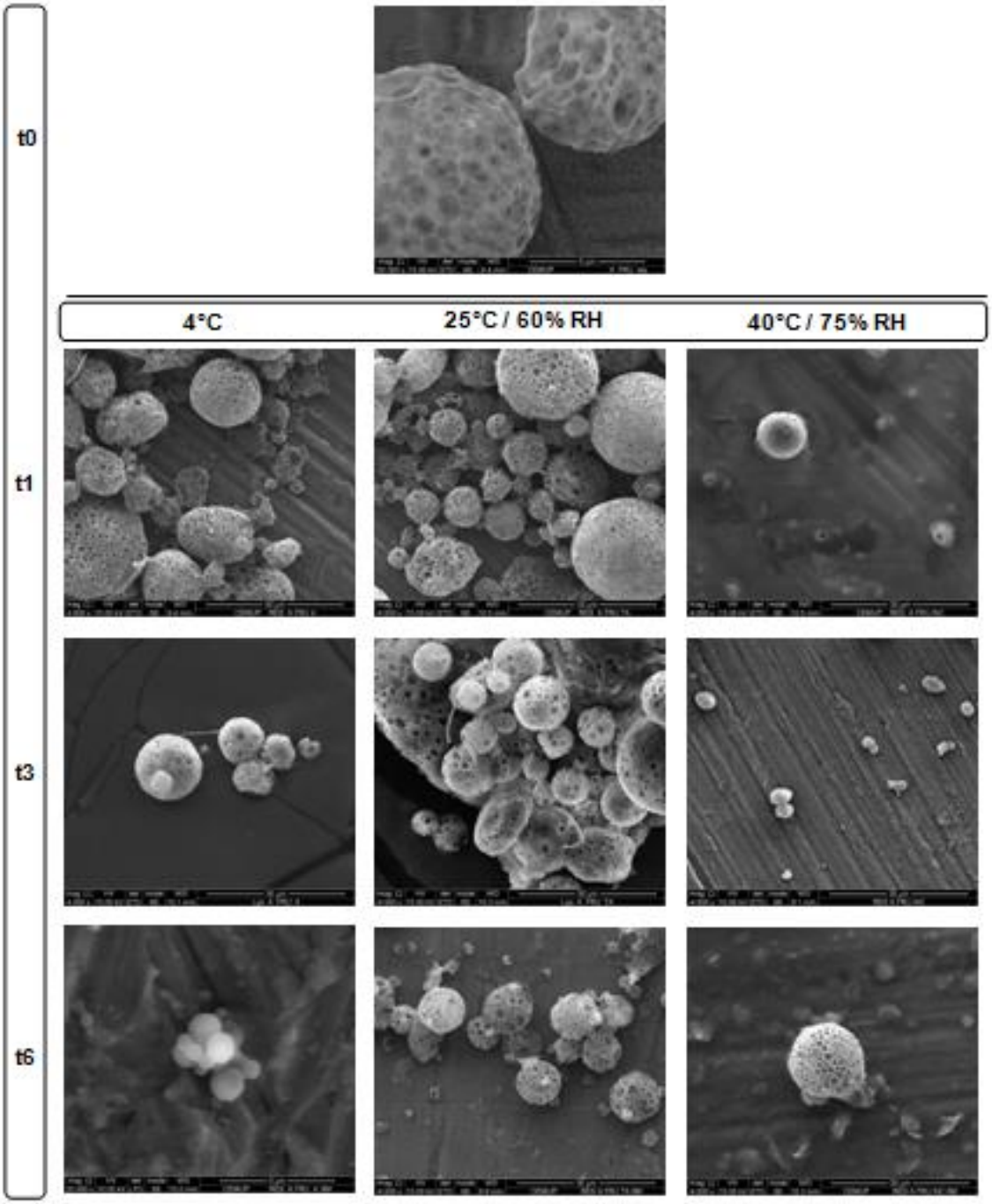

Figure 5.21. SEM microphotographs of freeze-dried insulin-PLGA nanoparticles + fructose formulations at t0, t1, t3 and t6, under the tested storage conditions. Scale bar: 30 µm, all microphotographs except t0, t6 4ºC at 5 µm; and t1 40ºC / 75% RH at 100 µm.

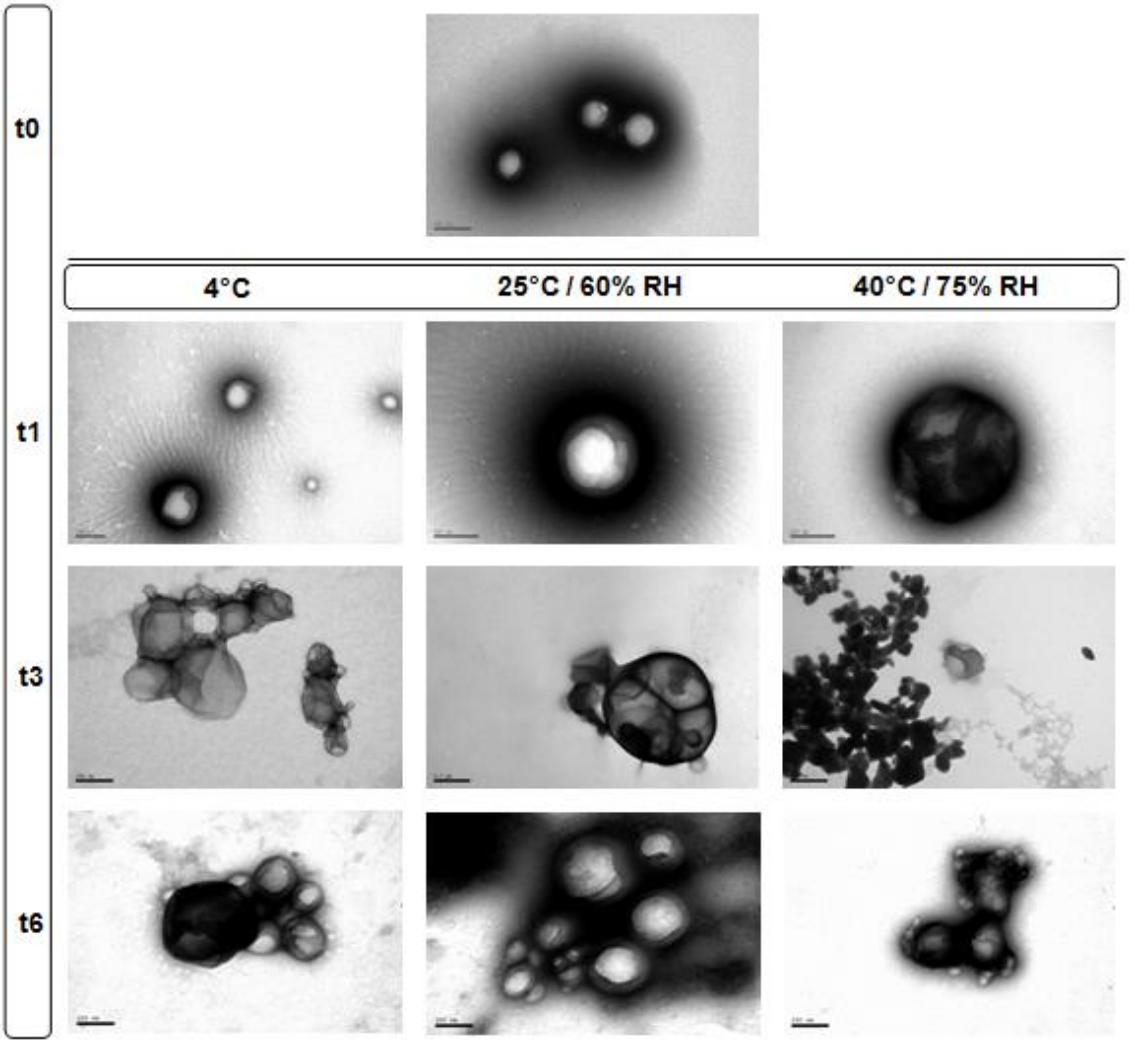

Figure 5.22. TEM microphotographs of freeze-dried insulin-PLGA nanoparticles + sorbitol formulations at t0, t1, t3 and t6, under the tested storage conditions. Scale bar: 200 nm, all microphotographs except t6 4ºC, t6 25ºC / 60% RH at 100 nm; and t3 25ºC / 60% RH at 0.5 µm.

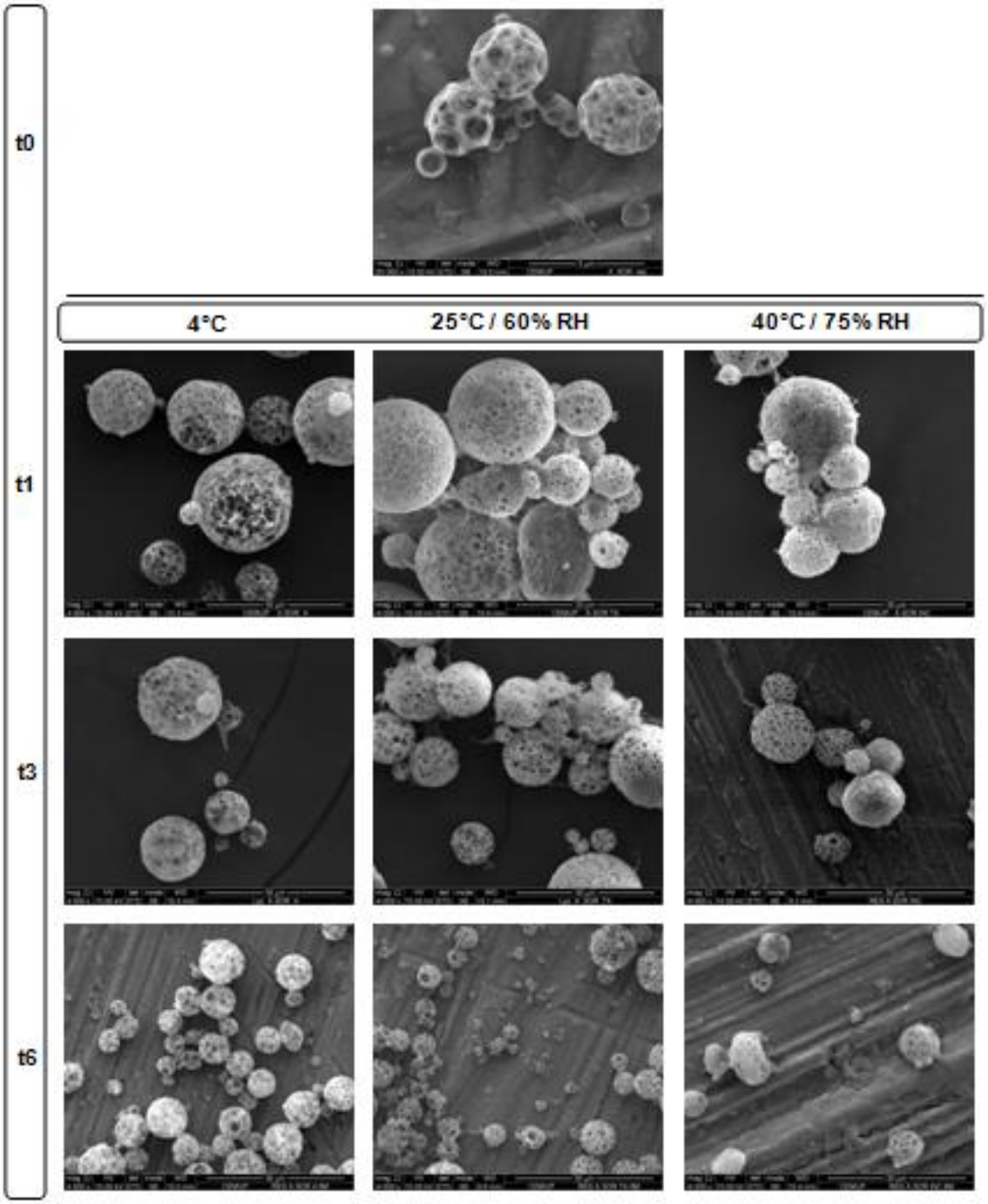

Figure 5.23. SEM microphotographs of freeze-dried insulin-PLGA nanoparticles + sorbitol formulations at t0, t1, t3 and t6, under the tested storage conditions. Scale bar: 30 µm, all microphotographs except t0 at 5 µm.

3.2. Insulin secondary structure

FTIR spectroscopy is one of the most useful techniques to assess the secondary structure of proteins loaded into nanoparticles in a non-invasive way. The amide I region (1710-1590 cm^{-1}) is the most representative region of the spectra to assess insulin secondary structure. The higher similarity between the second derivative spectra of native and loaded insulin corresponds to the lower protein structural changes. The amide I region of spectra can be perfectly used in the experiments because the signal of C=O stretching vibrations of PLGA occurs at around 1750 cm^{-1}, so does not interfere with the protein IR absorption.

3.2.1. Area of overlap and spectral correlation coefficient

AO values represent the similarity degree of the second derivative spectra of native insulin and the insulin loaded into the PLGA nanoparticles. The AO and SCC values obtained for the formulations, at the storage conditions over 6 months are shown in Figure 5.24. The general average of AO values was 72.8 ± 3.4% whereas for SCC was 86.1 ± 4.9%, showing that SCC was in average 13.3 % higher than AO. This occurred because SCC values may be overestimated, disagreeing with the visual impression of spectral similarity [253]. However, SCC is still a good complementary indicator, since the higher SCC values represent minor changes on the band positions. Thus, AO represents the quantitative change of insulin secondary structure and SCC gives an important information about the changes occurred in the band positions.

After production, insulin maintained its structure in about 88.1 ± 0.9% which means that insulin encapsulation process lead to a structure change of about 11.9%. After lyophilization (t0), the AO further significantly decreased, except for fructose added formulation, showing that the lyophilization process contributed to the destabilization of the loaded protein. Freeze-dried insulin-PLGA nanoparticles presented an AO of 71.1 ± 0.2%, whereas cryoprotectants obtained in average 78.5 ± 3.4 %, showing that cryoprotectant-added formulations presented better protein stabilization after lyophilization. Freeze-dried insulin-PLGA nanoparticles + fructose presented the highest AO of 81.5 ± 3.8% after lyophilization. Overall, it was found that after lyophilization, loaded protein stability was not relevantly different between formulations with collapsed and non-collapsed cakes. Similar results were found for lyophilized protein formulations in a previous work [254].

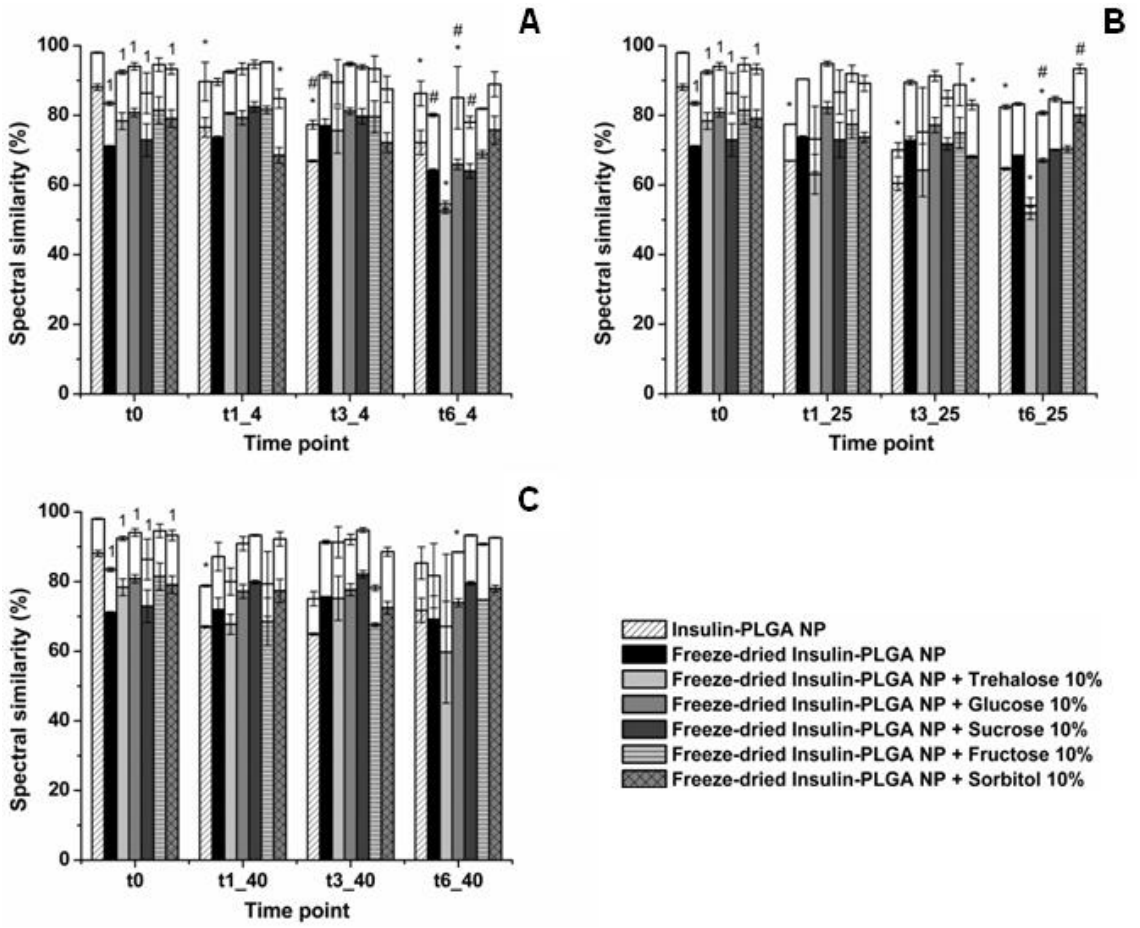

Figure 5.24. AO (colored bars) vs SCC (white bars) percentages of insulin-loaded PLGA nanoparticle formulations upon 6 months of storage at 4ºC (A), 25ºC / 60% RH (B) and 40ºC / 75% RH (C). Results are significantly different ($p < 0.05$) from insulin-PLGA nanoparticles after formulation, when marked with 1. When marked with * and #, results are significantly different ($p < 0.05$) from the corresponding formulation at t0, and from the corresponding formulation at the previous time point, respectively.

3.2.1.1. Insulin-PLGA nanoparticles and freeze-dried insulin-PLGA nanoparticles

Regarding insulin-PLGA nanoparticles it was noticed that after 1 month of storage at the storage conditions the AO significantly decreased, probably due to the hydrolytic degradation suffered by the polymer and the loaded insulin. Even though, nanoparticles were able to protect insulin structure upon 6 months storage, since almost the same level of protein structural change was maintained. The AO obtained after 6 months were 72.2 ± 3.5%, 64.7 ± 0.4% and 71.8 ± 3.5% for 4ºC, 25ºC / 60% RH and 40ºC / 75% RH, respectively, which shows the great insulin degradation suffered. The freeze-dried

insulin-PLGA nanoparticles at t0 had an AO of about 71.1 ± 0.2%, which showed that the lyophilization process contributed to an additional structural loss of about 17%. However, upon 6 months of storage at the storage conditions the same level of insulin structural change was maintained. The results obtained for lyophilized insulin-PLGA nanoparticles, showed that as expected, lyophilization better stabilized the loaded insulin upon storage comparatively to insulin-PLGA nanoparticles.

3.2.1.2. Cryoprotectant added formulations

As mentioned above, the overall cryoprotectant added formulations gave an extra protection to insulin structure, however some differences were found at the different storage conditions. Freeze-dried insulin-PLGA nanoparticles + trehalose maintained the AO level upon 3 months of storage, but it significantly decreased after 6 months to 52.5 ± 0.7%, 51.9 ± 1.8 and 59.7 ± 14.6 at 4ºC, 25ºC / 60% RH and 40ºC / 75% RH , respectively. This showed that trehalose added formulation lost almost half of its native structure after 6 months indicating that this cryoprotectant was not effective on the stabilization of the formulation. Contrary to trehalose-added formulation, all the other cryoprotectant-added formulations that collapsed after lyophilization showed enhanced insulin secondary structure stabilization. This occurred because collapsed cakes may show increased structural relaxation times, which highly reduced the global molecular mobility leading to a better protein stabilization [255]. A better protein stabilization in cakes collapsed after lyophilization was also reported in a previous work [256]. These results were in agreement with the obtained SEM microphotograps of the lyophilizates, since those structures may enhance the protection of the structure of loaded insulin. Besides some of the non-collapsed formulations collapsed upon storage, the formulations that collapsed after lyophilization still presented better protein stabilization. Freeze-dried insulin-PLGA nanoparticles + glucose presented an AO of 80.8 ± 1.2% at t0 and did not significantly changed upon 3 months of storage, however this formulation did not maintained the protein stability after 6 months storage, decreasing to 65.9 ± 1.5%, 67.1 ± 0.6 and 73.9 ± 1.1 at 4ºC, 25ºC / 60% RH and 40ºC / 75% RH, respectively. Freeze-dried insulin-PLGA nanoparticles + sucrose presented after lyophilization an AO of 72.9 ± 4.7%, and no significant changes were found after 6 months at the distinct storage conditions, except at 4ºC in which the AO significantly decreased down to 64.1 ± 2.1%. As mentioned above, for freeze-dried insulin-PLGA nanoparticles + fructose it was obtained an AO of 81.5 ± 3.8%, and no significant changes on insulin structure were obtained upon 6 months of storage at all the storage conditions. Freeze-dried insulin-PLGA nanoparticles + sorbitol presented an AO of 79.1 ± 2.5% at t0 and no significant

changes were found upon 6 months, being the formulation that presented the highest AO values after 6 months of 75.8 ± 4.0%, 80.1 ± 2.1% and 78.0 ± 0.9% at 4ºC, 25ºC/60% RH and 40ºC/75% RH, respectively.

3.2.2. Area-normalized second-derivative amide I spectra

The AO and SCC values give information about the quantitative changes of insulin structure, whereas the area-normalized second-derivative amide I spectra of the formulations shown in Figure 5.25 and 5.26 give information about the qualitative changes of protein secondary structure. Figure 5.25 stands for insulin-PLGA nanoparticles and lyophilized insulin-PLGA nanoparticles, whereas Figure 5.26 shows the results for all the cryoprotectant added formulations. Thus, the shown spectra allow the understanding of which modifications occurred in insulin secondary structure. It is known that the secondary structure of proteins are distinct in aqueous and lyophilized states [257]. Generally, lyophilization causes a decrease in α-helix and increase in β-sheet content. The latter is due to protein-protein interactions driving to the formation of intermolecular β-sheets when water is removed, so β-sheet content does not reflect its actual intramolecular structural content. Thus, it is considered that α-helix is the best indicator of protein structural integrity [258].

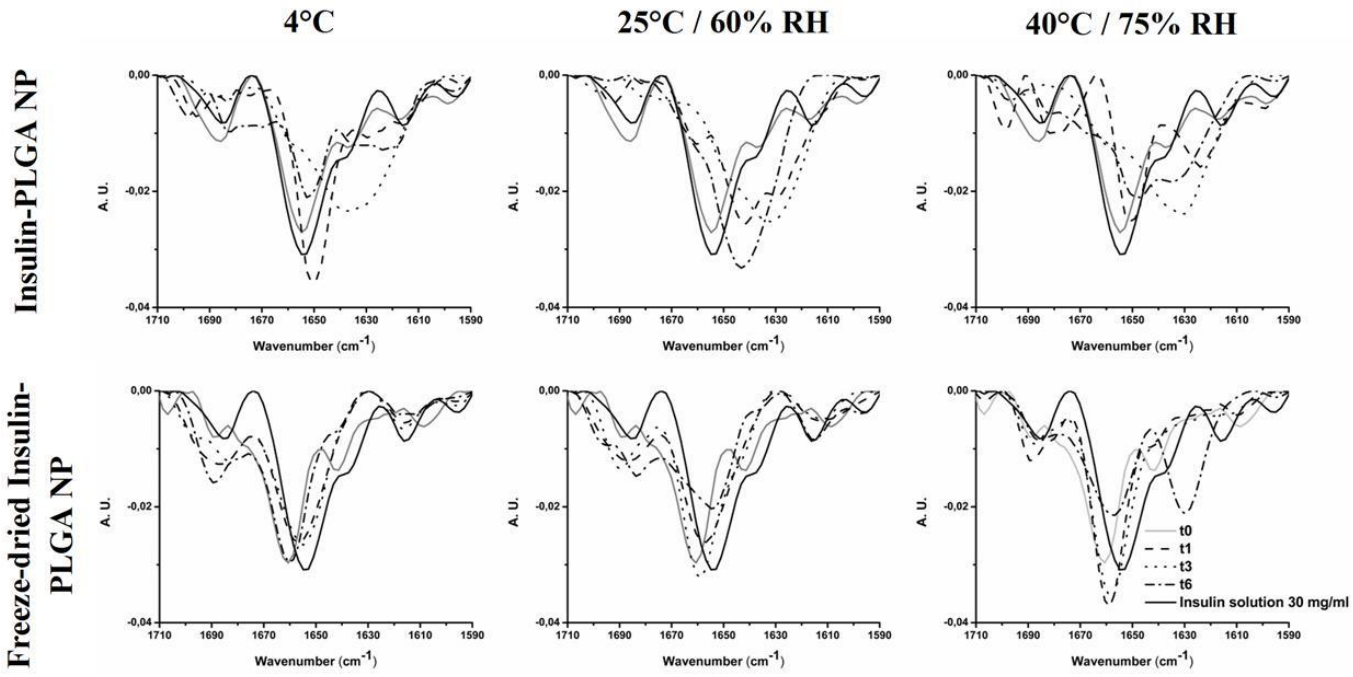

Figure 5.25. Second derivative amide I FTIR spectra of insulin-PLGA nanoparticles and freeze-dried insulin-PLGA nanoparticles stored over 6 months, at the different storage conditions. NP stands for nanoparticles.

The second-derivative FTIR spectrum of insulin shows that its secondary structure is dominated by α-helix (1655 cm^{-1}), and contains also β-sheets assignments from high-frequency (1685 cm^{-1}) and low-frequency (1616 cm^{-1}) [259]. The information about the modifications of these bands is crucial because it represent the changes that insulin suffered, leading to aggregation or denaturation that besides being therapeutically inactive, it may induce toxicity and immunogenicity problems after administration.

3.2.2.1. Insulin-PLGA nanoparticles and freeze-dried insulin-PLGA nanoparticles

In Figure 5.25 it is shown that for insulin-PLGA nanoparticles at t0, the insulin structure changed from a α-helix content decrease to a high-frequency β-sheet increase and over time at the different storage conditions, the α-helix of insulin shifted into a random coil between 1650-1630 cm^{-1}, and this shift was particularly evident at 25ºC / 60% RH and 40ºC / 75% RH. This showed that insulin loaded into PLGA nanoparticles in the suspension form was not stable during storage. For freeze-dried insulin-PLGA nanoparticles, the α-helix of insulin shifted into 1660 cm^{-1} after lyophilization, and besides some decrease of content of the α-helix band of the formulation upon storage, at the storage conditions it oscillated in the range of 1660-1655 cm^{-1} which is the characteristic α-helix band of insulin. A clear difference was observed at t6 for 40ºC / 75% RH with a loss of α-helix content and a random coil band formation at 1630 cm^{-1}. Regarding the information given by figure 5.25 it was possible to conclude that as expected, lyophilization improved the stability of insulin upon storage since the α-helix band of insulin was mainly located in its characteristic region.

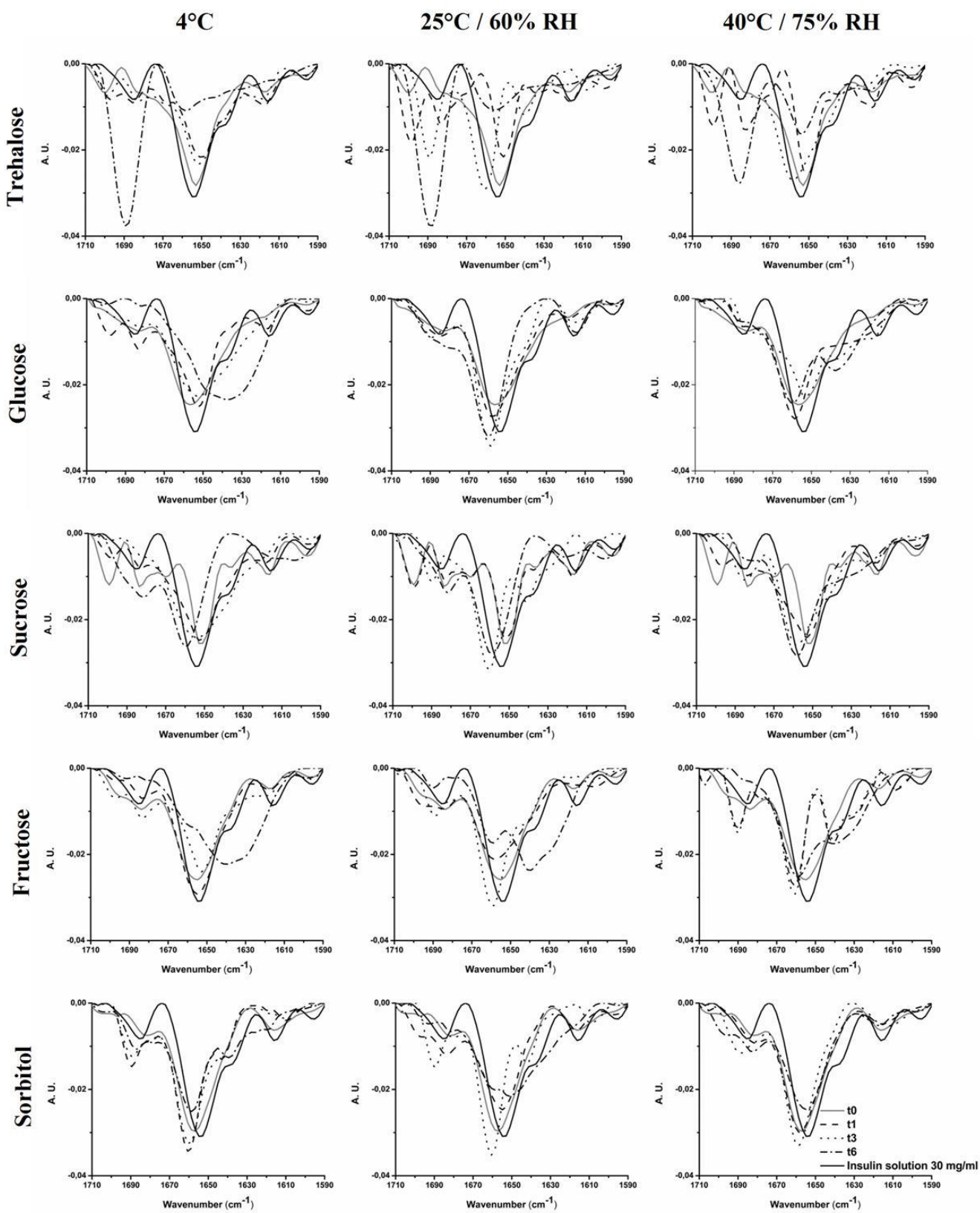

Figure 5.26. Second-derivative amide I FTIR spectra of freeze-dried insulin-PLGA nanoparticles added with cryoprotectants stored over 6 months, at the different storage conditions.

3.2.2.2. Cryoprotectant added formulations

In Figure 5.26 it is possible to visualize which kind of structural modifications occurred, when insulin-PLGA nanoparticles were lyophilized with the added cryoprotectants. It was observed a clear α-helix content loss after lyophilization for trehalose, glucose, sucrose and fructose added formulations. For freeze-dried insulin-PLGA nanoparticles + trehalose, it was noticed that insulin structure changed over time and for all the storage conditions at t6, the α-helix content drastically decreased and a large β-sheet band was formed at 1688 cm^{-1}, showing that insulin got denatured upon storage. In fact, trehalose added formulation it was the one in which insulin structure most changed. Trehalose is considered the preferable cryoprotectant due to its absence of internal hydrogen bonds allowing more flexible bonds formation with nanoparticles during lyophilization, low chemical reactivity and hygroscopicity and higher glass Tg'. However, our findings show up that trehalose used in a standard lyophilization cycle was not the best cryoprotectant on preserving the stability of insulin. For freeze-dried insulin-PLGA nanoparticles + glucose, it was observed that the α-helix band of insulin oscillated between 1660-1650 cm^{-1} and at t6 for 4ºC, a clear random coil band at 1638 cm^{-1} occurred. Freeze-dried insulin-PLGA nanoparticles + sucrose was the formulation in which α-helix content decreased the most after lyophilization (t0). Even though, the α-helix band of insulin upon storage, at the different conditions remained at the acceptable region of 1660-1650 cm^{-1}. For freeze-dried insulin-PLGA nanoparticles + fructose it was noticed a clear modification of insulin structure, over the 6 months at the storage conditions, with a loss of α-helix content and a formation of a random coil band at 1639 cm^{-1}. Regarding the overall results shown in Figure 5.26, it seems that for lyophilized insulin-PLGA nanoparticles + sorbitol, insulin secondary structure seemed to not change as much as other cryoprotectants. However differences in the α-helix content were still noticed. These results indicated that for a standard lyophilization process, sorbitol may be considered a good choice, since allowed a better maintenance of insulin structure comparatively to the other cryoprotectants over 6 months of storage. It was reported that the stereochemical conformation of polyalcohols may be responsible for a modified interaction with the frozen mass [167]. Sorbitol was the only cryoprotectant used that have tendency to form a different crystal morphology during lyophilization and storage, and this fact could benefit the stability of the loaded insulin.

Besides the effects of the lyophilization process, during storage the acidification of the environment around nanoparticles due to the polymer degradation products, lactic acid and glycolic acid, and the presence of PLGA carboxylic acid end groups may

expose proteins to an acidic environment and induce its degradation and instability or even block its release due to the interaction with the positive charges of the remaining encapsulated protein [219]. In addition, the use of reducing sugars such as glucose and fructose may present a problem as excipients because they are reactive with proteins, which may also be an additional problem for protein stability [260]. Even sucrose may be hydrolyzed forming glucose and fructose upon lyophilization and storage [256], so the use of these kind of cryoprotectants needs to be properly regarded.

3.2.3. Principal component analysis

All the changes in insulin structure after formulation, lyophilization and storage may be more intuitively compared by PCA. This technique allows a spatial distribution of formulations considering the type of insulin structural changes, and the differences in the secondary structure of insulin from obtained FTIR spectra may be more intuitively compared by the PCA represented in Figure 5.27. Considering the PCA shown in Figure 5.27-A, formulations could be grouped in 3 PCs with 95.55% of the captured total variance. The first PC was based on the native-like structure of insulin, which represented 84.08% of the dataset variance (Figure 5.27-B). Figure 5.27-A shows that the majority of the changes on insulin structure in the formulations and conditions over 6 months were close to the native like structure. It was for insulin-PLGA nanoparticles at all the storage conditions that the overall structural changes most deviated from insulin native structure, showing that lyophilization was crucial to preserve insulin structure. In addition, freeze-dried insulin-PLGA nanoparticles + trehalose at t6 for all the storage conditions was the formulation in which insulin structure mostly changed, showing up that this cryoprotectant was not as effective as others to preserve insulin structure upon 6 months of storage. A significant change on protein structure was also noticed for freeze-dried insulin-PLGA nanoparticles + sucrose at t1 and t6 for 25ºC / 60% RH. In addition, the changes of insulin structure in freeze-dried insulin-PLGA nanoparticles + sorbitol formulations at all the storage conditions seemed to be the closest ones, showing up that using this sugar as cryoprotectant helped to mitigate insulin structure modifications over storage time.

To further debrief smaller spectral modifications among formulations, all data set was mean-centered and the obtained new PCA shown in Figure 5.27-C explained 88.35% of the total variance in three PCs, with 47.87% in PC1, 24.52% in PC2 and 15.96% in PC3. Figure 5.27-D showed that the PCA-loadings were distributed by different secondary structure motifs. The overall results showed clearly the modifications occurred in insulin structure in all the formulations, showing different small variabilities

between samples and even among the same group of formulations. The highest noticed structural deviations occurred again for freeze-dried insulin-PLGA nanoparticles + trehalose at t6 for all the storage conditions and at t3 for 25ºC / 60% RH. Freeze-dried insulin-PLGA NP + fructose at t1 and t3 for 40ºC / 75% RH also presented some considerable insulin structural changes.

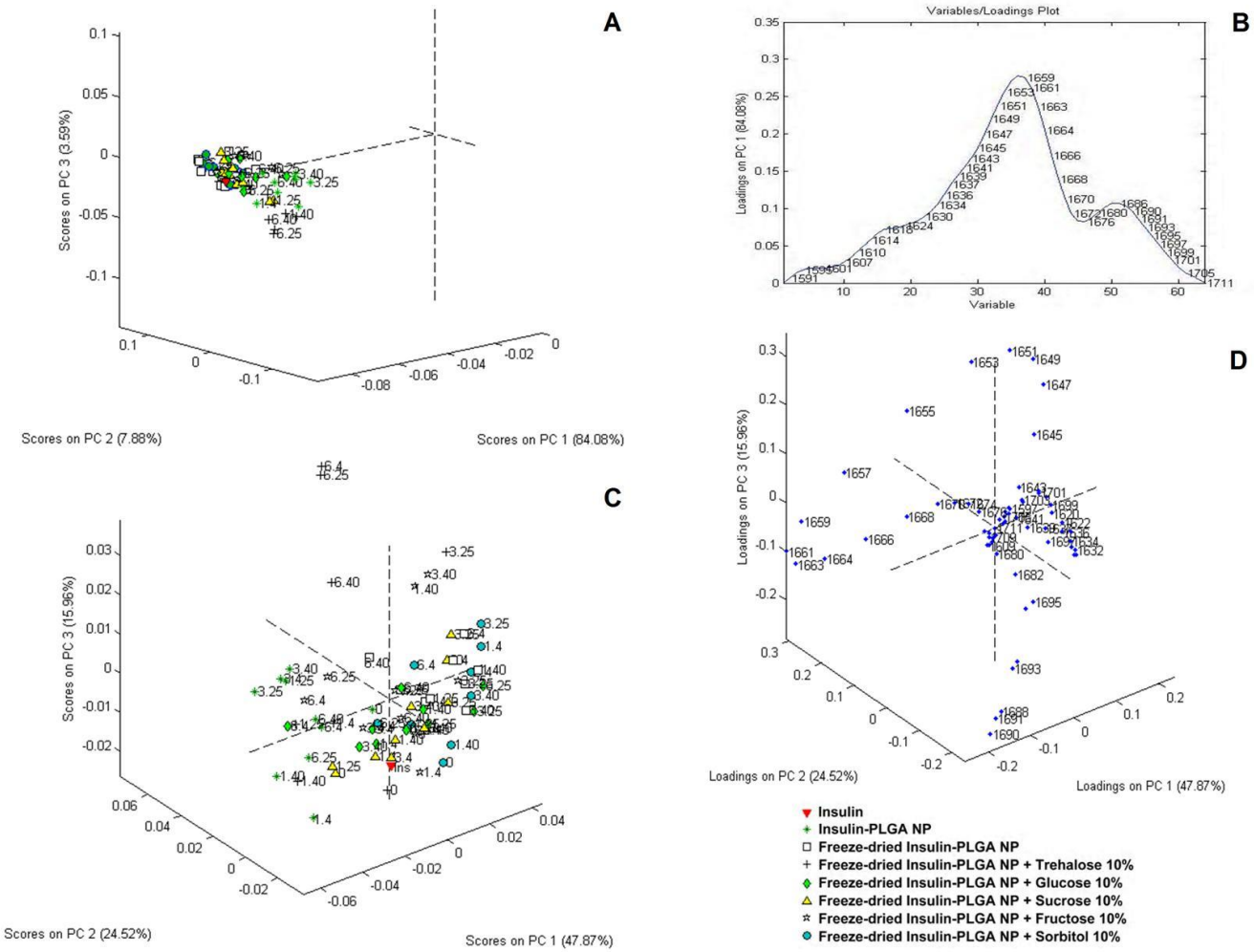

Figure 5.27. PCA from second-derivative amide I spectra of the formulations in three PCs (A), and the loadings plot on the first PC (B). PCA scores from mean-centered second-derivative amide I spectra (C), and the corresponding loadings plot (D). NP stands for nanoparticles.

4. Conclusion

The instability of insulin-PLGA nanoparticles upon storage was mitigated by lyophilization. The further addition of cryoprotectants prior lyophilization improved the stability of particles. The morphology of nanoparticles surface changed over time, but sorbitol provided better morphological stability at the storage conditions. Indeed, this was

the lyophilized formulation that presented less particle size increase supposing less aggregation. The lyophilization process contributed to the instability of insulin structure, which was attenuated by the addition of cryoprotectants. The formulations that collapsed after lyophilization showed enhanced protein stability, and presented the same level of insulin structural protection over 6 months. Among the cryoprotectants, sorbitol showed the highest insulin structure maintenance after 6 months of storage, and more similar structural modifications among all the storage conditions, revealing sorbitol as a versatile cryoprotectant.

In conclusion, it was noticed that the use of a non-optimized lyophilization process led to the collapse of some formulations with negative consequences to cake resuspension and nanoparticles aggregation over time. However, collapsed formulations presented better protein stabilization upon storage. Indeed, cryoprotectants enhanced particles stability upon lyophilization, but they presented different performances on the stabilization of the loaded protein. Therefore, it is highly recommendable to optimize the lyophilization process in order to make an optimal balance between obtaining a good cake that is easily resuspendable and avoiding nanoparticles aggregation upon storage, and to choose a proper cryoprotectant to achieve the highest stabilization of the protein loaded into PLGA nanoparticles.

Chapter 6

Co-encapsulation of Lyoprotectants as a Strategy to Improve the Stability of Protein-loaded PLGA Nanoparticles upon Lyophilization

Partially published in:

Pedro Fonte, Francisca Araújo, Vítor Seabra, Salette Reis, Marco van de Weert, Bruno Sarmento, Co-encapsulation of lyoprotectants improves the stability of protein-loaded PLGA nanoparticles upon lyophilization, Int J Pharm, 496 (2015) 850-862.

1. Introduction

Despite the benefits of lyophilization, the process itself may affect nanoparticle properties, and negatively impact the stability of the loaded protein. Lyoprotectants are often used to mitigate nanoparticle instability upon lyophilization, protecting the particles from mechanical stress of ice crystals and reduce aggregation by the formation of a glassy matrix. Lyoprotectants have been shown to prevent nanoparticle aggregation and assure their redispersion after freeze-thawing [261], and also to maintain protein native structure upon lyophilization [241, 242]. Two main theories have been suggested to justify the positive impact of lyoprotectants as protein formulation stabilizers. The water replacement theory states that lyoprotectants may form hydrogen bonds on the surface of proteins, and after removal of water during drying, sugars substitute the water molecules [170, 171]. The other theory states that proteins are stabilized due to their immobilization in a rigid and inert glass matrix formed by lyoprotectants [262, 263]. These principles may also be applied to nanoparticle formulations, and it is probably the combination of these two mechanisms that impacts the quality of the dried product. Commonly, a significant amount of lyoprotectant, often higher than the drug content, is used to preserve the structure of the lyophilizate and it is generally accepted that a faster freezing and higher lyoprotectant concentration lead to better nanoparticle redispersion properties [139, 140, 264]. However, the crystallization of lyoprotectants may induce irreversible aggregation [265].

During the encapsulation process, proteins may change their structure, which is potentially detrimental to their bioactivity. This may be caused by exposure to organic solvents, dehydration, shearing stress and interaction with hydrophobic interfaces [219]. Furthermore, the encapsulation of such hydrophilic molecules into hydrophobic polymeric carriers may result into unwanted protein-polymer and protein-protein interactions. Since lyoprotectants are usually added to nanoparticles prior to lyophilization, the influence of the loading of lyoprotectants together with proteins into nanoparticles may be a strategy to explore in order to improve the maintenance of the protein structure and nanoparticle characteristics upon lyophilization.

Thus, the aim of the present study was to assess the influence of the co-encapsulation of lyoprotectants and a therapeutic protein model, insulin, into PLGA nanoparticles, on the protein structural stability upon lyophilization. The effect of both reducing and non-reducing sugars was determined. In addition, the nanoparticle formulations and their lyophilizates were fully characterized, and their performance as drug delivery systems was evaluated *in vitro*.

2. Materials and Methods

2.1. Materials

For the nanoparticle production, PLGA 50:50 Resomer® RG 503 H (Mw 24,000-38,000; Tg 44-48 ºC) from Evonik Industries AG (Essen, Germany) was used. Recombinant human insulin, dichloromethane and PVA were obtained from Sigma-Aldrich (Steinheim, Germany). Trehalose, glucose, sucrose, fructose and sorbitol were also from Sigma-Aldrich (Steinheim, Germany). Trifluoroacetic acid from Acros Organics (Morris Plains, NJ, USA) and acetonitrile HPLC Gradient Grade from Fischer Scientific (Loughborough, UK) were used for the HPLC analysis. Chloroform from VWR (Soborg, Denmark) was used for protein extraction from nanoparticles prior to the CD analysis. Milli-Q water was produced in-house and other reagents were of analytical grade.

2.2. Preparation of PLGA nanoparticles

PLGA nanoparticles were produced following a previously developed protocol, based on a modified solvent emulsification-evaporation, w/o/w double emulsion technique [175]. Briefly, 200 mg of PLGA 50:50 were dissolved in 2 mL of dichloromethane, 0.2 mL of a 150 mg/mL insulin solution in HCl 0.1 M was added and then sonicated during 30 seconds at 70% of amplitude using a Bioblock vibracell 75186 sonicator from Fischer Bioblock Scientific (Rungis Complexe, France). This primary emulsion was poured into 25 mL of PVA 2% (w/v) at pH 7.4 and sonicated using the same previous conditions. Finally, the dichloromethane was removed under magnetic stirring for 3 hours. A similar encapsulation protocol was used to produce co-encapsulated lyoprotectant formulations, by dissolving insulin in a lyoprotectant HCL 0.1 M solution of trehalose, glucose, sucrose, fructose and sorbitol at 10 % (w/v). Unloaded nanoparticles were also produced.

2.3. Insulin association efficiency and loading capacity

The AE was calculated using the equation 4.1 (*see* Chapter 4), and loading capacity (LC) was calculated using the following equation:

$$LC = \frac{\text{Total amount of insulin} - \text{Free insulin in supernatant}}{\text{Total dry weight of nanoparticles}} \text{ x } 100 \qquad \textbf{(Eq. 6.1)}$$

The insulin present in the supernatant was obtained by centrifugation of formulations, using a Beckman Optima TL ultracentrifuge from Beckman Coulter (Brea, CA, U.S.A.) for 30 minutes at 40,000 x g and 4ºC. The dry mass was obtained after lyophilization of hydrated nanoparticles obtained by centrifugation. Insulin in the supernatant was quantified by a validated HPLC-UV method [233], and using a described protocol [175].

2.4. Freeze-thaw experiments

Freeze-thaw studies were performed in the chamber of a VirTis Advantage Plus Benchtop lyophilizer (SP Scientific, Warminster, PA, USA) with the vacuum pump switched off, to assess the effect of controlled freezing on the behavior of trehalose, glucose, sucrose, fructose and sorbitol at 10% (w/v) as lyoprotectants. Nanoparticles without lyoprotectant were used as control sample. The freezing step was performed by first cooling 1 mL of each sample from room temperature to 5ºC at a cooling rate of 5ºC/minute, followed by isothermal incubation for 15 minutes. Then, nanoparticles were frozen to -55ºC at a cooling rate of 1ºC/minute and held at this temperature for at least 60 minutes. In the thawing step, formulations were heated to 5ºC at 1ºC/minute. A set of triplicates of each formulation was used in the experiments.

2.5. Lyophilization of PLGA nanoparticles

Nanoparticles were washed three times with Milli-Q water, and the nanoparticles were collected after each washing step by centrifugation using a Heraeus Megafuge 1.0 R centrifuge (Thermo Scientific, Asheville, NC, USA) for 30 minutes at 23,000 x g. The particles were redispersed in water prior to lyophilization. Nanoparticle formulations intended to have external lyoprotectant were redispersed in water containing trehalose, glucose, sucrose, fructose and sorbitol at a concentration of 10% (w/v). The nanoparticles were poured into semi-stoppered glass vials with slotted rubber closures at a maximal height of 10 mm. All formulations were lyophilized in a VirTis Advantage Plus Benchtop lyophilizer (SP Scientific, Warminster, PA, USA), by freezing at -55ºC for 5 hours, followed by a first drying step at -45ºC and pressure of 400 mTorr during 40 hours, followed by a secondary drying step at 20ºC and pressure of 200 mTorr during 8 h.

2.6. Residual moisture content

The residual moisture content of the lyophilizates was determined by Karl Fischer titration using an 870 KF Titrino plus (Metrohm AG, Herisau, Switzerland). The same

amount of powder of each nanoparticle formulation was analyzed after lyophilization. A set of triplicates of each formulation were used in the experiment.

2.7. Reconstitution of lyophilizates

After lyophilization, samples were reconstituted by addition of distilled water in the inside wall of the vial and maintained during 10 minutes to ensure the cake wetting. Samples were then hand swirled to obtain complete homogenization.

2.8. Particle size and zeta potential analyses

Prior to particle size and zeta potential analyses, formulations in suspension and after reconstitution were diluted with Milli-Q water to obtain a suitable concentration. The mean particle size and zeta potential were analyzed following a described methodology [175]. The freeze-thawing ratio was calculated dividing the measured mean particle size of nanoparticles after with that before freeze-thawing. The lyophilization ratio was determined by dividing the measured mean particle size of nanoparticles after with that before lyophilization. A set of triplicates of each formulation was used in the experiments.

2.9. Scanning electron microscopy analysis

The morphology of PLGA nanoparticles was observed by SEM on a Quanta 400 FEG SEM from FEI (Hillsboro, OR, USA.). Formulations with lyoprotectants were resuspended in water and washed by centrifugation for 15 minutes at 23,000 x g and 4 ºC to remove the lyoprotectant. Prior to microscopic observation, all samples were mounted onto metal stubs and vacuum-coated with a layer of gold/palladium for 60 s using a 15 mA current.

2.10. X-Ray powder diffraction experiments

The diffractograms were collected using a X-ray powder diffractometer PANanalytical X'pert PRO with a PIXcel detector (PANanalytical B.V., Almelo, the Netherlands). XRPD patterns were obtained with a Cu Kα radiation (45 kV, 40 mA, λ = 1.54187 Å), and with a 96-well plate stage in transmission mode from 2-40º2θ with a scan speed of 0.067º/s.

2.11. Attenuated total reflectance-Fourier transform infrared spectroscopy analysis

The secondary structure of insulin loaded into PLGA nanoparticles was determined by ATR-FTIR. The insulin spectra were obtained following a previously described protocol [175]. All samples were analyzed and treated in triplicate.

2.11.1. Analysis of spectral similarity

The similarity of the area normalized second-derivative amide I spectra between the insulin loaded into PLGA nanoparticles and native insulin (dissolved in 0.1 M HCl), was quantitatively determined using the AO algorithm [244]. A 30 mg/mL insulin solution in HCl 0.1 M was used as reference, to obtain the spectral similarity to the native protein. The latter was used as reference, since it is generally recognized that the stability of a solid protein formulation increases with the increase of similarity to the FTIR spectra in solution [246]. Insulin lyophilized with and without lyoprotectants was also used as control sample in selected cases.

2.12. Circular dichroism analysis

To assess the structure of insulin loaded into the PLGA nanoparticles, insulin was extracted prior to CD analysis. Thus, chloroform was used to dissolve the nanoparticles polymer and the loaded insulin was redissolved in HCl 0.01 M. The measurements were obtained in an Olis DSM-10 CD Spectrophotometer (Olis Inc., Bogart, GA, USA). The CD spectra were determined from 250 to 190 nm using a 0.1 cm cell, a step size of 0.5 nm a bandwith of 1.5 nm, and an averaging time of 5 seconds. The lamp housing was purged with nitrogen and an average of 5 scans was obtained. All spectra were corrected by subtraction of the respective reference. The molar ellipticity of insulin was calculated as CD signal x MRW (mean residual weight of each insulin residue, 116 Da)[insulin concentration (mg/mL x cell pathlength (0.1 cm)]. The concentration of insulin was determined by UV absorption at 280 nm in a NanoDrop 2000c UV-Vis spectrophotometer (Thermo Scientific, Wilmington, DE, USA), using a molar extinction coefficient of 6200 $M^{-1}cm^{-1}$ for 1.0 mg/mL. A set of triplicates of each formulation was used in the experiments. An insulin solution at 0.2 mg/mL was used as reference, and samples of reconstituted lyophilized insulin containing lyoprotectants were also used as controls.

2.13. Insulin *in vitro* release study

The insulin *in vitro* release study was performed by dispersion of the lyophilizates into 10 mL of pH 7.4 PBS solution, and incubation at 37ºC under magnetic stirring at 100 rpm. Aliquots were collected at predetermined times of 0.5, 1, 2, 4, 8, 12, 24 and 48 hours, and replaced with similar volume of fresh medium. The collected samples were centrifuged for 30 minutes at 40,000 rpm and 4ºC, and insulin present in the supernatant was quantified using the HPLC method described above. A set of triplicates of each formulation was used in the experiments.

2.14. Statistical analysis

The statistical analysis was performed using a one-way ANOVA Tukey *post hoc* test, with a significance level of $p < 0.05$ in the OriginPro 8 software from OriginLab Corporation (Northampton, MA, USA).

3. Results and discussion

Insulin was used as a therapeutic protein model, and loaded into PLGA nanoparticles following a protocol previously optimized [101] in order to study the stability of the protein upon nanoparticle lyophilization. The criteria to choose the used lyoprotectants was to have two nonreducing sugars (trehalose and sucrose), two reducing sugars (glucose and fructose), and one sugar alcohol (sorbitol). Three different approaches were used, namely insulin-loaded PLGA nanoparticles with co-encapsulated lyoprotectant, with externally added lyoprotectant, and both with co-encapsulation and external addition of lyoprotectant. Therefore, insulin-loaded PLGA nanoparticles were co-encapsulated with trehalose (insulin-trehalose 10%-PLGA nanoparticles), glucose (insulin-glucose 10%-PLGA nanoparticles), sucrose (insulin-sucrose 10%-PLGA nanoparticles), fructose (insulin-fructose 10%-PLGA nanoparticles) and sorbitol (insulin-sorbitol 10%-PLGA nanoparticles) at 10% (w/v), as a function of the final volume of insulin solution. The externally added lyoprotectant was also added at 10% (w/v), but as a function of the final volume of the formulation. The concentration used in all lyoprotectant containing formulations was 10% (w/v) to obtain the highest acceptable lyoprotectant effect, since usually the level of lyoprotectant stabilization depends on its concentration [7]. To make a direct comparison, the same lyophilization process was used to lyophilize all samples.

Since in protein formulations, nonreducing sugars are preferable to avoid potential Maillard reaction, it was assessed the performance of the different lyoprotectants on the protection of the loaded protein, whether they are co-encapsulated or not. To determine the feasibility of co-encapsulating lyoprotectants, it was imperative to properly characterize the nanoparticles, the obtained lyophilizates, and the structural integrity of the loaded protein.

3.1. Particle size, zeta potential, association efficiency and loading capacity

The physical-chemical properties of insulin-loaded PLGA nanoparticles prior to lyophilization are depicted in Table 6.1. PLGA nanoparticles loading insulin without co-encapsulation of lyoprotectant (Insulin-PLGA nanoparticles) presented a mean particle size of 333 ± 19 nm and zeta potential of -26.3 ± 0.5 mV. The insulin-loaded PLGA nanoparticles with co-encapsulated lyoprotectants, with the exception of glucose, resulted in higher particle size ($p < 0.05$) than insulin-PLGA nanoparticles. Still, mean particle size for different formulations was lower than 500 nm. The PdI values were around 0.30.

Table 6.1. Physical-chemical properties and characterization of insulin AE and LC of insulin-loaded PLGA nanoparticles with or without co-encapsulated lyoprotectant ($n = 3$, mean ± SD). Results are significantly different ($p < 0.05$) from insulin-PLGA nanoparticles, when marked with *.

Formulation	Diameter (nm)	PdI	Zeta potential (mV)	AE (%)	LC (%)
Insulin-PLGA nanoparticles	333 ± 19	0.24 ± 0.18	-26.3 ± 0.5	88.2 ± 1.4	12.2 ± 0.1
Insulin-trehalose 10%-PLGA nanoparticles	418 ± 26*	0.31 ± 0.03	-36.0 ± 0.7*	89.0 ± 1.7	11.2 ± 0.1
Insulin-glucose 10%-PLGA nanoparticles	386 ± 16	0.33 ± 0.01	-38.2 ± 2.4*	91.1 ± 0.6	11.5 ± 0.1
Insulin-sucrose 10%-PLGA nanoparticles	424 ± 45*	0.33 ± 0.01	-36.3 ± 1.1*	91.0 ± 2.0	11.1 ± 1.0
Insulin-fructose 10%-PLGA nanoparticles	466 ± 15*	0.30 ± 0.02	-34.1 ± 1.6*	84.5 ± 2.2	10.1 ± 0.3
Insulin-sorbitol 10%-PLGA nanoparticles	433 ± 40*	0.31 ± 0.02	-35.2 ± 2.1*	89.8 ± 2.4	10.6 ± 0.2

The zeta potential analysis, showed that all nanoparticles presented a negative surface charge, which is characteristic of the acidic PLGA polymer [147]. The PLGA nanoparticles co-encapsulating lyoprotectants presented even lower zeta potential values, around, -35 mV. The zeta potential was significantly lower ($p < 0.05$) than PLGA

nanoparticles without co-encapsulated lyoprotectant, apparently because of the lyoprotectant contained in the nanoparticles. This may be explained by the presence of sugars that expand the location of the slipping plane during electrophoretic movement due to the formation of a viscous hydration layer on nanoparticles surface [248]. The same effect has been observed previously [175]. Thus, the co-encapsulation of lyoprotectants may increase the colloidal stability of PLGA nanoparticles, as the more negative zeta potential is expected to result in greater particle-particle repulsion.

The PLGA nanoparticles were also characterized in terms of insulin AE and LC to determine their ability to encapsulate the protein (Table 6.1). Insulin-PLGA nanoparticles obtained an AE of 88.2 ± 1.4 % and a LC of 12.2 ± 0.1, which are very good achievements considering the hydrophobic nature of the polymer and hydrophilic nature of insulin. All the other formulations with co-encapsulated lyoprotectants presented similar values of AE and a slightly lower LC of insulin, due to the presence of lyoprotectants loaded into the nanoparticles. This achievement demonstrates the robustness of the production protocol and the ability to co-encapsulate lyoprotectants, without negatively affecting insulin AE and LC.

3.2. Freeze-thaw study

The ability of lyoprotectants to avoid the aggregation of PLGA nanoparticles during lyophilization, at different lyoprotection levels: co-encapsulated (in), externally added (out) or both (in + out); was determined by a freeze-thaw experiment. The freeze-thawing ratio was obtained by dividing the mean particle size of nanoparticles after with that before freeze-thawing (Table 6.2). Thus, values around 1 represent that the mean particle size of nanoparticles was maintained upon freeze-thawing. The freeze-thawing ratio for insulin-PLGA nanoparticles was 0.87 ± 0.08, and for the PLGA nanoparticles with co-encapsulated lyoprotectants except fructose (1.28 ± 0.11), the freeze-thawing ratio did not show significant ($p < 0.05$) nanoparticle aggregation, indicating that the nanoparticle stability was not significantly affected by freeze-thawing.

Table 6.2. Characterization of freeze-thawing ratio, lyophilization ratio and residual moisture content of PLGA nanoparticles with different lyoprotection levels (n = 3, mean ± SD). The freeze-thawing results are significantly different (p < 0.05) from formulation containing no lyoprotectant, when marked with *.

Lyoprotectant level (w/v)	Freeze-thawing ratio	Lyophilization ratio	Residual moisture (%)
No lyoprotectant	0.87 ± 0.08	1.91 ± 0.15	0.98 ± 0.12
In			
Trehalose 10%	0.94 ± 0.03	0.50 ± 0.07	1.31 ± 0.49
Glucose 10%	1.19 ± 0.12	0.94 ± 0.09	0.91 ± 0.14
Sucrose 10%	1.06 ± 0.15	1.26 ± 0.11	1.82 ± 0.61
Fructose 10%	1.28 ± 0.11*	0.83 ± 0.18	1.74 ± 0.83
Sorbitol 10%	1.18 ± 0.18	0.36 ± 0.02	1.24 ± 0.59
Out			
Trehalose 10%	1.07 ± 0.11	0.51 ± 0.07	0.71 ± 0.11
Glucose 10%	0.95 ± 0.11	1.15 ± 0.13	0.84 ± 0.08
Sucrose 10%	1.11 ± 0.07	0.66 ± 0.09	0.87 ± 0.23
Fructose 10%	0.99 ± 0.05	1.29 ± 0.16	1.61 ± 0.47
Sorbitol 10%	0.91 ± 0.11	1.92 ± 0.22	1.59 ± 0.69
In + Out			
Trehalose 10%	0.85 ± 0.15	0.43 ± 0.02	0.70 ± 0.15
Glucose 10%	0.97 ± 0.04	0.72 ± 0.08	0.74 ± 0.10
Sucrose 10%	1.08 ± 0.03	0.75 ± 0.06	0.88 ± 0.16
Fructose 10%	1.06 ± 0.09	0.77 ± 0.04	0.80 ± 0.17
Sorbitol 10%	1.09 ± 0.24	0.56 ± 0.06	1.49 ± 0.29

3.3. Lyophilizate visual inspection and reconstitution

All the lyophilizates were visually inspected. It was expected that the lyoprotectants were able to facilitate the reconstitution of the lyophilizate and avoid nanoparticle aggregation [178]. The lyophilizates of PLGA nanoparticles with co-encapsulated lyoprotectants were white with cotton-like texture. For insulin-PLGA nanoparticles and all other formulations a slight shrinkage of the cake was observed upon lyophilization. Significant collapse of the lyophilizates was not observed, which was a good achievement since their collapse may negatively affect the nanoparticle redispersion. All the cakes were easy and fast to completely reconstitute obtaining good suspensions with no visual aggregates.

3.4. Particle size and zeta potential upon lyophilization

Prior to lyophilization, PLGA nanoparticles were centrifuged and washed with Milli-Q water to remove the surfactant PVA. Additionally, the removal of free drug by centrifugation and washing was important since its presence on nanoparticle surface may increase the zeta potential near to neutrality, increasing the probability of nanoparticle aggregation [7].

The lyophilization ratio was obtained by dividing the mean particle size of nanoparticles after with that before lyophilization. Thus, values around 1 represent that the mean particle size of nanoparticles was maintained after lyophilization. Figure 6.1 shows the characterization of all the PLGA nanoparticles in terms of mean particle size and zeta potential after lyophilization. Insulin-PLGA nanoparticles showed an increase mean particle size (637 ± 77 nm), resulting in a lyophilization ratio of 1.91 ± 0.15 (Table 6.2), which shows the high nanoparticle aggregation that may occur upon lyophilization.

The addition of external lyoprotectants to PLGA nanoparticles resulted in nanoparticle stabilization since no significant aggregation was noticed. The exception was the addition of external sorbitol that showed not to prevent nanoparticle aggregation, presenting a lyophilization ratio of 1.92 ± 0.22. The lyophilization of PLGA nanoparticles with co-encapsulated lyoprotectants presented different behaviors. Nanoparticles with glucose and fructose presented similar mean particle sizes after lyophilization whereas, lyophilization with sucrose showed a slight aggregation with a lyophilization ratio of 1.26 ± 0.11, and with trehalose and sorbitol a decreased particle size, resulting in a lyophilization ratio below 1, 0.50 ± 0.07 and 0.36 ± 0.02, respectively. The formulations containing trehalose showed the most similar particle size, obtaining a mean particle size of 206 ± 16 nm, 169 ± 26 nm and 179 ± 14 nm for co-encapsulated, added and both co-encapsulated and added lyoprotectant, respectively. In general, only few samples showed any significant aggregation, as determined by the lyophilization ratio, with only the insulin-PLGA nanoparticles and the formulation with externally added sorbitol showing a ratio above 1.3. The formulations with the smallest change in particle size after lyophilization were PLGA nanoparticles co-encapsulated or externally added with glucose, obtaining a lyophilization ratio of 0.94 ± 0.09 and 1.15 ± 0.13, respectively. With the exception of PLGA nanoparticles with the external fructose and sorbitol, the PdI values were below 0.4 (Table 6.3).

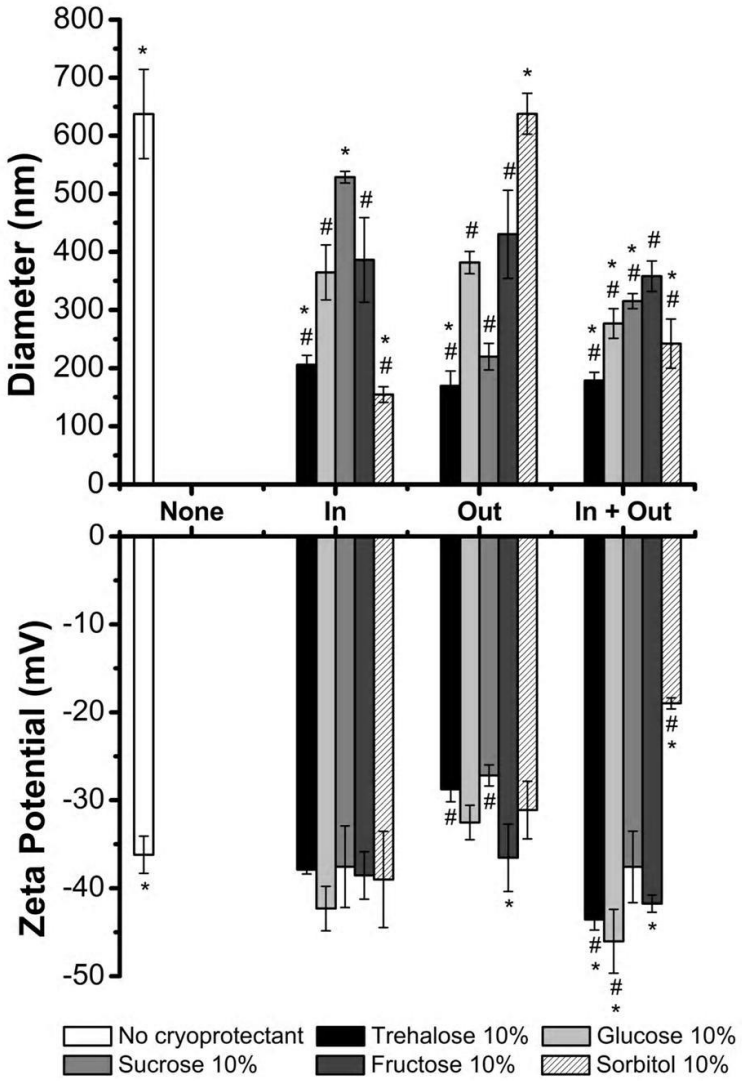

Figure 6.1. Mean particle size (top bars) and zeta potential (bottom bars) characterization of insulin-loaded PLGA nanoparticles lyophilized with different lyoprotection levels: no lyoprotectant (none), co-encapsulated lyoprotectant (In), added lyoprotectant (Out) and both co-encapsulated and added lyoprotectant (In + Out) (n = 3). Results are significantly different (p < 0.05) from insulin-PLGA nanoparticles after production, when marked with *; and significantly different (p < 0.05) from lyophilized insulin-PLGA nanoparticles, when marked with #.

After lyophilization and redispersion, the nanoparticles retained its characteristic negative surface charge. Insulin-PLGA nanoparticles showed a decreased zeta potential of -36.2 ± 2.1 mV. Similar behavior was also observed in previous works using a different lyophilization protocol [101, 175], although the cause of the decreased zeta potential remains elusive. The PLGA nanoparticles with co-encapsulated lyoprotectants showed the most similarity with PLGA nanoparticles containing no lyoprotectant, with -37.9 ± 0.5

mV, -42.3 ± 2.5 mV, -37.5 ± 4.6 mV, -38.5 ± 2.7 mV and -39.0 ± 5.5 mV, for trehalose, glucose, sucrose, fructose and sorbitol, respectively.

Table 6.3. PdI of insulin-loaded PLGA nanoparticles after lyophilization with different lyoprotection levels (*n* = 3, mean ± SD).

Formulation	PdI
No lyoprotectant	0.36 ± 0.03
In	
Trehalose 10%	0.23 ± 0.09
Glucose 10%	0.38 ± 0.01
Sucrose 10%	0.35 ± 0.01
Fructose 10%	0.39 ± 0.01
Sorbitol 10%	0.17 ± 0.09
Out	
Trehalose 10%	0.27 ± 0.08
Glucose 10%	0.38 ± 0.02
Sucrose 10%	0.32 ± 0.04
Fructose 10%	0.73 ± 0.24
Sorbitol 10%	0.47 ± 0.01
In + Out	
Trehalose 10%	0.28 ± 0.05
Glucose 10%	0.37 ± 0.01
Sucrose 10%	0.36 ± 0.01
Fructose 10%	0.38 ± 0.01
Sorbitol 10%	0.35 ± 0.02

3.5. Residual moisture content

The residual moisture content was determined for all the lyophilizates, since it is an important parameter to assure the long-term stability of PLGA nanoparticles, and the maintenance of the structure of the loaded protein [175]. Generally, lyoprotectants are amorphous but have a tendency to crystallize with increased residual moisture content, which in turn may be a source of nanoparticle instability [140]. Furthermore, the adsorption of moisture by lyophilized formulations during storage may decrease their Tg, promoting nanoparticle instability and lyophilizate collapse [250]. Generally it is accepted that the desired residual moisture content of lyophilizates should be around 1% or even less [7]. The residual moisture content of all the formulations is shown in Table 6.2, and were observed to be around 1%, indicating that the lyophilization process and particularly the secondary drying step was effective in removing water. The low water content is also crucial to avoid the hydrolysis of the PLGA matrix, improving the shelf-life of PLGA nanoparticles.

3.6. Nanoparticle morphology

3.6.1. Before lyophilization

All the samples were visualized by SEM (Figure 6.2). Along with nanoparticles, some non-particle shaped material could also be observed. The microphotograph of insulin-PLGA nanoparticles shows that nanoparticles presented spherical shape and smooth surface, characteristic of the encapsulation methodology. The same nanoparticle characteristics were verified when insulin was co-encapsulated with the different lyoprotectants. This indicated that the developed production protocol was capable of loading lyoprotectants inside nanoparticles without negatively affect their formation. The nanoparticle size range shown in all microphotographs was in agreement with the mean particle size characterization (section 3.1 of this chapter).

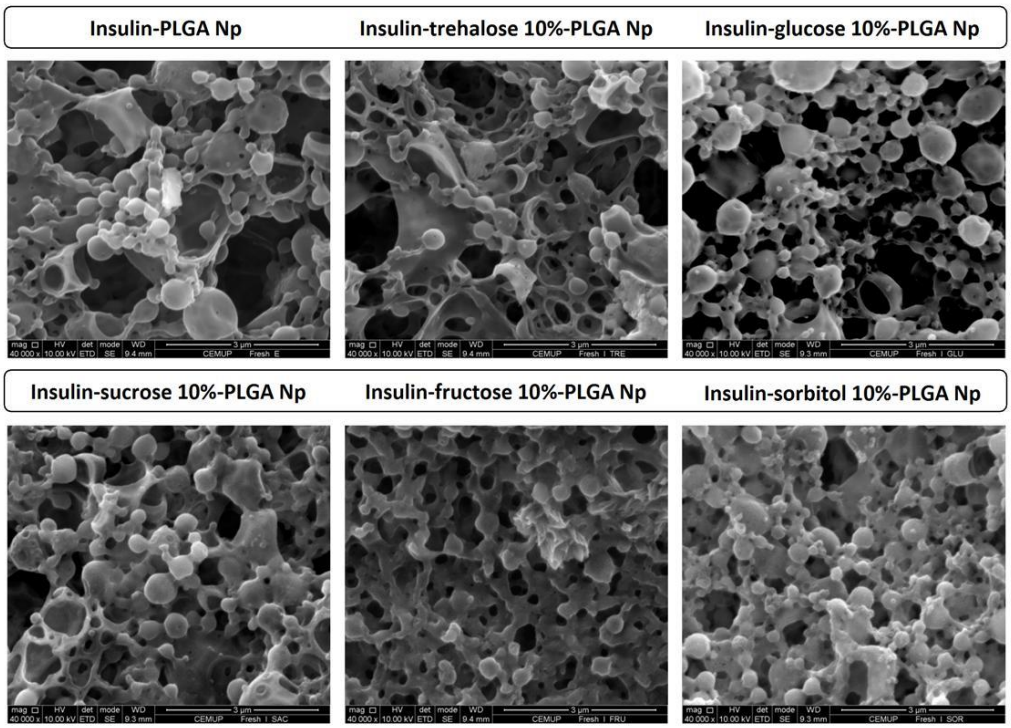

Figure 6.2. SEM microphotographs of insulin-loaded PLGA nanoparticles. Scale bar: all microphotographs at 3 µm. Np stands for nanoparticles.

3.6.2. After lyophilization

After resuspension of the lyophilizates all samples were observed by SEM (Figure 6.3). The microphotographs showed that insulin-PLGA nanoparticles maintained their spherical shape after lyophilization. However, an increased roughness of the nanoparticle surface was observed. This was probably due to the removal of water from the nanoparticles during the lyophilization process. This surface modification may increase the burst release of the loaded drug, which usually is undesirable. The ability of lyoprotectants to form hydrogen bonds with polar groups on the nanoparticle surface, replacing water as it freezes, may help mitigate nanoparticle roughness [101]. Thus, the effect of lyoprotectants on surface features was also tested.

The PLGA nanoparticles containing external lyoprotectants were washed with water before lyophilization, otherwise their visualization by SEM would be difficult when the concentration of lyoprotectants exceeds 5%, because of the formation of a continuous amorphous matrix embedding the nanoparticles [7, 101]. All the PLGA nanoparticles containing lyoprotectants, whether co-encapsulated and/or externally added, generally maintained the spherical shape and smooth surface of nanoparticles, showing that lyoprotectants and the lyophilization process preserved nanoparticle morphology and mitigated nanoparticles roughness. In addition, the particle size visualized in the microphotographs of all formulations was in agreement with the results of mean particle size (section 3.4 of this chapter).

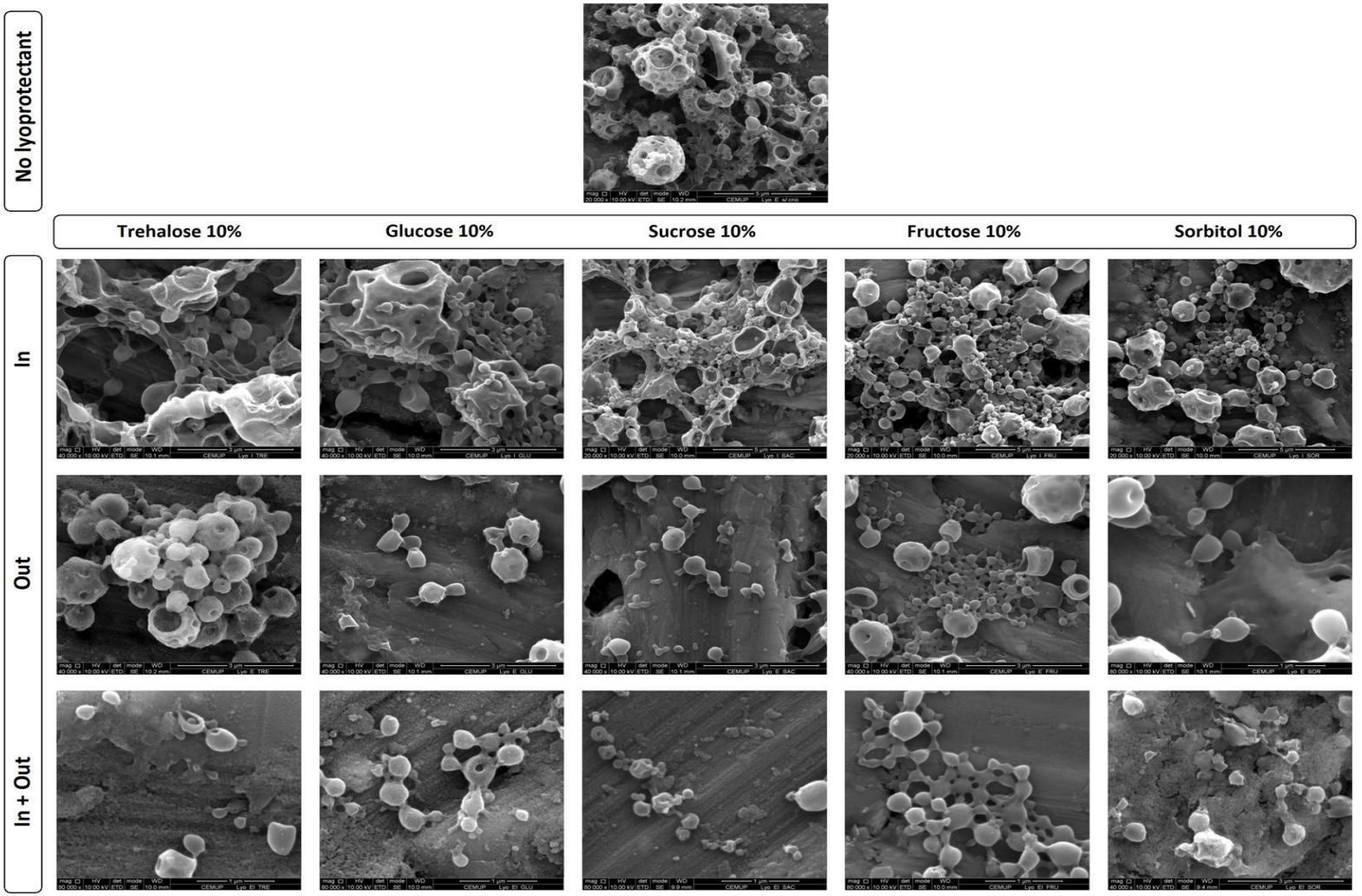

Figure 6. 3. SEM microphotographs of insulin-loaded PLGA nanoparticles, after lyophilization with different lyoprotection levels. Scale bar: all microphotographs at 1 µm; except In – trehalose 10%, In - glucose 10%, Out – trehalose 10%, glucose 10%, sucrose 10%, fructose 10% at 3 µm; and no lyoprotectant, In – sucrose 10%, fructose 10%, sorbitol 10%, at 5 µm.

3.7. X-ray powder diffraction analysis

XRPD is a very useful technique to study the crystalline state, and for characterization of polymorphs of solid materials such as lyophilizates. It has previously been stated that the crystallization of lyoprotectants during freezing, drying or storage may destabilize nanoparticles [140]. Nanoparticles and lyoprotectants in the amorphous state allow better hydrogen-bonding, which is one of the proposed stabilizing mechanisms of lyoprotectants, and thus the crystallization of lyoprotectants may have a negative effect on their performance as stabilizers. Therefore, all lyophilizates and control samples were analyzed by XRPD, to search for clear peaks in the XRPD diffractograms that indicate crystallinity. If no peaks were observed it means that formulations remained in the amorphous state. The obtained XRPD patterns are shown in Figure 6.4. As control samples, it were used the PLGA polymer and insulin bulk materials, lyophilized insulin, and lyophilized insulin added with lyoprotectants (Figure 6.4-A), and all those controls presented an amorphous state. Patterns indicative of amorphous state were also noticed for insulin-PLGA nanoparticles (Figure 6.4-C), and the PLGA nanoparticles with co-encapsulated lyoprotectants (Figure 6.4-B). Regarding the PLGA nanoparticles with added lyoprotectants prior lyophilization (Figure 6.4-C), the formulation with added trehalose remained in the amorphous state, and a few sharp peaks were found for the glucose, sucrose and fructose formulations. In contrast, clear evidence of crystallinity was noticed for the PLGA nanoparticles with added sorbitol. Considering the nanoparticle formulations with both co-encapsulated and added lyoprotectants, those containing trehalose and fructose were in the amorphous state and just a few peaks were observed for the sucrose formulation (Figure 6.4-D). A clear pattern of crystallinity was found for formulations containing glucose and sorbitol.

The overall XRPD diffractograms demonstrated that all PLGA nanoparticles with co-encapsulated lyoprotectants, yielded amorphous lyophilizates. These results showed that the co-encapsulation of lyoprotectants avoided crystallization upon lyophilization. The same amorphous state was verified for all the formulations containing trehalose, showing its versatility and good performance as lyoprotectant, as reported earlier [166]. A clear evidence of lyoprotectant crystallization upon lyophilization was observed for PLGA nanoparticles with sorbitol added and for formulations with both co-encapsulated and added glucose and sorbitol. The crystallization of sorbitol, is likely related to its higher intrinsic propensity to crystallize compared to lyoprotectants such as sucrose or fructose.

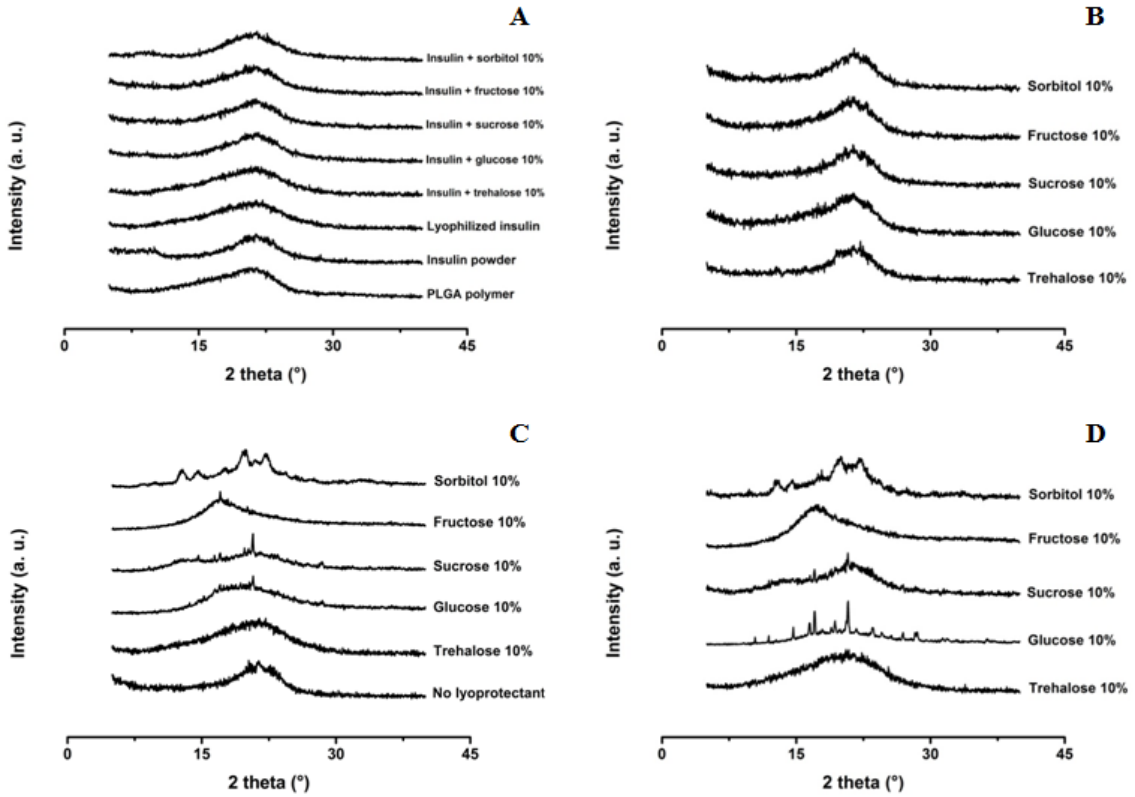

Figure 6.4. XRPD pattern of control samples, namely PLGA and insulin bulk materials, lyophilized insulin and lyophilized insulin added with lyoprotectants (A) and insulin-loaded PLGA nanoparticles lyophilized with different lyoprotection levels: in (B), out (C) and in and out (D).

3.8. Insulin secondary structure

3.8.1. Fourier transform infrared spectroscopy analysis

FTIR spectroscopy is a very useful technique to noninvasively assess the secondary structure of proteins loaded into nanoparticles [85]. To perform this analysis, the amide I region (1710-1590 cm^{-1}) is generally used, and the higher the similarity between the second derivative spectra of loaded insulin and native insulin, the better the maintenance of its secondary structure.

3.8.1.1. Area of overlap

The AO represents the degree of similarity between the area-normalized second-derivative spectra of native insulin and the insulin loaded into the different formulations. It was reported that proteins may lose their stability upon lyophilization potentially because

of their adsorption to the liquid/ice interface during the freezing step, which may lead to the loss of native conformation due to surface-induced denaturation [204]. The native structure of insulin was determined by the analysis of an insulin solution 30 mg/ml, and the AO values obtained for all the lyophilized PLGA nanoparticles are shown in Figure 6.5. The controls of lyophilized insulin and insulin with lyoprotectants at 10% (w/v), showed a similar AO around 85%.

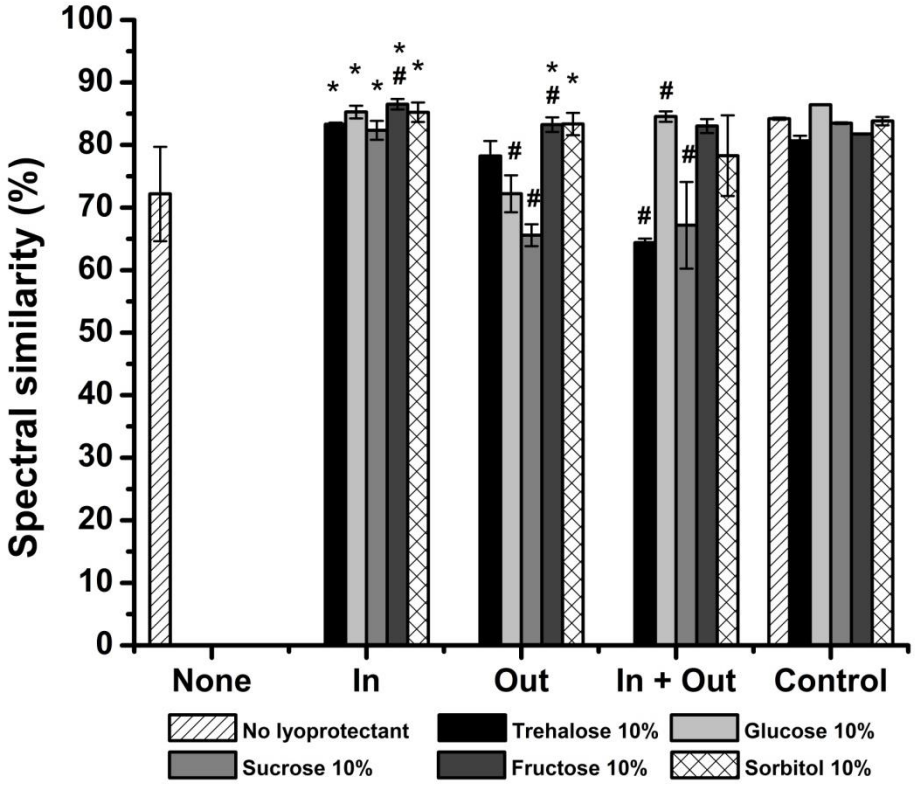

Figure 6.5. AO percentages of insulin loaded into PLGA nanoparticle formulations after lyophilization with different lyoprotection levels (n = 3). Formulations of insulin lyophilized with and without lyoprotectants were used as controls. Results are significantly different (p < 0.05) from formulation with no lyoprotectant, when marked with *, and from corresponding control formulation when marked with #.

Insulin-PLGA nanoparticles (no lyoprotectant, none) obtained an AO of 72.2 ± 7.5%, and this significant reduction in AO may be caused both by the encapsulation process and the lyophilization process. This result clearly indicates the need to use of stabilizers to better stabilize insulin structure. Compared to this formulation, all PLGA nanoparticles with co-encapsulated lyoprotectants significantly (p < 0.05) improved the stability of the loaded insulin, with AOs of 83.3 ± 0.3%, 85.3 ± 1.0%, 82.4 ± 1.5%, 86.5 ± 0.8% and 85.3 ± 1.6% for formulations with co-encapsulated trehalose, glucose,

sucrose, fructose and sorbitol, respectively. The insulin-loaded PLGA nanoparticles with added fructose and sorbitol also showed a significantly better insulin stabilization, whereas the other tested formulations showed no statistical improvement of insulin stability. The overall results showed that the co-encapsulation of lyoprotectants was a useful strategy to better preserve insulin structure.

Comparing the AO of insulin from all PLGA nanoparticles with the respective formulation with added lyoprotectant, which is the most common method to use sugars as lyoprotectants, it was observed that formulations co-encapsulated with the tested lyoprotectants, except sorbitol, showed an increase of insulin stabilization upon lyophilization, since the former showed an AO of 78.3 ± 2.4%, 72.2 ± 3.0%, 65.6 ± 1.8%, 83.3 ± 1.2% and 83.4 ± 1.8% for trehalose, glucose, sucrose, fructose and sorbitol, respectively. The strategy of co-encapsulating lyoprotectants into nanoparticles together with the protein also yielded the most similar AO values. These results clearly showed that the co-encapsulation of lyoprotectants, offered better insulin stabilization upon lyophilization over the conventional method of lyoprotectant addition prior lyophilization. This was also evidenced by the similar AO values of PLGA nanoparticles with co-encapsulated lyoprotectants and the controls of lyophilized insulin, which were about 84.2 ± 0.2%, 80.7 ± 0.8%, 86.4 ± 0.1%, 83.5 ± 0.1%, 81.7 ± 0.1% and 83.8 ± 0.7% for respectively no lyoprotectant, trehalose, glucose, sucrose, fructose and sorbitol containing formulations. The AO values obtained by comparing the spectra of the lyophilized formulations at the different lyoprotection levels with the respective lyophilized insulin controls (with lyoprotectants) (Figure 6.6), showed that PLGA nanoparticles with co-encapsulated lyoprotectant were most similar to the insulin controls. Surprisingly, the expected superior lyoprotection level by placing the lyoprotectant both inside and outside the nanoparticles did not offer higher insulin stability, comparatively to formulations with co-encapsulated lyoprotectants.

Depending on the lyoprotection level, lyoprotectants presented different performances; however, formulations containing fructose and sorbitol showed similar performances on insulin stabilization for all lyoprotection levels. However, it is likely ill-advised to use reducing sugars as lyoprotectants in close contact with a protein, as these may react with the protein over time forming a covalent sugar adduct (Maillard reaction) [260].

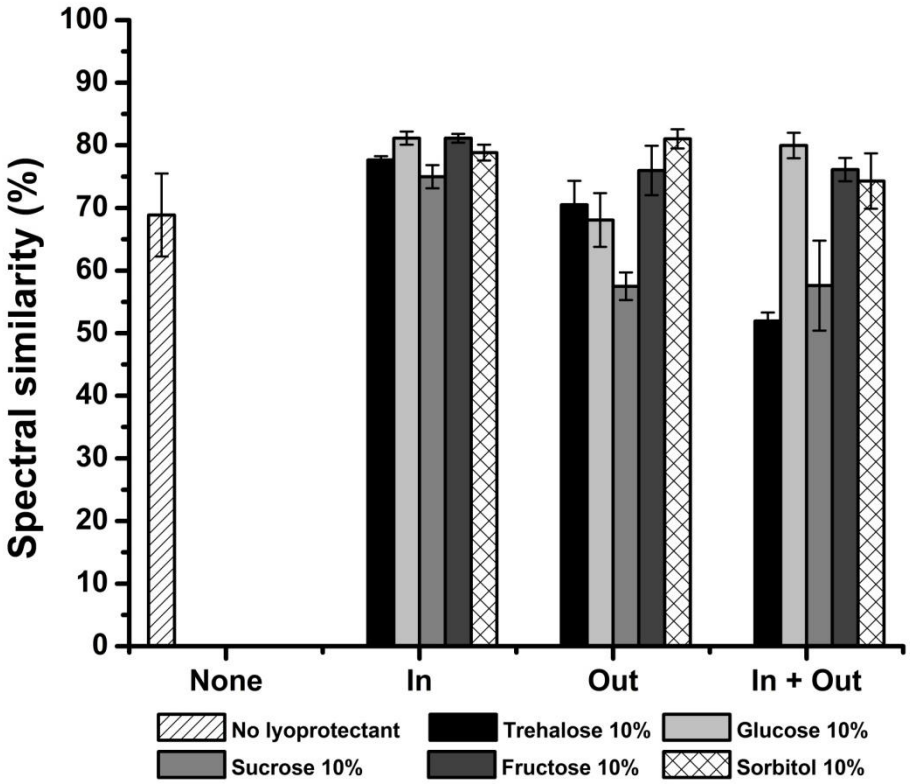

Figure 6.6. AO percentages of insulin loaded into PLGA nanoparticles formulations after lyophilization with different lyoprotection levels (*n* = 3), comparatively to respective lyophilized controls of insulin with and without lyoprotectant.

3.8.1.2. Visual comparison of area-normalized second-derivative amide I spectra

The AO values represent the quantitative maintenance of the native structure of insulin, whereas the visual comparison of the area-normalized second-derivative amide I spectra (Figure 6.7), gives information about the qualitative changes of insulin secondary structure. It has been described that the secondary structure of proteins is different in aqueous and lyophilized state [257]. Usually, the lyophilization process results in an increase in the β-sheet content, and a concomitant decrease in α-helix. The increase of β-sheet content is mainly due to protein-protein interactions, which drives to the formation of intermolecular β-sheets upon water removal, thus the β-sheet content does not properly represent protein intramolecular structural content. Therefore, it is accepted that the α-helix content is a better indicator of the protein structural integrity [258]. The area-normalized second-derivative FTIR spectrum of native insulin (Figure 6.7, insulin solution 30 mg/ml) fit well with the known secondary structure that is dominated by α-helix (1655 cm^{-1}), but also contain β-sheets (bands at 1638 and 1685 cm^{-1}) [259].

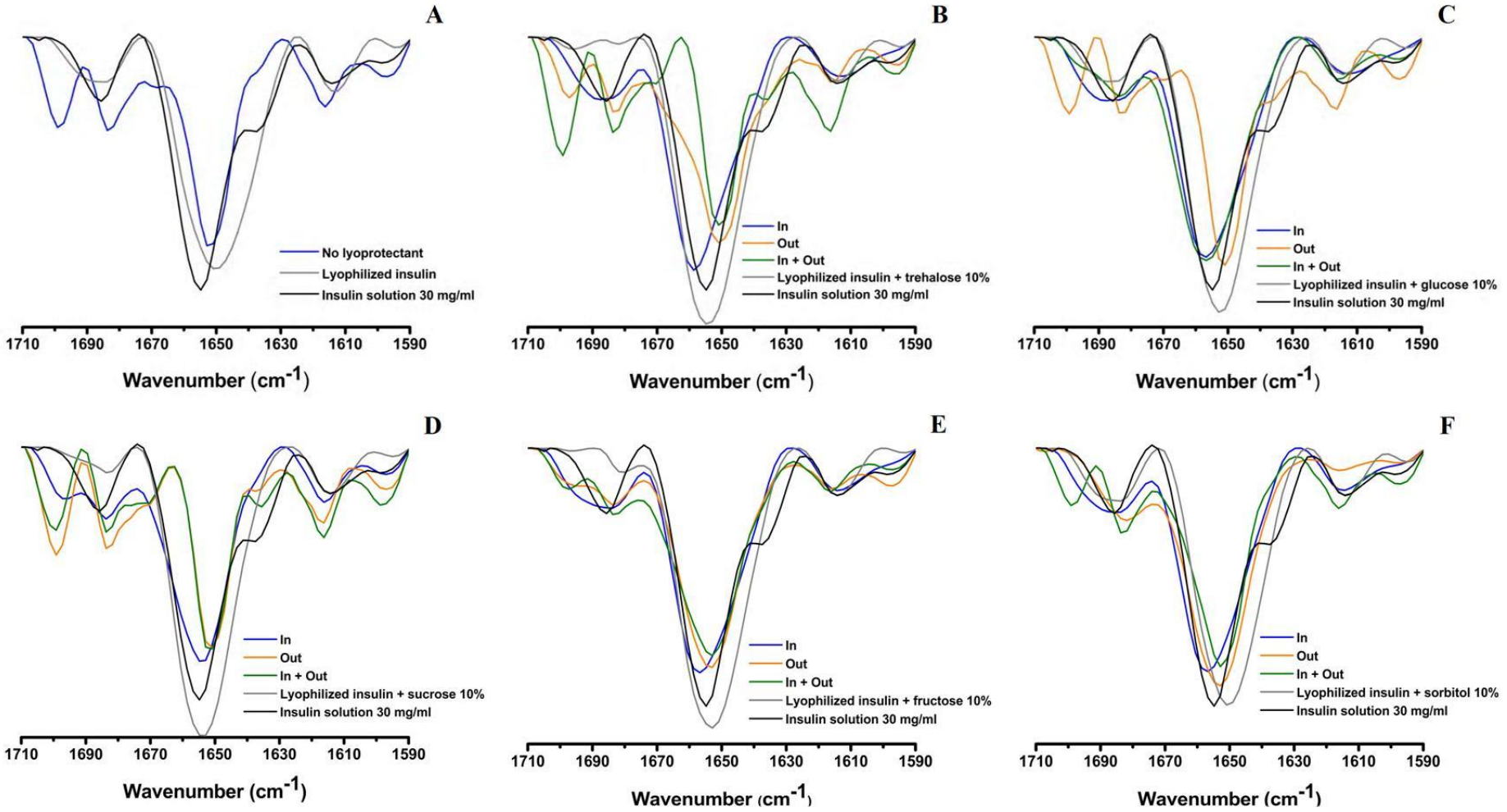

Figure 6.7. Area-normalized second-derivative amide I FTIR spectra of insulin loaded into lyophilized PLGA nanoparticles containing no lyoprotectant (A), trehalose 10% (B), glucose 10% (C), sucrose 10% (D), fructose 10% (E) and sorbitol 10% (F) at different lyoprotection levels.

The changes of these bands upon lyophilization represent the change of insulin structure. These changes may ultimately lead to aggregation or denaturation, which negatively impacts insulin bioactivity and may potentially cause adverse events upon administration.

It is shown in figure 6.7-A that insulin loaded into insulin-PLGA nanoparticles changed its structure upon lyophilization, verified by the decrease and slight shift of α-helix to 1653 cm^{-1} and increase of the β-sheet bands, in particular the potential intermolecular β-sheet bands at 1700 cm^{-1} and 1616 cm^{-1}. These structural changes show the necessity to use lyoprotectants to stabilize the protein upon lyophilization. Figures 6.7-B to 6.7-F, represent the area-normalized second-derivative spectra of the formulations at the different lyoprotection levels. Overall, when compared to the insulin solution 30 mg/ml, the controls of insulin lyophilized together with lyoprotectants, with exception of sorbitol, showed an increase in α-helix content, with also a band shift for formulations containing reducing sugars and sorbitol, showing the proposed stabilizing effect of lyoprotectants. Compared to the other trehalose containing formulations, the PLGA nanoparticles with co-encapsulated trehalose preserved the insulin structure best, with just a slight decrease and shift of α-helix to 1658 cm^{-1}. The other formulations containing trehalose showed a decrease and shift of α-helix into 1650 cm^{-1}. Regarding the β-sheet content, the formulation with added trehalose just slightly increased its high-frequency β-sheet, whereas the trehalose- in + out formulation surprisingly showed a significant increase in low- and high-frequency β-sheet and a possible intermolecular β-sheet band formation at 1618/1700 cm^{-1}.

The FTIR spectra of PLGA nanoparticles containing glucose (Figure 6.7-C) showed a similar insulin structure in glucose-in and glucose-in + out formulations with a slight decrease in the α-helix and shift to 1658 cm^{-1}. Insulin loaded into glucose-out PLGA nanoparticles suffered a higher structural modification with also a decrease and shift of α-helix to 1650 cm^{-1}, and an increase of low- and high- frequency β-sheet as well as possible intermolecular β-sheet band formation at about 1620/1700 cm^{-1}. The insulin loaded into all sucrose containing formulations showed a similar pattern of structure modifications, with the characteristic decrease in α-helix content and increase of low- and high-frequency β-sheet, and possible intermolecular β-sheet band formation at 1620/1700 cm^{-1}. However the insulin in sucrose-out and –in + out PLGA nanoparticles showed a similar and higher loss of α-helix content, than the sucrose-in formulation. The PLGA nanoparticles containing fructose showed most similarity among the different lyoprotection levels, which was mostly characterized by a slight decrease of α-helix. Finally, insulin loaded into PLGA nanoparticles containing sorbitol also showed a close similarity, with the exception of sorbitol-in + out which in addition to the slight decrease of

the α-helix content also increased its high-frequency β-sheet and intermoleculat β-sheet at 1620/1700 cm^{-1}.

Thus, the results showed that PLGA nanoparticles with co-encapsulated lyoprotectants demonstrated a higher protein structural stabilization than the other strategies. No apparent insulin aggregation was found in these formulations, as derived from the absence of intermolecular β-sheets bands, whereas in the PLGA nanoparticles containing trehalose (in + out), glucose (out), sucrose (out, in + out) and sorbitol (in + out) did show such bands. Surprisingly, the combination of lyoprotectant co-encapsulation and external addition performed worse than the co-encapsulation alone.

3.8.2. Circular dichroism experiments

All samples were analyzed by CD spectroscopy to also assess insulin secondary structure and confirm the results obtained by FTIR spectroscopy. In contrast to FTIR, to perform CD experiments it was necessary to extract insulin from nanoparticles to avoid spectral artifacts due to light scattering, and the obtained results are shown in Figure 6.8. The CD spectrum of 0.2 mg/ml insulin solution in HCl 0.01 was used as reference of insulin native structure and showed two minima at about 210 nm and 222 nm, which are characteristic of a predominant α-helix structure of the protein [266].

The insulin CD spectra of the lyophilized PLGA nanoparticles, showed a reduction of the α-helix structure of insulin. This was evident by the decrease in the intensity and the shift of insulin band from 192 nm to ca. 200 nm, and decrease of the bands at 210 nm and 222 nm. The results are then in agreement with the results obtained by FTIR, with an overall modification of insulin structure from α-helix, likely into β-sheet. The controls of lyophilized insulin containing lyoprotectants also showed reductions in α-helix content, as also observed by FTIR. More importantly, CD measurements showed that all the PLGA nanoparticles with co-encapsulated lyoprotectants better preserved the structure of insulin upon lyophilization, compared to the other formulations containing the same lyoprotectant. This was evident by the higher similarity CD spectra of those spectra, in particular the CD signals at 210 nm and 222 nm, with the spectrum of native insulin. Therefore, these results also show that the strategy of co-encapsulation of lyoprotectants together with insulin offered superior stability of insulin structure upon lyophilization, over the conventional method of lyoprotectant addition prior to lyophilization.

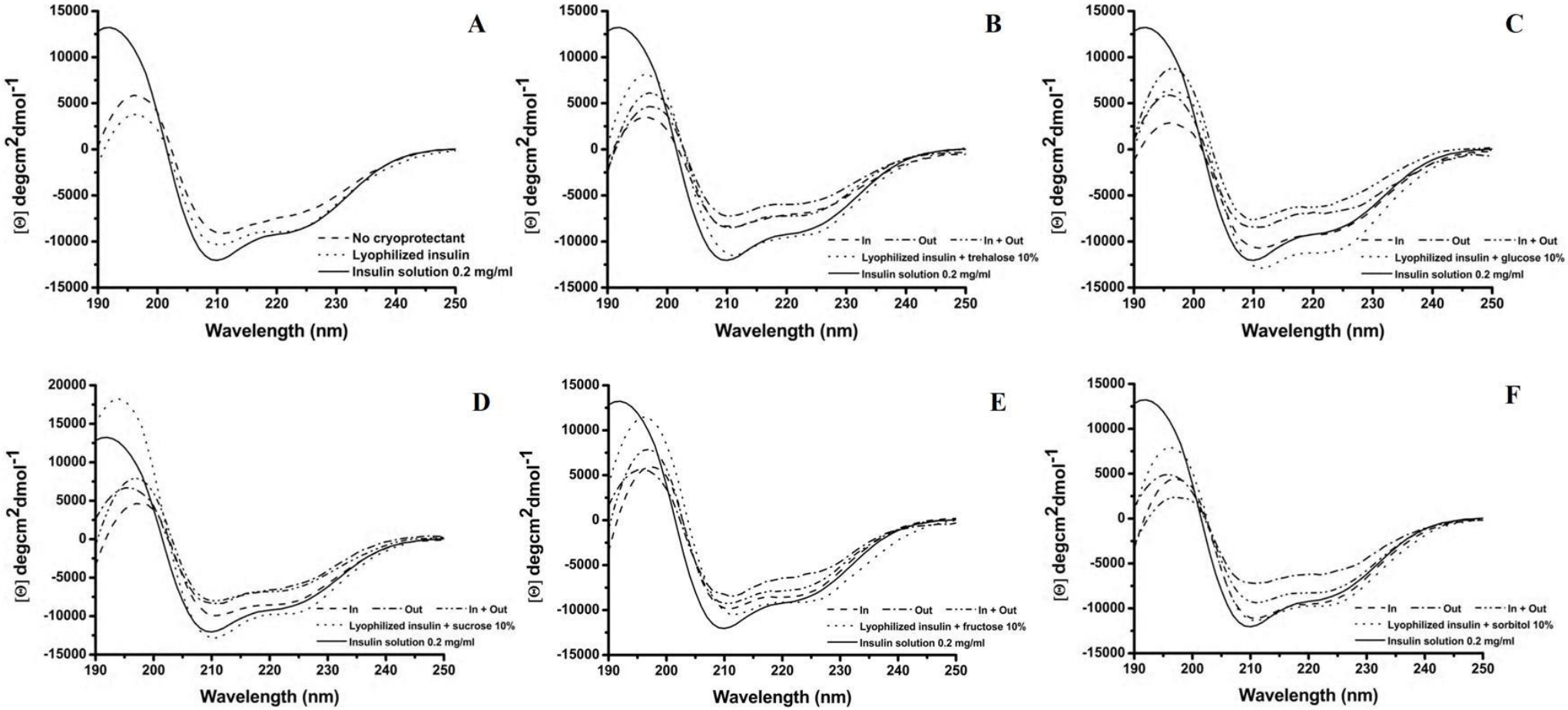

Figure 6.8. Far-UV CD spectra of insulin loaded into lyophilized PLGA nanoparticles containing no lyoprotectant (A), trehalose (B), glucose (C), sucrose (D), fructose (E) and sorbitol (F) at different lyoprotection levels.

Such strategy may also be successfully applied in the encapsulation of therapeutic proteins into other polymer-based or even lipid-based nanoparticles, such as PLA nanoparticles, PCL nanoparticles and solid lipid nanoparticles (SLN), with clear benefits to the stabilization of the loaded protein and consequent preservation of its bioactivity upon lyophilization.

3.9. *In vitro* release study

Just a few studies are known about the release profile of drugs by PLGA nanoparticles after lyophilization using lyoprotectants [101, 178]. To verify the potential of carriers to deliver the loaded drug, it is essential to assess the release profile of insulin under simulated *in vitro* conditions, from the developed PLGA nanoparticle formulations. The release patterns of insulin are shown in Figure 6.9. These results were slightly different from those obtained in a previous work [101], which could be explained by the use of a different lyophilization process that impacts the quality of the final product, and consequently the performance of PLGA nanoparticles as delivery systems.

The insulin-PLGA nanoparticles (no lyoprotectant) showed a release of insulin of 58.6 ± 4.7% in the first 2 hours, increasing the release up to 76.7 ± 2.7% until 48 h. The increase of nanoparticle porosity upon lyophilization is likely responsible for the release of more than 50% of insulin in the first 2 h. The formulations with co-encapsulated lyoprotectants showed a similar profile, achieving more than 60% of insulin release after 48 hours (Figure 6.9-A). Trehalose, glucose, sucrose, fructose and sorbitol formulations, achieved an insulin release after 48 hours of 82.5 ± 3.47%, 68.6 ± 4.2%, 69.7 ± 4.2%, 70.5 ± 3.5% and 73.5 ± 2.7%, respectively. The PLGA nanoparticles with added lyoprotectants showed a lower release of insulin (ca. 60%) after 48 hours (Figure 6.9-B) compared to the insulin-PLGA nanoparticles. This was particularly evident in the lower burst release of insulin in the first 2 hours, of 47.0 ± 4.0%, 36.6 ± 2.3%, 34.6 ± 4.4%, 43.1 ± 3.6% and 48.2 ± 4.0% for those added trehalose, glucose, sucrose, fructose and sorbitol, respectively. A similar behavior was also observed for formulations both with co-encapsulated and added lyoprotectants (Figure 6.9-C).

The overall formulations revealed a sustained release pattern of insulin, which is characteristic of PLGA nanoparticles [145, 147]. This consisted of an initial burst release in the first 2 hours followed by a sustained release until 48 h. This initial burst release may be explained by the increase of the porosity of the lyophilizates and nanoparticles. Indeed, the increase of nanoparticle porosity upon lyophilization facilitates the release of insulin, which leads to a higher release rate of insulin upon lyophilization of PLGA nanoparticles compared to the same carriers directly after production [101]. Then, after

this initial burst release, the erosion of the nanoparticle polymer overtime is responsible by the sustained release of insulin until 48 h.

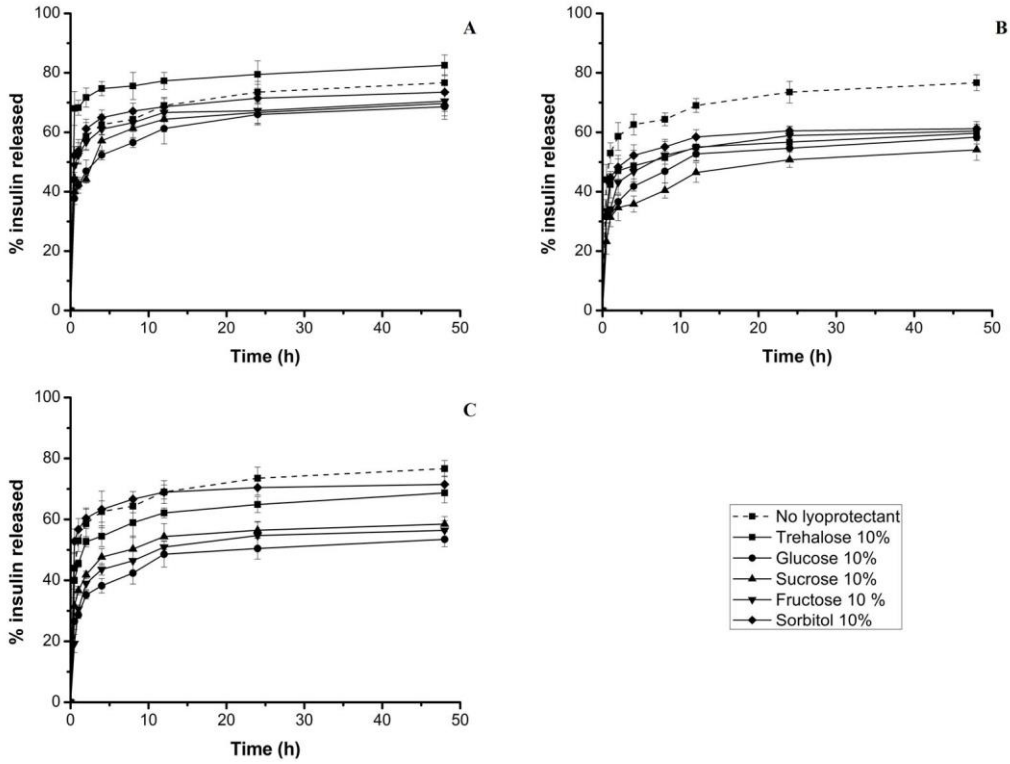

Figure 6.9. Cumulative release profile of insulin loaded into PLGA nanoparticles lyophilized with different lyoprotection levels: A: in, B: out and C: in + out. (*n* = 3, vertical lines represent SD).

The possible explanation, for the lower release of insulin from PLGA nanoparticle formulations containing lyoprotectants may be due to the presence of sugars that increase the osmotic pressure in the aqueous medium, decreasing significantly the burst release of insulin. This behavior has been previously described [267]. The increase of the osmotic pressure avoids the influx of water from the aqueous medium into the PLGA nanoparticles, reducing the formation of water channels which are responsible by the initial burst release [268]. Overall, besides the increase in porosity of nanoparticles upon lyophilization, the release of insulin could be mitigated by the presence of lyoprotectants on nanoparticle formulations.

4. Conclusion

Insulin-loaded PLGA nanoparticles with co-encapsulated lyoprotectants were successfully produced, and likely would have an improved colloidal stability. No

significant aggregation of PLGA nanoparticles was observed, indicating the suitability of the lyophilization process. The formulations with co-encapsulated lyoprotectants obtained a good lyophilizate with white cotton-like texture, whereas in the remainder formulations the lyophilizate slightly shrunk. The lyophilizate of PLGA nanoparticles with co-encapsulated lyoprotectants were amorphous, whereas formulations at the other tested lyoprotection levels presented some crystallinity. Those containing trehalose were, however, amorphous, revealing its versatility compared to the other lyoprotectants.

Regarding the stability of the loaded insulin, it was demonstrated that the co-encapsulation of lyoprotectants offered superior insulin stability compared to the conventional lyoprotectant addition method. In addition, these formulations showed the most similar structure maintenance among the lyoprotection levels. The simultaneous co-encapsulation and addition of lyoprotectant to the external phase could even be detrimental to insulin stabilization. Furthermore, the reducing sugars did not show an adverse effect on insulin stability, when they were co-encapsulated. The PLGA nanoparticles with added lyoprotectants showed a lower *in vitro* release of insulin, compared to formulations co-encapsulated with the same lyoprotectants.

In summary, the co-encapsulation of lyoprotectants together with insulin is a promising approach to better stabilize the protein upon lyophilization. At the same time this strategy uses much lower amount of lyoprotectant in formulations and improves the overall stability of insulin-loaded PLGA nanoparticles. Therefore, the findings achieved in this chapter may represent an impulse in the development of a new paradigm in the lyophilization of protein-loaded nanoparticles.

Chapter 7

Optimization of Lyophilization Cycle and Effect of Freezing on the Stability and Bioactivity of Protein-loaded PLGA Nanoparticles upon Lyophilization

To be partially published as:

Pedro Fonte, Fernanda Andrade, João Pinto, Vítor Seabra, Marco van de Weert, Salette Reis, Bruno Sarmento, Effect of the freezing step in the stability and bioactivity of protein-loaded PLGA nanoparticles upon lyophilization. *Submitted for publication.*

1. Introduction

The freezing step is considered the most determinant for product quality, since it impacts the type and size of ice crystals, influencing the water vapor flow during the drying steps, with obvious consequences to the final lyophilized product. The exact mechanism behind freezing during lyophilization is not well understood yet. Apparently, during freezing, ice crystals grow and nucleate, excluding the solutes in formulation into a cryoconcentrated phase in which a phase separation or even crystallization may occur [184]. The freezing step is also the most aggressive stage of the lyophilization process, leading to possible aggregation or even fusion of nanoparticles. Therefore, cryoprotectants are frequently added to formulations to protect nanoparticles from lyophilization stresses.

Different freezing methods may be used to obtain different freezing rates, as the shelf-ramped freezing [269] and the quench freezing using liquid nitrogen [184, 270]. Regardless the freezing method, the freezing step needs to occur at a temperature below the Tg' to guarantee the total solidification and, consequently, an acceptable lyophilized product. On its turn, the primary drying needs to occur below the Tc of the formulation, otherwise the obtained cake can collapse, which may lead to an inefficient water removal causing high residual moisture content and difficulty on redispersion of the lyophilizate [168, 204]. The optimization of the lyophilization cycle considering these critical temperatures is often neglected, and lyophilization is even used to dehydrate nanoparticle suspensions in a standard, empiric or even trial and error manner [7]. Previously, it was evaluated the influence of a standard lyophilization cycle using different cryoprotectants on the structure of a protein loaded into PLGA nanoparticles, and its stability upon 6 months of storage [175]. More recently, it was verified that the co-encapsulation of cryoprotectants improved the stability of protein-loaded PLGA nanoparticles after lyophilization [227]. In the present chapter, these approaches were taken further by assessing the influence of the freezing step, which is the most important one in lyophilization, on the structural stability of protein loaded into PLGA nanoparticles co-encapsulated with cryoprotectants, upon lyophilization using an optimized cycle.

Thus, the purpose of this chapter was to develop an optimized lyophilization cycle regarding the physical-chemical properties of the nanoparticles containing, insulin as a model therapeutic protein, and assess the effect of the freezing step in the structural stability of the encapsulated protein. In addition, it was determined the performance of several cryoprotectants in the preservation of insulin structure using different freezing

methods. Ultimately, the structural stability of the protein and consequent performance *in vivo* was also evaluated.

2. Materials and Methods

2.1. Materials

For the nanoparticles production it was used PLGA 50:50 Resomer® RG 503 H (Mw 24,000-38,000; Tg 44-48 ºC) from Evonik Industries AG (Essen, Germany). PVA, dichloromethane, recombinant human insulin, trehalose, sucrose, sorbitol and thioflavin T were from Sigma-Aldrich (Steinheim, Germany). For the HPLC analysis, it was used acetonitrile HPLC Gradient Grade from Fischer Scientific (Loughborough, UK) and trifluoroacetic acid from Acros Organics (Morris Plains, NJ, USA). Chloroform from Sigma-Aldrich (Steinheim, Germany) was used for protein extraction from nanoparticles. Streptozotocin used in the *in vivo* experiments was also from Sigma-Aldrich (Steinheim, Germany) and sodium citrate was from Merck KGaA (Darmstadt, Germany). The Milli-Q water was produced in-house and other reagents were of analytical grade.

2.2. Preparation of PLGA nanoparticles

The PLGA nanoparticles were produced by a modified solvent emulsification-evaporation, w/o/w double emulsion technique, which protocol was previously developed and optimized to co-encapsulate insulin and cryoprotectants into PLGA nanoparticles [227]. Briefly, 2 mL of dichloromethane were used to dissolve 200 mg of PLGA 50:50, and then added with 0.2 mL of a 150 mg/mL insulin solution in HCl 0.1 M containing also the different cryoprotectants used (trehalose, sucrose or sorbitol) at a concentration of 10% (w/v). This mixture was sonicated at 70% of amplitude for 30 seconds using a Bioblock vibracell 75186 sonicator from Fischer Bioblock Scientific (Rungis Complexe, France), forming the primary emulsion. The latter was then poured into 25 mL of PVA 2% (w/v) at pH 7.4, and again sonicated using the same previous conditions. Then, the organic solvent was removed by evaporation under magnetic stirring for 3 h. The same production method was also used to formulate both insulin loaded and unloaded PLGA nanoparticles to be used as controls. After production, nanoparticles were washed three times with Milli-Q water, and collected after each washing step by centrifugation for 30 minutes at 23,000 x *g* using a Heraeus Megafuge 1.0 R centrifuge (Thermo Scientific, Asheville, NC, USA). Finally, nanoparticles were redispersed in water.

2.3. Insulin association efficiency, loading capacity and retention efficiency

The AE was calculated using the equation 4.1 (*see* Chapter 4) and LC of insulin was calculated using equation 6.1 (*see* Chapter 6). The free insulin in supernatant was obtained by centrifugation of nanoparticles suspension at 40,000 x *g* at 4ºC for 30 min, in a Beckman Optima TL ultracentrifuge from Beckman Coulter (Brea, CA, U.S.A.). The dry mass of nanoparticles was obtained by lyophilization of nanoparticles after centrifugation. The insulin retention efficiency was determined by the amount of insulin which remained loaded after lyophilization, and was determined after reconstitution of nanoparticles and quantification of insulin present in supernatant after nanoparticle centrifugation. Insulin was quantified using a HPLC-UV method previously validated [233], in a Merck-Hitachi LaChrom HPLC instrument equipped with a LiChrospher 100 RP-18 guard column, 5 µm particle size from Merck (Whitehouse Station, NJ, U.S.A.) and also a XTerra RP 18 column, 5 µm particle size, 4.6 mm internal diameter x 250 mm length from Waters (Milford, MA, U.S.A.). All the obtained samples were run in triplicate.

2.4. Particle size and zeta potential analyses

The insulin-loaded PLGA nanoparticles in suspension and reconstituted after lyophilization were diluted with Milli-Q water to obtain a proper concentration, prior to the analysis of particle size and zeta potential. These analysis were respectively, performed by dynamic light scattering using a 90Plus Particle Size Analyser, and by phase analysis light scattering using a ZetaPALS Zeta Potential Analyser, both from Brookhaven Instruments Corporation (Holstville, NY, USA). The lyophilization ratio was calculated as the mean particle size after lyophilization, divided by the mean particle size before lyophilization.

2.5. Differential scanning calorimetry analysis

The thermal behavior of insulin-loaded PLGA nanoparticles during freezing was assessed using a Setaram DSC 131 from SETARAM instrumentation (Caluire, France) device equipped with a liquid nitrogen cooling system. 40 µL of each sample were placed into aluminum pans and frozen until -90ºC at a freezing rate of 5ºC/min. Then, samples were heated up at a rate of 1ºC/min and Tg' was obtained by the onset of the transition. An empty aluminum pan was used as reference.

2.6. Lyophilization microscopy

The Tc of each formulation was determined using a Linkam THMS350V lyophilization plate from Linkam Scientific Instruments (Tadworth, UK) assembled to an Olympus microscope (Osaka, Japan). Thus, samples were frozen at a rate of 10 ºC/min until -100 ºC, then held for 15 min and heated under vacuum at a rate of 5ºC/min. The Tc was obtained by the onset of product collapse during the drying of the frozen sample.

2.7. Lyophilization of nanoparticles

The insulin-loaded PLGA nanoparticles were placed into semi-stoppered glass vials, with slotted rubber closures at a maximal height of 10 mm. Three freezing conditions and temperatures were used, namely freezing samples at -80ºC in a freezer, freezing inside the lyophilizer chamber at -40ºC, and freezing in liquid nitrogen. The different freezing methods occurred during 4 hours, and all samples were dried following the same protocol in a VirTis Advantage Plus Benchtop lyophilizer from (SP Scientific (Warminster, PA, USA) at a condenser surface temperature of -60ºC. The primary drying occurred at -32ºC and 150 mtorr for 24 hours, followed by a secondary drying at 20ºC and 50 mtorr for 6 h (n = 3).

2.8. Macroscopic evaluation and residual moisture content of the lyophilizates

The lyophilizates were visually inspected to detect any shrinkage or collapse of the cake after lyophilization. The residual moisture content of the lyophilizates of insulin-loaded PLGA nanoparticles was determined using an A&D MX-50 moisture analyzer from A&D Company Ltd. (Tokyo, Japan). An equal amount of lyophilizate of each formulation was analysed, and the residual moisture content was quantified as percentage of containing moisture.

2.9. Reconstitution of lyophilizates

After lyophilization, all the samples were reconstituted by adding Milli-Q water on the inside wall of the vials and kept for 10 min, in order to assure the wetting of the cake. Then, samples were hand swirled until complete homogenization.

2.10. Scanning electron microscopy analysis

The morphology of insulin-loaded PLGA nanoparticles and the lyophilizates were observed by SEM using a FEI Quanta 400 FEG scanning electron microscope from FEI (Hillsboro, OR, USA). All the samples were mounted on metal stubs and coated under vacuum, with a layer of gold/palladium at a 15 mA current for 60 seconds prior to observation.

2.11. X-Ray powder diffraction analysis

The diffractograms of all formulations were obtained on a X-ray powder diffractometer PANanalytical X'pert PRO with a PIXcel detector (PANanalytical B. V., Almelo, Netherlands). The XRPD patterns were collected with a Cu Kα radiation (45 kV, 40 mA, λ = 1.54187 Å), and with a 96-well plate stage in transmission mode from 2-40º at 2θ with a scan speed of 0.067º/s.

2.12. Attenuated total reflectance-Fourier transform infrared spectroscopy analysis

ATR-FTIR was used to assess the secondary structure of insulin loaded into PLGA nanoparticles. The formulations were run on an ABB MB3000 FTIR spectrometer from ABB (Zurich, Switzerland) equipped with a MIRacle triple reflection ATR accessory from PIKE Technologies (Madison, WI, USA). The FTIR spectra were collected by 256 scans at a 4 cm^{-1} resolution in the 4000−600 cm^{-1} region. The insulin spectra were obtained by a double subtraction method [243], followed by a Savitzky-Golay second derivative of 15 points, and a 3-4 point baseline correction in the amide I region (1710−1590 cm^{-1}). Further, all the spectra were area-normalized for comparison. The spectral treatment was performed using the Horizon MB FTIR software from ABB. The similarity of the area normalized second-derivative amide I spectra, between native insulin and insulin loaded into PLGA nanoparticles was determined quantitatively, using the AO algorithm [244]. Therefore, it was used a 30 mg/mL insulin solution in HCl 0.1 M, to determine the percentage of spectral similarity. This solution was used as reference of native insulin, since it is considered that the stability of a solid protein formulation increases with the increase of the similarity to its spectra in solution [246].

2.13. Circular dichroism analysis

To assess the structure of insulin by CD, the protein was extracted from the PLGA nanoparticles by a treatment using a mixture of chloroform, to destroy the nanoparticles by dissolving the PLGA, and HCl 0.01 M to dissolve the extracted insulin. Then, all measurements were collected in a Jasco J-815 CD Spectrometer from Jasco Inc. (Easton, MD, USA) with the lamp housing continuously purged with nitrogen and at 25ºC. The CD spectra were obtained from an average of 5 scans in the 190-250 nm region, using a 0.1 cm cell, and with a step size of 0.5 nm, a bandwith of 1.5 nm, and an averaging time of 5 s. The reference sample spectrum was subtracted from the test sample spectra. The molar ellipticity of insulin was calculated as CD signal x MRW of each insulin residue (116 Da) [insulin concentration (mg/mL) x cell pathlength (0.1 cm)]. The concentration of insulin was determined by UV absorption at 280 nm in a NanoDrop 2000c UV-Vis Spectrophotometer (Thermo Scientific, Wilmington, DE, USA), using a molar extinction coefficient of 6200 $M^{-1}cm^{-1}$ for 1.0 mg/mL. As control sample of native insulin it was used a 0.2 mg/mL insulin solution in HCl 0.01 M.

2.14. Fluorescence spectroscopy analysis

Insulin-loaded PLGA nanoparticles were treated with chloroform and insulin was extracted prior to fluorescence spectroscopy analysis. The fluorescence emission spectra were obtained in a range of 290 to 450 nm with a 1 nm step in a Jasco FP-6500 Spectrofluorometer from Jasco Inc. (Easton, MD, USA) at 25ºC. The excitation occurred at 280 nm with excitation and emission slits set to 3 nm, an integration time per data point of 0.1 seconds and with 5 scans average. The reference sample spectrum was subtracted from the test sample spectra, and normalized based on insulin concentration.

2.15. Thioflavin T assay

The experiments were run in a Jasco FP-6500 Spectrofluorometer from Jasco Inc. (Easton, MD, USA) at 25ºC and the final concentration of insulin and thioflavin T were 11 µM and 25 µM, respectively. The samples of insulin extracted from nanoparticles were excited at 450 nm, and the fluorescence intensity was measured at 485 nm with slit widths of 5 nm. The reference sample spectrum was subtracted from the test sample spectra. Insulin fibrillated by incubation at 60ºC during 12 hours was used as a positive control.

2.16. *In vivo* activity analysis of insulin-loaded formulations

2.16.1. Animals

The animals were male Wistar Han rats (150-174 g) obtained from Harlan Laboratories (Sant Feliu de Codines, Spain), and were maintained for 7 days for nutritional, physiological and behavioral stabilization. They were kept accordingly to the recommendations of Federation of Laboratory Animal Science Associations (FELASA), and also to the European Parliament and Council Directive 2010/63/EU. A standard diet food from Mucedola srl (Settimo Milanese, Italy) and water *ad libitum* were given to animals. The floor of the cages were filled with Corn Cob ULTRA12 bedding from Ultragene (Santa Comba Dão, Portugal), and enriched with nesting materials. The room conditions were kept at 22ºC ± 2ºC, 55% ± 10% RH and 12/12 light exposition. Upon quarantine, the diabetes was induced to animals by intraperitoneal injection of streptozotocin with a concentration of 10 mg/mL in citrate buffer pH 4.5 at a dose of 60 mg/kg. After a week, the animals that presented fasted blood glucose levels higher than 250 mg/dL were grouped (n = 5) and used in the *in vivo* experiment.

2.16.2. In vivo pharmacological activity of insulin

The animals were fasted 12 hours before and during the experiment, but were allowed water *ad libitum*. The formulations were administered subcutaneously using a 25 G needle at a dose of 50 IU/kg bodyweight. An insulin solution in PBS at 2.5 IU/kg bodyweight administered subcutaneously was used as control. The blood samples were taken from the tail vein at 0.5, 1, 2, 4, 6, 8, 12 and 24 h and the plasma glucose levels were obtained using test strips from Abbot Laboratories (Amadora, Portugal) in a Precision Xtra blood glucose meter from the same supplier. In order to evaluate the cumulative hypoglycemic effect over time, the plasma glucose levels were plotted against time, as percentage of values at the beginning of the experiment. The PA of the formulations was determined using the equation:

$$PA = \frac{\frac{\text{AAC test}}{\text{Dose test}}}{\frac{\text{AAC control}}{\text{Dose control}}} \times 100 \qquad \textbf{(Eq. 7.1)}$$

The area above the curve (AAC) test and control refers to the AAC of subcutaneous formulations and subcutaneous insulin solution in PBS (2.5 IU/kg bodyweight), respectively. Simultaneously, the dose test and control refers to the insulin dose at IU/kg bodyweight of subcutaneous formulations and subcutaneous insulin solution, respectively.

2.17. Statistical analysis

All the statistical analyses were performed using a one-way ANOVA Tukey *post hoc* test, with a significance level of $p < 0.05$ in the OriginPro 8 software from OriginLab Corporation (Northampton, MA, USA).

3. Results and discussion

The therapeutic protein model, insulin, was loaded into PLGA nanoparticles following a protocol previously developed [101]. The strategy of co-encapsulation of cryoprotectants together with insulin into PLGA nanoparticles showed to better protect the protein structure upon lyophilization, comparatively to the conventional cryoprotectant addition method immediately prior to lyophilization [227]. Therefore, this approach was used to study the effect of the freezing step of lyophilization in the structure of the loaded insulin.

The freezing step is the one that most influences the properties of the final product [184], nevertheless its impact in the structure of the loaded protein was not investigated so far. In the present study, several cryoprotectants were used, namely, two nonreducing sugars, trehalose and sucrose, and one sugar alcohol, sorbitol. The concentration of cryoprotectants used in formulations was 10% (w/v) to obtain the highest acceptable cryoprotectant effect, since its level of formulation stabilization depends on its concentration [7]. To assess the effect of the freezing step, additionally to the characterization of insulin structure, it was also characterized the properties of nanoparticles, the obtained lyophilizates and, likewise, the *in vivo* therapeutic performance of formulations.

3.1. Particle size, zeta potential, association efficiency and loading capacity

It was produced insulin-loaded PLGA nanoparticles containing no cryoprotectant (insulin-PLGA nanoparticles) and also co-encapsulated with trehalose (insulin-trehalose 10%-PLGA nanoparticles), sucrose (insulin-sucrose 10%-PLGA nanoparticles) and

sorbitol (insulin-sorbitol 10%-PLGA nanoparticles). The mean particle size, PdI and zeta potential characterizations of insulin-loaded PLGA nanoparticles are depicted in Figure 7.1. Insulin-PLGA nanoparticles, without any cryoprotectant, presented a particle size of 339 ± 10 nm, in agreement with that obtained in a previous work [227]. The insulin-loaded PLGA nanoparticles co-encapsulated with cryoprotectants ranged between 243 nm and 394 nm. On its turn the PdI of such formulations ranged between 0.17 and 0.25, which shows the low heterogeneity of nanoparticles.

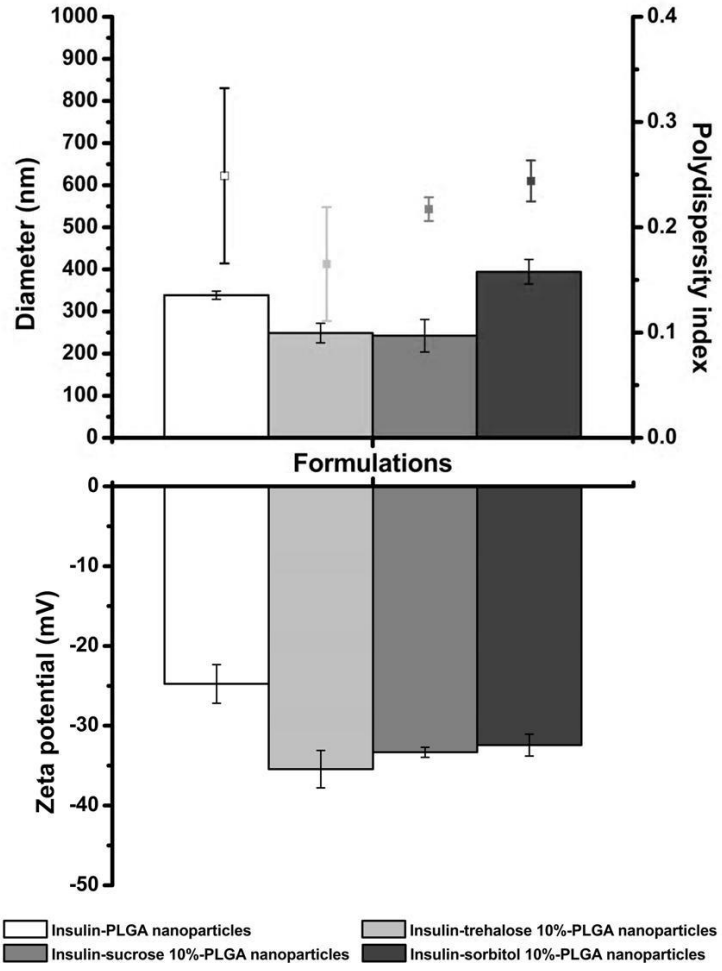

Figure 7.1. Mean particle size (top bars), PdI, and zeta potential (bottom bars) characterization of insulin-loaded PLGA nanoparticles (*n* = 3, mean ± SD).

All insulin-loaded PLGA nanoparticles had a negative surface charge, characteristic of the acidic PLGA polymer [147]. The insulin-loaded PLGA nanoparticles containing co-encapsulated cryoprotectants presented lower zeta potential, comparatively to the formulation without co-encapsulated cryoprotectant. These results were similar with those obtained previously [227], and may be explained by the presence

of cryoprotectants able to expand the location of the slipping plane during the electrophoretic movement, due to the formation of a viscous layer on the surface of nanoparticles [248]. Therefore, the co-encapsulation of cryoprotectants may increase the colloidal stability of the nanoparticles, since the more negative zeta potential results in greater particle-particle repulsion.

The insulin-loaded PLGA nanoparticles were further characterized in terms of insulin AE and LC (Table 7.1). The insulin AE of formulations was higher than 90%, a very good achievement considering the hydrophilic nature of insulin and hydrophobic nature of the PLGA polymer. Regarding the insulin LC it was noticed a slight decrease for insulin-loaded PLGA nanoparticles co-encapsulated with cryoprotectants, due to the presence of cryoprotectants loaded into nanoparticles. Both AE and LC were in agreement with those obtained previously [227], demonstrating the robustness of the production protocol and its ability to load insulin together with cryoprotectants, without prejudice the encapsulation of the protein.

Table 7.1. Characterization of insulin AE and LC of insulin-loaded PLGA nanoparticles (*n* = 3, mean ± SD).

Formulation	AE (%)	LC (%)
Insulin-PLGA nanoparticles	94.1 ± 0.3	12.5 ± 0.5
Insulin-trehalose 10%-PLGA nanoparticles	90.2 ± 0.4	11.4 ± 0.4
Insulin-sucrose 10%-PLGA nanoparticles	90.7 ± 0.5	11.7 ± 0.3
Insulin-sorbitol 10%-PLGA nanoparticles	93.7 ± 0.3	11.9 ± 0.4

3.2. Design of the lyophilization cycle

To obtain a lyophilized product with high quality, it is necessary to focus both in the formulation and in the lyophilization cycle. Most of the research works on the lyophilization of nanoparticles have been done following trial and error observations, without considering the scientific principles of such process. Thus, the lyophilization cycle needs to be developed following engineering and physical-chemical principles of nanoparticles, in order to preserve its characteristics and obtain a good lyophilizate [7, 140, 153].

The critical properties of formulations, necessary to design an adequate lyophilization process are the Tg' and the Tc. Thus, nanoparticles need to be cooled below its Tg' to assure the total solidification of the formulation [163], and the Tc is the maximum allowable temperature of product during the primary drying [193]. If product is

heated above Tc, the lyophilized product may collapse losing its macroscopic structure [195]. The obtained Tg' and Tc results of the produced formulations are depicted in Table 7.2, and it was noticed a decrease on those parameters when cryoprotectants were co-encapsulated. It has been reported that when cryoprotectants are added to nanoparticle formulations, the success of the lyophilization cycle depends just on the thermal properties of the cryoprotectants [153]. However, with the approach of co-encapsulating the cryoprotectant the success of the lyophilization cycle relies on the thermal properties of the formulation as a whole. Focusing in the Tg' and Tc results, it were designed three different lyophilization cycles. The used temperatures of the freezing and primary drying steps were defined considering the lower Tg' and Tc values obtained, since the formulations were lyophilized together in the different lyophilization cycles. The variation in the freezing step was performed to assess the contribution of different freezing methods in lyophilization, to the maintenance of the structure of insulin loaded into PLGA nanoparticles with and without cryoprotectants co-encapsulated.

Besides being simple, the freezing step is the one in which most of the water is removed, and being the first step, its effectiveness determines the success of the lyophilization cycle [184]. Therefore, the freezing step needs to be properly regarded, and it is important to distinguish between cooling rate and freezing rate, since they may not be necessarily related. The first is related with the rate that a formulation is cooled, whereas the freezing rate is the rate of postnucleation growth of ice crystals that is influenced by the supercooling amount prior to nucleation [270, 271]. Both cooling and freezing rates are influenced by the freezing method, such as the freezing at -80ºC, freezing inside the lyophilizer (ramped cooling) or freezing in liquid nitrogen. These different freezing methods, result in different ice crystals growth regarding its size, shape and number, and consequently result into different stresses to nanoparticles. Furthermore, the morphology of ice crystals is strictly related with the sublimation rate [185].

Table 7.2. Tg' and Tc of insulin-loaded PLGA nanoparticles**.**

Formulation	Tg' (°C)	Tc (°C)
Insulin-PLGA nanoparticles	-25.0	-23.2
Insulin-trehalose 10%-PLGA nanoparticles	-27.3	-25.7
Insulin-sucrose 10%-PLGA nanoparticles	-29.1	-27.8
Insulin-sorbitol 10%-PLGA nanoparticles	-31.3	-29.3

3.3. Lyophilizate visual inspection, reconstitution and residual moisture content

The freezing method decisively influences the characteristics of the lyophilized product such as its morphology, physical state, uniformity, reconstitution time, and residual moisture content. The lyophilizates obtained from the different lyophilization cycles were visually inspected, and all of them were white with cotton-like texture, and were occupying the same volume of the original frozen mass, without shrinkage or cake collapse, indicating that the used lyophilization cycles were properly optimized. The cakes of all the insulin-loaded PLGA nanoparticles were easy and fast to completely reconstitute obtaining good suspensions with no visual aggregates. The product collapse is a problem to avoid, since leads to high residual moisture content and large reconstitution times of nanoparticles, due to the absence of a porous structure [168, 173, 194].

Table 7.3. Lyophilization ratio, insulin retention efficiency and residual moisture content of insulin-loaded PLGA nanoparticles after lyophilization at different freezing conditions (n = 3, mean ± SD).

Formulation	Lyophilization ratio	Insulin retention efficiency (%)	Residual moisture content (%)
-80 °C			
Insulin-PLGA nanoparticles	1.07 ± 0.10	97.7 ± 0.8	1.27 ± 0.28
Insulin-trehalose 10%-PLGA nanoparticles	1.09 ± 0.19	98.2 ± 1.2	1.35 ± 0.32
Insulin-sucrose 10%-PLGA nanoparticles	1.11 ± 0.35	97.1 ± 1.5	1.28 ± 0.44
Insulin-sorbitol 10%-PLGA nanoparticles	0.98 ± 0.08	97.4 ± 0.8	1.40 ± 0.15
Ramped cooling			
Insulin-PLGA nanoparticles	1.01 ± 0.16	97.8 ± 0.9	1.55 ± 0.68
Insulin-trehalose 10%-PLGA nanoparticles	1.14 ± 0.08	97.7 ± 1.2	1.39 ± 0.59
Insulin-sucrose 10%-PLGA nanoparticles	1.14 ± 0.14	98.1 ± 1.2	1.36 ± 0.44
Insulin-sorbitol 10%-PLGA nanoparticles	1.12 ± 0.06	98.3 ± 1.5	1.48 ± 0.36
Liquid nitrogen			
Insulin-PLGA nanoparticles	0.82 ± 0.09	95.9 ± 0.8	1.22 ± 0.25
Insulin-trehalose 10%-PLGA nanoparticles	1.05 ± 0.04	96.9 ± 1.8	1.24 ± 0.12
Insulin-sucrose 10%-PLGA nanoparticles	1.01 ± 0.34	97.1 ± 1.6	1.16 ± 0.32
Insulin-sorbitol 10%-PLGA nanoparticles	0.72 ± 0.01	97.9 ± 1.9	1.25 ± 0.17

The secondary drying removes the adsorbed water that did not separated as ice upon freezing, and therefore did no sublimate during the primary drying. The residual moisture content obtained from the analysis of the lyophilizates is shown in Table 7.3, and the overall results were about 1%. This was a good achievement, since lyophilized products need to have very low residual moisture content, and it is considered that for pharmaceutical products, it should be around 1% [150]. A high residual moisture content is able to destabilize nanoparticles upon storage due to the crystallization of the containing cryoprotectant [140], and may also lead to a low Tg of the PLGA formulations, which can catalyze the PLGA hydrolysis, hampering the shelf-life stability of PLGA nanoparticles

In addition, the obtained results also revealed that the different freezing methods were suitable on freezing the formulations and the lyophilization cycle, particularly the secondary drying, was effective on removing water in order to obtain such low residual moisture content.

3.4. Particle size, zeta potential and drug retention efficiency upon lyophilization

Before lyophilization, insulin-loaded PLGA nanoparticles were washed with Milli-Q water to remove the surfactant PVA, to avoid its cryoprotectant action. A washing step was also important to remove the free drug, since its presence may increase the zeta potential up to neutrality, increasing the probability of nanoparticles aggregation [7]. Figure 7.2 shows the mean particle size, PdI and zeta potential characterization of insulin-loaded PLGA nanoparticles after lyophilization, using the different freezing methods. In addition, the Table 7.3 shows the lyophilization ratio of formulations, which was obtained by dividing the mean particle size of nanoparticles after with that before lyophilization. Therefore, a lyophilization ratio around 1 represents that the mean particle size of nanoparticles was kept after lyophilization. The overall results of mean particle size showed that insulin-loaded nanoparticles maintained its particle size upon lyophilization. There were just two exceptions for insulin-PLGA nanoparticles and insulin-sorbitol 10%-PLGA nanoparticles frozen in liquid nitrogen, which presented a lower mean particle size ($p < 0.05$) after lyophilization, achieving a lyophilization ratio of 0.82 ± 0.09 and 0.72 ± 0.01, respectively. The freezing stresses suffered by nanoparticles at this freezing condition may be responsible of such particle size change. On their turn, trehalose and sucrose helped to mitigate the stresses of freezing in liquid nitrogen. The lyophilization ratio of the remainder formulations were around 1 demonstrating the maintenance of nanoparticles size upon lyophilization. Besides being higher than prior lyophilization, the PdI also demonstrated the low heterogeneity of nanoparticles size in

all formulations. Additionally, with the exception of insulin-sucrose 10%-PLGA nanoparticles frozen at -80ºC and in liquid nitrogen, the zeta potential values of the different formulations were similar upon lyophilization, demonstrating the good colloidal stability of nanoparticles.

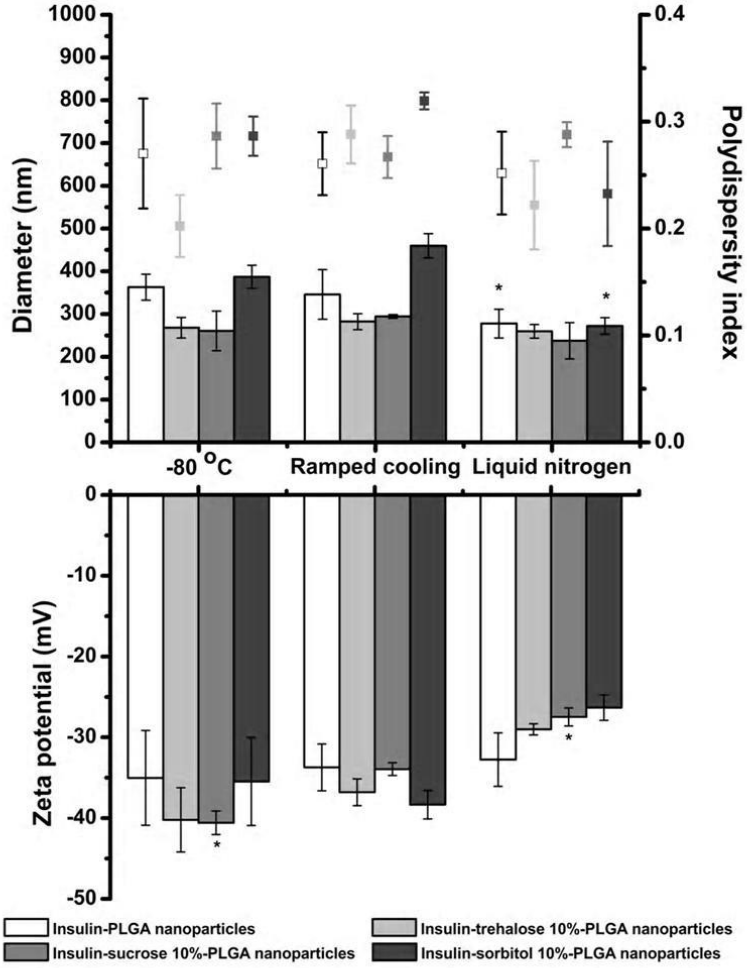

Figure 7.2. Mean particle size (top bars), PdI and zeta potential (bottom bars) characterization of insulin-loaded PLGA nanoparticles, after lyophilization at different freezing conditions (n = 3, mean ± SD). Results are significantly different (p < 0.05) from the respective formulation prior lyophilization, when marked with *.

During freezing, the crystallization of ice leads to a phase separation and nanoparticles cryoconcentration, leading to their possible aggregation or fusion. Higher supercooling as occurs during freezing in liquid nitrogen, may result in smaller ice crystals and higher surface area of ice, which decreases the mechanical stresses suffered by nanoparticles, avoiding their aggregation [185]. Such ice crystals originated by freezing in liquid nitrogen, lead to lower primary drying rates comparatively to shelf-ramped freezing. Furthermore, the intra-vial heterogeneity of ice crystals or solutes

contributes to unpredictable modifications in the sublimation rate, causing potentially unacceptable quality of products [188, 272] Thus, the multidirectional growth of ice crystals as occurs during freezing in a -80ºC freezer or in liquid nitrogen may be detrimental to nanoparticles stability. This could be the possible explanation for the differences found in particle size of nanoparticles after lyophilization using freezing in liquid nitrogen. Generally, the lower the equilibration temperature in the sample, the more heterogeneous the ice crystals are formed. With a slower freezing occurred in ramped cooling, there is more time for nanoparticles to concentrate ahead of the advancing freezing front.

The insulin retention efficiency in the formulations is depicted in Table 7.3. The occurrence of drug leakage after lyophilization may indicate modifications in the integrity of nanoparticles. Besides the results showed a very slight leakage of insulin from nanoparticles upon lyophilization, the drug retention efficiency values in the formulations were superior to about 96% in all the freezing conditions, demonstrating that the lyophilization cycles were able to preserve the integrity of nanoparticles.

3.5. Nanoparticle morphology

3.5.1. Before lyophilization

The morphology of insulin-loaded PLGA nanoparticles and the lyophilizates may be visualized by SEM, since this technique allows evaluating the size, shape and surface of nanoparticles. This information is crucial to infer the nanoparticles stability, and consequently the stability of the loaded protein. The purification of insulin-loaded PLGA nanoparticles prior to the microscopy analysis was necessary to remove the PVA, because it forms a continuous film that difficult the observation of polymeric nanoparticles by SEM [153].

The SEM microphotographs are shown in Figure 7.3, and it was noticed that the nanoparticles of all formulations were characteristically similar with a spherical shape and smooth surface, which is characteristic of the used encapsulation method. The size range of nanoparticles is also in accordance with the mean particle size characterization mentioned in section 3.1. In addition, the microphotographs also showed that the encapsulation methodology was able to co-encapsulate the cryoprotectants allowing the formation of nanoparticles, as it was also previously reported [227].

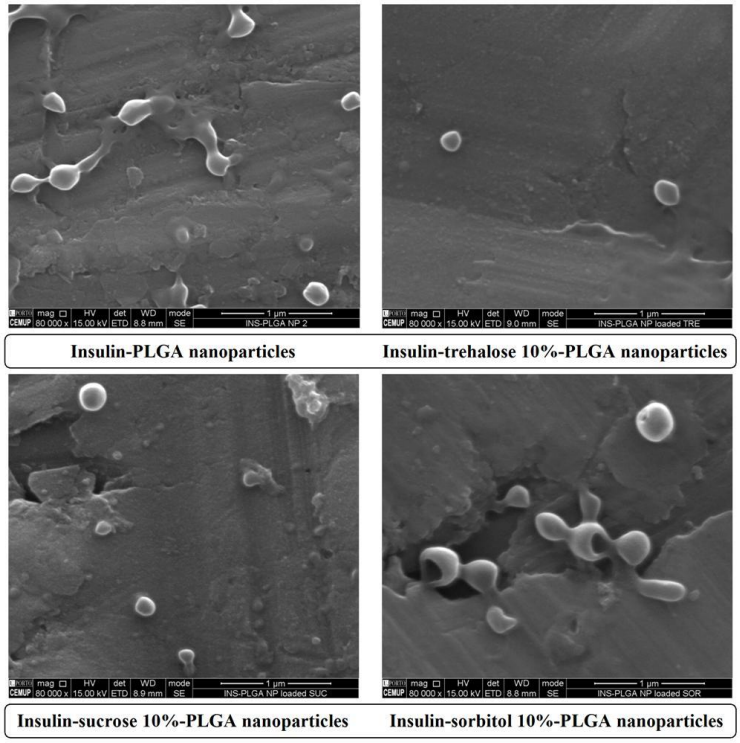

Figure 7.3. SEM microphotographs of insulin-loaded PLGA nanoparticles. Scale bar: 1 µm.

3.5.2. After lyophilization

The lyophilizates were observed by SEM, and the results are shown in Figure 7.4. Generally, the porosity and texture of the dried cake are influenced by the ice crystal growth during freezing. Regarding the freezing methods, the shelf ramped freezing is recognized to originate a high freezing rate after slow cooling, resulting in a sponge-like matrix and a small spherulitic pores [272]. On its turn, the freezing in liquid nitrogen originates a directional solidification, combined with a high freezing rate forming small lamellar-shaped pores [273]. All the lyophilizates showed a porous structure, which is important to the nanoparticles resuspension. In the lyophilizates of insulin-PLGA nanoparticles (no cryoprotectant), it was easily observable the nanoparticles with their round shape in the three freezing methods. However, in the formulations containing cryoprotectants co-encapsulated, the visualization of nanoparticles was not so clear, and instead, more tight structures were observed. This difference is due to the presence of some amount of cryoprotectants in formulation that may leak from inside and surround nanoparticles forming a protective matrix upon lyophilization. In fact, the ability of cryoprotectants to form a protective matrix has previously been reported [163], and their ability to form such a tight structures able to protect nanoparticles was also described

[175]. Some leakage of insulin and the lower zeta potential values of insulin-loaded PLGA nanoparticles co-encapsulated with cryoprotectants mentioned above, may also confirm this possibility.

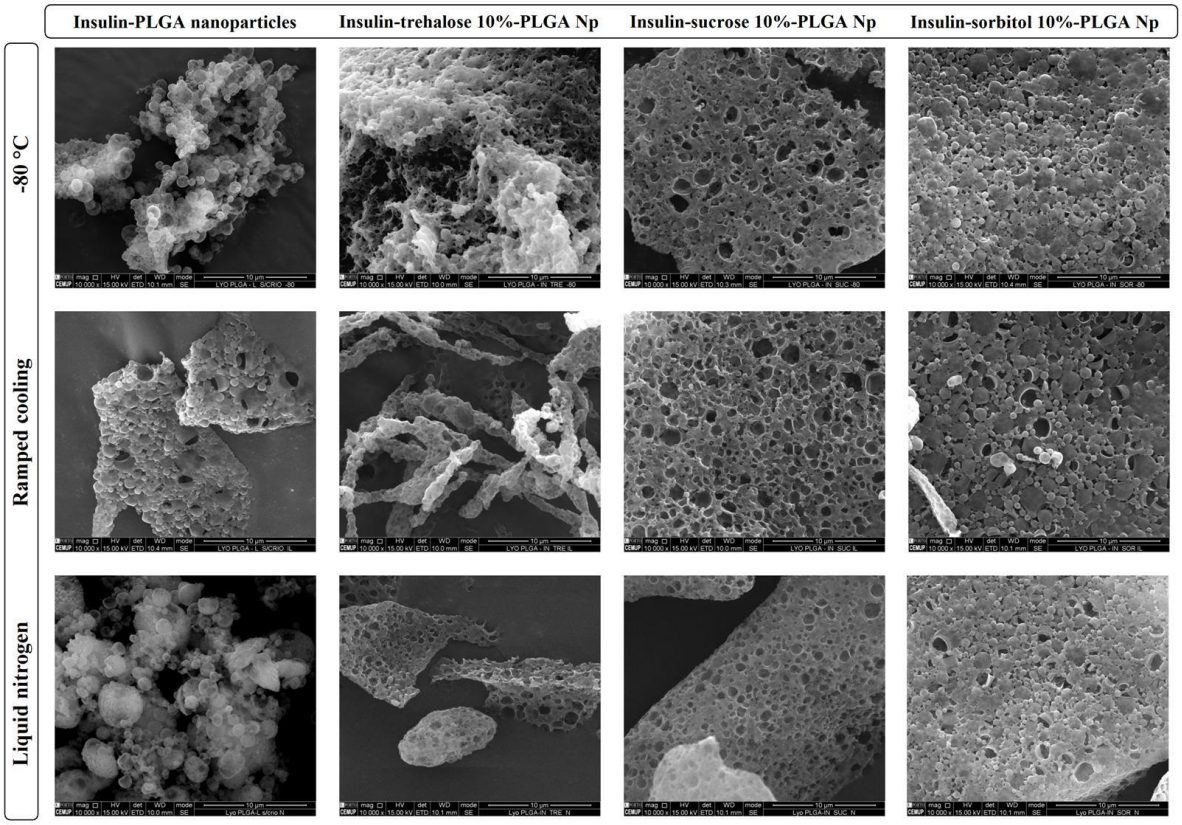

Figure 7.4. SEM microphotographs of the lyophilizates of insulin-loaded PLGA nanoparticles. Scale bar: 10 µm. Np stands for nanoparticles.

Regarding the lyophilizates of insulin-PLGA nanoparticles (no cryoprotectant) at the different freezing conditions, it was observed that those obtained using freezing at -80ºC and freezing in liquid nitrogen were similar, whereas the lyophilizate obtained using a ramped cooling presented a more tight shape. This difference may be due to a faster cooling in the first two methods originating many small ice crystals, whereas the ramped cooling originates larger ice crystals, and during the separation of ice it is also originated a more concentrated phase of nanoparticles. The same explanation applies to insulin-trehalose 10%-PLGA nanoparticles with a ramped cooling, in which the filamentary structures that were observed may be due to the presence of those nanoparticles in the interfaces of the ice formation phase and the cryoconcentrated phase containing nanoparticles. Both insulin-sucrose 10%-PLGA nanoparticles and insulin-sorbitol 10%-PLGA nanoparticles obtained very similar lyophilizates among the different freezing methods, achieving porous lyophilizates. These results demonstrated the versatility of

sucrose and sorbitol to be used in different freezing methods, achieving very similar lyophilizates.

The lyophilizates were resuspended and observed by SEM (Figure 7.5). The microphotographs showed that insulin-loaded PLGA nanoparticles maintained their spherical shape after lyophilization, and corroborated the mean particle size described in section 3.4 of this chapter. These results confirmed that the three optimized lyophilization cycles, and also the cryoprotectants used were able to preserve the features of nanoparticles upon lyophilization, which is the main purpose in nanoparticles lyophilization.

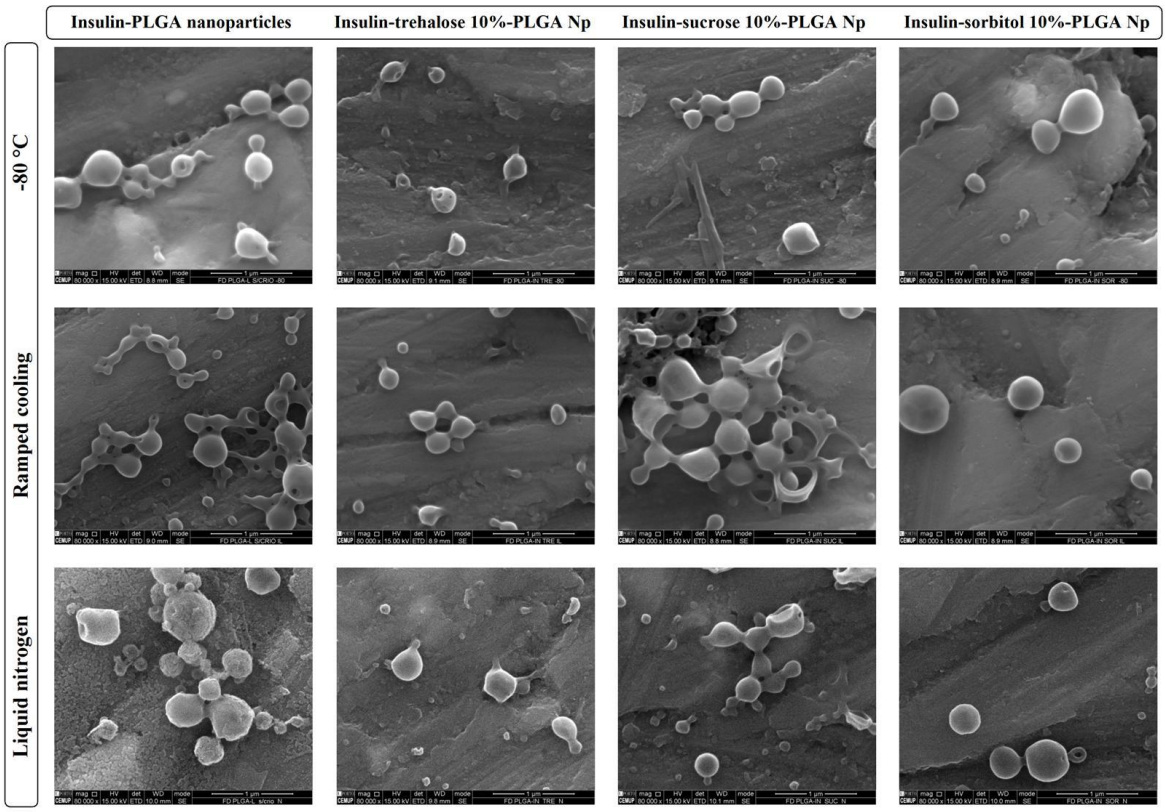

Figure 7.5. SEM microphotographs of lyophilized insulin-loaded PLGA nanoparticles after resuspension. Scale bar: 1 µm. Np stands for nanoparticles.

3.6. X-ray powder diffraction analysis

XRPD is the best technique to assess the crystalline state, and characterize possible polymorphs of solid materials such as lyophilizates. It has been reported that the crystallization of cryoprotectants during freezing, drying or even storage may prejudice nanoparticles stability [140]. Thus, both nanoparticles and cryoprotectants in amorphous state allow a better hydrogen-bonding, which is a stabilizing ability of

cryoprotectants. Regarding insulin, it was reported that upon storage this protein in the amorphous state was more stable than in the crystalline state [274]. The lyophilizates of insulin-loaded PLGA nanoparticles were assessed by XRPD, and the results are depicted in Figure 7.6. The amorphous state of a sample is elucidated in XRPD diffractograms if no clear peaks are observed. In a previous work from our group, it was showed that the PLGA polymer and insulin bulk materials, as well as a lyophilized insulin and lyophilized insulin added with cryoprotectants were amorphous [227]. It was also demonstrated that the co-encapsulation of cryoprotectants together with insulin yielded amorphous lyophilizates.

The XRPD diffractograms demonstrated that all lyophilizates were amorphous upon lyophilization, using the three different freezing methods. Just a small and not significant peak appeared in lyophilized insulin-PLGA nanoparticles frozen with liquid nitrogen. Therefore, the overall obtained results showed that the used lyophilization cycles were adequate to obtain good amorphous lyophilizates, which are necessary to have a good perspective on their storage stability.

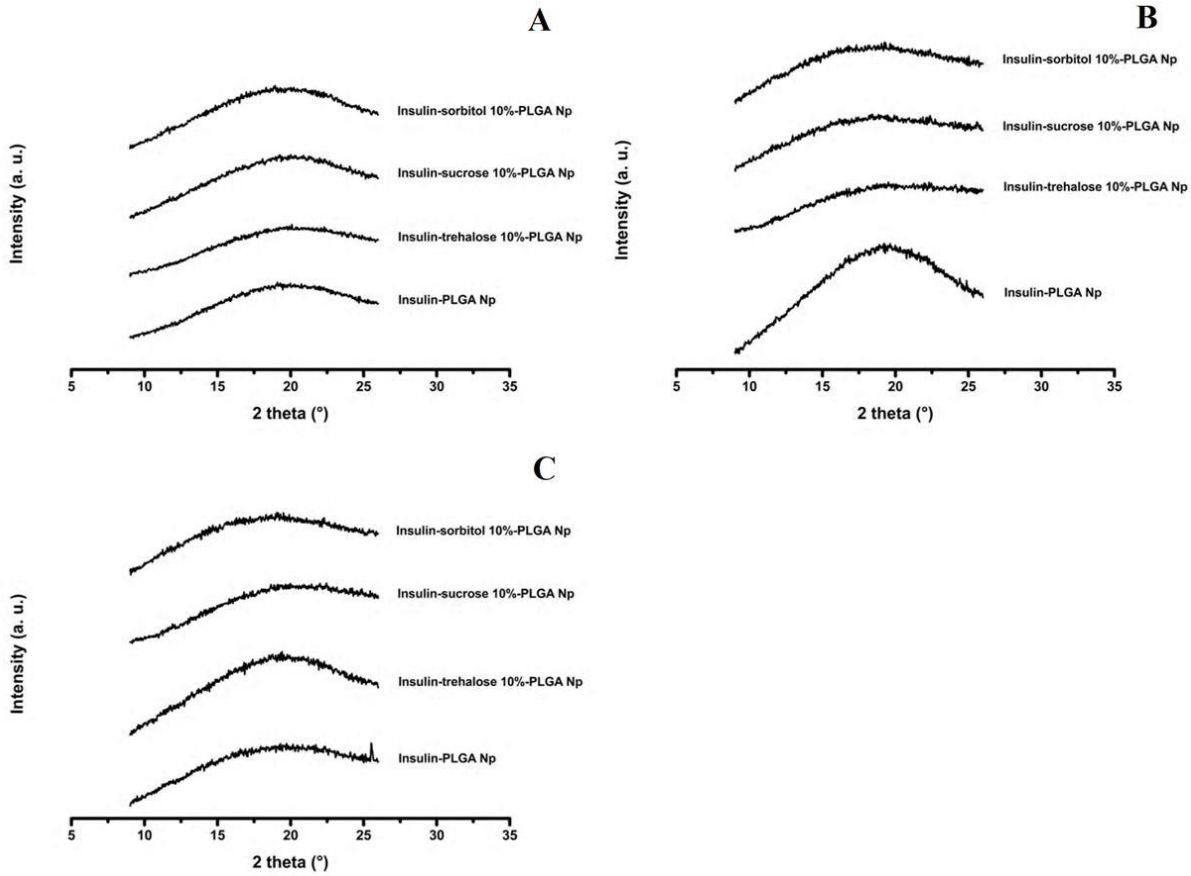

Figure 7.6. XRPD pattern of insulin-loaded PLGA nanoparticles lyophilized using freezing at -80ºC (A), ramped cooling (B) and liquid nitrogen (C). Np stands for nanoparticles.

3.7. Insulin structural integrity

3.7.1. Fourier transform infrared spectroscopy analysis

FTIR spectroscopy is a widely used technique, that may be applied in the assessment of the secondary structure of proteins loaded into nanoparticles in a non-invasive way [85]. Regarding a protein spectra, the amide I region (1710-1590 cm^{-1}) is commonly used to establish the similarity between the second derivative spectra of native and loaded proteins. Thus, the higher the similarity between them, better the maintenance of the secondary structure of the protein.

3.7.1.1. Area of overlap

The AO is a quantitative measurement of the similarity degree between the area-normalized second derivative spectra of native insulin, and insulin loaded into PLGA nanoparticles. In protein formulations, the detrimental effects on protein stability during freezing may be correlated to the used freezing method. The main aspects that can influence the stability of proteins during freezing are the cold denaturation, ice formation and freeze-concentration [270]. However, most of the significant changes in protein stability occur during ice crystallization, that originates a freeze-concentration and large liquid/ice interfaces in which proteins may adsorb and lose its native conformation due to a surface-induced denaturation [204]. Similarly, in protein-loaded nanoparticle formulations these phenomena also occur, but in the protein environment inside the nanoparticles.

The native structure of insulin was obtained by the FTIR analysis of an insulin solution 30 mg/mL, and the AO values obtained for the lyophilized PLGA nanoparticles are depicted in Figure 7.7. The results showed that upon lyophilization using freezing at -80ºC, the insulin-loaded PLGA nanoparticles co-encapsulated with cryoprotectants showed higher insulin stability ($p < 0.05$) comparatively to insulin-PLGA nanoparticles (no cryoprotectant). The AO of insulin co-encapsulated with cryoprotectants was in the range of 83-85%, comparatively to only about 74.5 ± 0.7 % of insulin-PLGA nanoparticles. Regarding the formulations lyophilized using the other two freezing methods, with just the exception of insulin-sucrose 10%-PLGA nanoparticles, the formulations containing co-encapsulated cryoprotectants did not show a clear improvement in insulin stability comparatively to insulin-PLGA nanoparticles. However, when comparing the AO values from the different freezing methods, it was noticed that

the freezing method influenced the AO of insulin loaded into PLGA nanoparticles without cryoprotectant co-encapsulated. Indeed, the AO of insulin was higher for lyophilization with ramped cooling with 89.0 ± 1.4 %, followed by the one frozen in liquid nitrogen with 79.6 ± 1.0 % and freezing at -80ºC with 74.5 ± 0.7%. These differences may be explained by the distinct formation of liquid/ice interfaces in the protein environment, originated by the different freezing methods.

The freezing methods that originate higher freezing rates as occurred in freezing at -80 and in liquid nitrogen, result in smaller ice crystals and consequently larger ice-water interfaces, leading to a higher extent of surface-induced denaturation of proteins [204]. It was described that the increase in the surface area of ice crystals originated modifications in protein structure, and also protein aggregation [275]. Thus, this may be the explanation why in those two freezing methods, the insulin stability was lower than in the ramped cooling. Similar behavior was found in a previous study in which a lower amount of insoluble aggregates of bovine IgG were found for shelf-ramped freezing, comparatively to the immersion in liquid nitrogen [276]. The same tendency was observed in a freeze-thawing study of a human growth hormone solution [277]. Different proteins also showed less turbidity in a slow freezing after freeze-thawing, comparatively to freezing in liquid nitrogen [278]. The difference of about 5% of AO between freezing at -80ºC and in liquid nitrogen may be explained by the faster freezing occurred in the latter freezing method. Indeed, it was reported that a faster freezing reduced the loss of LDH activity comparatively to slow freezing, since a faster freezing reduces the time that a protein remain in the freeze-concentrated phase in which degradation reactions occur [279].

Considering the formulations containing cryoprotectants, a positive outcome was that the co-encapsulation of cryoprotectants helped to mitigate the differences in AO observed in the formulations without cryoprotectants. In fact, it was observed very similar insulin stabilization obtaining an AO of around 80% among the different freezing methods. These results demonstrated that the presence of cryoprotectants together with insulin inside the nanoparticles was important to mitigate the different freezing stresses caused by the freezing methods. It is known that cryoprotectants are able to stabilize proteins during freezing by a preferential exclusion [280]. In fact, cryoprotectants have tendency to be excluded from the protein surface leading to a preferential hydration of the protein, and increasing the thermodynamic stability of its native state. Simultaneously, cryoprotectants can also stabilize the protein by reducing its adsorption on the ice surface occurring during freezing and also by increasing the viscosity of the freeze-concentrate [269].

It was previously reported that when using a controlled but not optimized lyophilization process, the co-encapsulation of cryoprotectants showed better protein stabilization comparatively to the conventional cryoprotectant addition method [227]. In the present work, this approach was taken further and it was observed that using optimized lyophilization cycles, the co-encapsulation of cryoprotectants may be determinant in insulin stability maintenance, when using specific freezing methods such as freezing at -80ºC. Furthermore and more importantly, the co-encapsulation of cryoprotectants allows very similar protein stabilization among the freezing methods, mitigating the different freezing stresses occurred.

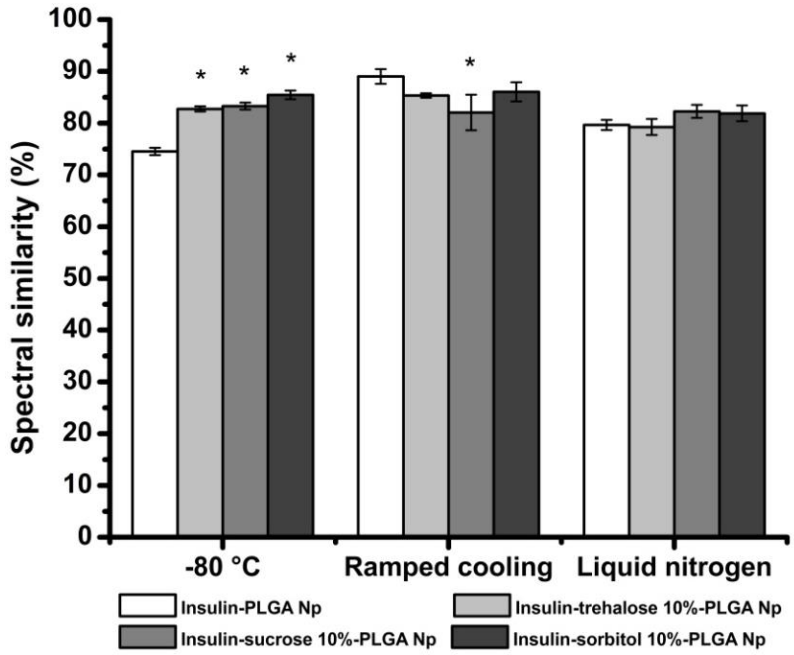

Figure 7.7. AO percentages of insulin loaded into PLGA nanoparticle formulations after lyophilization at different freezing conditions (n = 3, mean ± SD). Np stands for nanoparticles. Results are significantly different (p < 0.05) from formulation with no cryoprotectant co-encapsulated, insulin-PLGA nanoparticles, when marked with *.

3.7.1.2. Visual comparison of area-normalized second-derivative amide I spectra

The AO values represent the quantitative maintenance of the native structure of insulin, whereas the qualitative changes of insulin structure are obtained by the analysis of the area-normalized second-derivative amide I spectra depicted in Figure 7.8. Commonly, upon lyophilization the protein structure suffers a decrease in α-helix, with a simultaneous increase in the β-sheet content, and it is generally accepted that the α-helix content is a better indicator of the structural integrity of proteins [258]. The area-

normalized second-derivative FTIR spectrum of native insulin (insulin solution 30 mg/mL, Figure 7.8) corresponds to the known secondary structure of insulin that is dominated by α-helix (1658 cm^{-1}), containing also β-sheets (bands at 1640 and 1690 cm^{-1}) [85, 259, 281]. Thus, the changes of these bands occurred upon lyophilization corresponds to changes in insulin secondary structure, that may lead to protein denaturation or aggregation, affecting insulin bioactivity or even cause potential adverse effects upon administration.

Considering the freezing at -80°C, it was observed that insulin-PLGA nanoparticles (no cryoprotectant) showed a slight decrease and a shift in α-helix into 1653 cm^{-1}, presenting also a shift in its high wavenumber β-sheet content into 1684 cm^{-1}, as well as a intermolecular β-sheet formation bands at 1616/1700 cm^{-1}. These modifications showed a significant change in insulin secondary structure. On its turn, besides some differences among them, the insulin-loaded PLGA nanoparticles containing cryoprotectants co-encapsulated, demonstrated a similar structural behavior with no shift in α-helix content, a similar decrease and shift of the band of high wavenumber β-sheet content, and with no formation of intermolecular β-sheet at 1700 cm^{-1}. Regarding the α-helix content, it was found a maintenance, increase and decrease of the content of this structural feature for insulin-loaded PLGA nanoparticles co-encapsulated with trehalose, sucrose and sorbitol, respectively. These results are in agreement with those obtained in the AO values, and clearly showed the superior stability offered by the insulin-loaded PLGA nanoparticles containing cryoprotectants co-encapsulated, comparatively to the formulation containing no cryoprotectant upon lyophilization with freezing at -80ºC.

By analyzing the spectra of the formulations frozen by ramped cooling, it was possible to observe that, comparatively to the other freezing methods, the obtained spectra presented the most similarity among them. No significant shifts in α-helix were observed and just a more evident increase of this structural feature was observed for insulin-sucrose 10%-PLGA nanoparticles. The high frequency β-sheet content at 1690 cm^{-1} was very similar, with just a significant decrease in this content for insulin-trehalose 10%-PLGA nanoparticles. Regarding the insulin-PLGA nanoparticles (no cryoprotectant) it was evident a decrease in α-helix and an increase both in high and low wavenumber β-sheet. This latter increase in β-sheet content was also observed for insulin-sorbitol 10%-PLGA nanoparticles; however the α-helix of insulin was better preserved than for the formulation containing no cryoprotectant. The overall results observed for formulations frozen in a ramped cooling, showed that besides insulin-PLGA nanoparticles presented a slight higher AO, the formulations containing cryoprotectants allowed a superior maintenance of insulin secondary structure. This gives rise to the importance of

analyzing together, the quantitative and qualitative maintenance of insulin secondary structure.

Regarding the samples frozen in liquid nitrogen, it was observed some variability in the insulin spectra upon lyophilization. It was verified a similar behavior of insulin structure for insulin-PLGA nanoparticles containing no cryoprotectant as observed in freezing at -80ºC. Thus, there was also a similar decrease and shift in the α-helix band into 1653 cm^{-1}, and a shift in the high wavenumber β-sheet content into 1684 cm^{-1}, as well as an intermolecular β-sheet band formation at 1616/1700 cm^{-1}. The spectra of insulin loaded into PLGA nanoparticles containing cryoprotectants showed some variability. Insulin-trehalose 10%-PLGA nanoparticles showed an increase and shift in α-helix into 1660 cm^{-1}, together with a significant decrease in the low wavenumber β-sheet content. The insulin-sucrose 10%-PLGA nanoparticles presented no shift and no change in the intensity of the α-helix band, with just a shift and decrease in the high wavenumber β-sheet content. On its turn, the formulation containing sorbitol showed the worst performance among the cryoprotectant co-encapsulated formulations, with a significant decrease and a slight shift in the α-helix band into 1656 cm^{-1}. Considering the overall results of formulations frozen at liquid nitrogen it was observed a superior performance on insulin stabilization in insulin-loaded PLGA nanoparticles with cryoprotectants co-encapsulated, comparatively to the one containing no cryoprotectants.

Since the aggregation and denaturation of proteins are noticed by a decrease in α-helix with a simultaneous increase in β-sheet content, it was possible to infer that no clear significant denaturation or aggregation of insulin was observed. The ramped cooling was the method in which formulations presented the most similar insulin structure and maintenance. More importantly, in all the three freezing conditions the insulin-loaded PLGA nanoparticles containing cryoprotectants co-encapsulated offered better insulin stabilization upon lyophilization, comparatively to the formulation containing no cryoprotectant. In addition, and considering that α-helix is the best indicator of insulin stability, it was observed that in the three freezing methods the formulations containing trehalose and sucrose presented a better protein stabilization than those containing sorbitol.

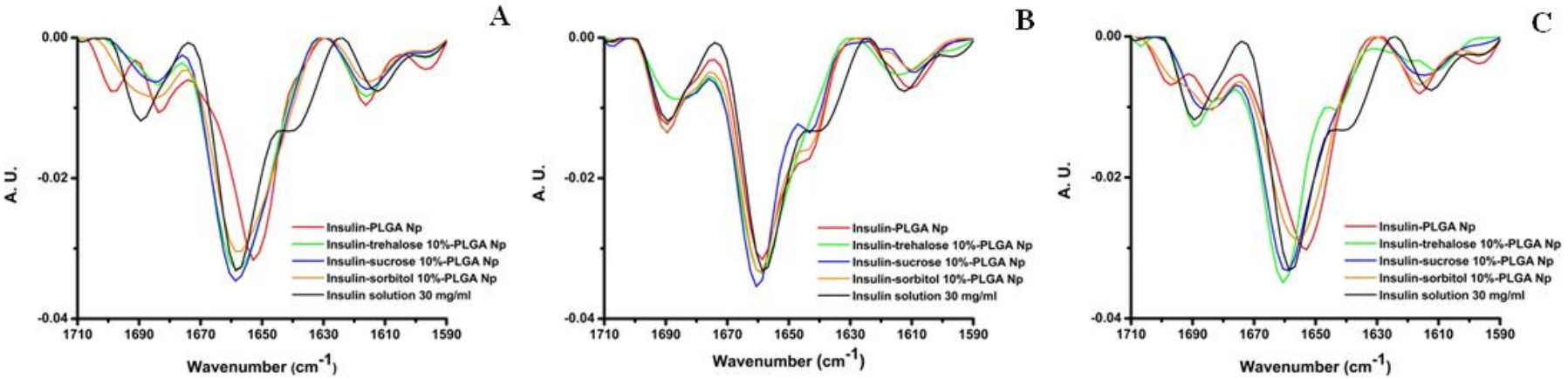

Figure 7.8. Area-normalized second-derivative amide I FTIR spectra of insulin loaded into PLGA nanoparticles lyophilized using freezing at -80ºC (A), ramped cooling (B) and liquid nitrogen (C). Np stands for nanoparticles.

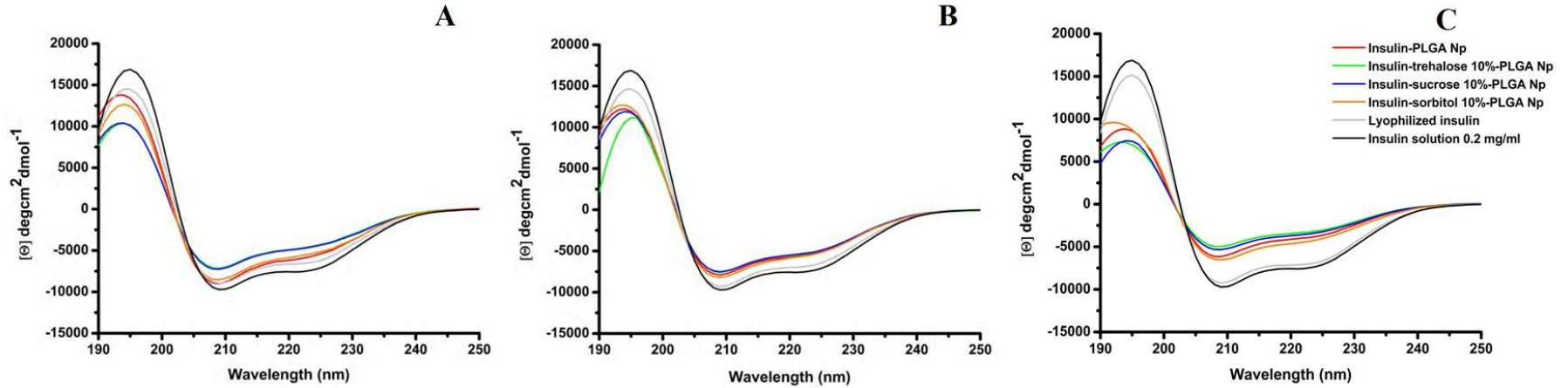

Figure 7.9. Far-UV CD spectra of insulin extracted from insulin-loaded PLGA nanoparticles lyophilized using freezing at -80ºC (A), ramped cooling (B) and liquid nitrogen (C). Insulin 0.2 mg/mL in 0.01 HCl used as reference. Np stands for nanoparticles.

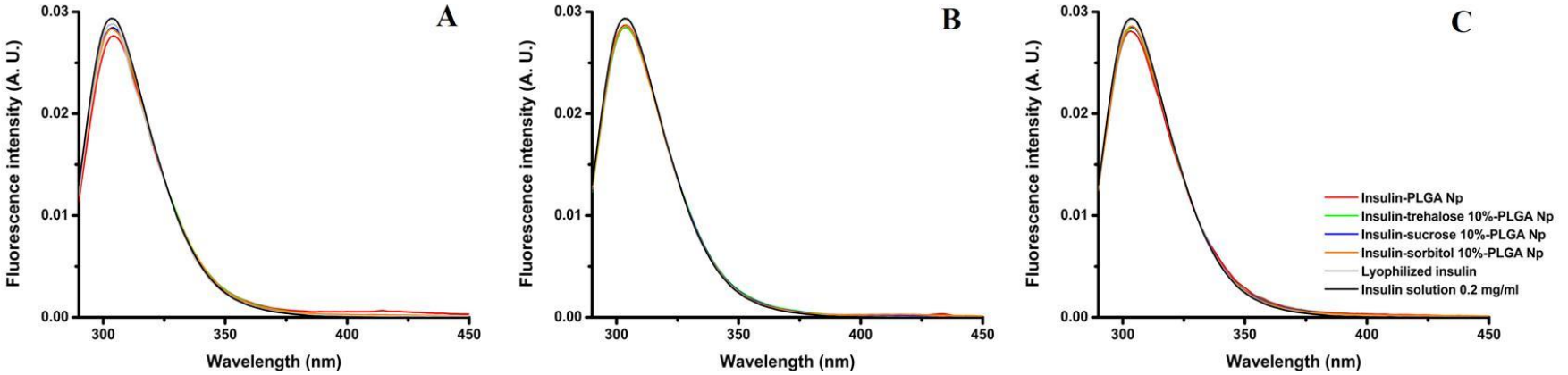

Figure 7.10. Fluorescence spectra of insulin extracted from insulin-loaded PLGA nanoparticles lyophilized using freezing at -80ºC (A), ramped cooling (B) and liquid nitrogen (C). Insulin 0.2 mg/mL in 0.01 HCl used as reference. Np stands for nanoparticles.

3.7.2. Circular dichroism experiments

CD spectroscopy was also used to assess the secondary structure of insulin, and confirm the results obtained by FTIR. To obtain the CD spectra it was necessary to extract insulin from nanoparticles, to avoid spectral artifacts due to light scattering. The obtained far-UV CD spectra are shown in Figure 7.9. The spectrum of native insulin corresponds to the spectrum of 0.2 mg/mL insulin used as reference, and it was observed two minima at about 208 nm and 222 nm, which are characteristic of the predominant α-helix structure of the protein [266]. The obtained native insulin spectrum is in accordance with that described in other research works [85, 282].

All CD spectra of insulin extracted from nanoparticles showed no relevant shifts in the two minima, demonstrating the predominant α-helical structure of insulin. The denaturation, aggregation or even fibrillation of insulin is characterized by the presence of considerable and predominant β-sheet content, represented by a minima of ellipticity at around 216 nm [143, 283]. Since this structural modification from α-helix into β-sheet was not observed, it is supposed that insulin from all formulations kept its bioactivity. Some variability in the decrease of the negative ellipticity signal of insulin was observed, which represents the modifications in the secondary structure of insulin. Since the CD characterization of insulin structure was performed in an invasive way, together with the structural modifications caused both by the encapsulation and the lyophilization processes, some variability in the CD spectra of insulin may be also explained by the extraction process of insulin from nanoparticles. Despite the concerns about the extraction process and its possible influence, the results were similar to those obtained in non-invasive way by FTIR data. For instance, the insulin-loaded PLGA nanoparticles lyophilized using a ramped cooling demonstrated the closest similarity among them, as it was observed by FTIR. Thus, it was again demonstrated that the lyophilization using this freezing method, helped to mitigate the structural modifications of insulin, comparatively to the other freezing methods.

3.7.3. Fluorescence spectroscopy

The fluorescence spectroscopy was used to assess the tertiary structure of insulin extracted from PLGA nanoparticles. Since insulin lacks tryptophan, its fluorescence depends on the four tyrosine residues [284]. Thus, the changes in the intensity of the emission spectra of intrinsic protein fluorescence are indicators of modifications in the conformation of insulin. The fluorescence spectra of insulin are

depicted in Figure 7.10. The spectrum of native insulin was obtained by the analysis of an insulin solution 0.2 mg/mL in HCl 0.01 M, and it was showed a maximum of fluorescence intensity at the wavelength of 304 nm. The insulin spectrum was in agreement with those obtained in previous works [285-287]. The overall insulin spectra showed no shift in the fluorescence intensity maxima, indicating that the overall structure of insulin was preserved. However the decrease in the intensity of fluorescence occurred in insulin from the lyophilized PLGA nanoparticles, suggested some conformational changes [288].

Regarding the spectra of insulin from formulations lyophilized using freezing at -80ºC, it was observed that insulin-PLGA nanoparticles (no cryoprotectant) showed lower fluorescence intensity comparatively to the samples containing cryoprotectants co-encapsulated. Additionally this formulation showed slight formation of a peak at around 414 nm, which may be caused by a potential tyrosine oxidation [289]. These results were in agreement with those obtained by FTIR, and showed that cryoprotectants offered superior stability to insulin upon lyophilization using freezing at -80ºC. Similar better insulin stabilization was observed for formulations containing cryoprotectants upon lyophilization using freezing at liquid nitrogen. The formulations lyophilized using ramped cooling showed the most similar insulin conformation, since the fluorescence intensity was very similar in all formulations. The overall results are in agreement with those obtained for the characterization of the secondary structure of insulin by FTIR and CD.

3.8. Thioflavin T assay

The thioflavin T is a cationic benzothiazole dye able to bind to amyloid fibrils with crossed β-sheet structures, exhibiting an enhancement of fluorescence emission at 485 nm and shift of its excitation maximum from 340 to 450 nm [290, 291]. Amyloid fibrils are a particular class of protein aggregates, so its presence in formulation means that the protein structure and consequent bioactivity is drastically compromised. Insulin may form amyloid-like fibrils caused by various stress factors, with different morphologies depending on the arrangement of its protofilaments [292, 293].The enhancement in thioflavin T fluorescence intensity shows the insulin aggregation, whereas no signal enhancement shows no aggregation of insulin [287].

All insulin samples from formulations showed no presence of thioflavin T-positive filaments, suggesting no formation of amyloid fibrils, since no enhancement on fluorescence emission at 485 nm was observed. Since all the normalized data were around zero, the data is not shown. On its turn, the positive control of fibrillated insulin showed enhanced fluorescence emission. The results showed that neither the method of

nanoparticles production nor the lyophilization processes acted as stress factors for insulin instability that could lead to its fibrillation. These results are also in agreement with the structural characterization mentioned above, since no fibrillation was evidenced by FTIR, CD and fluorescence spectroscopy.

3.9. *In vivo* bioactivity analysis of insulin-loaded formulations

The bioactivity of insulin loaded into PLGA nanoparticles was evaluated *in vivo* using a diabetic animal model. Since the formulations lyophilized using ramped cooling presented the closest structural similarity of insulin, their performance *in vivo* was evaluated. Thus, it were tested the insulin-PLGA nanoparticles (no cryoprotectant) and also one formulation with cryoprotectant co-encapsulated, insulin-trehalose 10%-PLGA nanoparticles. The latter was chosen as a representative of the formulations with cryoprotectants co-encapsulated, since it was demonstrated a close structural similarity of insulin. The insulin-loaded PLGA nanoparticles were subcutaneously administered to overnight fasted diabetic rats, and blood samples were collected at predetermined time points for glucose quantification. These formulations were administered at an insulin dose of 50 IU/kg, to have a high acceptable hypoglycemic effect. The obtained reduction of the initial glucose levels over time after subcutaneous administration of insulin-loaded PLGA nanoparticles, subcutaneous insulin and unloaded nanoparticles is shown in Figure 7.11. The baseline value of mean plasma glucose level was taken as 100%. In addition, the parameters for plasma glucose levels and relative PA are depicted in Table 7.4.

After subcutaneous administration of insulin solution (2.5 IU/kg), the glycemia decreased significantly to 30.9 ± 13.5 % after 1 hour, achieving a maximal decrease after 4 h. The formulations of insulin-loaded PLGA nanoparticles showed the minima of glucose levels at around 4-6 hours followed by an increase in glucose, but this increase was quite lower than that obtained for subcutaneous insulin, demonstrating that PLGA nanoparticles were able to prolong the hypoglycemic effect of insulin. The pattern of plasma glucose percentage for these formulations was in agreement with their *in vitro* release pattern, characterized by an initial burst release, and followed by a controlled release of insulin [227]. The initial burst release seems to be related with the increase of nanoparticles porosity upon lyophilization [101], whereas the following controlled release occurs mainly due to the erosion of the polymer matrix. Regarding the insulin-trehalose 10%-PLGA nanoparticles, it was observed that the plasma blood glucose percentage was significantly higher ($p < 0.05$) than that obtained by subcutaneous insulin in the first 2 hours, which was naturally explained by the faster availability of insulin into the

bloodstream provided by the subcutaneous insulin. On contrary, from 6 to 24 hours the plasma glucose percentage was significantly lower ($p < 0.05$) than that obtained by subcutaneous insulin, which is clearly caused by the sustained release of insulin from PLGA nanoparticles, prolonging its hypoglycemic effect.

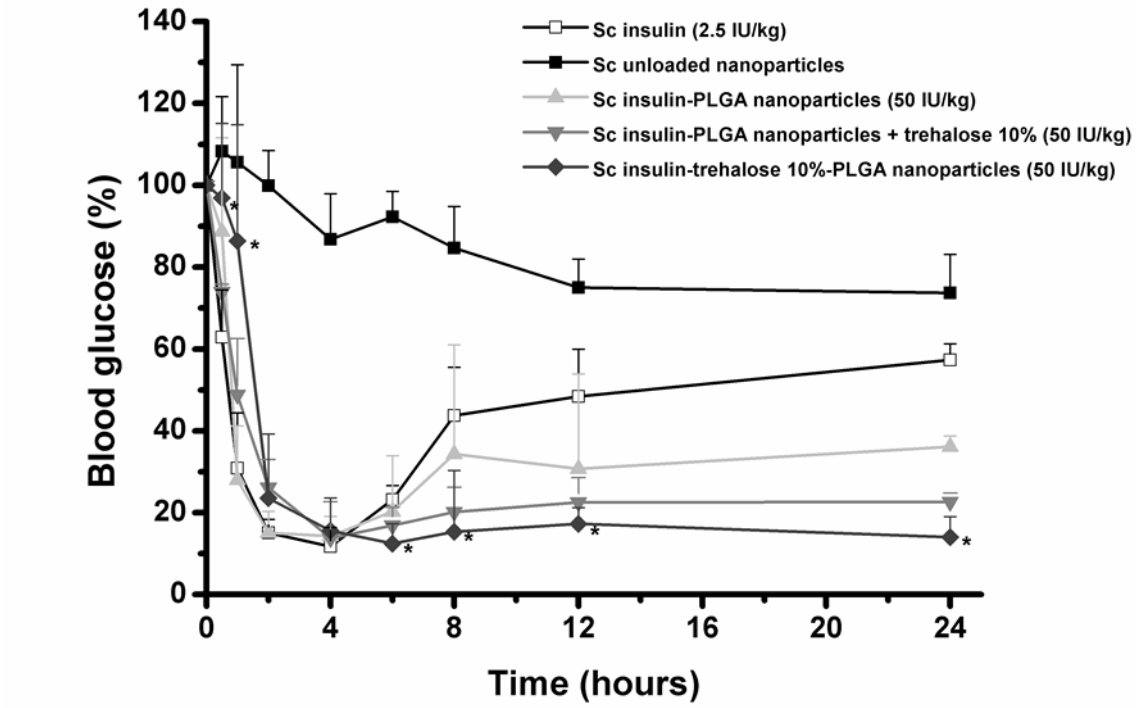

Figure 7.11. Plasma glucose levels in diabetic rats over time as percentage of initial levels, after subcutaneous administration of an insulin solution (2.5 IU/kg), unloaded nanoparticles, insulin-PLGA nanoparticles (50 IU/kg), insulin-PLGA nanoparticles + trehalose 10% (50 IU/kg) and insulin-trehalose 10%-PLGA nanoparticles (50 IU/kg). Data represent the mean ± SD, n = 5/group. Results are significantly different ($p < 0.05$) from subcutaneous insulin when marked with *. Sc stands for subcutaneous.

As a control sample it was also administered to rats a formulation of insulin-PLGA nanoparticles added with trehalose at 10% (w/w) prior lyophilization using ramped cooling (insulin-PLGA nanoparticles + trehalose 10%). The formulation with co-encapsulated trehalose showed an enhanced hypoglycemic effect comparatively to the other insulin-loaded PLGA nanoparticles, caused by both a higher release rate [227], and superior insulin stabilization and bioactivity. The PA results (Table 7.4) also corroborate the superior hypoglycemic effect provided by insulin-loaded PLGA nanoparticles co-encapsulated with cryoprotectant.

Table 7.4. Parameters for plasma glucose levels and relative pharmacological availability percentage. Data represent the mean ± SD, *n* = 5/group.

	Subcutaneous insulin	**Insulin-PLGA nanoparticles**	**Insulin-PLGA nanoparticles + trehalose 10%**	**Insulin-trehalose 10%-PLGA nanoparticles**
Insulin dose (IU/kg)	2.5	50	50	50
Cmin (%)	11.7 ± 4.7	14.3 ± 4.9	13.8 ± 8.9	12.4 ± 4.9
Tmin (h)	4	4	4	6
PA (%)	-	6.1 ± 1.2	6.7 ± 0.8	7.0 ± 0.6

4. Conclusion

In this chapter, it was evaluated the influence of the freezing step of lyophilization in the structure of a therapeutic protein, insulin, loaded into PLGA nanoparticles. In addition, it was assessed the performance of different co-encapsulated cryoprotectants, in the protection of insulin-loaded PLGA nanoparticles upon lyophilization.

The overall results regarding the mean particle size, zeta potential and insulin retention efficiency, besides some differences, demonstrated that the features of insulin-loaded PLGA nanoparticles were preserved upon the optimized lyophilization cycles. The lyophilizates of insulin-loaded nanoparticles with cryoprotectants co-encapsulated, presented a more tight structure comparatively to nanoparticles containing no cryoprotectants, forming a protective matrix that could be important to protect both nanoparticles and the loaded protein. In addition, all lyophilization cycles produced amorphous lyophilizates, which resulted in a good perspective for the storage stability of nanoparticles.

Regarding the structure of insulin loaded into PLGA nanoparticles, it was verified that in absence of cryoprotectants, the insulin structure presented some variability depending on the freezing method, and it was the ramped cooling that presented the higher structural maintenance of insulin. Such structural loss of native conformation was mitigated when cryoprotectants were co-encapsulated, demonstrating that their presence in formulation reduced the different freezing stresses and better preserved the structure of insulin upon lyophilization, comparatively to formulations containing no cryoprotectant. It was also in the ramped cooling at -40ºC that formulations both with and without cryoprotectants co-encapsulated, presented the most insulin structural similarity and maintenance. In addition, in the three freezing methods, the formulations containing trehalose and sucrose presented better protein stabilization than those containing

sorbitol. Furthermore, it was found that neither the encapsulation process nor the lyophilization cycles acted as stress factors for insulin-loaded PLGA nanoparticles that could lead to insulin fibrillation.

The *in vivo* bioactivity experiments found that the insulin-loaded PLGA nanoparticles were able to prolong the hypoglycemic effect of insulin, comparatively to the subcutaneously administered insulin. Such hypoglycemic effect was even enhanced by the formulation with cryoprotectant co-encapsulated, in comparison with the other insulin-loaded PLGA nanoparticles, essentially caused by the superior insulin stabilization and bioactivity.

Overall, this chapter gave rise to the importance of optimizing the lyophilization process in order to obtain a good lyophilized product. It was also clearly demonstrated that the freezing process used in lyophilization, may have a detrimental effect in the structure of the protein loaded into nanoparticles. This could be avoided by the use of cryoprotectants co-encapsulated that better preserve insulin structure and bioactivity upon lyophilization.

Chapter 8

Optimization of Lyophilization Cycle Using Annealing and its Effect on the Stability of Protein-loaded PLGA Nanoparticles

To be partially published as:

Pedro Fonte, Paulo R. Lino, Vítor Seabra, António Almeida, Salette Reis, Bruno Sarmento, Annealing as a tool for the optimization of lyophilization and ensuring of the stability of protein-loaded PLGA nanoparticles. *Submitted for publication.*

1. Introduction

The freezing step is considered the most important one in lyophilization, since it influences the size of ice crystals and consequently the duration of the drying steps [188]. Generally, the optimization of the lyophilization cycle is mainly focused on decreasing the time needed for the primary drying, which is the longest step in lyophilization. The shelf temperature and chamber pressure are the main lyophilization parameters that may improve the sublimation rate. However, if they are not properly adjusted it may lead to undesired product overheating and collapse.

The annealing is a processing step in lyophilization in which samples are kept at a determined subfreezing temperature above the Tg', during a period of time [190]. This process influences the size distribution of ice crystals, leading to their growth. Their size distribution during annealing is ruled by Ostwald ripening, which states that crystals smaller than a critical size decrease, whereas the larger ones grow [190]. Therefore, the increase of the size of ice crystals during annealing may accelerate the sublimation rate by increasing the diameter of pores, in spaces that were previously occupied by ice crystals, and by a decrease of the mass transfer resistance by the dried layer [191]. The annealing may also decrease the heterogeneity of the drying rate between samples, in order to obtain a more inter-vial homogeneous cake structure [163, 294]. Overall, annealing may be a useful tool to obtain a dried cake with good quality in a shorter period of time.

The annealing step has been applied in the lyophilization of protein formulations. In a rhIFN-ɣ formulation, the application of an annealing step avoided the cracking of the cakes, originated more native-like secondary structure of protein in the solid product and prevented the aggregation of the protein upon reconstitution [273]. Regarding nanoparticle formulations, just a few works have been focusing on the influence of annealing in the stability of nanoparticles [153, 191, 192]. It was demonstrated that annealing accelerated the sublimation, with simultaneous maintenance of size of polymeric nanoparticles [153]. However, the influence of annealing in the structure and stability of loaded proteins has not been studied so far. The possible modification of the structure of loaded proteins during annealing needs to be properly regarded, since it has been demonstrated that the freezing step in lyophilization influences the structure of proteins loaded into nanoparticles [295].

The main aim of this study was to develop an optimized lyophilization cycle using annealing, in order to decrease the time needed to lyophilize protein-loaded polymeric nanoparticles, assuring simultaneously the stability of nanoparticles and the structural

maintenance of the loaded protein. Additionally, it was assessed the influence of the cryoprotectant effect during annealing, in the stability of nanoparticles and with upmost importance, in the stability of the encapsulated protein upon lyophilization.

2. Materials and Methods

2.1. Materials

PLGA 50:50 Resomer® RG 503 H (Mw 24,000-38,000; Tg 44-48 ºC) from Evonik Industries AG (Essen, Germany) was used for nanoparticles production. PVA, dichloromethane, recombinant human insulin and trehalose were from Sigma-Aldrich (Steinheim, Germany). For the HPLC analysis, it was used acetonitrile HPLC Gradient Grade from Fischer Scientific (Loughborough, UK) and trifluoroacetic acid from Acros Organics (Morris Plains, NJ, USA). Chloroform from Sigma-Aldrich (Steinheim, Germany) was used for protein extraction from nanoparticles. The milli-Q water was produced in-house and other reagents were of analytical grade.

2.2. Preparation of PLGA nanoparticles

The PLGA nanoparticles were produced following a previously developed and optimized protocol to co-encapsulate insulin and trehalose into PLGA nanoparticles [227]. Thus, 200 mg of PLGA 50:50 were dissolved in 2 mL of dichloromethane, and then added with 0.2 mL of a 150 mg/mL insulin solution in HCl 0.1 M containing trehalose at a concentration of 10% (w/v). The primary emulsion was obtained by sonication at 70% of amplitude for 30 seconds, using a Bioblock vibracell 75186 sonicator from Fischer Bioblock Scientific (Rungis Complexe, France). The emulsion was then poured into 25 mL of PVA 2% (w/v) at pH 7.4, and sonicated again using the same previous conditions. The organic solvent was removed by evaporation for 3 h under magnetic stirring. The production method was also used to formulate both nanoparticles without co-encapsulated cryoprotectant and unloaded nanoparticles. After production, nanoparticles were washed three times with milli-Q water, and collected after each washing step by centrifugation for 30 minutes at 23,000 x *g* using a Heraeus Megafuge 1.0 R centrifuge (Thermo Scientific). Finally, nanoparticles were redispersed in water.

2.3. Insulin association efficiency, loading capacity and retention efficiency

The AE was calculated using the equation 4.1 (*see* Chapter 4) and LC of insulin was calculated using equation 6.1 (*see* Chapter 6). The nanoparticles suspension was centrifuged at 40,000 x *g* at 4ºC for 30 min in a Beckman Optima TL ultracentrifuge from Beckman Coulter (Brea, CA, USA.), and it was collected the supernatant containing free insulin. Centrifuged nanoparticles were lyophilized to obtain the dry mass of nanoparticles. Upon reconstitution of lyophilized nanoparticles, the suspension was centrifuged and the supernatant was collected for insulin quantification and determination of insulin retention efficiency. The insulin free in supernatant was quantified by a HPLC-UV method previously validated [233], in a Merck-Hitachi LaChrom HPLC instrument equipped with a LiChrospher 100 RP-18 guard column, 5 µm particle size from Merck (Whitehouse Station, NJ, U.S.A.) and also a XTerra RP 18 column, 5 µm particle size, 4.6 mm internal diameter x 250 mm length from Waters (Milford, MA, U.S.A.). All the samples were run in triplicate.

2.4. Particle size and zeta potential analysis

To perform the analysis of mean particle size, PdI and zeta potential, the nanoparticles in suspension and reconstituted after lyophilization were diluted with milli-Q water to achieve a suitable concentration. These analyses were performed by dynamic light scattering using a 90Plus Particle Size Analyser, and by phase analysis light scattering using a ZetaPALS Zeta Potential Analyser, from Brookhaven Instruments Corporation (Holstville, NY, USA). The lyophilization ratio was calculated as the ratio between the mean particle size after lyophilization, and that before lyophilization.

2.5. Lyophilization of nanoparticles

The insulin-loaded PLGA nanoparticles suspensions were poured into semi-stoppered glass vials at a maximal height of 10 nm, and lyophilized in a VirTis Advantage Plus Benchtop lyophilizer from SP Scientific (Warminster, PA, USA). Thus, samples were frozen by ramped cooling at -40ºC during 4 hours, and primary drying occurred at -32ºC and 150 mtorr for 24 h, followed by a secondary drying at 20ºC and 50 mtorr for 6 h, at a condenser surface temperature of -60ºC (n = 3). When the thermal treatment of annealing was included in the lyophilization cycle, the nanoparticle formulations were frozen by ramped cooling at -40ºC and the temperature was raised to

the annealing temperature of -10ºC and held for 2 h. Then, samples were cooled to -40ºC and held for another 2 h. The primary drying occurred at -32ºC and 150 mtorr for 15 h, followed by a secondary drying at 20ºC and 50 mtorr for 6 h, at a condenser surface temperature of -60ºC (*n* = 3).

2.6. Macroscopic evaluation, residual moisture content and reconstitution of the lyophilizates

The lyophilizates were visually inspected to assess the aspect of the cake, and the residual moisture content was evaluated using an A&D MX-50 moisture analyzer from A&D Company Ltd. (Tokyo, Japan). Thus, an equal amount of lyophilizate of each formulation was analysed, and the residual moisture content was quantified as percentage of containing moisture. The lyophilizates were reconstituted by adding milli-Q water on the inside wall of the vials to guarantee the cake wetting. Finally, formulations were swirled until complete homogenization.

2.7. Scanning electron microscopy analysis

The insulin-loaded PLGA nanoparticles morphology was evaluated by SEM, using a FEI Quanta 400 FEG scanning electron microscope from FEI (Hillsboro, Oregon, USA). Both nanoparticle suspensions and lyophilizates were mounted on metal stubs, and coated under vacuum with a layer of gold/palladium with a 15 mA current for 60 seconds prior to observation.

2.8. Attenuated Total Reflectance-Fourier transform infrared spectroscopy analysis

The secondary structure of insulin loaded into PLGA nanoparticles was assessed by ATR-FTIR. The samples were analysed in an ABB MB3000 FTIR spectrometer from ABB (Zurich, Switzerland) equipped with a MIRacle triple reflection ATR accessory from PIKE Technologies (Madison, WI, USA). The FTIR spectra were collected in the 4000−600 cm^{-1} region after 256 scans at a 4 cm^{-1} resolution. The insulin spectra were obtained by a double subtraction method [243], followed by a Savitzky-Golay second derivative of 15 points, and a 3-4 point baseline correction in the amide I region (1710−1590 cm^{-1}). This spectral treatment was performed using the Horizon MB FTIR software from ABB, and all the spectra were area-normalized for further comparison. The AO algorithm was used to assess the quantitative similarity of the area normalized

second-derivative amide I spectra between native insulin and insulin loaded into PLGA nanoparticles [244]. A 30 mg/ml insulin solution in HCl 0.1 M was analysed and used as the native insulin spectrum to determine the percentage of spectral similarity, since it is considered that the stability of a solid protein formulation increases with the increase of the similarity to its spectra in solution [246].

2.9. Circular dichroism analysis

Insulin was extracted from the PLGA nanoparticles using chloroform and HCl 0.01 M to dissolve insulin, prior to the CD analysis. All samples were analysed at 25ºC with the lamp housing continuously purged with nitrogen, in a Jasco J-815 CD Spectrometer from Jasco Inc. (Easton, MD, USA). The CD spectra were obtained using a 0.1 cm cell in the range of 190 to 250 nm with an average of 5 scans, with a step size of 0.5 nm, a bandwith of 1.5 nm, and an averaging time of 5 s. The spectrum of reference sample was subtracted from the test sample spectra. The molar ellipticity of insulin was calculated as CD signal x MRW (mean residual weight of each insulin residue, 116 Da) [insulin concentration (mg/mL) x cell pathlength (0.1 cm)]. The insulin concentration was determined by UV absorption at 280 nm in a NanoDrop 2000c UV-Vis Spectrophotometer (Thermo Scientific, Wilmington, DE, USA), using a molar extinction coefficient of 6200 $M^{-1}cm^{-1}$ for 1.0 mg/mL. As control sample of native insulin, it was used a 0.2 mg/mL insulin solution in HCl 0.01 M.

2.10. Fluorescence spectroscopy analysis

Insulin was extracted from the PLGA nanoparticles using chloroform and HCl 0.01 M to dissolve insulin, prior to the fluorescence spectroscopy analysis. The emission spectra were obtained at 25ºC in the range of 290 to 450 nm with 1 nm step in a Jasco FP-6500 Spectrofluorometer from Jasco Inc. (Easton, MD, USA). The excitation occurred at 280 nm with both emission and excitation slits set to 3 nm, with an integration time per data point of 0.1 seconds and an average of 5 scans. The spectrum of reference sample was subtracted from the sample spectra, and normalized based on insulin concentration. As control sample of native insulin, it was used a 0.2 mg/mL insulin solution in HCl 0.01 M.

2.11. Thioflavin T assay

The samples of extracted insulin were incubated with Thioflavin T and analyzed in a Jasco FP-6500 Spectrofluorometer from Jasco Inc. (Easton, MD, USA) at 25ºC and the final concentration of insulin and thioflavin T were 11 µM and 25 µM, respectively. They were excited at 450 nm, and the fluorescence intensity was determined at 485 nm with slit widths of 5 nm. The reference sample spectrum was subtracted from the test sample spectra. As a positive control it was used insulin fibrillated by incubation at 60ºC during 12 hours.

2.12. Statistical analysis

The statistical analyses were performed in the OriginPro 8 software from OriginLab Corporation (Northampton, MA, USA), using a one-way ANOVA Tukey *post hoc* test, with a significance level of $p < 0.05$.

3. Results and discussion

It is generraly accepted that the annealing process influences the sublimation rate and the quality of the lyophilized protein drug product. However, its impact on the stability of the protein loaded into nanoparticles was not investigated so far. In addition, the influence of the cryoprotectant effect in the stabilization of the loaded protein upon lyophilization using annealing needs to be scrutinized.

Insulin was used as a model of therapeutic protein, and was co-encapsulated into PLGA nanoparticles together with a cryoprotectant, since this approach demonstrated to better preserve the protein structure upon lyophilization, comparatively to the conventional cryoprotectant addition method [227]. In this study, trehalose was used as cryoprotectant, because it demonstrated to be a versatile cryoprotectant to stabilize protein-loaded nanoparticles upon lyophilization using different freezing methods [295]. Trehalose was used at a concentration of 10% (w/v) to obtain the highest acceptable cryoprotectant effect, since the level of stabilization provided depends on its concentration [7]. To characterize the influence of annealing in the lyophilized formulations, the properties of nanoparticles and the lyophilizates were assessed, and was evaluated the structural maintenance of the loaded protein.

3.1. Particle size, zeta potential, association efficiency and loading capacity analyses

Insulin-loaded nanoparticles co-encapsulated with trehalose (insulin-trehalose 10%-PLGA nanoparticles) and without cryoprotectant encapsulated (insulin-PLGA nanoparticles) were produced to allow the comparison and assessment of the stabilization effect provided by the cryoprotectant.

The mean particle size, PdI and zeta potential characterization of insulin-loaded PLGA nanoparticles is shown in Table 8.1. Both formulations presented a close particle size in the range of about 250-300 nm and a low PdI, demonstrating the robustness of the encapsulation protocol [295]. Considering the zeta potential analysis, it was observed that nanoparticles had a negative surface charge, characteristic of the acidic PLGA polymer [147]. The zeta potential of insulin-trehalose 10%-PLGA nanoparticles was even slightly lower, which indicated a potential better colloidal stability of these nanoparticles, comparatively to insulin-PLGA nanoparticles.

Table 8.1. Mean particle size, polydispersity index, zeta potential, and insulin AE and LC characterization of insulin-loaded PLGA nanoparticles (*n* = 3, mean ± SD).

Formulation	Mean particle size (nm)	PdI	Zeta potential (mV)	AE (%)	LC (%)
Insulin-PLGA nanoparticles	294 ± 15	0.26 ± 0.02	-20.4 ± 2.5	92.6 ± 0.7	12.1 ± 0.6
Insulin-trehalose 10%-PLGA nanoparticles	249 ± 14	0.23 ± 0.08	-23.8 ± 2.5	90.5 ± 0.5	11.2 ± 0.4

The insulin AE and LC of formulations are also depicted in Table 8.1. Both formulations presented an AE higher than 90%, which was a good achievement considering the hydrophilic nature of insulin and the hydrophobic nature of nanoparticles polymer. The AE and LC results were similar with those obtained in previous works [227, 295], which demonstrated once again the robustness of the encapsulation protocol, and its ability to co-encapsulate the cryoprotectant together with the protein.

3.2. Design of the lyophilization cycle

The lyophilization cycle needs to be designed considering the engineering principles of the process and the physical-chemical properties of nanoparticles, to obtain a lyophilizate with high quality and to properly preserve the nanoparticles features [7, 140, 153]. The knowledge of physical-chemical properties of formulations, such as the Tg' and Tc, is necessary to design an optimal lyophilization cycle [163, 193]. In a previous chapter, these parameters of formulations were characterized in order to design an optimal lyophilization cycle that was also used in the present work [295]. This cycle was the basis to design another one including an annealing step.

To assess the effect of annealing in the formulations and simultaneously decrease the time of primary drying, an annealing step of 2 h at -10ºC was included in the freezing stage that kept its duration time of 4 h, and the duration of primary drying was shorten from 24 h to 15 h. This modification represented a decrease of the primary drying duration of about 38%, and the reduction of the duration of the lyophilization cycle of about 26%. Previously, annealing was applied in the lyophilization of polymeric nanoparticles, and it was observed that the sublimation rate was increased when the annealing temperature was well above the Tg' of the formulation [191]. It has been also reported that when annealing occurred below the Tg', the sublimation rate was not increased [190]. Therefore, it was used the temperature of annealing of -10ºC for being well above the Tg' of the formulations. When this occurs, the ice melts and the smaller ice crystals melt faster than the larger ones. The size distribution of ice crystals during annealing is ruled by the Ostwald ripening, in which the crystals smaller than a critical size decrease, whereas those larger than that critical size increase in size [185]

Overall, it is recognized that the morphology of ice crystals is directly related with the sublimation rate [185]. Since annealing promotes the growth of ice crystals and increases the sublimation rate due to the increase of pore size of the product, it was used this approach to decrease the duration of primary drying, which is the longest step in lyophilization. This possibility it is only feasible, if both the nanoparticles features and the stability of loaded protein are preserved upon lyophilization.

3.3. Visual inspection, reconstitution and residual moisture content of the lyophilizates

The lyophilizates obtained from nanoparticles lyophilization with and without annealing were inspected, and they presented a cotton-like texture and white colour. The

lyophilizates occupied the same volume of the original frozen mass and no shrinkage or cake collapse were observed, which demonstrated that particularly the lyophilization with an annealing step allowed obtaining good lyophilizates. The cake collapse is a problem to avoid, because it originates prolonged reconstitution times and high residual moisture content [168, 173]. All the lyophilizates were easily reconstituted obtaining suspensions with no visual aggregates. The complete reconstitution of the lyophilizates of formulations lyophilized with annealing was even in average about 10 seconds faster, than those lyophilized with no annealing. This property may be explained by the larger pores of the lyophilizates that were previously occupied by larger ice crystals formed during annealing [191]. Such pores allowed a faster reconstitution of the lyophilizates obtained by lyophilization with annealing.

The residual moisture content of the lyophilizates is depicted in Table 8.2. The nanoparticles lyophilized using annealing obtained a similar residual moisture content of those lyophilized without annealing, around 1%, which demonstrated that annealing allowed the decrease of the primary drying time in about 38%, without increasing the residual moisture content. These results showed that the lyophilization process was effective on removing the water from formulations, since they need to have very low residual moisture content, which for pharmaceutical products should be around 1% [150]. This result is also explained by the faster sublimation rate promoted by the porous structure of annealed formulations. Another possible explanation for a faster sublimation rate that allowed a decrease in the duration time of primary drying, without compromising the low residual moisture content of the lyophilizates, was the ability of annealing to eliminate the thin skin layer on the top surface of the cake [296]. Such thin layer occurs due to the migration of nanoparticles and cryoprotectant during ice crystallization, hampering the water removal from the product.

3.4. Particle size, zeta potential and drug retention efficiency after lyophilization

After resuspension of the lyophilizates, the nanoparticle suspensions were characterized in terms of mean particle size, PdI and zeta potential and the results are depicted in Table 8.2. The overall mean particle size of nanoparticles after lyophilization were similar with that after nanoparticles production, with just the exception for insulin-PLGA nanoparticles lyophilized with annealing that presented a significant size modification ($p < 0.05$). This result showed the importance of the presence of co-encapsulated trehalose, acting as cryoprotectant, when annealing was used. The potential residual leakage of trehalose from nanoparticles may protect them in a localized manner, by forming a protective matrix around nanoparticles [163, 295]. The

lyophilization ratio is also shown in Table 8.2. This ratio was obtained by dividing the mean particle size of nanoparticles after with that before lyophilization. Thus, a value around 1 demonstrates that the mean particle size of nanoparticles was maintained after lyophilization. The lyophilization ratio of nanoparticles were around 1 demonstrating that the lyophilization process used did not led to significant particle aggregation or fusion. When using annealing in the lyophilization of nanoparticle suspensions, the main problem is the mechanical stress of ice crystals that may lead to nanoparticles aggregation or fusion, since this effect on nanoparticles stability is more accentuated for larger ice crystals than for smaller ones [185, 191, 295]. Therefore, the mean particle size and lyophilization ratio results clearly showed that the nanoparticles stability was maintained upon lyophilization using annealing. The PdI of nanoparticles were similar after lyophilization, also demonstrating the low heterogeneity of nanoparticles size and the absence of significant particle aggregation.

Table 8.2. Lyophilization ratio, insulin retention efficiency, residual moisture content, mean particle size, PdI and zeta potential characterization of insulin-loaded PLGA nanoparticles after lyophilization with and without annealing (n = 3, mean ± SD). Results are significantly different (p < 0.05) from the respective formulation prior lyophilization, when marked with *.

Formulation	Mean particle size (nm)	PdI	Zeta potential (mV)	Lyophilization ratio	Insulin retention efficiency (%)	Residual moisture content (%)
No annealing						
Insulin-PLGA nanoparticles	280 ± 10	0.26 ± 0.01	-29.2 ± 3.5*	0.95 ± 0.07	99.1 ± 0.4	1.33 ± 0.41
Insulin-trehalose 10%-PLGA nanoparticles	245 ± 18	0.25 ± 0.02	-31.6 ± 2.5*	0.98 ± 0.08	99.0 ± 0.5	1.45 ± 0.35
Annealing						
Insulin-PLGA nanoparticles	270 ± 4*	0.21 ± 0.01	-33.1 ± 1.8*	0.91 ± 0.04	98.5 ± 0.9	1.55 ± 0.27
Insulin-trehalose 10%-PLGA nanoparticles	250 ± 23	0.26 ± 0.07	-30.8 ± 1.5*	1.00 ± 0.09	98.7 ± 0.4	1.48 ± 0.37

Regarding the zeta potential, it was observed a significant decrease (p < 0.05) of the surface charge of nanoparticles upon lyophilization, leading to a better colloidal

stability of nanoparticles. The drug leakage during lyophilization may occur due to possible modifications of nanoparticles integrity. Therefore, it was evaluated the insulin retention efficiency in nanoparticles after lyophilization, which is shown in Table 8.2. The leakage of insulin from nanoparticles during lyophilization was negligent, demonstrating that the integrity of nanoparticles was preserved after lyophilization. These results also showed the annealing did not induced stresses to nanoparticles that could damage them and lead to insulin leakage.

3.5. Morphology of nanoparticles

3.5.1. Prior lyophilization

The morphology of nanoparticles and lyophilizates were assessed by SEM to assess the shape, surface and size of nanoparticles. These features are important to infer the stability of nanoparticles and the loaded protein. Figure 8.1 shows the insulin-loaded PLGA nanoparticles after production. The nanoparticles of both formulations were similar presenting a smooth surface and spherical shape, which are characteristic of the used encapsulation method and of the nanoparticles polymer. The size range of nanoparticles is also in accordance with the mean particle size described in section 3.1 of this chapter.

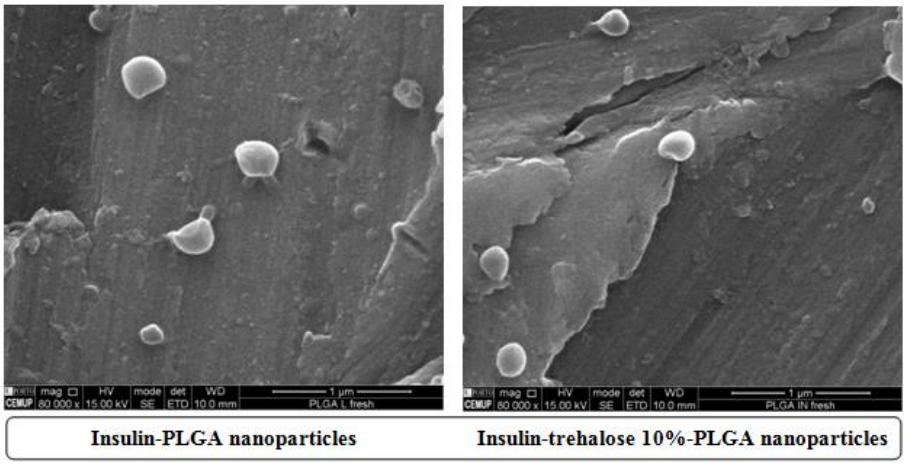

Figure 8.1. SEM microphotographs of insulin-loaded PLGA nanoparticles after production. Scale bar: 1 µm.

3.5.2. After lyophilization

Figure 8.2 shows the SEM microphotographs of the lyophilizates obtained by lyophilization with and without annealing. The lyophilizates presented a porous structure, which were formed during water sublimation and are necessary to the adequate resuspension of nanoparticles. In the lyophilizates it was possible to visualize the arrangement of nanoparticles that maintained its spherical shape upon lyophilization. However, the lyophilizates obtained using annealing showed a more homogenous structure, comparatively to those obtained without annealing. This occurred mainly due to the decrease of the heterogeneity of the sublimation rate caused by annealing, obtaining a more homogeneous cake structure [163, 294].

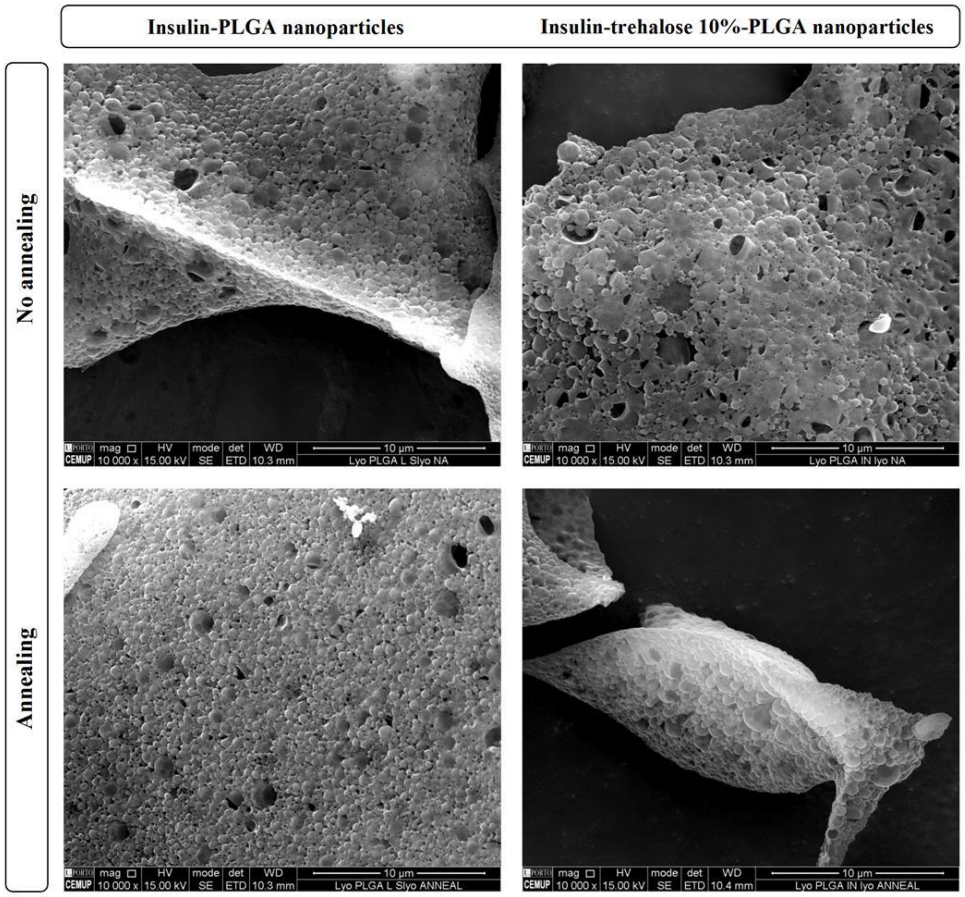

Figure 8.2. SEM microphotographs of the lyophilizates of insulin-loaded PLGA nanoparticles. Scale bar: 10 µm.

After resuspension of the lyophilizates, nanoparticles were observed by SEM (Figure 8.3). The nanoparticles of all formulations maintained their spherical shape and smooth surface after lyophilization and resuspension. The size range observed in the

microphotographs was also in accordance with the mean particle size described in section 3.4 of this chapter. The microphotographs clearly demonstrated that the lyophilization process with and without annealing was able to preserve the integrity of nanoparticles, which is the main aim in nanoparticles lyophilization.

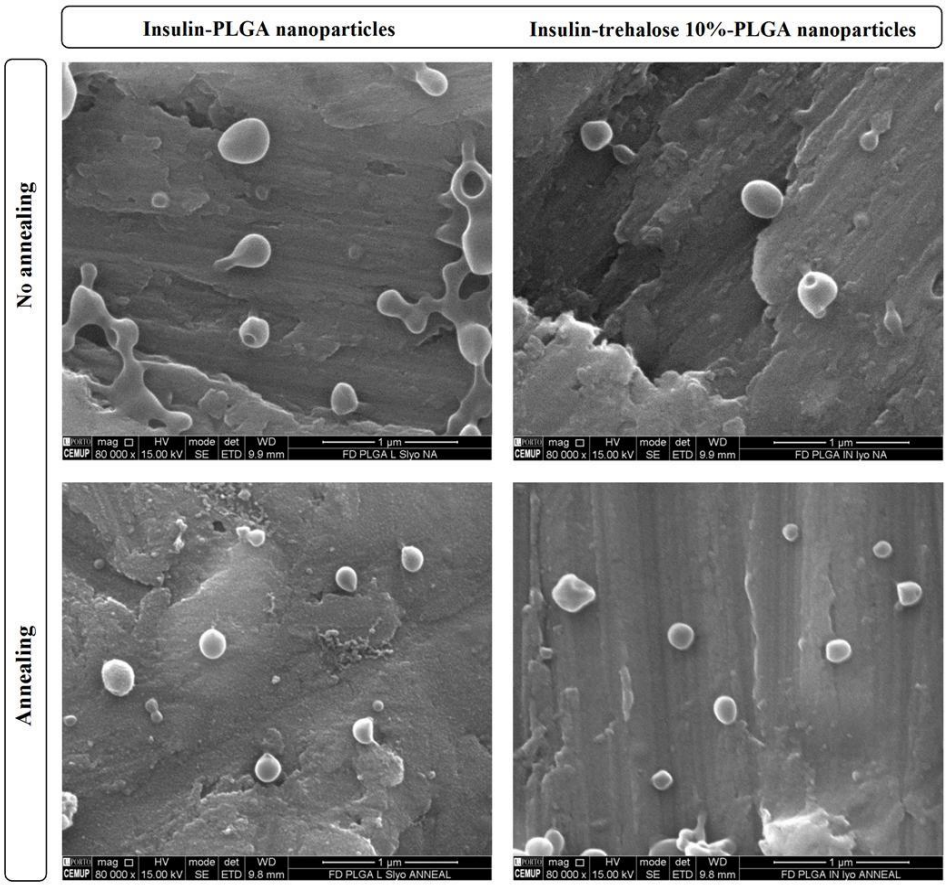

Figure 8.3. SEM microphotographs of lyophilized insulin-loaded PLGA nanoparticles after resuspension. Scale bar: 1 µm.

3.6. Insulin structural integrity

3.6.1. Fourier-transform infrared spectroscopy analysis

FTIR spectroscopy is a powerful technique in the assessment of the secondary structure of proteins loaded into nanoparticles, in a non-invasive manner [85]. In a protein spectra, the amide I region at 1710-1590 cm^{-1} is used to evaluate the similarity of the second derivative spectra of the native protein with that of the loaded protein. Therefore, the highest the similarity between those spectra represents the highest maintenance of the secondary structure of the protein. This protein structure may be

assessed quantitatively and qualitatively, by analyzing the AO and the area-normalized second derivative amide I spectra, respectively.

3.6.1.1. Area of overlap

The AO measures the degree of similarity between the area-normalized second derivative spectra of native insulin, and the insulin loaded into PLGA nanoparticles. The spectrum of native insulin was obtained by the FTIR analysis of an insulin solution 30 mg/ml in HCl 0.1 M. The AO results for the lyophilized insulin-loaded PLGA nanoparticles are depicted in Figure 8.4.

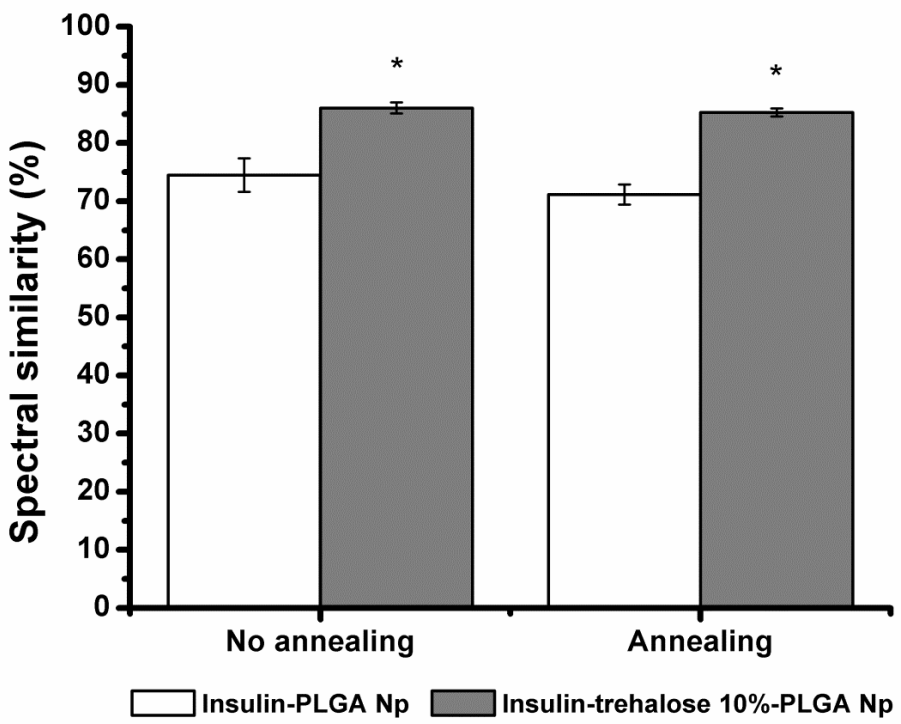

Figure 8.4. AO percentages of insulin loaded into PLGA nanoparticle formulations after lyophilization with and without annealing (n = 3, mean ± SD). Np stands for nanoparticles. Results are significantly different (p < 0.05) from formulation with no cryoprotectant co-encapsulated, insulin-PLGA nanoparticles, when marked with *.

It was observed that either for lyophilization with and without annealing, the nanoparticles co-encapsulated with trehalose had a significantly higher AO of insulin (p < 0.05), comparatively to the formulation containing no cryoprotectant. The AO of insulin-trehalose 10%-PLGA nanoparticles was 85.3 ± 0.7% and 86.0 ± 1.0% for annealing and no annealing conditions, respectively. These results demonstrated that the presence of

trehalose as cryoprotectant, better preserved the structure of insulin loaded into PLGA nanoparticles upon lyophilization both for annealing and no annealing conditions. This may be explained by the ability of cryoprotectants, to stabilize proteins by a preferential exclusion during freezing [280]. The cryoprotectant co-encapsulated with insulin into PLGA nanoparticles has tendency to be excluded from the protein surface, originating a preferential hydration of insulin and increasing the thermodynamic stability of its native state. Additionally, the cryoprotectant may also preserve the insulin structure by reducing its adsorption on the ice surface during freezing, and also by increasing the freeze-concentrate viscosity [269].

Regarding the comparison of lyophilization with and without annealing, no differences were observed in the AO of both insulin-PLGA nanoparticles and insulin-trehalose 10%-PLGA nanoparticles. The insulin AO of those formulations, for annealing and no annealing conditions was even almost identical. This was a particularly good result, since it was clearly demonstrated that annealing allowed the optimization of the lyophilization cycle by decreasing its duration time, and simultaneously ensuring the structural stability of the loaded protein. The possible explanation for this phenomenon is that the stability of proteins loaded into nanoparticles may be more related with the freezing method, rather than the annealing conditions during freezing [295].

3.6.1.2. Visual comparison of area-normalized second derivative amide I spectra

The AO is a quantitative indicator of the preservation of insulin native structure, whereas the analysis of the area-normalized second-derivative amide I spectra allows the evaluation of the qualitative changes of insulin structure. This data is depicted in Figure 8.5.

Generally, upon lyophilization, the protein structure suffers a decrease in α-helix, with a concomitant increase in the β-sheet content, and it is usually accepted that the α-helix content is the best indicator of the integrity of protein structure [258]. The area-normalized second-derivative FTIR spectrum of native insulin was obtained by the analysis of an insulin solution 30 mg/ml. The spectrum showed the insulin structure was dominated by α-helix band at 1657 cm^{-1}, including also β-sheets with bands at 1640 cm^{-1} and 1690 cm^{-1}. These band features of insulin were in agreement with those reported in previous works [85, 281, 295]. The changes of such bands occurring during lyophilization, represent the changes in the secondary structure of insulin that may lead to its denaturation or aggregation, hampering insulin bioactivity or even causing possible adverse effects after administration [259].

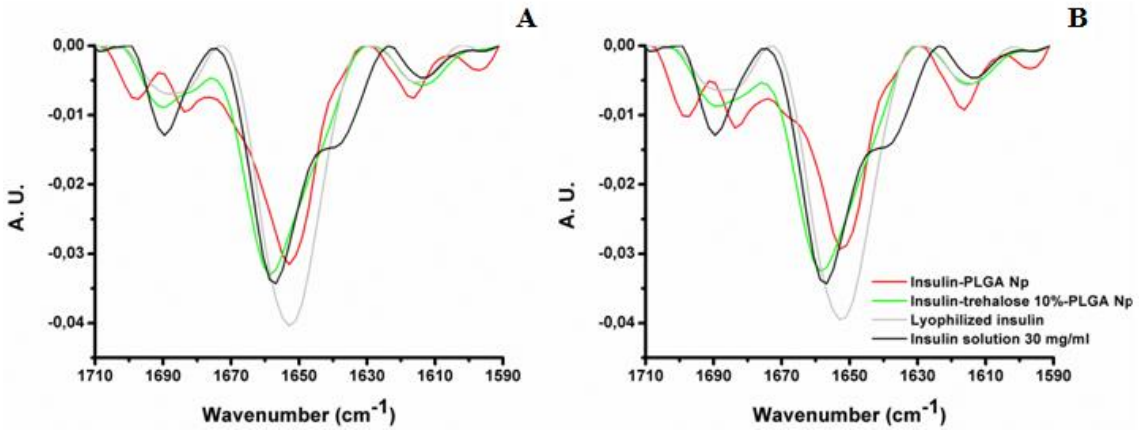

Figure 8.5. Area-normalized second-derivative amide I FTIR spectra of insulin loaded into PLGA nanoparticles lyophilized using no annealing (A), and annealing (B). Np stands for nanoparticles.

Overall, no denaturation or aggregation of insulin was noticed upon lyophilization of the formulations, since these phenomena are evidenced by a clear decrease in α-helix content and a concomitant increase in β-sheet. This result was a good indicator that insulin could maintain its bioactivity upon lyophilization with and without annealing. Previously, it was demonstrated the *in vivo* bioactivity of insulin loaded into the PLGA nanoparticles used in the present work, upon lyophilization without annealing [295]. The insulin contained in formulations presented distinct structural rearrangements upon lyophilization. Interestingly, the structural features of insulin in the different formulations lyophilized both with and without annealing were practically identical, demonstrating the robustness of the lyophilization cycles, and also that the distinct morphology of ice crystals and liquid/water interfaces formed during annealing, in which surface-induced denaturation of insulin may occur [204], had not a detrimental effect on the structural stability of insulin.

The insulin-trehalose 10%-PLGA nanoparticles presented the closest similarity with native insulin, with just a slight decrease and shift of α-helix band into 1659 cm^{-1}, and a decrease of the high-wavenumber β-sheet content. On its turn, the nanoparticles containing no cryoprotectant showed a more pronounced decrease of the α-helix band and its shift into 1653 cm^{-1}, which modification was similar to that of the respective band position of lyophilized insulin. These structural features demonstrated that the co-encapsulation of the cryoprotectant was crucial, to better preserve the structure of insulin loaded into PLGA nanoparticles upon lyophilization with and without annealing.

3.6.2. Circular dichroism analysis

The CD spectroscopy was also used to evaluate the secondary structure of insulin. Prior to the analysis, insulin was extracted from PLGA nanoparticles to avoid spectral artifacts caused by light scattering. During the extraction process, it can occur some minor modifications of insulin structure, nevertheless CD is still a good tool to corroborate the results obtained by FTIR spectroscopy. The far-UV CD spectra of insulin are depicted in Figure 8.6. To obtain the spectrum of native insulin, it was analyzed a solution of insulin 0.2 mg/ml in HCl 0.01 M, obtaining a spectrum with two ellipticity minima characteristic of the predominant α-helical structure of the protein, at 208 nm and 222 nm [266]. The spectrum of native insulin was similar to those described in previous works [85, 282].

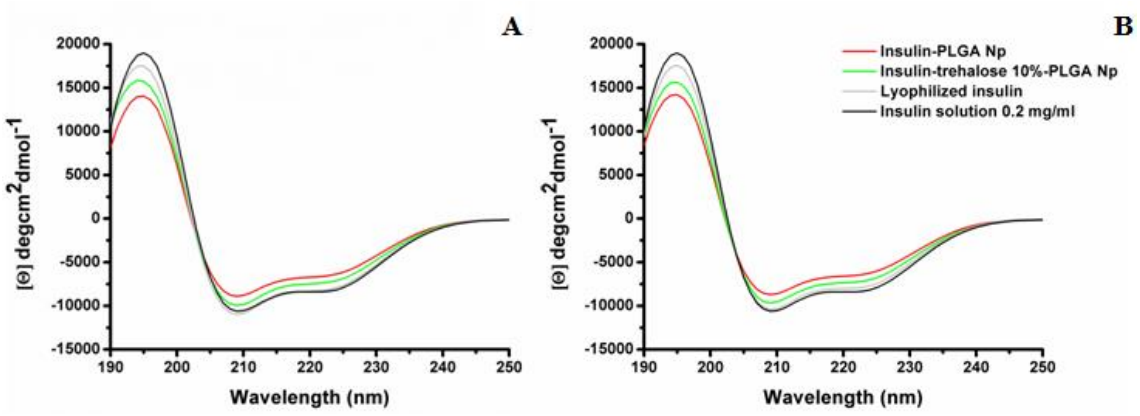

Figure 8.6. Far-UV CD spectra of insulin extracted from insulin-loaded PLGA nanoparticles lyophilized using no annealing (A), and annealing (B). Np stands for nanoparticles.

Overall, the spectra of insulin did not showed relevant shifts of the characteristic minima, demonstrating the prevalent α-helical structure of insulin. The structural modification that could lead to the denaturation, aggregation or fibrillation of insulin is evidenced by prevalent β-sheet content, with an ellipticity minimum around 216 nm [143, 283]. Once this detrimental modification did not occur, the CD results were in agreement with those of FTIR on demonstrating the ability of the lyophilization cycles with and without annealing, to preserve insulin structure in such a way that it could maintain its bioactivity.

The variability in the rearrangement of insulin structure upon lyophilization was demonstrated by the decrease of the negative ellipticity signal. Despite the possible influence of the extraction process of insulin, the CD results were similar to those obtained by FTIR. For instance, the CD spectra of insulin from formulations lyophilized

with no annealing were practically identical, to those obtained after lyophilization with annealing. Furthermore, the insulin from formulations with co-encapsulated trehalose showed a closer similarity with native insulin, comparatively to the insulin from PLGA nanoparticles containing no cryoprotectant co-encapsulated, since the latter evidenced a more pronounced decrease of the negative ellipticity signal. These results confirmed both that annealing had not a detrimental effect in insulin structure, and that PLGA nanoparticles co-encapsulated with trehalose presented a superior structural stability of insulin, comparatively to nanoparticles without cryoprotectant co-encapsulated.

3.6.3. Fluorescence spectroscopy analysis

The fluorescence spectroscopy is another technique used in the evaluation of proteins, particularly their tertiary structure [288]. Prior analysis, insulin was also extracted from PLGA nanoparticles to avoid potential spectral artifacts. Insulin lacks tryptophan, so the protein fluorescence is mostly dependent on the four tyrosine residues [284]. Therefore, the modification of the emission spectra of insulin fluorescence is an indicator of possible changes in the protein structure. Figure 8.7 shows the fluorescence spectra of insulin from nanoparticles, in which the spectrum of native insulin (insulin solution 0.2 mg/ml), evidenced a maximum fluorescence intensity at 304 nm. The spectrum of native insulin was in agreement with those previously reported [285-287, 295].

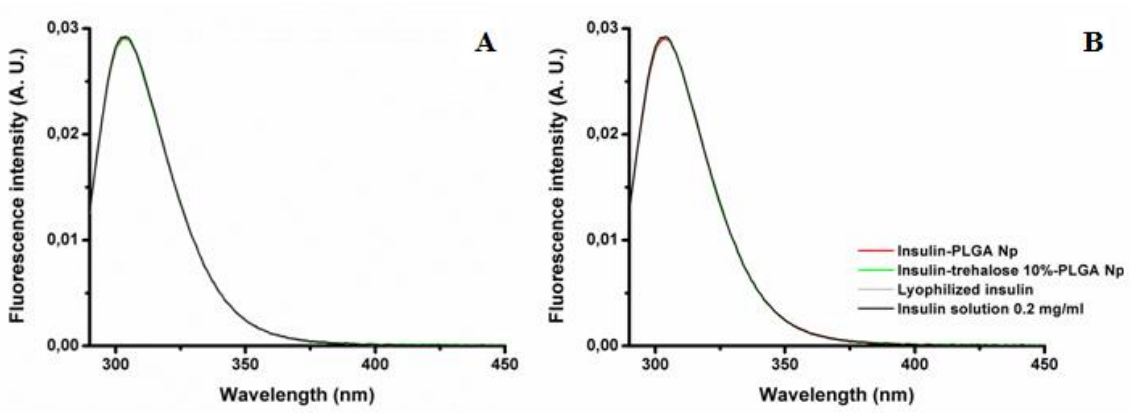

Figure 8.7. Fluorescence spectra of insulin extracted from insulin-loaded PLGA nanoparticles lyophilized using no annealing (A), and annealing (B). Np stands for nanoparticles.

The structural modifications configured with insulin denaturation, aggregation or fibrillation are characterized by a decrease in the intensity of fluorescence emission and the shift of its maxima [284]. Since all the insulin spectra were practically identical, it was possible to conclude that those structural modifications did not occur, and the

lyophilization cycles both with and without annealing were able to preserve the stability of insulin in order to assure its bioactivity. No differences were found between the insulin spectra from nanoparticles lyophilized using annealing, with those lyophilized with no annealing.

3.7. Thioflavin T experiment

The thioflavin T experiment is a useful tool to assess the fibrillation of insulin, which may occur during nanoparticles processing and lyophilization. The amyloid fibrils are proteins aggregates that indicate the protein structure and its bioactivity are decisively compromised. The thioflavin T is a dye able to bind to amyloid fibrils with crossed β-sheet structures, leading to a shift of the fluorescence excitation maximum from 340 nm to 450 nm, and an increase of fluorescence emission at 485 nm [290, 291]. Thus, the enhancement of the thioflavin T fluorescence intensity is indicative of insulin aggregation/fibrillation [287].

The insulin from PLGA nanoparticles did not evidenced the presence of amyloid fibrils, since it was not verified a fluorescence emission at 485 nm (data not shown). In turn, the positive control of fibrillated insulin showed a clear fluorescence emission. These results were in agreement with aforementioned structural characterization of insulin, and were elucidative on demonstrating that both the nanoparticles production and lyophilization cycles with and without annealing, did not acted as stress factors that could originate insulin fibrillation.

4. Conclusion

In this chapter, the main objective was to develop an optimized lyophilization cycle using annealing to decrease the duration time of the process, and simultaneously ensure the stability of nanoparticles and with upmost importance the maintenance of the loaded protein stability. Additionally, it was assessed the cryoprotectant effect in this stabilization process. Insulin and PLGA nanoparticles were used as models in this study.

Annealing allowed obtaining good lyophilizates with no cake collapse, and its reconstitution was even faster than the lyophilizates obtained without annealing. The lyophilizates obtained using annealing had similar residual moisture content of those without annealing. The presence of cryoprotectant co-encapsulated was found important to better stabilize the nanoparticles size during lyophilization with annealing, mitigating the stresses caused by ice crystals growth. However, no nanoparticles aggregation or fusion, and a superior colloidal stability of nanoparticles were observed after

lyophilization. The lyophilizates obtained using annealing demonstrated a more homogenous structure, comparatively to those obtained without annealing, due to the decrease of heterogeneity of the sublimation rate caused by annealing.

Regarding the maintenance of protein structure upon lyophilization, no insulin denaturation, aggregation or fibrillation was observed, being a good indicator that the lyophilization process was able to preserve the bioactivity of insulin. It was demonstrated that nanoparticle formulations with co-encapsulated cryoprotectant, better preserved the structure of insulin upon lyophilization, comparatively to nanoparticles without cryoprotectant co-encapsulated. Indeed, the structural features of insulin loaded into nanoparticles co-encapsulated with trehalose presented the closest similarity with those of native insulin. The level of insulin structural maintenance of nanoparticles lyophilized using annealing was similar to that obtained without annealing, demonstrating that annealing allowed the optimization of lyophilization cycle by decreasing its duration time with a simultaneous preservation of protein structure.

Overall, this work gave rise to the importance of the optimization of lyophilization cycle of polymeric nanoparticles loaded with proteins, and particularly recognized annealing as a tool to decrease the duration of the process and simultaneously ensure the stability of nanoparticles and the structural preservation of the encapsulated protein.

Chapter 9

General Conclusions and Future Perspectives

The therapeutic proteins are the most common biopharmaceuticals available in the market, usually in the lyophilized form. Benefiting from the development of the nanotechnology field in the last decades, proteins have been encapsulated into polymeric nanoparticles mainly due to its ability to load, protect, release in a sustained manner and deliver proteins to a specific target. A good example is the PLGA polymer, regularly used in the production of nanoparticles, mainly due to its biodegradability, biocompatibility and good sustained release properties. However, PLGA nanoparticles in aqueous suspension are unstable, due to the hydrolytically unstable polyester. The lyophilization is a dehydration process commonly used in the pharmaceutical industry to increase the long term stability, and allow easy handling and storage of products. Besides its stabilizing effects, the lyophilization steps may induce different stresses to formulations with detrimental and irreversible consequences both to nanoparticles and the loaded protein. To mitigate such stresses, several excipients such as cryo- and lyoprotectants have been used. Despite being an easy process, lyophilization is based in several engineering principles that must be properly regarded. These principles and the physical-chemical properties of formulations are usually neglected, and lyophilization is often used empirically or in a trial and error way, with obvious negative and unpredictable consequences to the formulation as a whole, namely to the lyophilizate, nanoparticles and loaded protein.

In the present Thesis, it was developed an optimization of the lyophilization parameters of polymeric nanoparticles for delivery of therapeutic proteins, using PLGA nanoparticles and insulin as models. Those parameters focused on every component involved in the lyophilization of nanoparticles, as are the nanoparticle formulations and the lyophilization cycle. The general purpose followed in the optimization of lyophilization parameters was obtaining the best preservation of nanoparticle features and with upmost importance, assures the superior stability of the loaded protein. Therefore, the nanoparticles were first optimized in order to obtain acceptable features regarding its size, zeta potential and insulin association efficiency. It was also assessed the influence of cryoprotectants and a standard lyophilization process in the porosity of nanoparticles. Then, the nanoparticles added with cryoprotectants were used to evaluate their stability and the structural maintenance of insulin, upon storage during 6 months at different storage conditions. Using a more controlled lyophilization cycle, it was proposed an approach in the lyophilization of nanoparticles by co-encapsulating the lyoprotectants with insulin, as a way to better stabilize the structure and bioactivity of the loaded protein. The success of this strategy allows saving some lyoprotectant, since the amount needed is quite lower than that used in the conventional lyoprotectant addition method, and also

to avoid this latter processing step, which may be interesting from an up-scale and industrial point of view. After precisely assessing the physical-chemical properties of nanoparticles, it was developed an optimized lyophilization cycle and was evaluated the influence of different freezing methods in the stability of insulin-loaded nanoparticles, and the performance of cryoprotectants as excipients to avoid possible freezing stresses to nanoparticles. Finally, after choosing a cryoprotectant with good stabilizing performance, it was evaluated the effect of annealing in the stability of insulin-loaded nanoparticles and its ability to decrease the duration time of lyophilization.

All the objectives proposed for this Thesis were met. The formulation containing PLGA 50:50 as polymer and PVA 2% as surfactant was the one that presented the best features regarding its size, zeta potential and association efficiency, and was chosen for further experiments. The porosity of nanoparticles was enhanced upon lyophilization, especially when cryoprotectants were added as excipients, namely trehalose, glucose, sucrose, fructose and sorbitol. The release profile of insulin from nanoparticles showed a burst release in the first 2 h, followed by a sustained release up to 48 hours. The release of insulin was increased after nanoparticles lyophilization, potentially due to the porosity enhancement. The insulin released from nanoparticles showed different performances dependent on the cryoprotectant used. It was hypothesized that nanoparticles porosity and cryoprotectants presence may have distinct influences in the stability of insulin-loaded nanoparticles.

In the 6 months storage stability study, it was observed that the use of a standard lyophilization cycle led to the collapse of several formulations with detrimental effects to lyophilizates resuspension and nanoparticles aggregation. Interestingly, collapsed formulations showed better protein stabilization upon storage, than non-collapsed ones. The cryoprotectants enhanced the nanoparticles stability, but they presented different performances on the stabilization of insulin structure. Sorbitol showed better performance over the other cryoprotectants, which was surprising since it is known the propensity of sorbitol to crystallize, which may interfere with the storage stability of formulations. These results showed the variability occurred when a standard lyophilization cycle was used.

The co-encapsulation of lyoprotectants with the protein into nanoparticles revealed to be a promising strategy. Insulin-loaded PLGA nanoparticles co-encapsulated with lyoprotectants obtained a mean particle size of 386-466 nm, and a zeta potential ranging between -34 and -38 mV, dependent on the lyoprotectant used. The AE and LC of formulations were about 85-91% and 10-12%, respectively. These formulations obtained no cake collapse and amorphous lyophilizates. This strategy offered superior insulin stability with an AO of about 82-87%, comparatively to the conventional

lyoprotectant addition method achieving an AO of 66-83%. The reducing sugars used as cryoprotectants did not show an adverse effect on insulin stability, when they were co-encapsulated. Surprisingly, the concomitant co-encapsulation and addition of lyoprotectant prior lyophilization showed to be even detrimental to insulin stability. Regarding the *in vitro* release of insulin, the nanoparticles added with lyoprotectants prior lyophilization showed a lower release of insulin, comparatively to nanoparticles co-encapsulated with the same lyoprotectant. This ability may be used to provide benefits to diabetes therapy.

The lyophilization cycle was optimized considering the physical-chemical properties of nanoparticle formulations. Then, it was assessed the influence of the freezing step of lyophilization in the stability of insulin-loaded nanoparticles co-encapsulated with cryoprotectants. In this work it were used the two nonreducing sugars and the sugar alcohol as cryoprotectants, used previously. The features of nanoparticles were preserved upon lyophilization using the different freezing methods. The lyophilization cycle of each freezing condition produced amorphous lyophilizates, which was a good perspective for their storage stability. Insulin-loaded nanoparticles lyophilized without cryoprotectant showed some variability in the structure of the protein depending on the freezing method, being the ramped cooling at -40ºC that obtained the highest structural maintenance of insulin with an AO of about 89%. Such structural variability was mitigated when cryoprotectants were co-encapsulated, showing that they reduced the freezing stresses and better preserved the insulin structure. The ramped cooling at -40ºC was the freezing method in which the formulations both with and without cryoprotectants co-encapsulated, obtained the most similar structural maintenance of insulin. Trehalose and sucrose showed better cryoprotectant performance than sorbitol. Both the encapsulation and lyophilization processes, did not acted as stress factors to insulin that could lead to its fibrillation. More importantly, the formulation containing trehalose was used in the assessment of the *in vivo* bioactivity of insulin-loaded nanoparticles upon lyophilization and reconstitution, and was observed that the carriers were able to prolong the hypoglycemic effect of insulin, comparatively to subcutaneous insulin. The hypoglycemic effect was even enhanced by the nanoparticles co-encapsulated with trehalose, comparatively to both nanoparticles without and with trehalose added prior lyophilization, essentially caused by the superior insulin stabilization and bioactivity.

After optimization and choosing the most suitable freezing method, the lyophilization cycle was included with an annealing step in order to increase the sublimation rate and thus, decrease the duration time of lyophilization. In this process the stability of insulin-loaded nanoparticles with co-encapsulated trehalose had to be

assured. The lyophilization using annealing obtained good lyophilizates with no cake collapse, and their reconstitution was even faster than the lyophilizates produced without annealing. The residual moisture content of lyophilizates obtained with annealing was similar to those without annealing, demonstrating that the time reduction of lyophilization using annealing was possible and equally effective on water removal. The presence of trehalose co-encapsulated mitigated the freezing stresses of ice crystals growth caused by annealing, and was important to stabilize nanoparticles. As previously observed, nanoparticles co-encapsulated with trehalose preserved better the insulin structure, than nanoparticles without cryoprotectant. The structural maintenance of insulin obtained by annealing was similar to that without annealing, showing that the inclusion of an annealing step in the lyophilization cycle allowed to decrease its duration time in about 26%, with no detrimental effects to protein structure.

The work underlying this Thesis has to be seen as an ongoing work. In research, there is always another experiment to be done. At this point, the performed work may be a good contribution to the biopharmaceutics and nanomedicine fields. The importance of optimization of the parameters involved in protein-loaded nanoparticles lyophilization, from the formulations itself to the lyophilization cycle was highlighted here. Future works may extend these principles to improve the stability of different proteins loaded into other nanocarriers, polymeric or not. The strategy of co-encapsulating cryo- and lyoprotectants together with proteins with the purpose of better stabilizing it may open a new paradigm in the lyophilization of biopharmaceutic products. From an upscale and industrial point of view, it might be important since allows eliminating the cryo- and lyoprotectant addition step between nanoparticles production and lyophilization, and at the same time reduces drastically the amount of excipient needed. More importantly, since therapeutic proteins are usually expensive, the superior maintenance of insulin native structure and consequent enhanced bioactivity may be valuable from a cost-benefit perspective. In the following years, it will be also interesting to apply the technologies of monotorization and management of lyophilization that have been developed, in the lyophilization of nanoparticle-based products, in order to improve their quality and storage stability with a simultaneous decrease of the duration and cost of lyophilization.

References

[1] Z. Antosova, M. Mackova, V. Kral, T. Macek, Therapeutic application of peptides and proteins: parenteral forever?, Trends Biotechnol, 27 (2009) 628-635.

[2] P. Fonte, F. Araújo, C. Silva, C. Pereira, S. Reis, H.A. Santos, B. Sarmento, Polymer-based nanoparticles for oral insulin delivery: Revisited approaches, Biotechnol Adv, 33 (2015) 1342-1354.

[3] P. Fonte, F. Araújo, S. Reis, B. Sarmento, Oral insulin delivery: how far are we?, J Diabetes Sci Technol, 7 (2013) 520-531.

[4] H.M. Courrier, N. Butz, T.F. Vandamme, Pulmonary drug delivery systems: recent developments and prospects, Crit Rev Ther Drug Carrier Syst, 19 (2002) 425-498.

[5] J.W. Yoo, E. Chambers, S. Mitragotri, Factors that control the circulation time of nanoparticles in blood: Challenges, solutions and future prospects, Curr Pharm Des, 16 (2010) 2298-2307.

[6] D. Lemoine, C. Francois, F. Kedzierewicz, V. Preat, M. Hoffman, P. Maincent, Stability study of nanoparticles of poly(epsilon-caprolactone), poly(D,L-lactide) and poly(D,L-lactide-co-glycolide), Biomaterials, 17 (1996) 2191-2197.

[7] W. Abdelwahed, G. Degobert, S. Stainmesse, H. Fessi, Freeze-drying of nanoparticles: formulation, process and storage considerations, Adv Drug Deliv Rev, 58 (2006) 1688-1713.

[8] F. Franks, Freeze-drying of bioproducts: putting principles into practice, Eur J Pharm Biopharm, 45 (1998) 221-229.

[9] M.K. Lee, M.Y. Kim, S. Kim, J. Lee, Cryoprotectants for freeze drying of drug nano-suspensions: Effect of freezing rate, J Pharm Sci, 98 (2009) 4808-4817.

[10] T. Arakawa, S. Prestrelski, W. Kenney, J. Carpenter, Factors affecting short-term and long-term stabilities of proteins, Adv Drug Deliv Rev, 46 (2001) 307-326.

[11] D.R. Whiting, L. Guariguata, C. Weil, J. Shaw, IDF diabetes atlas: global estimates of the prevalence of diabetes for 2011 and 2030, Diabetes Res Clin Pract, 94 (2011) 311-321.

[12] S. Wild, G. Roglic, A. Green, R. Sicree, H. King, Global prevalence of diabetes: estimates for the year 2000 and projections for 2030, Diabetes Care, 27 (2004) 1047-1053.

[13] S. Hosseininasab, R. Pashaei-Asl, A.A. Khandaghi, H.T. Nasrabadi, K. Nejati-Koshki, A. Akbarzadeh, S.W. Joo, Y. Hanifehpour, S. Davaran, Synthesis, characterization, and in vitro studies of PLGA-PEG nanoparticles for oral insulin delivery, Chem Biol Drug Des, 84 (2014) 307-315.

[14] D. Meetoo, P. McGovern, R. Safadi, An epidemiological overview of diabetes across the world, Br J Nurs, 16 (2007) 1002-1007.

[15] F.G. Banting, C.H. Best, The internal secretion of the pancreas, J Lab Clin Med, 7 (1922) 251-266.

[16] P. Reichard, B.Y. Nilsson, U. Rosenqvist, The effect of long-term intensified insulin treatment on the development of microvascular complications of diabetes mellitus, N Engl J Med, 329 (1993) 304-309.

[17] The effect of intensive treatment of diabetes on the development and progression of long-term complications in insulin-dependent diabetes mellitus. The Diabetes Control and Complications Trial Research Group, N Engl J Med, 329 (1993) 977-986.

[18] Effect of intensive therapy on the microvascular complications of type 1 diabetes mellitus, Jama, 287 (2002) 2563-2569.

[19] E.P. Herrero, M.J. Alonso, N. Csaba, Polymer-based oral peptide nanomedicines, Ther Deliv, 3 (2012) 657-668.

[20] K. Chaturvedi, K. Ganguly, M.N. Nadagouda, T.M. Aminabhavi, Polymeric hydrogels for oral insulin delivery, J Control Release, 165 (2013) 129-138.

[21] M. Morishita, N.A. Peppas, Is the oral route possible for peptide and protein drug delivery?, Drug Discov Today, 11 (2006) 905-910.

[22] L. Plapied, N. Duhem, A. des Rieux, V. Préat, Fate of polymeric nanocarriers for oral drug delivery, Curr Opin Colloid Interface Sci, 16 (2011) 228-237.

[23] M.R. Rekha, C.P. Sharma, Oral delivery of therapeutic protein/peptide for diabetes--future perspectives, Int J Pharm, 440 (2013) 48-62.

[24] J.G. Still, Development of oral insulin: progress and current status, Diabetes Metab Res Rev, 18 Suppl 1 (2002) S29-37.

[25] E.M. Pridgen, F. Alexis, O.C. Farokhzad, Polymeric nanoparticle technologies for oral drug delivery, Clin Gastroenterol Hepatol, 12 (2014) 1605-1610.

[26] M.C. Chen, K. Sonaje, K.J. Chen, H.W. Sung, A review of the prospects for polymeric nanoparticle platforms in oral insulin delivery, Biomaterials, 32 (2011) 9826-9838.

[27] A. des Rieux, V. Fievez, M. Garinot, Y.J. Schneider, V. Preat, Nanoparticles as potential oral delivery systems of proteins and vaccines: a mechanistic approach, J Control Release, 116 (2006) 1-27.

[28] A.C. Hunter, J. Elsom, P.P. Wibroe, S.M. Moghimi, Polymeric particulate technologies for oral drug delivery and targeting: a pathophysiological perspective, Nanomedicine, 8 Suppl 1 (2012) S5-20.

[29] J. Hochman, P. Artursson, Mechanisms of absorption enhancement and tight junction regulation, J Control Release, 29 (1994) 253-267.

[30] A. des Rieux, V. Pourcelle, P.D. Cani, J. Marchand-Brynaert, V. Preat, Targeted nanoparticles with novel non-peptidic ligands for oral delivery, Adv Drug Deliv Rev, 65 (2013) 833-844.

[31] B.F. Choonara, Y.E. Choonara, P. Kumar, D. Bijukumar, L.C. du Toit, V. Pillay, A review of advanced oral drug delivery technologies facilitating the protection and absorption of protein and peptide molecules, Biotechnol Adv, 32 (2014) 1269-1282.

[32] T.H. Yeh, L.W. Hsu, M.T. Tseng, P.L. Lee, K. Sonjae, Y.C. Ho, H.W. Sung, Mechanism and consequence of chitosan-mediated reversible epithelial tight junction opening, Biomaterials, 32 (2011) 6164-6173.

[33] H.W. Sung, K. Sonaje, Z.X. Liao, L.W. Hsu, E.Y. Chuang, pH-responsive nanoparticles shelled with chitosan for oral delivery of insulin: from mechanism to therapeutic applications, Acc Chem Res, 45 (2012) 619-629.

[34] M.R. Avadi, A. Jalali, A.M. Sadeghi, K. Shamimi, K.H. Bayati, E. Nahid, A.R. Dehpour, M. Rafiee-Tehrani, Diethyl methyl chitosan as an intestinal paracellular enhancer: ex vivo and in vivo studies, Int J Pharm, 293 (2005) 83-89.

[35] J.M. Smith, M. Dornish, E.J. Wood, Involvement of protein kinase C in chitosan glutamate-mediated tight junction disruption, Biomaterials, 26 (2005) 3269-3276.

[36] M. Werle, H. Takeuchi, A. Bernkop-Schnurch, Modified chitosans for oral drug delivery, J Pharm Sci, 98 (2009) 1643-1656.

[37] K. Sonaje, E.Y. Chuang, K.J. Lin, T.C. Yen, F.Y. Su, M.T. Tseng, H.W. Sung, Opening of epithelial tight junctions and enhancement of paracellular permeation by chitosan: microscopic, ultrastructural, and computed-tomographic observations, Mol Pharm, 9 (2012) 1271-1279.

[38] S.D. Conner, S.L. Schmid, Regulated portals of entry into the cell, Nature, 422 (2003) 37-44.

[39] M.H. Jang, M.N. Kweon, K. Iwatani, M. Yamamoto, K. Terahara, C. Sasakawa, T. Suzuki, T. Nochi, Y. Yokota, P.D. Rennert, T. Hiroi, H. Tamagawa, H. Iijima, J. Kunisawa, Y. Yuki, H. Kiyono, Intestinal villous M cells: an antigen entry site in the mucosal epithelium, Proc Natl Acad Sci U S A, 101 (2004) 6110-6115.

[40] G.M. Cooper, The Cell Surface, in: The Cell: A Molecular Approach, Sunderland (MA): Sinauer Associates, 2000.

[41] H. Hillaireau, P. Couvreur, Nanocarriers' entry into the cell: relevance to drug delivery, Cell Mol Life Sci, 66 (2009) 2873-2896.

[42] F. Araújo, C. Pereira, P.L. Granja, H.A. Santos, B. Sarmento, Functionalized nanoparticles for targeting the gastrointestinal apical membrane receptors, in: R.D. Vooght-Johnson (Ed.) Advances and Challenges in Oral Delivery of Macromolecules, Future Science Group, 2014.

[43] R. Singh, J. Lillard Jr, Nanoparticle-based targeted drug delivery, Exp Mol Pathol, 86 (2009) 215-223.

[44] A. Chaudhury, S. Das, Recent advancement of chitosan-based nanoparticles for oral controlled delivery of insulin and other therapeutic agents, AAPS PharmSciTech, 12 (2011) 10-20.

[45] X. Du, J. Zhang, Y. Zhang, S. Li, X. Lin, X. Tang, Y. Zhang, Y. Wang, Decanoic acid grafted oligochitosan nanoparticles as a carrier for insulin transport in the gastrointestinal tract, Carbohydr Polym, 111 (2014) 433-441.

[46] K.B. Chalasani, G.J. Russell-Jones, S.K. Yandrapu, P.V. Diwan, S.K. Jain, A novel vitamin B12-nanosphere conjugate carrier system for peroral delivery of insulin, J Control Release, 117 (2007) 421-429.

[47] K.B. Chalasani, G.J. Russell-Jones, A.K. Jain, P.V. Diwan, S.K. Jain, Effective oral delivery of insulin in animal models using vitamin B12-coated dextran nanoparticles, J Control Release, 122 (2007) 141-150.

[48] V. Agarwal, I.K. Reddy, M.A. Khan, Oral Delivery of Proteins: Effect of chicken and duck ovomucoid on the stability of insulin in the presence of α-chymotrypsin and trypsin, Pharm Pharmacol Commun, 6 (2000) 223-227.

[49] H. Liu, R. Tang, W.S. Pan, Y. Zhang, H. Liu, Potential utility of various protease inhibitors for improving the intestinal absorption of insulin in rats, J Pharm Pharmacol, 55 (2003) 1523-1529.

[50] M.E. Lane, M. O'Driscoll C, O.I. Corrigan, Quantitative estimation of the effects of bile salt surfactant systems on insulin stability and permeability in the rat intestine using a mass balance model, J Pharm Pharmacol, 57 (2005) 169-175.

[51] C.L. Li, Y.J. Deng, Oil-based formulations for oral delivery of insulin, J Pharm Pharmacol, 56 (2004) 1101-1107.

[52] A. Fasano, S. Uzzau, Modulation of intestinal tight junctions by Zonula occludens toxin permits enteral administration of insulin and other macromolecules in an animal model, J Clin Invest, 99 (1997) 1158-1164.

[53] E.J. Nielsen, S. Yoshida, N. Kamei, R. Iwamae, E.-S. Khafagy, J. Olsen, U.L. Rahbek, B.L. Pedersen, K. Takayama, M. Takeda-Morishita, In vivo proof of concept of oral insulin delivery based on a co-administration strategy with the cell-penetrating peptide penetratin, J Control Release, 189 (2014) 19-24.

[54] N. Kamei, M. Morishita, K. Takayama, Importance of intermolecular interaction on the improvement of intestinal therapeutic peptide/protein absorption using cell-penetrating peptides, J Control Release, 136 (2009) 179-186.

[55] R. Muzzarelli, Chemical and technological advances in chitins and chitosans useful for the Formulation of biopharmaceuticals, in: B. Sarmento, J. das Neves (Eds.)

Chitosan-based systems for biopharmaceuticals: Delivery, Targeting and Polymer Therapeutics., John Wiley & Sons, Ltd., 2012, pp. 3-21.

[56] Q. Gan, T. Wang, Chitosan nanoparticle as protein delivery carrier--systematic examination of fabrication conditions for efficient loading and release, Colloids Surf B Biointerfaces, 59 (2007) 24-34.

[57] R. Hejazi, M. Amiji, Chitosan-based gastrointestinal delivery systems, J Control Release, 89 (2003) 151-165.

[58] A. Makhlof, Y. Tozuka, H. Takeuchi, Design and evaluation of novel pH-sensitive chitosan nanoparticles for oral insulin delivery, Eur J Pharm Sci, 42 (2011) 445-451.

[59] Y. Pan, Y.J. Li, H.Y. Zhao, J.M. Zheng, H. Xu, G. Wei, J.S. Hao, F.D. Cui, Bioadhesive polysaccharide in protein delivery system: chitosan nanoparticles improve the intestinal absorption of insulin in vivo, Int J Pharm, 249 (2002) 139-147.

[60] P. Mukhopadhyay, K. Sarkar, M. Chakraborty, S. Bhattacharya, R. Mishra, P.P. Kundu, Oral insulin delivery by self-assembled chitosan nanoparticles: In vitro and in vivo studies in diabetic animal model, Mater Sci Eng C Mater Biol Appl, 33 (2013) 376-382.

[61] Z. Ma, H.H. Yeoh, L.Y. Lim, Formulation pH modulates the interaction of insulin with chitosan nanoparticles, J Pharm Sci, 91 (2002) 1396-1404.

[62] Z. Ma, T.M. Lim, L.Y. Lim, Pharmacological activity of peroral chitosan-insulin nanoparticles in diabetic rats, Int J Pharm, 293 (2005) 271-280.

[63] K.A. Janes, P. Calvo, M.J. Alonso, Polysaccharide colloidal particles as delivery systems for macromolecules, Adv Drug Deliv Rev, 47 (2001) 83-97.

[64] S.M. van der Merwe, J.C. Verhoef, J.H. Verheijden, A.F. Kotze, H.E. Junginger, Trimethylated chitosan as polymeric absorption enhancer for improved peroral delivery of peptide drugs, Eur J Pharm Biopharm, 58 (2004) 225-235.

[65] R.J. Verheul, M. Amidi, S. van der Wal, E. van Riet, W. Jiskoot, W.E. Hennink, Synthesis, characterization and in vitro biological properties of O-methyl free N,N,N-trimethylated chitosan, Biomaterials, 29 (2008) 3642-3649.

[66] G. Sandri, M.C. Bonferoni, S. Rossi, F. Ferrari, C. Boselli, C. Caramella, Insulin-loaded nanoparticles based on N-trimethyl chitosan: in vitro (Caco-2 model) and ex vivo (excised rat jejunum, duodenum, and ileum) evaluation of penetration enhancement properties, AAPS PharmSciTech, 11 (2010) 362-371.

[67] Y. Jin, Y. Song, X. Zhu, D. Zhou, C. Chen, Z. Zhang, Y. Huang, Goblet cell-targeting nanoparticles for oral insulin delivery and the influence of mucus on insulin transport, Biomaterials, 33 (2012) 1573-1582.

[68] A.M. Sadeghi, F.A. Dorkoosh, M.R. Avadi, P. Saadat, M. Rafiee-Tehrani, H.E. Junginger, Preparation, characterization and antibacterial activities of chitosan, N-trimethyl chitosan (TMC) and N-diethylmethyl chitosan (DEMC) nanoparticles loaded with insulin using both the ionotropic gelation and polyelectrolyte complexation methods, Int J Pharm, 355 (2008) 299-306.

[69] A. Bayat, B. Larijani, S. Ahmadian, H.E. Junginger, M. Rafiee-Tehrani, Preparation and characterization of insulin nanoparticles using chitosan and its quaternized derivatives, Nanomedicine, 4 (2008) 115-120.

[70] A. Bayat, F.A. Dorkoosh, A.R. Dehpour, L. Moezi, B. Larijani, H.E. Junginger, M. Rafiee-Tehrani, Nanoparticles of quaternized chitosan derivatives as a carrier for colon delivery of insulin: ex vivo and in vivo studies, Int J Pharm, 356 (2008) 259-266.

[71] A.M. Sadeghi, F.A. Dorkoosh, M.R. Avadi, M. Weinhold, A. Bayat, F. Delie, R. Gurny, B. Larijani, M. Rafiee-Tehrani, H.E. Junginger, Permeation enhancer effect of chitosan and chitosan derivatives: comparison of formulations as soluble polymers and nanoparticulate systems on insulin absorption in Caco-2 cells, Eur J Pharm Biopharm, 70 (2008) 270-278.

[72] L. Yin, J. Ding, C. He, L. Cui, C. Tang, C. Yin, Drug permeability and mucoadhesion properties of thiolated trimethyl chitosan nanoparticles in oral insulin delivery, Biomaterials, 30 (2009) 5691-5700.

[73] M.R. Rekha, C.P. Sharma, Synthesis and evaluation of lauryl succinyl chitosan particles towards oral insulin delivery and absorption, J Control Release, 135 (2009) 144-151.

[74] A. Elsayed, M. Al-Remawi, N. Qinna, A. Farouk, K.A. Al-Sou'od, A.A. Badwan, Chitosan-sodium lauryl sulfate nanoparticles as a carrier system for the in vivo delivery of oral insulin, AAPS PharmSciTech, 12 (2011) 958-964.

[75] M.R. Avadi, A.M. Sadeghi, N. Mohammadpour, S. Abedin, F. Atyabi, R. Dinarvand, M. Rafiee-Tehrani, Preparation and characterization of insulin nanoparticles using chitosan and arabic gum with ionic gelation method, Nanomedicine, 6 (2010) 58-63.

[76] M.R. Avadi, A.M. Sadeghi, N. Mohamadpour Dounighi, R. Dinarvand, F. Atyabi, M. Rafiee-Tehrani, Ex vivo evaluation of insulin nanoparticles using chitosan and arabic gum, ISRN Pharm, 2011 (2011) 860109.

[77] S.C. Chen, Y.C. Wu, F.L. Mi, Y.H. Lin, L.C. Yu, H.W. Sung, A novel pH-sensitive hydrogel composed of N,O-carboxymethyl chitosan and alginate cross-linked by genipin for protein drug delivery, J Control Release, 96 (2004) 285-300.

[78] N. Zhang, J. Li, W. Jiang, C. Ren, J. Xin, K. Li, Effective protection and controlled release of insulin by cationic beta-cyclodextrin polymers from alginate/chitosan nanoparticles, Int J Pharm, 393 (2010) 212-218.

[79] L. Huang, J. Xin, Y. Guo, J. Li, A novel insulin oral delivery system assisted by cationic β-cyclodextrin polymers, J Appl Polym Sci, 115 (2010) 1371-1379.

[80] P. Mukhopadhyay, R. Mishra, D. Rana, P.P. Kundu, Strategies for effective oral insulin delivery with modified chitosan nanoparticles: A review, Prog Polym Sci, 37 (2012) 1457-1475.

[81] M.C. Chen, F.L. Mi, Z.X. Liao, C.W. Hsiao, K. Sonaje, M.F. Chung, L.-W. Hsu, H.W. Sung, Recent advances in chitosan-based nanoparticles for oral delivery of macromolecules, Adv Drug Deliv Rev, 65 (2013) 865-879.

[82] B. Sarmento, A. Ribeiro, F. Veiga, D. Ferreira, Development and characterization of new insulin containing polysaccharide nanoparticles, Colloids Surf B Biointerfaces, 53 (2006) 193-202.

[83] B. Sarmento, A. Ribeiro, F. Veiga, D. Ferreira, R. Neufeld, Oral bioavailability of insulin contained in polysaccharide nanoparticles, Biomacromolecules, 8 (2007) 3054-3060.

[84] B. Sarmento, A.J. Ribeiro, F. Veiga, D.C. Ferreira, R.J. Neufeld, Insulin-loaded nanoparticles are prepared by alginate ionotropic pre-gelation followed by chitosan polyelectrolyte complexation, J Nanosci Nanotechnol, 7 (2007) 2833-2841.

[85] B. Sarmento, D. Ferreira, L. Jorgensen, M. van de Weert, Probing insulin's secondary structure after entrapment into alginate/chitosan nanoparticles, Eur J Pharm Biopharm, 65 (2007) 10-17.

[86] B. Sarmento, A. Ribeiro, F. Veiga, P. Sampaio, R. Neufeld, D. Ferreira, Alginate/chitosan nanoparticles are effective for oral insulin delivery, Pharm Res, 24 (2007) 2198-2206.

[87] C.B. Woitiski, R.J. Neufeld, F. Veiga, R.A. Carvalho, I.V. Figueiredo, Pharmacological effect of orally delivered insulin facilitated by multilayered stable nanoparticles, Eur J Pharm Sci, 41 (2010) 556-563.

[88] C.B. Woitiski, B. Sarmento, R.A. Carvalho, R.J. Neufeld, F. Veiga, Facilitated nanoscale delivery of insulin across intestinal membrane models, Int J Pharm, 412 (2011) 123-131.

[89] C.B. Woitiski, R.J. Neufeld, A.F. Soares, I.V. Figueiredo, F.J. Veiga, R.A. Carvalho, Evaluation of hepatic glucose metabolism via gluconeogenesis and glycogenolysis after oral administration of insulin nanoparticles, Drug Dev Ind Pharm, 38 (2012) 1441-1450.

[90] Y.H. Lin, F.L. Mi, C.T. Chen, W.C. Chang, S.F. Peng, H.F. Liang, H.W. Sung, Preparation and characterization of nanoparticles shelled with chitosan for oral insulin delivery, Biomacromolecules, 8 (2007) 146-152.

[91] K. Sonaje, Y.J. Chen, H.L. Chen, S.P. Wey, J.H. Juang, H.N. Nguyen, C.W. Hsu, K.J. Lin, H.W. Sung, Enteric-coated capsules filled with freeze-dried chitosan/poly(gamma-glutamic acid) nanoparticles for oral insulin delivery, Biomaterials, 31 (2010) 3384-3394.

[92] Y.H. Lin, K. Sonaje, K.M. Lin, J.H. Juang, F.L. Mi, H.W. Yang, H.W. Sung, Multi-ion-crosslinked nanoparticles with pH-responsive characteristics for oral delivery of protein drugs, J Control Release, 132 (2008) 141-149.

[93] K. Sonaje, Y.H. Lin, J.H. Juang, S.P. Wey, C.T. Chen, H.W. Sung, In vivo evaluation of safety and efficacy of self-assembled nanoparticles for oral insulin delivery, Biomaterials, 30 (2009) 2329-2339.

[94] F.Y. Su, K.J. Lin, K. Sonaje, S.P. Wey, T.C. Yen, Y.C. Ho, N. Panda, E.Y. Chuang, B. Maiti, H.W. Sung, Protease inhibition and absorption enhancement by functional nanoparticles for effective oral insulin delivery, Biomaterials, 33 (2012) 2801-2811.

[95] L. Han, Y. Zhao, L. Yin, R. Li, Y. Liang, H. Huang, S. Pan, C. Wu, M. Feng, Insulin-loaded pH-sensitive hyaluronic acid nanoparticles enhance transcellular delivery, AAPS PharmSciTech, 13 (2012) 836-845.

[96] X.Y. Xiong, Y.P. Li, Z.L. Li, C.L. Zhou, K.C. Tam, Z.Y. Liu, G.X. Xie, Vesicles from Pluronic/poly(lactic acid) block copolymers as new carriers for oral insulin delivery, J Control Release, 120 (2007) 11-17.

[97] X.Y. Xiong, Q.H. Li, Y.P. Li, L. Guo, Z.L. Li, Y.C. Gong, Pluronic P85/poly(lactic acid) vesicles as novel carrier for oral insulin delivery, Colloids Surf B Biointerfaces, 111 (2013) 282-288.

[98] F. Araújo, N. Shrestha, M.-A. Shahbazi, P. Fonte, E.M. Mäkilä, J.J. Salonen, J.T. Hirvonen, P.L. Granja, H.A. Santos, B. Sarmento, The impact of nanoparticles on the mucosal translocation and transport of GLP-1 across the intestinal epithelium, Biomaterials, 35 (2014) 9199-9207.

[99] N. Reix, A. Parat, E. Seyfritz, R. Van Der Werf, V. Epure, N. Ebel, L. Danicher, E. Marchioni, N. Jeandidier, M. Pinget, Y. Frère, S. Sigrist, In vitro uptake evaluation in Caco-2 cells and in vivo results in diabetic rats of insulin-loaded PLGA nanoparticles, Int J Pharm, 437 (2012) 213-220.

[100] J. Yang, H. Sun, C. Song, Preparation, characterization and in vivo evaluation of pH-sensitive oral insulin-loaded poly(lactic-co-glycolicacid) nanoparticles, Diabetes Obes Metab, 14 (2012) 358-364.

[101] P. Fonte, S. Soares, A. Costa, J. Andrade, V. Seabra, S. Reis, B. Sarmento, Effect of cryoprotectants on the porosity and stability of insulin-loaded PLGA nanoparticles after freeze-drying, Biomatter, 2 (2012) 329-339.

[102] S. Davaran, Y. Omidi, Mohammad Reza Rashidi, M. Anzabi, A. Shayanfar, S. Ghyasvand, N. Vesal, F. Davaran, Preparation and in vitro evaluation of linear and star-branched PLGA nanoparticles for insulin delivery, J Bioact Compat Polym, 23 (2008) 115-131.

[103] F. Cui, K. Shi, L. Zhang, A. Tao, Y. Kawashima, Biodegradable nanoparticles loaded with insulin–phospholipid complex for oral delivery: Preparation, in vitro characterization and in vivo evaluation, J Control Release, 114 (2006) 242-250.

[104] S. Sun, N. Liang, H. Piao, H. Yamamoto, Y. Kawashima, F. Cui, Insulin-S.O (sodium oleate) complex-loaded PLGA nanoparticles: formulation, characterization and in vivo evaluation, J Microencapsul, 27 (2010) 471-478.

[105] M.J. Santander-Ortega, D. Bastos-Gonzalez, J.L. Ortega-Vinuesa, M.J. Alonso, Insulin-loaded PLGA nanoparticles for oral administration: an in vitro physico-chemical characterization, J Biomed Nanotechnol, 5 (2009) 45-53.

[106] G. Sharma, C.F. van der Walle, M.N.V. Ravi Kumar, Antacid co-encapsulated polyester nanoparticles for peroral delivery of insulin: Development, pharmacokinetics, biodistribution and pharmacodynamics, Int J Pharm, 440 (2013) 99-110.

[107] F. Cui, A. Tao, D. Cun, L. Zhang, K. Shi, Preparation of insulin loaded PLGA-Hp55 nanoparticles for oral delivery, J Pharm Sci, 96 (2007) 421-427.

[108] Z.M. Wu, L. Ling, L.Y. Zhou, X.D. Guo, W. Jiang, Y. Qian, K.Q. Luo, L.J. Zhang, Novel preparation of PLGA/HP55 nanoparticles for oral insulin delivery, Nanoscale Res Lett, 7 (2012) 299.

[109] Z.M. Wu, L. Zhou, X.D. Guo, W. Jiang, L. Ling, Y. Qian, K.Q. Luo, L.J. Zhang, HP55-coated capsule containing PLGA/RS nanoparticles for oral delivery of insulin, Int J Pharm, 425 (2012) 1-8.

[110] X. Zhang, M. Sun, A. Zheng, D. Cao, Y. Bi, J. Sun, Preparation and characterization of insulin-loaded bioadhesive PLGA nanoparticles for oral administration, Eur J Pharm Sciences, 45 (2012) 632-638.

[111] G.P. Carino, J.S. Jacob, E. Mathiowitz, Nanosphere based oral insulin delivery, J Control Release, 65 (2000) 261-269.

[112] S. Jain, V.V. Rathi, A.K. Jain, M. Das, C. Godugu, Folate-decorated PLGA nanoparticles as a rationally designed vehicle for the oral delivery of insulin, Nanomedicine (Lond), 7 (2012) 1311-1337.

[113] X. Liu, C. Liu, W. Zhang, C. Xie, G. Wei, W. Lu, Oligoarginine-modified biodegradable nanoparticles improve the intestinal absorption of insulin, Int J Pharm, 448 (2013) 159-167.

[114] C. Damgé, P. Maincent, N. Ubrich, Oral delivery of insulin associated to polymeric nanoparticles in diabetic rats, J Control Release, 117 (2007) 163-170.

[115] M. Socha, A. Sapin, C. Damgé, P. Maincent, Influence of polymers ratio on insulin-loaded nanoparticles based on poly-ε-caprolactone and Eudragit® RS for oral administration, Drug Deliv, 16 (2009) 430-436.

[116] C. Damgé, M. Socha, N. Ubrich, P. Maincent, Poly(ε-caprolactone)/eudragit nanoparticles for oral delivery of aspart-insulin in the treatment of diabetes, J Pharm Sci, 99 (2010) 879-889.

[117] B. Deutel, M. Greindl, M. Thaurer, A. Bernkop-Schnurch, Novel insulin thiomer nanoparticles: in vivo evaluation of an oral drug delivery system, Biomacromolecules, 9 (2008) 278-285.

[118] G. Perera, M. Greindl, T.F. Palmberger, A. Bernkop-Schnürch, Insulin-loaded poly(acrylic acid)-cysteine nanoparticles: Stability studies towards digestive enzymes of the intestine, Drug Deliv, 16 (2009) 254-260.

[119] A.C. Foss, T. Goto, M. Morishita, N.A. Peppas, Development of acrylic-based copolymers for oral insulin delivery, Eur J Pharm Biopharm, 57 (2004) 163-169.

[120] M.G. Li, W.L. Lu, J.C. Wang, X. Zhang, X.Q. Wang, A.P. Zheng, Q. Zhang, Distribution, transition, adhesion and release of insulin loaded nanoparticles in the gut of rats, Int J Pharm, 329 (2007) 182-191.

[121] S. Sajeesh, C.P. Sharma, Cyclodextrin–insulin complex encapsulated polymethacrylic acid based nanoparticles for oral insulin delivery, Int J Pharm, 325 (2006) 147-154.

[122] M.S. Mesiha, M.B. Sidhom, B. Fasipe, Oral and subcutaneous absorption of insulin poly(isobutylcyanoacrylate) nanoparticles, Int J Pharm, 288 (2005) 289-293.

[123] Y. Zhang, X. Wu, L. Meng, Y. Zhang, R. Ai, N. Qi, H. He, H. Xu, X. Tang, Thiolated Eudragit nanoparticles for oral insulin delivery: preparation, characterization and in vivo evaluation, Int J Pharm, 436 (2012) 341-350.

[124] M. Jelvehgari, P. Zakeri-Milani, M.R. Siahi-Shadbad, B.D. Loveymi, A. Nokhodchi, Z. Azari, H. Valizadeh, Development of pH-sensitive insulin nanoparticles using Eudragit L100-55 and chitosan with different molecular weights, AAPS PharmSciTech, 11 (2010) 1237-1242.

[125] C. Tyagi, L. Tomar, P. Kumar, Y.E. Choonara, L.D. Toit, H. Singh, V. Pillay, pH responsive polymeric nanoparticles for oral insulin delivery, Int J Pharmacol Pharm Tech, 1 (2012) 6-10.

[126] C.J. Thompson, L. Tetley, I.F. Uchegbu, W.P. Cheng, The complexation between novel comb shaped amphiphilic polyallylamine and insulin—Towards oral insulin delivery, Int J Pharm, 376 (2009) 46-55.

[127] C.J. Thompson, L. Tetley, W.P. Cheng, The influence of polymer architecture on the protective effect of novel comb shaped amphiphilic poly(allylamine) against in vitro enzymatic degradation of insulin—Towards oral insulin delivery, Int J Pharm, 383 (2010) 216-227.

[128] C.J. Thompson, W. Cheng, P. Gadad, K. Skene, M. Smith, G. Smith, A. McKinnon, R. Knott, Uptake and transport of novel amphiphilic polyelectrolyte-insulin nanocomplexes by Caco-2 Cells—Towards oral insulin, Pharm Res, 28 (2011) 886-896.

[129] Access Pharmaceuticals web page, in: http://www.accesspharma.com, 2014.

[130] NanoMega Medical Corporation web page, in: http://www.nanomegamedical.com, 2014.

[131] NOD Pharmaceuticals, Inc. web page, in: http://www.nodpharm.com, 2014.

[132] A.T. Florence, Issues in oral nanoparticle drug carrier uptake and targeting, J Drug Target, 12 (2004) 65-70.

[133] S. Hossain, E.H. Chowdhury, T. Akaike, Nanoparticles and toxicity in therapeutic delivery: the ongoing debate, Ther Deliv, 2 (2011) 125-132.

[134] M. Goldberg, I. Gomez-Orellana, Challenges for the oral delivery of macromolecules, Nat Rev Drug Discov, 2 (2003) 289-295.

[135] K. Gowthamarajan, G. Kulkarni, Oral Insulin: fact or fiction? Possibilities of achieving oral delivery for insulin, Resonance, 8 (2003) 38-46.

[136] C.P. Reis, F. Veiga, P. Nunes, A.F. Soares, T. Laranjeira, R. Carvalho, J. Jones, I.V. Figueiredo, A.J. Ribeiro, A.M.S. Cabrita, Toxicological in vivo studies of an oral insulin nanosystem, Toxicol Lett, 172 (2007) S90-S90.

[137] C.P. Reis, I.V. Figueiredo, R.A. Carvalho, J. Jones, P. Nunes, A.F. Soares, C.F. Silva, A.J. Ribeiro, F.J. Veiga, C. Damgé, A.M.S. Cabrita, R.J. Neufeld, Toxicological assessment of orally delivered nanoparticulate insulin, Nanotoxicology, 2 (2008) 205-217.

[138] L. Wu, J. Zhang, W. Watanabe, Physical and chemical stability of drug nanoparticles, Adv Drug Deliv Rev, 63 (2011) 456-469.

[139] S. Hirsjarvi, L. Peltonen, L. Kainu, J. Hirvonen, Freeze-drying of low molecular weight poly(L-lactic acid) nanoparticles: effect of cryo- and lyoprotectants, J Nanosci Nanotechnol, 6 (2006) 3110-3117.

[140] W. Abdelwahed, G. Degobert, H. Fessi, Investigation of nanocapsules stabilization by amorphous excipients during freeze-drying and storage, Eur J Pharm Biopharm, 63 (2006) 87-94.

[141] E.N. Baker, T.L. Blundell, J.F. Cutfield, S.M. Cutfield, E.J. Dodson, G.G. Dodson, D.M. Hodgkin, R.E. Hubbard, N.W. Isaacs, C.D. Reynolds, et al., The structure of 2Zn pig insulin crystals at 1.5 A resolution, Philos Trans R Soc Lond B Biol Sci, 319 (1988) 369-456.

[142] U. Derewenda, Z. Derewenda, G.G. Dodson, R.E. Hubbard, F. Korber, Molecular structure of insulin: the insulin monomer and its assembly, Br Med Bull, 45 (1989) 4-18.

[143] A. Ahmad, V.N. Uversky, D. Hong, A.L. Fink, Early events in the fibrillation of monomeric insulin, J Biol Chem, 280 (2005) 42669-42675.

[144] L. Nielsen, S. Frokjaer, J. Brange, V.N. Uversky, A.L. Fink, Probing the mechanism of insulin fibril formation with insulin mutants, Biochemistry, 40 (2001) 8397-8409.

[145] H. Makadia, S. Siegel, Poly lactic-co-glycolic acid (PLGA) as biodegradable controlled drug delivery carrier, Polymers, 3 (2011) 1377-1397.

[146] X.S. Wu, N. Wang, Synthesis, characterization, biodegradation, and drug delivery application of biodegradable lactic/glycolic acid polymers. Part II: biodegradation, J Biomater Sci Polym Ed, 12 (2001) 21-34.

[147] F. Danhier, E. Ansorena, J. Silva, R. Coco, A. Le Breton, V. Preat, PLGA-based nanoparticles: an overview of biomedical applications, J Control Release, 161 (2012) 505-522.

[148] NCBI, PubChem database, in: https://pubchem.ncbi.nlm.nih.gov, 2015.

[149] N.-O. Chung, M.K. Lee, J. Lee, Mechanism of freeze-drying drug nanosuspensions, Int J Pharm, 437 (2012) 42-50.

[150] N.A. Williams, G.P. Polli, The lyophilization of pharmaceuticals: a literature review, J Parenter Sci Technol, 38 (1984) 48-59.

[151] S.K. Sahoo, J. Panyam, S. Prabha, V. Labhasetwar, Residual polyvinyl alcohol associated with poly (D,L-lactide-co-glycolide) nanoparticles affects their physical properties and cellular uptake, J Control Release, 82 (2002) 105-114.

[152] M.F. Zambaux, F. Bonneaux, R. Gref, P. Maincent, E. Dellacherie, M.J. Alonso, P. Labrude, C. Vigneron, Influence of experimental parameters on the

characteristics of poly(lactic acid) nanoparticles prepared by a double emulsion method, J Control Release, 50 (1998) 31-40.

[153] W. Abdelwahed, G. Degobert, H. Fessi, A pilot study of freeze drying of poly(epsilon-caprolactone) nanocapsules stabilized by poly(vinyl alcohol): Formulation and process optimization, Int J Pharm, 309 (2006) 178-188.

[154] B. Seijo, E. Fattal, L. Roblot-Treupel, P. Couvreur, Design of nanoparticles of less than 50 nm diameter: preparation, characterization and drug loading, Int J Pharm, 62 (1990) 1-7.

[155] H. Murakami, M. Kobayashi, H. Takeuchi, Y. Kawashima, Further application of a modified spontaneous emulsification solvent diffusion method to various types of PLGA and PLA polymers for preparation of nanoparticles, Powder Technol, 107 (2000) 137-143.

[156] S. Galindo-Rodriguez, E. Allemann, H. Fessi, E. Doelker, Physicochemical parameters associated with nanoparticle formation in the salting-out, emulsification-diffusion, and nanoprecipitation methods, Pharm Res, 21 (2004) 1428-1439.

[157] F. De Jaeghere, E. Allemann, J. Leroux, W. Stevels, J. Feijen, E. Doelker, R. Gurny, Formulation and lyoprotection of poly(lactic acid-co-ethylene oxide) nanoparticles: influence on physical stability and in vitro cell uptake, Pharm Res, 16 (1999) 859-866.

[158] H. Murakami, M. Kobayashi, H. Takeuchi, Y. Kawashima, Preparation of poly(DL-lactide-co-glycolide) nanoparticles by modified spontaneous emulsification solvent diffusion method, Int J Pharm, 187 (1999) 143-152.

[159] M. Berton, E. Allemann, C.A. Stein, R. Gurny, Highly loaded nanoparticulate carrier using an hydrophobic antisense oligonucleotide complex, Eur J Pharm Sci, 9 (1999) 163-170.

[160] D. Quintanar-Guerrero, A. Ganem-Quintanar, E. Allemann, H. Fessi, E. Doelker, Influence of the stabilizer coating layer on the purification and freeze-drying of poly(D,L-lactic acid) nanoparticles prepared by an emulsion-diffusion technique, J Microencapsul, 15 (1998) 107-119.

[161] S. de Chasteigner, G. Cavé, H. Fessi, J.-P. Devissaguet, F. Puisieux, Freeze-drying of itraconazole-loaded nanosphere suspensions: a feasibility study, Drug Dev Res, 38 (1996) 116-124.

[162] J. Molpeceres, M.R. Aberturas, M. Chacon, L. Berges, M. Guzman, Stability of cyclosporine-loaded poly-sigma-caprolactone nanoparticles, J Microencapsul, 14 (1997) 777-787.

[163] X. Tang, M. Pikal, Design of freeze-drying processes for pharmaceuticals: practical advice, Pharm Res, 21 (2004) 191-200.

[164] S.D. Allison, M.C. Molina, T.J. Anchordoquy, Stabilization of lipid/DNA complexes during the freezing step of the lyophilization process: the particle isolation hypothesis, Biochim Biophys Acta, 1468 (2000) 127-138.

[165] P. Stupar, V. Pavlović, J. Nunić, S. Cundrič, M. Filipič, M. Stevanović, Development of lyophilized spherical particles of poly(epsilon-caprolactone) and examination of their morphology, cytocompatibility and influence on the formation of reactive oxygen species, J Drug Deliv Sci Technol, 24 (2014) 191-197.

[166] L. Crowe, D. Reid, J. Crowe, Is trehalose special for preserving dry biomaterials?, Biophys J, 71 (1996) 2087-2093.

[167] A. Saez, M. Guzmán, J. Molpeceres, M. Aberturas, Freeze-drying of polycaprolactone and poly(d,l-lactic-glycolic) nanoparticles induce minor particle size changes affecting the oral pharmacokinetics of loaded drugs, Eur J Pharm Biopharm, 50 (2000) 379-387.

[168] M. Sameti, G. Bohr, M.N.V. Ravi Kumar, C. Kneuer, U. Bakowsky, M. Nacken, H. Schmidt, C.-M. Lehr, Stabilisation by freeze-drying of cationically modified silica nanoparticles for gene delivery, Int J Pharm, 266 (2003) 51-60.

[169] M.A. Moretton, D.A. Chiappetta, A. Sosnik, Cryoprotection-lyophilization and physical stabilization of rifampicin-loaded flower-like polymeric micelles, J R Soc Interface, 9 (2012) 487-502.

[170] J. Crowe, L. Crowe, J. Carpenter, Preserving dry biomaterials: the water replacement hypothesis, BioPharm, 6 (1993) 28-37.

[171] S. Allison, A. Dong, J. Carpenter, Counteracting effects of thiocyanate and sucrose on chymotrypsinogen secondary structure and aggregation during freezing, drying, and rehydration, Biophys J, 71 (1996) 2022-2032.

[172] F. De Jaeghere, E. Allemann, J. Feijen, T. Kissel, E. Doelker, R. Gurny, Freeze-drying and lyopreservation of diblock and triblock poly(lactic acid)-poly(ethylene oxide) (PLA-PEO) copolymer nanoparticles, Pharm Dev Technol, 5 (2000) 473-483.

[173] S. Bozdag, K. Dillen, J. Vandervoort, A. Ludwig, The effect of freeze-drying with different cryoprotectants and gamma-irradiation sterilization on the characteristics of ciprofloxacin HCl-loaded poly(D,L-lactide-glycolide) nanoparticles, J Pharm Pharmacol, 57 (2005) 699-707.

[174] M. Chacon, J. Molpeceres, L. Berges, M. Guzman, M.R. Aberturas, Stability and freeze-drying of cyclosporine loaded poly(D,L lactide-glycolide) carriers, Eur J Pharm Sci, 8 (1999) 99-107.

[175] P. Fonte, S. Soares, F. Sousa, A. Costa, V. Seabra, S. Reis, B. Sarmento, Stability study perspective of the effect of freeze-drying using cryoprotectants on the structure of insulin loaded into PLGA nanoparticles, Biomacromolecules, 15 (2014) 3753-3765.

[176] B. Wilson, L. Paladugu, S.R. Priyadarshini, J.J. Jenita, Development of albumin-based nanoparticles for the delivery of abacavir, Int J Biol Macromol, 81 (2015) 763-767.

[177] A. Curic, B.L. Keller, R. Reul, J. Moschwitzer, G. Fricker, Development and lyophilization of itraconazole loaded poly(butylcyanoacrylate) nanospheres as a drug delivery system, Eur J Pharm Sci, 78 (2015) 121-131.

[178] Y. Jeong, Y. Shim, C. Kim, G. Lim, K. Choi, C. Yoon, Effect of cryoprotectants on the reconstitution of surfactant-free nanoparticles of poly(DL-lactide-co-glycolide), J Microencapsul, 22 (2005) 593-601.

[179] A. Jain, K. Thakur, G. Sharma, P. Kush, U.K. Jain, Fabrication, characterization and cytotoxicity studies of ionically cross-linked docetaxel loaded chitosan nanoparticles, Carbohydr Polym, 137 (2016) 65-74.

[180] E. Trappler, Lyophilization Equipment, in: H.R. Constantino, M.J. Pikal (Eds.) Lyophilization of Biopharmaceuticals, AAPS Press, Arlington, VA, USA, 2004, pp. 3-41.

[181] M.J. Pikal, Freeze-drying of proteins : process, formulation and stability, in: Formulation and Delivery of Proteins and Peptides, American Chemical Society, 1994, pp. 120-133.

[182] M. Holzer, V. Vogel, W. Mäntele, D. Schwartz, W. Haase, K. Langer, Physico-chemical characterisation of PLGA nanoparticles after freeze-drying and storage, Eur J Pharm Biopharm, 72 (2009) 428-437.

[183] F. Franks, Freeze-drying: from empiricism to predictability. The significance of glass transitions, Dev Biol Stand, 74 (1992) 9-18.

[184] J.C. Kasper, W. Friess, The freezing step in lyophilization: Physico-chemical fundamentals, freezing methods and consequences on process performance and quality attributes of biopharmaceuticals, Eur J Pharm Biopharm, 78 (2011) 248-263.

[185] J.A. Searles, J.F. Carpenter, T.W. Randolph, The ice nucleation temperature determines the primary drying rate of lyophilization for samples frozen on a temperature-controlled shelf, J Pharm Sci, 90 (2001) 860-871.

[186] Z. Cui, C.H. Hsu, R.J. Mumper, Physical characterization and macrophage cell uptake of mannan-coated nanoparticles, Drug Dev Ind Pharm, 29 (2003) 689-700.

[187] M.S. Shaik, O. Ikediobi, V.D. Turnage, J. McSween, N. Kanikkannan, M. Singh, Long-circulating monensin nanoparticles for the potentiation of immunotoxin and anticancer drugs, J Pharm Pharmacol, 53 (2001) 617-627.

[188] T.W. Patapoff, D.E. Overcashier, The importance of freezing on lyophilization cycle development, BioPharm, 15 (2002) 16-21.

[189] B.S. Chang, S.Y. Patro, Freeze-drying process development for protein pharmaceuticals, in: H.R. Costantino, M.J. Pikal (Eds.) Lyophilization of Biopharmaceuticals, AAPS Press, Arlington, VA, USA, 2004, pp. 113-138.

[190] J.A. Searles, J.F. Carpenter, T.W. Randolph, Annealing to optimize the primary drying rate, reduce freezing-induced drying rate heterogeneity, and determine T(g)' in pharmaceutical lyophilization, J Pharm Sci, 90 (2001) 872-887.

[191] W. Abdelwahed, G. Degobert, H. Fessi, Freeze-drying of nanocapsules: Impact of annealing on the drying process, Int J Pharm, 324 (2006) 74-82.

[192] A.-M. Shi, L.-J. Wang, D. Li, B. Adhikari, The effect of annealing and cryoprotectants on the properties of vacuum-freeze dried starch nanoparticles, Carbohydr Polym, 88 (2012) 1334-1341.

[193] M.J. Pikal, S. Shah, M.L. Roy, R. Putman, The secondary drying stage of freeze drying: drying kinetics as a function of temperature and chamber pressure, Int J Pharm, 60 (1990) 203-207.

[194] Y. Konan, R. Gurny, E. Allémann, Preparation and characterization of sterile and freeze-dried sub-200 nm nanoparticles, Int J Pharm, 233 (2002) 239-252.

[195] M.J. Pikal, S. Shah, The collapse temperature in freeze drying: dependance on measurement methodology and rate of water removal from the glassy state, Int J Pharm, 62 (1990) 165-186.

[196] T. Kodama, M. Takeuchi, N. Wakiyama, K. Terada, Optimization of secondary drying condition for desired residual water content in a lyophilized product using a novel simulation program for pharmaceutical lyophilization, Int J Pharm, 469 (2014) 59-66.

[197] Stability testing of new drug substances and products Q1A(R2) in: ICH, Geneva, Switzerland, 2003.

[198] A. Gürsoy, L. Eroğlu, S. Ulutin, M. Taşyürek, H. Fessi, F. Puisieux, J.-P. Devissaguet, Evaluation of indomethacin nanocapsules for their physical stability and inhibitory activity on inflammation and platelet aggregation, Int J Pharm, 52 (1989) 101-108.

[199] W.Y. Ayen, N. Kumar, A systematic study on lyophilization process of polymersomes for long-term storage using doxorubicin-loaded (PEG)(3)-PLA nanopolymersomes, Eur J Pharm Sci, 46 (2012) 405-414.

[200] M. Dadparvar, S. Wagner, S. Wien, F. Worek, H. von Briesen, J. Kreuter, Freeze-drying of HI-6-loaded recombinant human serum albumin nanoparticles for improved storage stability, Eur J Pharm Biopharm, 88 (2014) 510-517.

[201] G.R. Nireesha, L. Divya, C. Sowmya, N. Venkateshan, M. Niranjan Babu, V. Lavakumar, Lyophilization/Freeze drying - A review, Int J Novel Trends Pharm Sci, 3 (2013) 87-98.

[202] A. Millqvist-Fureby, M. Malmsten, B. Bergenstahl, Surface characterisation of freeze-dried protein/carbohydrate mixtures, Int J Pharm, 191 (1999) 103-114.

[203] K.S. Soppimath, T.M. Aminabhavi, A.R. Kulkarni, W.E. Rudzinski, Biodegradable polymeric nanoparticles as drug delivery devices, J Control Release, 70 (2001) 1-20.

[204] W. Wang, Lyophilization and development of solid protein pharmaceuticals, Int J Pharm, 203 (2000) 1-60.

[205] S.S. Davis, Delivery of peptide and non-peptide drugs through the respiratory tract, Pharm Sci Technolo Today, 2 (1999) 450-456.

[206] S. Frokjaer, D.E. Otzen, Protein drug stability: a formulation challenge, Nat Rev Drug Discov, 4 (2005) 298-306.

[207] J.E. Talmadge, The pharmaceutics and delivery of therapeutic polypeptides and proteins, Adv Drug Deliv Rev, 10 (1993) 247-299.

[208] I. Bala, S. Hariharan, M. Kumar, PLGA nanoparticles in drug delivery: the state of the art, Crit Rev Ther Drug Carrier Syst, 21 (2004) 387-422.

[209] J.L. Cleland, M.F. Powell, S.J. Shire, The development of stable protein formulations: a close look at protein aggregation, deamidation, and oxidation, Crit Rev Ther Drug Carrier Syst, 10 (1993) 307-377.

[210] J.F. Carpenter, M.J. Pikal, B.S. Chang, T.W. Randolph, Rational design of stable lyophilized protein formulations: some practical advice, Pharm Res, 14 (1997) 969-975.

[211] B.S. Bhatnagar, M.J. Pikal, R.H. Bogner, Study of the individual contributions of ice formation and freeze-concentration on isothermal stability of lactate dehydrogenase during freezing, J Pharm Sci, 97 (2008) 798-814.

[212] X.C. Tang, M.J. Pikal, Measurement of the kinetics of protein unfolding in viscous systems and implications for protein stability in freeze-drying, Pharm Res, 22 (2005) 1176-1185.

[213] S. Luthra, J.P. Obert, D.S. Kalonia, M.J. Pikal, Investigation of drying stresses on proteins during lyophilization: differentiation between primary and secondary-drying stresses on lactate dehydrogenase using a humidity controlled mini freeze-dryer, J Pharm Sci, 96 (2007) 61-70.

[214] S. Luthra, J.P. Obert, D.S. Kalonia, M.J. Pikal, Impact of critical process and formulation parameters affecting in-process stability of lactate dehydrogenase during the secondary drying stage of lyophilization: a mini freeze dryer study, J Pharm Sci, 96 (2007) 2242-2250.

[215] A. Baheti, L. Kumar, A.K. Bansal, Excipients used in lyophilization of small molecules, J Excipients Food Chem, 1 (2010) 41-54.

[216] H. Katas, Z. Hussain, S.A. Rahman, Storage stabilisation of albumin-loaded chitosan nanoparticles by lyoprotectants, Trop J Pharm Res, 12 (2013) 135-142.

[217] S. Rodrigues, C. Cordeiro, B. Seijo, C. Remunan-Lopez, A. Grenha, Hybrid nanosystems based on natural polymers as protein carriers for respiratory delivery: Stability and toxicological evaluation, Carbohydr Polym, 123 (2015) 369-380.

[218] M. Dionisio, C. Cordeiro, C. Remunan-Lopez, B. Seijo, A.M. Rosa da Costa, A. Grenha, Pullulan-based nanoparticles as carriers for transmucosal protein delivery, Eur J Pharm Sci, 50 (2013) 102-113.

[219] M. van de Weert, W. Hennink, W. Jiskoot, Protein instability in poly(lactic-co-glycolic acid) microparticles, Pharm Res, 17 (2000) 1159-1167.

[220] M.D. Blanco, M.J. Alonso, Development and characterization of protein-loaded poly(lactide-co-glycolide) nanospheres, Eur J Pharm Biopharm, 43 (1997) 287-294.

[221] S. Sharif, D.T. O'Hagan, A comparison of alternative methods for the determination of the levels of proteins entrapped in poly(lactide-co-glycolide) microparticles, Int J Pharm, 115 (1995) 259-263.

[222] H. Sah, A new strategy to determine the actual protein content of poly(lactide-co-glycolide) microspheres, J Pharm Sci, 86 (1997) 1315-1318.

[223] M. Diop, N. Auberval, A. Viciglio, A. Langlois, W. Bietiger, C. Mura, C. Peronet, A. Bekel, D. Julien David, M. Zhao, M. Pinget, N. Jeandidier, C. Vauthier, E. Marchioni, Y. Frere, S. Sigrist, Design, characterisation, and bioefficiency of insulin-chitosan nanoparticles after stabilisation by freeze-drying or cross-linking, Int J Pharm, 491 (2015) 402-408.

[224] K.T. Mody, D. Mahony, A.S. Cavallaro, F. Stahr, S.Z. Qiao, T.J. Mahony, N. Mitter, Freeze-drying of ovalbumin loaded mesoporous silica nanoparticle vaccine formulation increases antigen stability under ambient conditions, Int J Pharm, 465 (2014) 325-332.

[225] N. Samadi, C.F. van Nostrum, T. Vermonden, M. Amidi, W.E. Hennink, Mechanistic studies on the degradation and protein release characteristics of

poly(lactic-co-glycolic-co-hydroxymethylglycolic acid) nanospheres, Biomacromolecules, 14 (2013) 1044-1053.

[226] X. Lu, H. Gao, C. Li, Y.W. Yang, Y. Wang, Y. Fan, G. Wu, J. Ma, Polyelectrolyte complex nanoparticles of amino poly(glycerol methacrylate)s and insulin, Int J Pharm, 423 (2012) 195-201.

[227] P. Fonte, F. Araújo, V. Seabra, S. Reis, M. van de Weert, B. Sarmento, Co-encapsulation of lyoprotectants improves the stability of protein-loaded PLGA nanoparticles upon lyophilization, Int J Pharm, 496 (2015) 850-862.

[228] M. van de Weert, L. Jorgensen, E. Horn Moeller, S. Frokjaer, Factors of importance for a successful delivery system for proteins, Expert Opin Drug Deliv, 2 (2005) 1029-1037.

[229] A. Kumari, S. Yadav, S. Yadav, Biodegradable polymeric nanoparticles based drug delivery systems, Colloids Surf B Biointerfaces, 75 (2010) 1-18.

[230] K. Izutsu, Y. Fujimaki, A. Kuwabara, N. Aoyagi, Effect of counterions on the physical properties of l-arginine in frozen solutions and freeze-dried solids, Int J Pharm, 301 (2005) 161-169.

[231] M. García-Fuentes, D. Torres, M.J. Alonso, Design of lipid nanoparticles for the oral delivery of hydrophilic macromolecules, Colloids Surf B Biointerfaces, 27 (2003) 159-168.

[232] N. Zhang, Q. Ping, G. Huang, W. Xu, Y. Cheng, X. Han, Lectin-modified solid lipid nanoparticles as carriers for oral administration of insulin, Int J Pharm, 327 (2006) 153-159.

[233] B. Sarmento, A. Ribeiro, F. Veiga, D. Ferreira, Development and validation of a rapid reversed-phase HPLC method for the determination of insulin from nanoparticulate systems, Biomed Chromatogr, 20 (2006) 898-903.

[234] P. Fonte, T. Nogueira, C. Gehm, D. Ferreira, B. Sarmento, Chitosan-coated solid lipid nanoparticles enhance the oral absorption of insulin, Drug Deliv Transl Res, 1 (2011) 299-308.

[235] W. Mehnert, K. Mader, Solid lipid nanoparticles: production, characterization and applications, Adv Drug Deliv Rev, 47 (2001) 165-196.

[236] H. Takeuchi, H. Yamamoto, T. Toyoda, H. Toyobuku, T. Hino, Y. Kawashima, Physical stability of size controlled small unilameller liposomes coated with a modified polyvinyl alcohol, Int J Pharm, 164 (1998) 103-111.

[237] L. Šikurova, M. Kristeková, Fluorescence anisotropy and light-scattering studies of the interaction of insulin with liposomes, J Fluoresc, 3 (1993) 215-217.

[238] Y.-Y. Yang, T.-S. Chung, X.-L. Bai, W.-K. Chan, Effect of preparation conditions on morphology and release profiles of biodegradable polymeric microspheres

containing protein fabricated by double-emulsion method, Chem Eng Sci, 55 (2000) 2223-2236.

[239] A. Giteau, M.C. Venier-Julienne, A. Aubert-Pouessel, J.P. Benoit, How to achieve sustained and complete protein release from PLGA-based microparticles?, Int J Pharm, 350 (2008) 14-26.

[240] J. Buske, C. König, S. Bassarab, A. Lamprecht, S. Mühlau, K.G. Wagner, Influence of PEG in PEG–PLGA microspheres on particle properties and protein release, Eur J Pharm Biopharm, 81 (2012) 57-63.

[241] M. Heller, J. Carpenter, T. Randolph, Protein formulation and lyophilization cycle design: Prevention of damage due to freeze-concentration induced phase separation, Biotechnol Bioeng, 63 (1999) 166-174.

[242] S. Kadoya, K. Fujii, K. Izutsu, E. Yonemochi, K. Terada, C. Yomota, T. Kawanishi, Freeze-drying of proteins with glass-forming oligosaccharide-derived sugar alcohols, Int J Pharm, 389 (2010) 107-113.

[243] A. Dong, P. Huang, W. Caughey, Protein secondary structures in water from second-derivative amide i infrared spectra, Biochemistry, 29 (1990) 3303-3308.

[244] B. Kendrick, A. Dong, S. Allison, M. Manning, J. Carpenter, Quantitation of the area of overlap between second-derivative amide I infrared spectra to determine the structural similarity of a protein in different states, J Pharm Sci, 85 (1996) 155-158.

[245] S. Prestrelski, N. Tedeschi, T. Arakawa, J. Carpenter, Dehydration-induced conformational transitions in proteins and their inhibition by stabilizers, Biophys J, 65 (1993) 661-671.

[246] M. Maltesen, S. Bjerregaard, L. Hovgaard, S. Havelund, M. Van De Weert, Analysis of insulin allostery in solution and solid state with FTIR, J Pharm Sci, 98 (2009) 3265-3277.

[247] G. Maisuradze, A. Liwo, H. Scheraga, Principal component analysis for protein folding dynamics, J Mol Biol, 385 (2009) 312-329.

[248] S. Matsumoto, Proteins and sugars affecting the zeta potential and stability of dispersed vesicular globules in w/o/w emulsions, in: K. Nishinari, E. Doi (Eds.) Food Hydrocolloids, Springer US, 1993, pp. 399-408.

[249] F. Franks, Long-term stabilization of biologicals, Biotechnology, 12 (1994) 253-256.

[250] C. Oksanen, G. Zografi, The relationship between the glass transition temperature and water vapor absorption by poly(vinylpyrrolidone), Pharm Res, 7 (1990) 654-657.

[251] H. Sasaki, J. Kikuchi, T. Maeda, H. Kuboniwa, Impact of different elastomer formulations on moisture permeation through stoppers used for lyophilized products stored under humid conditions, PDA J Pharm Sci Technol, 64 (2010) 63-70.

[252] E. Schmitt, D. Law, G. Zhang, Nucleation and crystallization kinetics of hydrated amorphous lactose above the glass transition temperature, J Pharm Sci, 88 (1999) 291-296.

[253] J. D'Antonio, B. Murphy, M. Manning, W. Al-Azzam, Comparability of protein therapeutics: quantitative comparison of second-derivative amide I infrared spectra, J Pharm Sci, 101 (2012) 2025-2033.

[254] K. Schersch, O. Betz, P. Garidel, S. Muehlau, S. Bassarab, G. Winter, Systematic investigation of the effect of lyophilizate collapse on pharmaceutically relevant proteins I: Stability after freeze-drying, J Pharm Sci, 99 (2010) 2256-2278.

[255] K. Schersch, O. Betz, P. Garidel, S. Muehlau, S. Bassarab, G. Winter, Systematic investigation of the effect of lyophilizate collapse on pharmaceutically relevant proteins, part 2: Stability during storage at elevated temperatures, J Pharm Sci, 101 (2012) 2288-2306.

[256] K. Schersch, O. Betz, P. Garidel, S. Muehlau, S. Bassarab, G. Winter, Systematic investigation of the effect of lyophilizate collapse on pharmaceutically relevant proteins III: Collapse during storage at elevated temperatures, Eur J Pharm Biopharm, 85 (2013) 240-252.

[257] K. Griebenow, A. Klibanov, Lyophilization-induced reversible changes in the secondary structure of proteins, Proc Natl Acad Sci U S A, 92 (1995) 10969-10976.

[258] K. Griebenow, A. Klibanov, On protein denaturation in aqueous−organic mixtures but not in pure organic solvents, J Am Chem Soc, 118 (1996) 11695-11700.

[259] M. van de Weert, J. Hering, P. Haris, Fourier transform infrared spectroscopy, in: W. Jiskoot, D. Crommelin (Eds.) Methods for Structural Analysis of Protein Pharmaceuticals, AAPS Press, 2005, pp. 131-166.

[260] S. Li, T. Patapoff, D. Overcashier, C. Hsu, T. Nguyen, R. Borchardt, Effects of reducing sugars on the chemical stability of human relaxin in the lyophilized state, J Pharm Sci, 85 (1996) 873-877.

[261] F. Kesisoglou, S. Panmai, Y. Wu, Nanosizing — Oral formulation development and biopharmaceutical evaluation, Adv Drug Deliv Rev, 59 (2007) 631-644.

[262] L. Chang, D. Shepherd, J. Sun, D. Ouellette, K. Grant, X. Tang, M. Pikal, Mechanism of protein stabilization by sugars during freeze-drying and storage:

native structure preservation, specific interaction, and/or immobilization in a glassy matrix?, J Pharm Sci, 94 (2005) 1427-1444.

[263] L. Chang, D. Shepherd, J. Sun, X. Tang, M. Pikal, Effect of sorbitol and residual moisture on the stability of lyophilized antibodies: Implications for the mechanism of protein stabilization in the solid state, J Pharm Sci, 94 (2005) 1445-1455.

[264] A. Layre, P. Couvreur, J. Richard, D. Requier, N. Eddine Ghermani, R. Gref, Freeze-drying of composite core-shell nanoparticles, Drug Dev Ind Pharm, 32 (2006) 839-846.

[265] S. Kamiya, T. Kurita, A. Miyagishima, S. Itai, M. Arakawa, Physical properties of griseofulvin-lipid nanoparticles in suspension and their novel interaction mechanism with saccharide during freeze-drying, Eur J Pharm Biopharm, 74 (2010) 461-466.

[266] S. Kelly, T. Jess, N. Price, How to study proteins by circular dichroism, Biochim Biophys Acta, 1751 (2005) 119-139.

[267] G. Jiang, B. Thanoo, P. DeLuca, Effect of osmotic pressure in the solvent extraction phase on BSA release profile from PLGA microspheres, Pharm Dev Technol, 7 (2002) 391-399.

[268] B. Amsden, Review of osmotic pressure driven release of proteins from monolithic devices, J Pharm Pharm Sci, 10 (2007) 129-143.

[269] J. Searles, Freezing and Annealing Phenomena in Lyophilization, in: L. Rey, J.C. May (Eds.) Freeze drying/Lyophilization of pharmaceutical and biological products, Informa Healthcare, 2010, pp. 52-81.

[270] B.S. Bhatnagar, R.H. Bogner, M.J. Pikal, Protein stability during freezing: separation of stresses and mechanisms of protein stabilization, Pharm Dev Technol, 12 (2007) 505-523.

[271] J.J. Schwegman, J.F. Carpenter, S.L. Nail, Evidence of partial unfolding of proteins at the ice/freeze-concentrate interface by infrared microscopy, J Pharm Sci, 98 (2009) 3239-3246.

[272] J. Liu, T. Viverette, M. Virgin, M. Anderson, D. Paresh, A study of the impact of freezing on the lyophilization of a concentrated formulation with a high fill depth, Pharm Dev Technol, 10 (2005) 261-272.

[273] S.D. Webb, J.L. Cleland, J.F. Carpenter, T.W. Randolph, Effects of annealing lyophilized and spray-lyophilized formulations of recombinant human interferon-gamma, J Pharm Sci, 92 (2003) 715-729.

[274] M.J. Pikal, D.R. Rigsbee, The stability of insulin in crystalline and amorphous solids: observation of greater stability for the amorphous form, Pharm Res, 14 (1997) 1379-1387.

[275] G.B. Strambini, E. Gabellieri, Proteins in frozen solutions: evidence of ice-induced partial unfolding, Biophys J, 70 (1996) 971-976.

[276] J.M. Sarciaux, S. Mansour, M.J. Hageman, S.L. Nail, Effects of buffer composition and processing conditions on aggregation of bovine IgG during freeze-drying, J Pharm Sci, 88 (1999) 1354-1361.

[277] B.M. Eckhardt, J.Q. Oeswein, T.A. Bewley, Effect of freezing on aggregation of human growth hormone, Pharm Res, 8 (1991) 1360-1364.

[278] B.S. Chang, B.S. Kendrick, J.F. Carpenter, Surface-induced denaturation of proteins during freezing and its inhibition by surfactants, J Pharm Sci, 85 (1996) 1325-1330.

[279] S. Nema, K.E. Avis, Freeze-thaw studies of a model protein, lactate dehydrogenase, in the presence of cryoprotectants, J Parenter Sci Technol, 47 (1993) 76-83.

[280] J.F. Carpenter, T. Arakawa, J.H. Crowe, Interactions of stabilizing additives with proteins during freeze-thawing and freeze-drying, Dev Biol Stand, 74 (1992) 225-238; discussion 238-229.

[281] L. Jørgensen, C. Vermehren, S. Bjerregaard, S. Froekjaer, Secondary structure alterations in insulin and growth hormone water-in-oil emulsions, Int J Pharm, 254 (2003) 7-10.

[282] Z. Yong, D. Yingjie, W. Xueli, X. Jinghua, L. Zhengqiang, Conformational and bioactivity analysis of insulin: Freeze-drying TBA/water co-solvent system in the presence of surfactant and sugar, Int J Pharm, 371 (2009) 71-81.

[283] M. Bouchard, J. Zurdo, E.J. Nettleton, C.M. Dobson, C.V. Robinson, Formation of insulin amyloid fibrils followed by FTIR simultaneously with CD and electron microscopy, Protein Sci, 9 (2000) 1960-1967.

[284] I.B. Bekard, D.E. Dunstan, Tyrosine autofluorescence as a measure of bovine insulin fibrillation, Biophys J, 97 (2009) 2521-2531.

[285] M. Falconi, M. Bozzi, M. Paci, A. Raudino, R. Purrello, A. Cambria, M. Sette, M.T. Cambria, Spectroscopic and molecular dynamics simulation studies of the interaction of insulin with glucose, Int J Biol Macromol, 29 (2001) 161-168.

[286] M. Amidi, H.C. Pellikaan, A.H. de Boer, D.J. Crommelin, W.E. Hennink, W. Jiskoot, Preparation and physicochemical characterization of supercritically dried insulin-loaded microparticles for pulmonary delivery, Eur J Pharm Biopharm, 68 (2008) 191-200.

[287] R. Malik, I. Roy, Probing the mechanism of insulin aggregation during agitation, Int J Pharm, 413 (2011) 73-80.

[288] J.R. Lakowicz, Principles of fluorescence spectroscopy, Springer US, New York, 2006.

[289] C. Arigita, W. Jiskoot, J. Westdijk, C. van Ingen, W.E. Hennink, D.J. Crommelin, G.F. Kersten, Stability of mono- and trivalent meningococcal outer membrane vesicle vaccines, Vaccine, 22 (2004) 629-642.

[290] H. LeVine, Thioflavine T interaction with amyloid β-sheet structures, Amyloid, 2 (1995) 1-6.

[291] A.A. Maskevich, V.I. Stsiapura, V.A. Kuzmitsky, I.M. Kuznetsova, O.I. Povarova, V.N. Uversky, K.K. Turoverov, Spectral properties of thioflavin T in solvents with different dielectric properties and in a fibril-incorporated form, J Proteome Res, 6 (2007) 1392-1401.

[292] L. Nielsen, R. Khurana, A. Coats, S. Frokjaer, J. Brange, S. Vyas, V.N. Uversky, A.L. Fink, Effect of environmental factors on the kinetics of insulin fibril formation: elucidation of the molecular mechanism, Biochemistry, 40 (2001) 6036-6046.

[293] J.L. Jimenez, E.J. Nettleton, M. Bouchard, C.V. Robinson, C.M. Dobson, H.R. Saibil, The protofilament structure of insulin amyloid fibrils, Proc Natl Acad Sci U S A, 99 (2002) 9196-9201.

[294] S.L. Nail, S. Jiang, S. Chongprasert, S.A. Knopp, Fundamentals of freeze-drying, Pharm Biotechnol, 14 (2002) 281-360.

[295] P. Fonte, F. Andrade, J. Pinto, V. Seabra, M. van de Weert, S. Reis, B. Sarmento, Effect of the freezing step in the stability and bioactivity of protein-loaded PLGA nanoparticles upon lyophilization.

[296] F. Nemati, G.N. Cavé, P. Couvreur, Lyophilization of substances with low water permeability by a modification of crystallized structures during freezing, in: Assoc. Pharm. Galenique Ind., vol. 3, 1992, pp. 487-493.

This page was intentionally left in blank